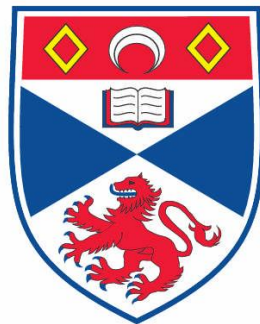


Investigations into temporal and spatial variability of zooplankton at the Svalbard archipelago

Ananda Rabindranath



This thesis is submitted in partial fulfilment for the degree of PhD

at the

University of St Andrews

2013

I, Ananda Rabindranath, hereby certify that this thesis, which is approximately 76,000 words in length, has been written by me, that it is the record of work carried out by me and that it has not been submitted in any previous application for a higher degree.

I was admitted as a research student in September, 2008 and as a candidate for the degree of Doctor of Philosophy in September, 2009; the higher study for which this is a record was carried out in the University of St Andrews between 2008 and 2012.

Date signature of candidate

I hereby certify that the candidate has fulfilled the conditions of the Resolution and Regulations appropriate for the degree of Doctor of Philosophy in the University of St Andrews and that the candidate is qualified to submit this thesis in application for that degree.

Date signature of supervisor

In submitting this thesis to the University of St Andrews I understand that I am giving permission for it to be made available for use in accordance with the regulations of the University Library for the time being in force, subject to any copyright vested in the work not being affected thereby. I also understand that the title and the abstract will be published, and that a copy of the work may be made and supplied to any bona fide library or research worker, that my thesis will be electronically accessible for personal or research use unless exempt by award of an embargo as requested below, and that the library has the right to migrate my thesis into new electronic forms as required to ensure continued access to the thesis. I have obtained any third-party copyright permissions that may be required in order to allow such access and migration, or have requested the appropriate embargo below.

The following is an agreed request by candidate and supervisor regarding the electronic publication of this thesis:

Embargo on both of printed copy and electronic copy for the same fixed period of two years on the following ground:

publication would preclude future publication;

Date signature of candidate signature of supervisor

Abstract

Plankton are generally considered good indicators for ocean climate variability, but plankton data from the Arctic are still comparatively scarce. Due to this scarcity of information, the prevalence of vertical migration behaviour at high latitude is still debated. Atlantic inflow is a key process governing biological diversity in the Arctic Ocean, and the location of the Svalbard archipelago makes it an ideal study area to monitor this inflow. Comparing the zooplankton community within the fjords of Svalbard at various latitudes allowed us to assess the influence of Atlantic inflow and any subsequent changes in zooplankton composition that may have implications for higher trophic levels. Using sediment traps deployed on oceanic moorings, Chapter 3 of this thesis analysed long term observations from sea-ice dominated Rijpfjorden for the first time, and compared the zooplankton to Atlantic Water influenced Kongsfjorden. Chapters 4 and 5 investigated the spatial relevance of our moored observations using shipboard observations, and chapters 6 and 7 present observations of vertical migration across a range of conditions.

Kongsfjorden was dominated by *Calanus* copepods associated with Arctic and Atlantic water, and strongly influenced by Atlantic Water advection. Rijpfjorden was largely influenced by sea-ice formation with higher proportional abundances of macrozooplankton species. Advection brought Atlantic associated species into Rijpfjorden during warmer years. Prevailing hydrology and bathymetry were highlighted as factors forcing zooplankton distribution, while advection was identified as responsible for much of the observed small scale spatial variation amongst weaker swimmers. At an aggregation scale of 0.5 nautical miles, zooplankton distribution was highly patchy and moored observations could only be reliably expanded outwards to a maximum of 1 nautical mile. Low amplitude diel vertical migration (especially by younger copepodids) was identified in surface waters when a food source was available. These observations must be considered within the dynamic framework of advection highlighted by this thesis.

Acknowledgements

Supervision. I would like to thank my supervisor A.S. Brierley for his help and support during my PhD and his willingness to allow me to travel and conduct my research with very few limitations. I would also like to thank my tutor Chris Todd for his advice at every review of my progress.

Financial support. The Pelagic Ecology Research Group (PERG) at the University of St Andrews and A.S. Brierley. The Norwegian Polar Institute (NPI – particularly Stig Falk-Petersen and Haakon Hop) and The University Centre on Svalbard (UNIS – particularly Jørgen Berge).

Logistical support. Officers and crew of the *RRS James Clark Ross*, *RV Lance* and *RV Jan Mayen* and all members of the Scottish Association for Marine Science (SAMS), NPI and UNIS who granted me permission to participate on their cruises. Personnel at UNIS (Longyearbyen) who allowed me to spend a number of months on Svalbard.

Research support. Martin James Cox for his willingness to fit me into a busy schedule and always assist with training and queries on acoustic and spatial analysis. Margaret Wallace for her assistance at the early stages of my research. Malin Daase for her advice and training on zooplankton analysis. The NPI (particularly Malin Daase, Stig Falk-Petersen, Haakon Hop, Anette Wold) for supplying zooplankton and acoustic data and assisting during manuscript publication. Igor Berchenko (Murmansk Marine Biological Institute) for supplying zooplankton data. Slawek Kwasniewski and members of the zooplankton taxonomic team at IOPAS for patient training in zooplankton taxonomic identification. Jørgen Berge (UNIS) for supplying sediment trap zooplankton data and allowing my participation on courses AB320 and AB321 at Svalbard. Finlo Cottier and Colin Griffiths (SAMS) for supplying hydrographic moored data and allowing me to visit SAMS for training. Anna Birgitta Ledang, Arild Sundfjord, Vladimir Pavlov (NPI) and Estelle Dumont (SAMS) for supplying CTD data and training me in its collection and processing. Zach West Brown (Stanford University) for supplying SST data.

Personal support. My family for supporting me with enthusiasm and financial support. My colleagues at PERG and my close friends at University (Yasmeen Chaudhry, Charlotte Owen and Catharina Andrew) for always being available.

Contents

1. General Introduction	1
1.1. General research aim	1
1.2. Climate change in the Arctic	2
1.3. The Svalbard archipelago as a zooplankton study area.....	8
1.3.1. Important Svalbard hydrology	14
1.3.2. Ecology and importance of key Svalbard zooplankton species	22
1.3.3. Vertical migration of zooplankton in the High Arctic.....	26
1.4. Summary of climate change impacts on zooplankton in the high Arctic with implications for carbon flux.....	31
1.5. Zooplankton patchiness with implications for moored observations	35
1.5.1. Currents at Kongsfjorden and Rijpfjorden.....	36
1.6. Data chapter summary	48
2. General Methods	50
2.1. Moored observations	50
2.2. Depth stratified vertical net hauls	55
2.3. Multi-frequency active acoustics	58
2.4. Multivariate analysis	64
3. Moored seasonal observations of zooplankton at Kongsfjorden and Rijpfjorden	71
3.1. Introduction.....	71
3.2. Materials and methods.....	74
3.2.1. Sampling location.....	74
3.2.2. Environmental parameters	76
3.2.3. Sediment trap zooplankton sampling	77
3.2.4. Multivariate analysis	78
3.3. Results	80
3.3.1. Sediment trap zooplankton	80
3.3.2. Kongsfjorden.....	82
3.3.3. Kongsfjorden hydrography	88
3.3.4. Rijpfjorden	93
3.3.5. Rijpfjorden hydrography.....	103
3.3.6. Correlations between hydrography and sediment trap zooplankton	111
3.4. Discussion.....	113

3.4.1.	Hydrodynamic control on zooplankton community composition.....	113
3.4.2.	Conclusion	121
4.	Small scale spatial variation in zooplankton around moorings at Kongsfjorden, Rijpfjorden and Billefjorden	122
4.1.	Introduction.....	122
4.2.	Materials and methods.....	125
4.2.1.	Sampling locations	125
4.2.2.	Environmental parameters	128
4.2.3.	Zooplankton sampling	129
4.2.4.	Acoustic observations.....	129
4.2.5.	Multivariate and Wilcoxon signed-rank analysis.....	130
4.3.	Results	132
4.3.1.	Environmental conditions	132
4.3.2.	Copepod populations and vertical distribution of <i>Calanus</i> and <i>Metridia longa</i>	141
4.3.3.	Multivariate analysis of net samples	152
4.3.4.	Acoustic observations.....	155
4.3.5.	Multivariate analysis of acoustic observations	160
4.4.	Discussion.....	161
4.4.1.	Variations in zooplankton between locations	161
4.4.2.	Variations in zooplankton within locations	170
4.4.3.	Conclusion	176
5.	Broad scale spatial variation in zooplankton around the Svalbard archipelago	178
5.1.	Introduction.....	178
5.2.	Materials and methods.....	180
5.2.1.	Sampling location.....	180
5.2.2.	Zooplankton sampling	184
5.2.3.	Acoustic observations.....	185
5.2.4.	Multivariate clustering.....	185
5.2.5.	Auto-correlation functions and characteristic scale	186
5.3.	Results	190
5.3.1.	Broad scale station clustering	190
5.3.2.	Characteristic scale.....	205
5.4.	Discussion.....	209
5.4.1.	Hydrodynamic control on zooplankton spatial distribution	209

5.4.2.	Autocorrelation distances and implications for moored observations	212
5.4.3.	Conclusion	216
6.	Seasonal and diel vertical migration of zooplankton at Svalbard	218
6.1.	Introduction.....	218
6.2.	Materials and methods.....	221
6.2.1.	Sampling location.....	221
6.2.2.	Environmental parameters	222
6.2.3.	Zooplankton sampling	223
6.2.4.	Acoustic observations.....	223
6.2.5.	Multivariate analysis	225
6.2.6.	ANOVA analysis.....	226
6.3.	Results	227
6.3.1.	Ice cover.....	227
6.3.2.	Environmental conditions	228
6.3.3.	Copepod populations and vertical distribution	231
6.3.4.	Vertical distribution of <i>Calanus</i> biomass	235
6.3.5.	Multivariate analysis of net samples	235
6.3.6.	Acoustic observations.....	238
6.3.7.	Multivariate analysis of acoustic observations	241
6.3.8.	ANOVA of acoustic observations	245
6.4.	Discussion.....	245
6.4.1.	Seasonal ‘snapshot’	245
6.4.2.	Copepod DVM behaviour.....	248
6.4.3.	Conclusion	253
7.	Summer diel vertical migration of zooplankton in ice-covered waters.....	254
7.1.	Introduction.....	254
7.2.	Materials and methods.....	255
7.2.1.	Sampling location.....	255
7.2.2.	Environmental parameters	257
7.2.3.	Zooplankton sampling	258
7.2.4.	Acoustic observations.....	259
7.2.5.	Multivariate analysis	261
7.2.6.	Kruskal-Wallis and ANOVA analysis of mean depth (Z_m).....	262
7.3.	Results	264
7.3.1.	Environmental conditions	264
7.3.2.	Copepod populations and vertical distribution	270

7.3.3.	Multivariate analysis of net samples	281
7.3.4.	Acoustic observations.....	282
7.3.5.	Multivariate analysis of acoustic observations	288
7.4.	Discussion.....	289
7.4.1.	Zooplankton DVM behaviour at ice-covered locations	289
7.4.3.	Conclusion	297
8.	General discussion	298
8.1.	Hydrodynamic control of zooplankton.....	298
8.2.	Spatial relevance of moored observations	303
8.3.	The prevalence of summer diel vertical migration	309

1. General Introduction

1.1. General research aim

The aim of this PhD research was to investigate zooplankton temporal and spatial variation in the high Arctic Svalbard archipelago, and compare locations of Atlantic influence to areas of Arctic dominance. The Scottish Association for Marine Science (SAMS) and Norwegian Polar Institute (NPI) have deployed and maintained a number of long term oceanographic moorings in the fjords of Svalbard (Billefjorden, Kongsfjorden and Rijpfjorden) since 2002. Although the moorings are primarily designed to measure the physical properties of the water column, they have also been collecting information on zooplankton using sediment traps and Acoustic Doppler Current Profilers (ADCP's). Many important findings on phenomena such as zooplankton advection and diel vertical migration (e.g. Willis et al. 2006; Berge et al. 2009; Wallace et al. 2010) have arisen from these long term monitoring platforms.

This thesis will use sediment trap collected zooplankton to investigate annual cycles in zooplankton community structure, and compare an Atlantic influenced fjord to a predominantly Arctic one (Ch 3). This comparative investigation will shed further light on the expected changes in zooplankton community composition within a warming Arctic. The expected changes are not straightforward, as outlined in Nature by Holtcamp (2010). In this article on zooplankton in the Bering Sea, it is highlighted that the traditional hypothesis of zooplankton in general becoming more abundant in warmer years is likely to be wrong. Although small zooplankton species thrived in warmer conditions, larger more lipid rich species did not. This can have important effects on predators which preferentially target the larger species.

However, although much important information can be gathered from the moorings, zooplankton spatial variation (patchiness) around these moorings has not been

1. General Introduction

thoroughly investigated to date over a range of scales. Thus, the implications of these moored observations cannot be accurately extrapolated either within the fjords themselves or over a broader Arctic system. This thesis will investigate zooplankton spatial distribution around each mooring and a wider Svalbard area (Ch 4 and 5), and highlight any differences in aggregation between areas of Atlantic and Arctic influence.

Finally, I shall investigate zooplankton diel vertical migration (DVM) around the archipelago to identify the prevalence of this behaviour at high latitude (Ch 6 and 7). The occurrence of DVM behaviour at high latitude is currently debated, and this thesis will bring new evidence to this debate. Zooplankton diel vertical migration is known to affect spatial aggregation, and so has both a temporal and spatial implication which is relevant to our spatial investigations.

In order to describe the motivation and provide background information for this research, this first chapter will review the importance of the Arctic marine system, its historic changes and future vulnerability to climate change, and its zooplankton.

1.2. Climate change in the Arctic

The Arctic system is characterised by extremes, including very cold winter temperatures, a highly seasonal cycle of solar radiation input, dominant snow cover and relatively low precipitation (Hinzman et al. 2005). One paradigm of polar marine ecology is that the seasonal change in sea ice cover significantly influences ecosystem processes (Cisewski et al. 2009), and many features of the Arctic system such as the intense seasonality in primary production (Søreide et al. 2003) arise from this extreme seasonality of the high north.

One of the primary conclusions arising from the IPCC's Second Assessment Report (Fitzharris 1996) was the extreme vulnerability of the Arctic to projected climate change (Manabe et al. 1991; Manabe and Stouffer 1995; Houghton et al. 1996, 2001; Watson et al. 1998). In addition to the vulnerability of the Arctic to climate change, the effects are

1. General Introduction

also expected to be more acute in this region (Manabe et al. 1992; Mitchell et al. 1995; Zwiers 2002; Holland and Bitz 2003; ACIA 2004; Kattsov and Kallen 2005).

Furthermore, high resolution climate records indicate that the Arctic system can shift relatively rapidly from one climate regime to another, indicated by both a rapid shift in diatom assemblages in frozen pond sediment cores (Douglas et al. 1994) and changes in indicators of ocean surface cooling in deep-sea sediment cores (Bond et al. 1999).

Within a regime of variability, the rate of temperature change observed within the last few decades is unprecedented (Overpeck et al. 1997; Overpeck 1996; Serreze et al. 2000).

Variations in sea-ice cover have been noted to be the major influence behind changes in the Arctic marine ecosystem, including sedimentation rate changes (Stein et al. 1994) and changes in primary production levels (Stein et al. 2001). Although sea-ice variations are generally consistent with air temperature anomalies (Chapman and Walsh 1993), the two are not always linked. The 20th Century has been shown to have been the warmest in the northern hemisphere for the past 400 years (Overpeck et al. 1997) (Fig 1.1b), and many of these changes either started or accelerated in the mid 1970's (Hinzman et al. 2005) (Fig 1.1a).

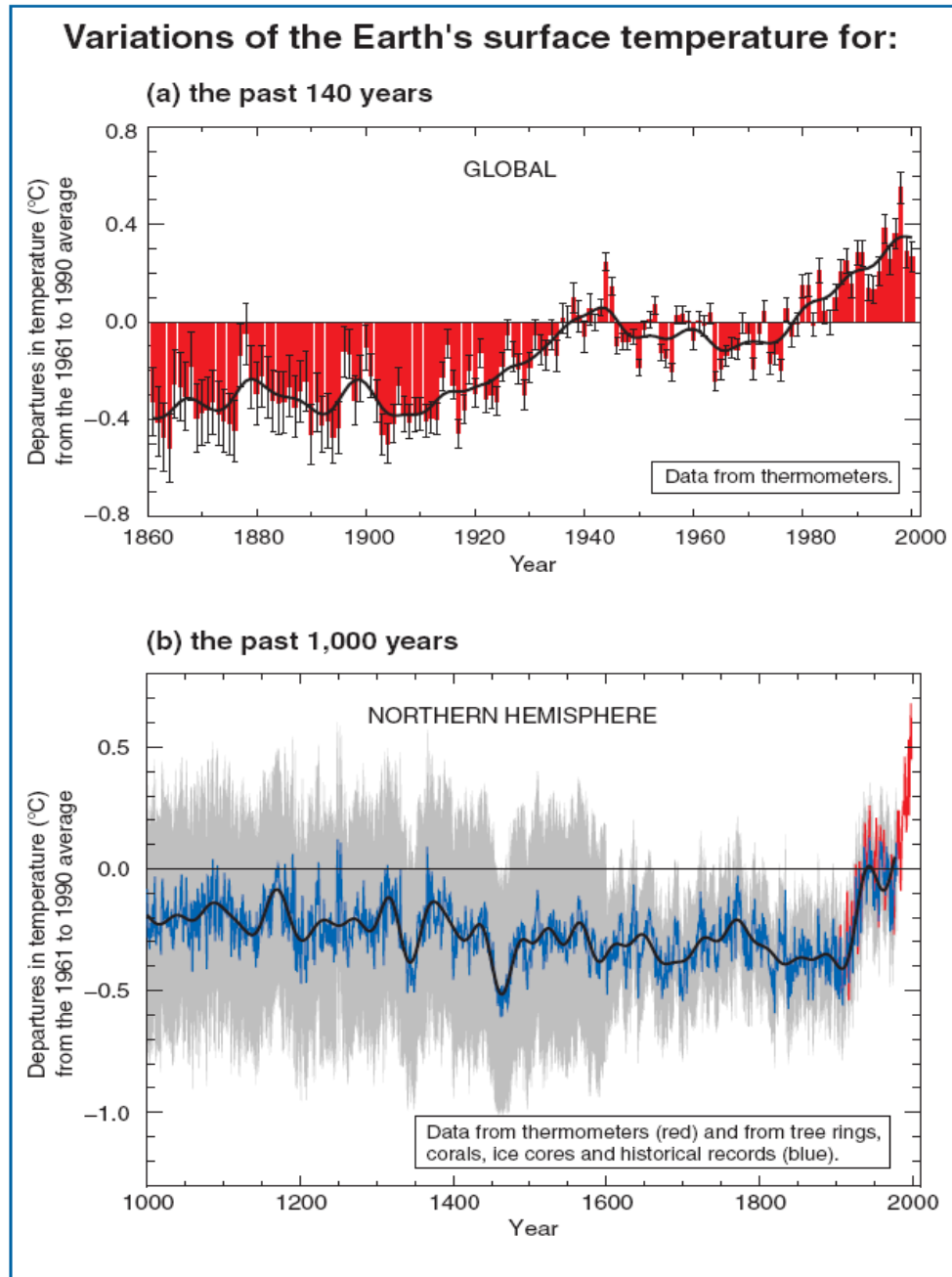


Fig 1.1) Variations of the Earth's surface temperature (a)Black curve describes approximate decadal temperature values (10 year averages) [error bars of 95% CI in annual data] (b)Black curve describes 50 year average temperature values [grey area representing 95% CI from 'proxy data'] (Adapted from Fig 1 in IPCC 2001 *Summary for Policymakers* – based upon (a) Chapter 2, Fig 2.7c & (b) Chapter 2, Fig 2.20 in IPCC, 2001: *Climate Change 2001: The Scientific Basis. Contribution of Working Group I to the Third Assessment Report of the Intergovernmental Panel on Climate Change*]

In terms of daily maximum temperature, the magnitude of warming in the Arctic has been approximately 5°C per century (from observations over the 20th century), although

1. General Introduction

there are regional differences in this trend (Koerner and Lundgaard 1996; Borzenkova 1999; Jones et al. 1999; Serreze et al. 2000; Hinzman et al. 2005). Within a regime of variation, the overall picture remains one of warming especially during the winter months (Chapman and Walsh 1993).

During the 1920's and 1930's, a warming event in the northern North Atlantic and the high Arctic occurred, and the changes were sufficient to produce significant changes in marine ecosystems (ICES 1949; Cushing 1982). More recently, air temperature in the Arctic has risen by 0.9°C between 1987 and 1997 (Alexandrov and Maistrova 1998). The summer melting period of sea-ice over a large portion of the Arctic has increased by 5.3 days (8%) per decade between 1979 and 1996 (Smith 1998). Greenland's ice sheet has been observed to be thinning dramatically, with a net loss of approximately 51 km³ of ice per year (Krabill et al. 1999, 2000). Arctic sea-ice extent, defined as daily, monthly and annual overall extent, has decreased by 3% per decade between 1978 and 1996, especially during the summer months (Cavalieri et al. 1997; Parkinson et al. 1999; Johannessen et al. 1999; Serreze et al. 2000) (Fig 1.2). This loss in sea-ice appears to be intensifying, as the most significant contractions in extent to date were first recorded in 1990, 1993 and 1995 (Maslanik et al. 1996), and more recently the six lowest seasonal minimum ice extents since satellite records began in 1976 have all been recorded between 2007 and 2012 (NSIDC 2012). On September 16 2012, sea ice extent in the Arctic dropped to 3.41 million square km, its record lowest extent (NSIDC 2012). Using general climate models, Flato and Boer (2001) have predicted that the Arctic Ocean will be clear of ice entirely during summer by the end of the 21st Century (Fig 1.2).

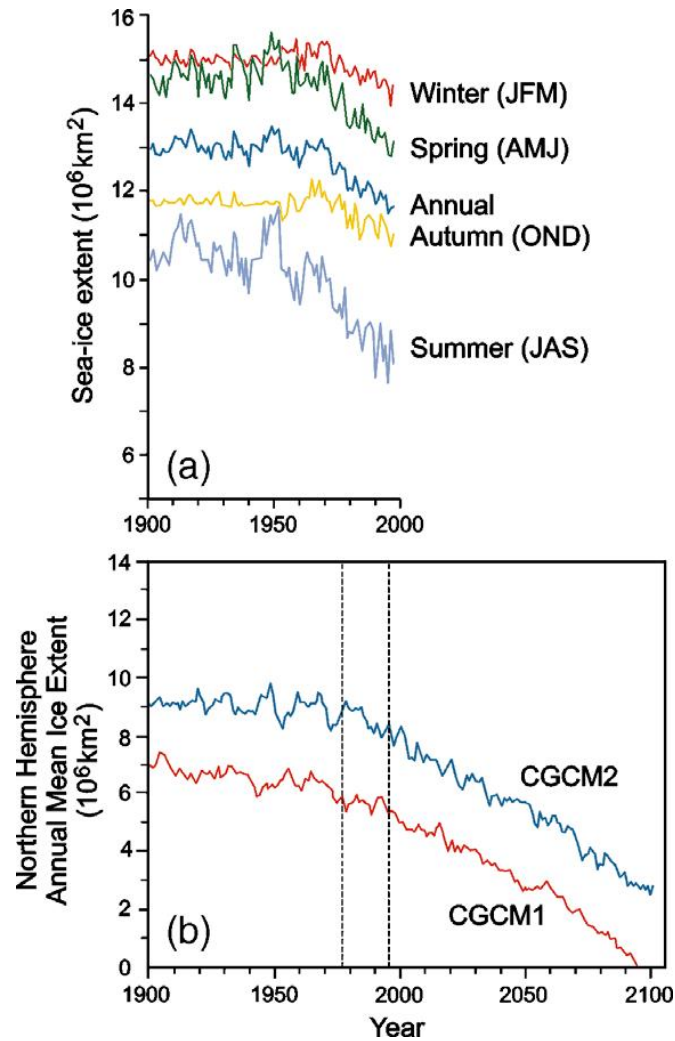


Fig 1.2) (a) Annual and seasonal sea-ice extent in the Northern Hemisphere between 1900 and 2000 (adapted from Vinnikov et al., 1999). (b) Model projections of annual mean sea-ice extent for the Northern Hemisphere (CGCM1 and CGCM2). CGCM2 differs from CGCM1 in its mixing parameterization (for details see Flato and Boer, 2001 – Fig from Flato and Boer, 2001)

It is not sea-ice extent alone that is changing in the Arctic, but also sea-ice thickness. Rothrock et al. (1999) have found that ice thickness at the end of the melt season has decreased by approximately 1.3 m over much of the deepwater Arctic Ocean (15% per decade). Furthermore, multiyear ice (i.e. ice that has survived more than one annual season) is also being lost from the Arctic Ocean at 7% per decade, an even greater rate than the figures for overall sea-ice loss (Johannessen and Miles 2000).

These trends and changes in sea-ice must be considered within the framework of the roughly 10 year climate cycle in the Arctic which is linked to the North Atlantic

1. General Introduction

Oscillation (NAO) (Mysak and Venegas 1998) (see Deser 2000; Serreze et al. 2000 for descriptions of the NAO). The NAO is highly correlated with the Arctic Oscillation (AO), which describes how the surface strength of the polar vortex changes over time (Hodges 2000). Circa 1988-89, the NAO/AO entered a strong positive phase, resulting in a below average sea-level pressure around the North Pole. This positive NAO/AO state promoted stronger counter-clockwise atmospheric circulation (Serreze et al. 2000), and the major oceanographic consequence of this positive NAO/AO index is an increase in the Northward flow of warmer AtW (temperature $> 3^{\circ}\text{C}$) into the Arctic Ocean (Dickson et al. 2000) (Fig 1.3). This greater influx of warmer AtW has played a major role in promoting the observed decreases in sea-ice extent and thickness in the Arctic (Kotlyakov 1997; Steele and Boyd 1998; Wang and Ikeda 2001). However, the observed decreases in Arctic sea-ice extent have been described as larger than would be expected from this natural climatic variation alone (Vinnikov et al. 1999).

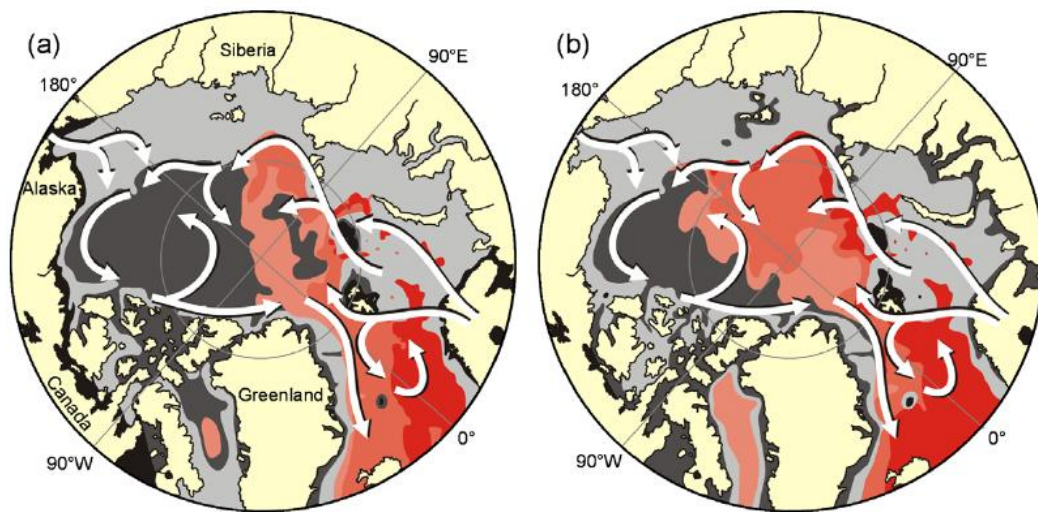


Fig 1.3) The increase in Atlantic water (red) inflow to the Arctic produced by the strong shift from AO-/NAO- (a) to AO+/NAO+ (b) circa 1989. White arrows indicate Atlantic layer boundary currents. [Based on Hodges (2000), Maslowski et al. (2000), McLaughlin et al. (1996), & Morison et al. (1998, 2000) – Adapted from Macdonald et al. 2005]

The present climate scenario throughout the Arctic Ocean has been described as an ‘internally perpetuating’ state of accelerated sea ice melting (Lindsay & Zhang 2005), where changes in upper ocean circulation have flushed thick multi-year ice out of the Arctic Basin creating large areas of open water and affecting ice-albedo feedback

mechanisms. The majority of evidence thus points towards a regime shift in the Arctic, from an 'icehouse' state to 'greenhouse' conditions. Regardless of the debated precise timing of such a shift, Lenton et al. (2008) stipulate that a summer ice-loss threshold (which when passed will create positive feedback towards summer ice-free conditions in the Arctic); if not already passed, may be very close and a regime shift may occur well within this century.

1.3. The Svalbard archipelago as a zooplankton study area

In terms of direct contact and exchange with other oceans, the Arctic oceanic system is constrained by its geography and its almost total encirclement by land masses. Arctic oceanic circulation is thus closely linked to bathymetry due to the topographic steering of currents (Rudels et al. 1994). Due to the prevailing topography, bathymetry and global distribution of oceanic salinity, water from the Pacific Ocean will tend to enter the Arctic rather than leave, but the shallow sill at the Bering Strait (50 m depth) will exclude deeper water exchange and allow only surface water to pass over and enter the Arctic Ocean (Weaver et al. 1999). This limited exchange at low rates (Overland and Roach 1987) tends to limit the influence of Pacific water influx on the Arctic in terms of warming. However, deep basin water from the Atlantic Ocean can enter the Arctic through the deep channel at the Fram Strait (2500 m depth) (Fig 1.4). Along with the Fram Strait, the Barents Sea (that contains the Svalbard archipelago) is also an important pathway for AtW to enter the Arctic Ocean (Ingvaldsen and Loeng 2009). For thorough reviews of the characteristics of the Barents Sea and the Fram Strait, please see Wassmann et al. (2006) and Hop et al. (2006). The West Spitsbergen Current (WSC) carries relatively warm ($\sim 3^{\circ}\text{C}$) and saline (~ 35 psu) AtW northward along the western side of the Svalbard archipelago (Weaver et al. 1999) (Fig 1.4).

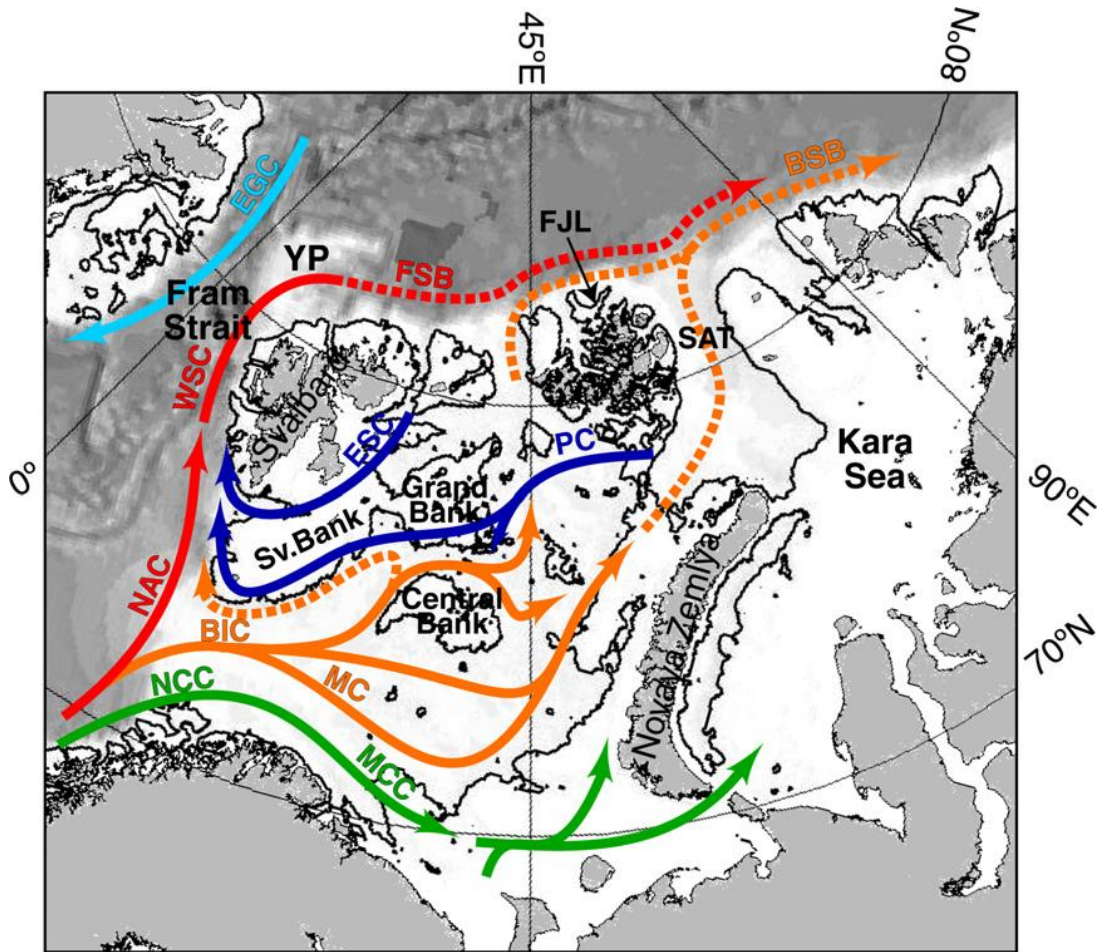


Fig 1.4) Bathymetry and surface currents of the Barents Sea from Norway (bottom) to Svalbard (centre). Black line indicates 200 m depth. Green arrows represent coastal water currents, red and orange represent water of Atlantic origin and blue represents water of Arctic origin. Broken lines represent subduction of currents under Arctic Water. [BIC = Bear Island Channel, BSB = Barents Sea Branch, SAT = St. Anna Trough, Sv Bank = Svalbard Bank, FJL = Franz Josef Land, YP = Yermak Plateau, NCC = Norwegian Coastal Current, NAC = Norwegian Atlantic Current, **WSC = West Spitsbergen Current**, EGC = East Greenland Current, MCC = Murman Coastal Current, MC = Murman Current, PC = Persey Current, **ESC = East Spitsbergen Current**]. (Wassmann et al. 2006)

The WSC is considered to be the major pathway for both heat and water volume transport into the Arctic Ocean (Aagaard and Greisman 1975), and it is the warm core confined to the upper continental slope of Svalbard that transports the majority of all heat into the Arctic Ocean (Schauer et al. 2004). As mentioned in the previous section, an increase in influx of AtW has been the major factor behind much of the observed warming in the Arctic Ocean, and this influx occurs through the WSC alongside the Svalbard archipelago. As Arctic conditions warm and the influx of AtW increases,

1. General Introduction

Arctic zooplankton communities (dominated by larger coldwater species), tend to retreat further northwards and are replaced by smaller zooplankton associated with warmer more southerly waters (Beaugrand et al. 2002) (Fig 1.5). Coastal areas around the southern and western Svalbard archipelago are particularly sensitive to the influence of both contrasting Arctic and Atlantic water masses (Slubowska-Woldengen et al. 2007), and are strongly influenced by two contrasting ocean currents. The Sørkapp Current (or South Cape Current, a branch of the ESC on Fig 1.4) carries cold Arctic waters (ArW) southward and with it a zooplankton community characterised by larger calanoid crustaceans (such as the copepod *Calanus glacialis*). The West and South Spitsbergen Currents carry warm AtW northwards and with it smaller copepods (such as *Calanus finmarchicus*) (Stempniewicz et al. 2007) (Fig 1.5).

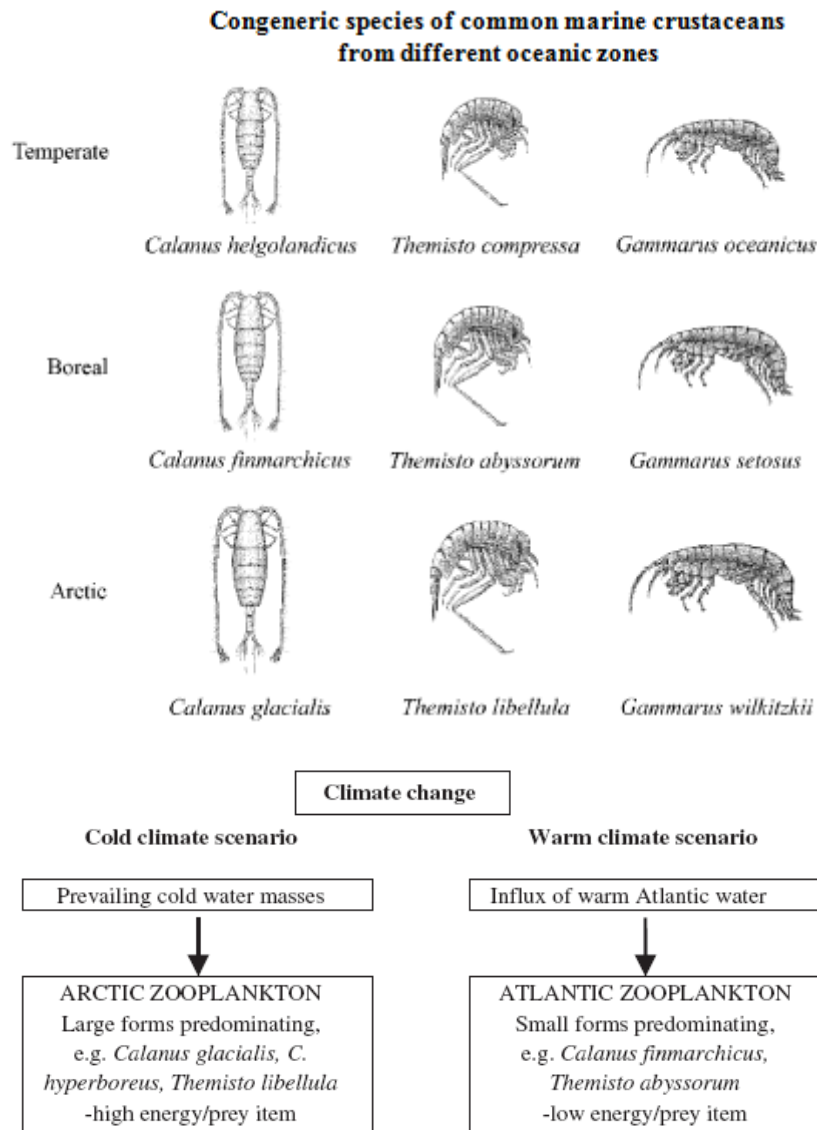


Fig 1.5) [Above] Closely related species of zooplankton (columns) classed by oceanic zones (rows) – (Boreal Zone represents influx of Atlantic Water into the Arctic). Relative sizes of adults approximated by image sizes. [Below] Climate change scenario effects on zooplankton around Southwest Svalbard [adapted from Stempniewicz et al. 2007 – diagrams of zooplankton based upon Weslawski unpublished materials]

As the proportions of these species (i.e. closely related forms of characteristic different sizes) can be assessed as an indicator of the different water masses present and thus as a proxy for climate change, the Svalbard archipelago becomes the perfect study area to assess the effects of climate change in the Arctic. Changes in the relative proportions of these zooplankton species also have important knock on effects throughout the food chain. The importance and ecology of these zooplankton species and the motivation for

1. General Introduction

studying them in particular will be discussed more thoroughly in section 1.3.2. Although total zooplankton biomass is similar in the two contrasting water masses, the scarcity of large (> 3 mm) crustaceans in AtW decreases the feeding efficiency of planktivorous seabirds (Weslawski et al. 1999). For example, with an increasing influx of AtW, the energy budget of little auks markedly deteriorates (Stempniewicz 2001), and the southernmost little auk populations of south Greenland and Iceland have already collapsed. Similar negative effects may occur to marine mammals through the loss of their favoured prey (Polar Cod and amphipods – see Fig 1.6 for simplified Arctic Ocean food web) that are associated with biologically productive ice edges which will be lost to increased ice-melt (Tynan and DeMaster 1997; Anisimov and Fitzharris 2001).

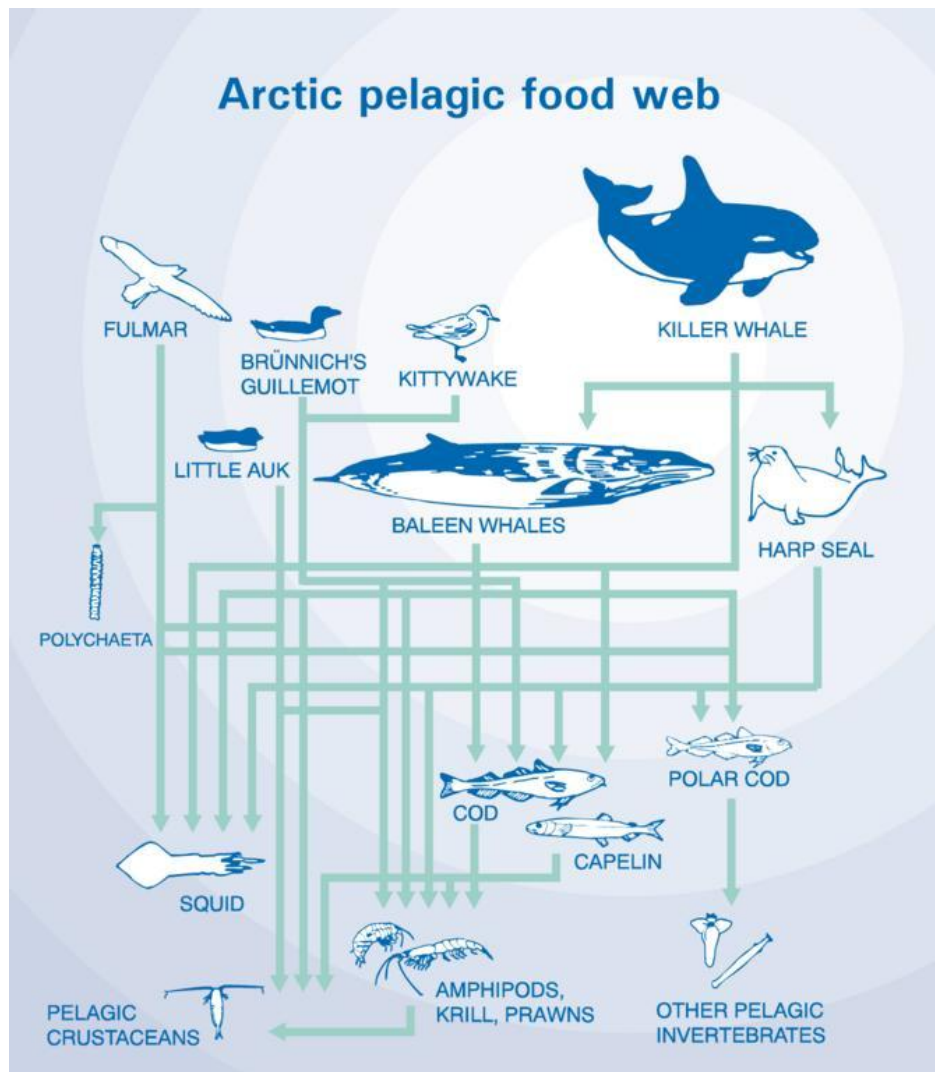


Fig 1.6) Simplified Arctic pelagic food web [UNEP/GRID-Arendal, accessed online]

1. General Introduction

Changes in sea-ice cover and associated zooplankton may also influence a restructuring of the Arctic food web that changes the number of trophic levels or the flow of carbon between pelagic and benthic food webs (Macdonald et al. 2005). Research on Arctic shelves suggests that pelagic and benthic systems are more tightly coupled than in warmer seas (Petersen and Curtis 1980; Ambrose and Renaud 1995; Piepenburg 2005). However, with an increasing influx of AtW and its associated zooplankton, primary production in the water column may undergo changes in grazing, altering this coupling. In fact, there are many publications that outline how Arctic marine ecosystems may be altered by changes in dominant water masses and changes in associated populations (e.g. Sakshaug et al. 1991; Hunt et al. 1999; Saar 2000; Dippner and Ottersen 2001; Feder et al. 2003). Clearly then the study of zooplankton as a key component of the food chain is especially important within the current era of warming, and the Svalbard archipelago is well placed geographically to monitor the confluence zones of the dominant water masses. Due to the influences of these different water masses, the Svalbard archipelago contains many contrasting marine locations (fjords, shelf areas and deeper trenches) that when observed can help us assess the differences between the current high Arctic conditions and a warmer Arctic in the future. More detailed hydrology of key locations investigated in this thesis is discussed in the next section.

1. General Introduction

1.3.1. Important Svalbard hydrology

Firstly, please refer to Fig 1.7 for place names around the Svalbard archipelago.

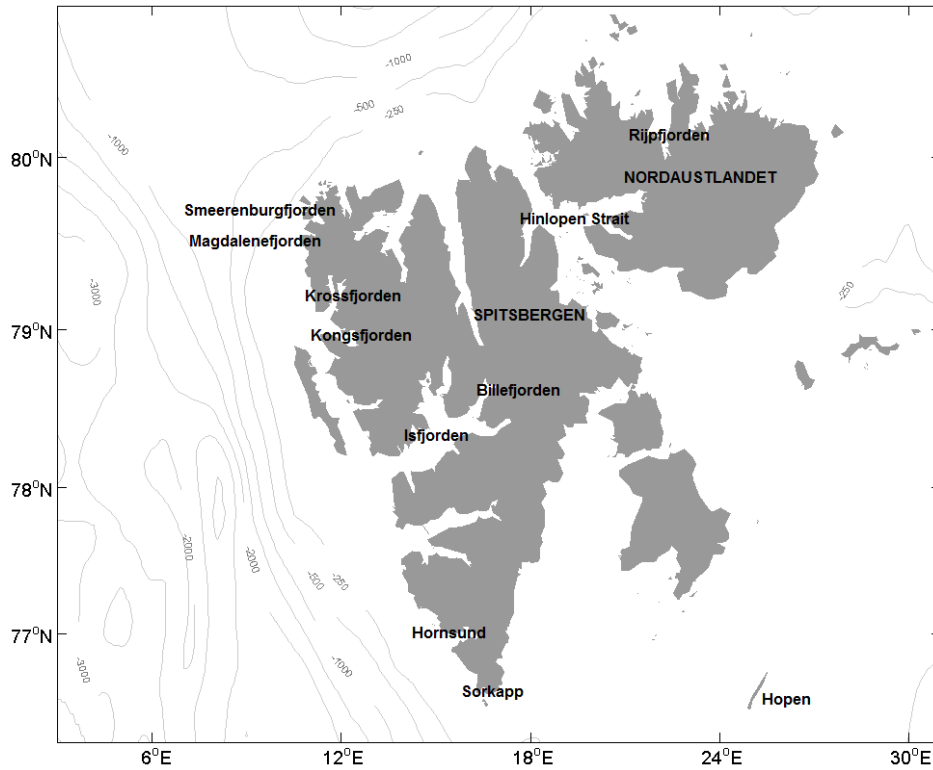


Fig 1.7) Map of the Svalbard archipelago with locations referred to in this thesis labelled.

The waters surrounding the Svalbard archipelago are mainly influenced by Atlantic, Arctic, locally produced and glacial water masses. Although definitions for these water masses vary slightly through the literature, I have chosen to use the following definitions from Svendsen et al. (2002 (Table 1.1)).

Table 1.1) Water mass definitions for the Barents Sea (Svendsen et al. 2002)

Water Mass	Temperature (°C)	Salinity
Atlantic Water (AtW)	> 3	> 34.9
Transformed Atlantic Water (TAtW)	> 1	> 34.7
Arctic Water (ArW)	< 1	34.3 – 34.8
Local Water (LW)	< 1	> 34.4
Winter Cooled Water (WCW)	< - 0.5	> 34.4
Surface Water (SW)	> 1	< 34
Intermediate Water (IW)	> 1	34 – 34.7

Atlantic Water (AtW) is defined by a salinity > 34.9 and temperature > 3°C. However, the temperature of this AtW varies seasonally from 3.5 – 7.5°C, and both temperature and salinity decrease in north and eastward directions from its inflow source (Ingvaldsen and Loeng 2009). AtW originates from the warm Gulf Stream, and is generally found between 200-800 m depth as the Atlantic layer (Schlosser et al. 1995). Transformed AtW (TAtW) resembles AtW apart from its lower salinity (> 34.7) and wider temperature range, and is formed when locally produced and glacial water masses mix with AtW (Loeng 1991; Harris et al. 1998). Arctic Water (ArW) is characterised by low salinity (34.3 – 34.8) and temperatures below 1°C. Low temperature (< 1°C) Local Water (LW) is produced in fjords during autumn/winter by convectional cooling (Svendsen et al. 2002), while Winter Cooled Water (WCW) (temperature < -0.5°C, salinity > 34.4) is formed as a result of sea ice formation and the sinking of dense cold brine. Although its temperature is highly variable due to solar warming, Surface Water (SW) is created by melting processes especially during summer, and is characterised by low salinity (down to < 28). This layer can have a thickness of 5-20 m (Ingvaldsen and Loeng 2009). The SW layer is sometimes referred to as Melt Water (MW) (Ingvaldsen and Loeng 2009). Between deeper AtW masses and SW, a transitional layer of Intermediate Water (IW) often forms with salinity lower than in TAtW but higher than SW (34 < salinity < 34.7), and this layer can be tens of metres thick (Svendsen et al. 2002).

However, alongside these general definitions of water masses, water sources mix and are modified through contact with the atmosphere and local processes such as wind, waves and tidal currents (Pfirman et al. 1994; Svendsen et al. 2002). There are a number of key fjords in the Svalbard archipelago that together describe much of the variation found throughout the archipelago and the contrast between AtW and ArW dominance. These fjords are labelled in Fig 1.8. Kongsfjorden, Rijpfjorden and Billefjorden have all contained long term oceanic moorings deployed by SAMS/NPI and used in this thesis.

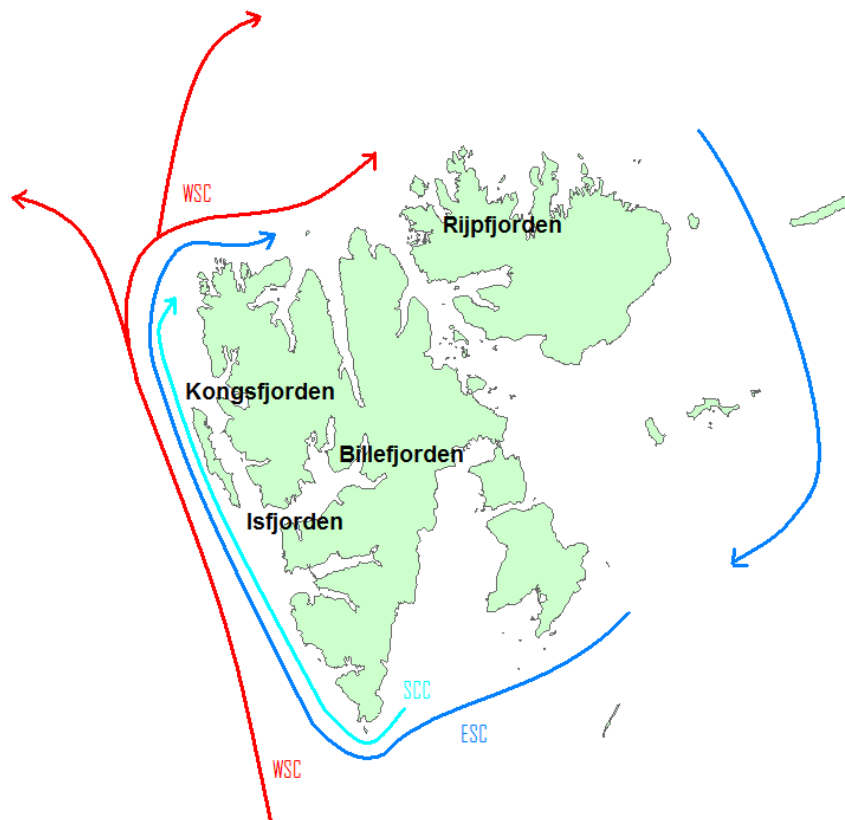


Fig 1.8) Map of the Svalbard archipelago describing the dominant currents [WSC carrying AtW (red), ESC carrying ArW (dark blue), SCC carrying Coastal Water (light blue)] and the key fjords investigated in this thesis [Isfjorden, Billefjorden, Kongsfjorden and Rijpfjorden] (adapted from Wiktor 2008 pers. comm.)

Kongsfjorden

Kongsfjorden is an open glacial fjord with no sill located on the northwest coast of Spitsbergen in the Svalbard archipelago (Fig 1.8). This fjord is an extension of

1. General Introduction

Kongsfjordrenna, a trench that cuts across the Spitsbergen shelf (Kwasniewski 2003). As Kongsfjorden is relatively wide and lacks a sill, it is heavily influenced by processes on the adjacent shelf (Hop et al. 2006), where the water mass is a mix of onshore transported AtW (assisted by Kongsfjordrenna), ArW on the shelf and locally produced (glacier melt, precipitation etc) fresher water (Saloranta and Svendsen 2001; Hop et al. 2006). This shelf water mass is often referred to as Transformed Atlantic Water (TAtW). The fjord consists of two basins separated by a 30 m deep ridge, and the depth of the fjord gradually decreases towards the inner end (from > 300 m in the outer basin to 60 – 90 m in the inner basin) (Kwasniewski 2003). Kongsfjorden is heavily influenced by three large glaciers – Kongsbreen, Kongsvergen and Blomstrandbreen. The fjord also displays strong seasonal changes between a state of ArW dominance (cold and fresh) in winter and through much of the year (Wallace et al. 2010) and one of AtW dominance (warm and saline) in summer (Hop et al. 2006). During the ArW dominance of autumn and winter, glacial melt water mixes with the AtW below it and produces Intermediate Water (Svendsen et al. 2002). Surface cooling and sea-ice formation then creates water with temperatures < 0°C that can persist in the deep basins in the fjord throughout the rest of the annual season (Svendsen et al. 2002; Cottier et al. 2005). During this winter period, the vertical stratification of the fjord is relatively weak.

Kongsfjorden can then undergo a rapid shift to an AtW dominated system. As the fjord gradually warms through mixing with warmer and fresher melt water, the front which separates fjord and shelf water weakens (Cottier et al. 2005). This allows the TAtW to enter the fjord, although it mostly remains in the outer fjord basin (Svendsen et al. 2002). This regime change in Kongsfjorden during summer occurs mostly in the intermediate and deep water layers that are separated by strong stratification from the upper layer (Weslawski et al. 1991; Svendsen et al. 2002; Cottier et al. 2005). With this variation in water mass dominance, the sea-ice extent in Kongsfjorden is highly variable, but the inner fjord is generally ice covered from December to June (Svendsen et al. 2002). Stable ice cover does not develop in the middle and outer fjord at any point in most years (Weslawski et al. 1994; Ito and Kudoh 1997). In fact, a larger than average inflow of AtW into the fjord during the winter of 2005/06 (Cottier et al. 2007)

led to the fjord remaining free of sea-ice from 2006 to 2008 (Wallace et al. 2010). These unique conditions mean that Kongsfjorden displays many sub-Arctic characteristics despite its high latitude (79°N). In years of weaker AtW influence, the zooplankton community consists more of Arctic species, and the community shifts towards boreal species in years of stronger AtW influence (Kwasniewski et al. 2003). Thus Kongsfjorden is an ideal location in which to both monitor climate change in the Arctic, and also investigate the effects of a warming Arctic on zooplankton.

Rijpfjorden

Rijpfjorden is located on the north coast of Nordaustlandet in the Svalbard archipelago (Fig 1.8). The fjord is approximately 30 km long and opens to a width of 10 km (Howe et al. 2010). The bathymetry of Rijpfjorden is comparatively poorly mapped, but the maximum depth is known to be approximately 240 m and the fjord is separated from the Arctic Basin to the north by a plateau at 100 m depth (Falk-Petersen et al. 2008). The fjord also contains at least two basins separated by sills (Howe et al. 2010). Although Rijpfjorden has a broad mouth to the east and narrow channels between islands to the north (Wallace et al. 2010), there is less AtW influence on the fjord as the mouth is further from the shelf break than at Kongsfjorden and there is no deep connecting trench (Howe et al. 2010). Rijpfjorden lies at 80°N and is covered by fast ice for 6 – 8 months of the year and dominated by typically Arctic conditions (Berge et al. 2009; Wallace et al. 2010). These typically Arctic conditions include water temperatures close to freezing for much of the year, stratification of the water column and high productivity (Howe et al. 2010). With these conditions, Rijpfjorden tends to be dominated by a characteristically Arctic zooplankton community. Howe et al. (2010) describe how Rijpfjorden ‘has no documented major influence of AtW’ (although AtW does circulate along the northern shelf slope of Svalbard, Ivanov et al. 2008), and support this using sediment trap collected cyst assemblages that are dominated by an Arctic species. AtW may influence this fjord however, as in August 2004 when a high proportion of the Atlantic copepod species *Calanus finmarchicus* was observed in the fjord (Falk-Petersen et al. 2008). With its Arctic dominance, Rijpfjorden becomes an ideal comparison with Kongsfjorden in terms of an Arctic vs. Atlantic perspective with

implications for a warming Arctic (i.e. from an Arctic dominated system i.e. Rijpfjorden to a more Atlantic influenced one i.e. Kongsfjorden). However, with the more recent challenge to the accepted paradigm of an Arctic Rijpfjorden, the monitoring of zooplankton in the fjord has become even more important as a signal for the northward expansion of AtW and its associated zooplankton assemblage.

Billefjorden

Billefjorden is the north-eastern extension of Isfjorden and the largest fjord of the Svalbard archipelago (Fig 1.8) (Szczucinski and Kajaczkowski 2012). It lies at 78°N on the western coast of the Svalbard archipelago. The fjord consists of an outer basin (maximum depth ~230 m) which is separated from Isfjorden by a sill depth of 80 m, and a shallower inner basin (maximum depth ~ 190 m)(Arnkvaern et al. 2005). Due to the sill at the entrance to the fjord, Billefjorden is separated from the typically AtW characterised Isfjorden system and less influenced by advection into the fjord (Arnkvaern et al. 2005; Nilsen et al. 2008). Due to the lack of influence from warmer AtW, fast ice covers the inner fjord annually during winter/spring (January - June) (Arnkvaern et al. 2005). The sill then allows Billefjorden to retain locally produced brine water from ice formation (which sinks to form Winter Cooled Water) from the previous winter season (Nilsen et al. 2008). This sill creates a contrasting fjord system in Billefjorden to that in Kongsfjorden which is open to the influx of AtW from the shelf, and Billefjorden can be considered useful for studies of typically Arctic zooplankton communities. Although the influence of advection is minimal at Billefjorden, winter ice-formation may flush the fjord to a certain extent and this can have a minor but measurable effect on the zooplankton community (Breur 2003). Although Billefjorden is at lower latitude than Kongsfjorden and Rijpfjorden, it may in fact be the most consistent indicator of Arctic conditions, with the least advection of zooplankton into or out of the fjord.

Prevailing sea-ice conditions during this research

Images of Arctic sea-ice concentrations (observed by AMSR-E and projected using arctic grids from NSIDC at 6.25 km resolution by the University of Bremen) were obtained as daily averages on July, August and September 15 in order to provide comparable broad-scale sea-ice conditions between the years of sampling during this research. These images are displayed in Fig 1.9. Significant variation between years dependant on the magnitude of AtW inflow to the archipelago is noticeable in these images, and highlights the dynamic nature of this system.

1. General Introduction

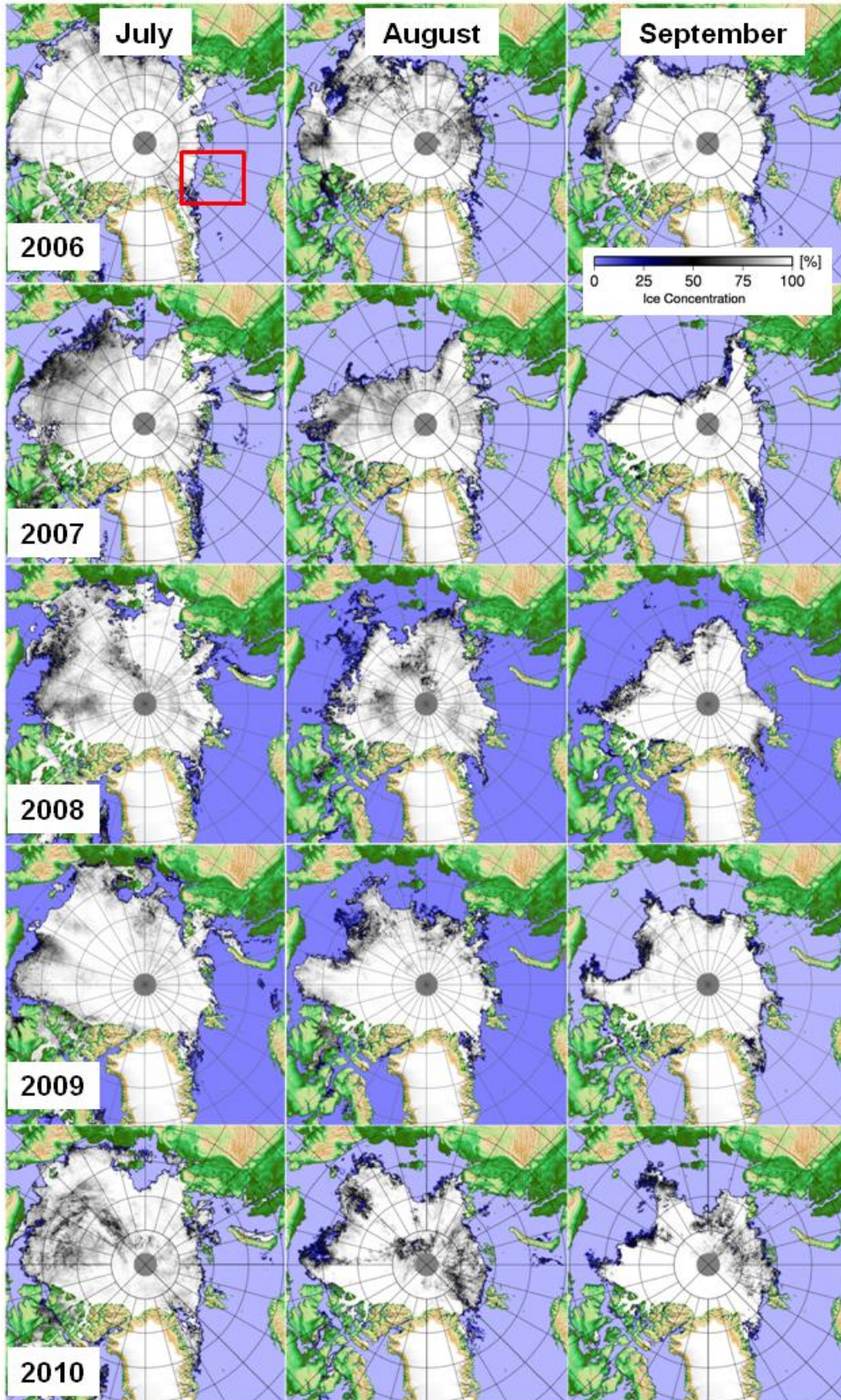


Fig 1.9) Images of Arctic sea-ice concentrations (AMSR-E projected using arctic grids from NSIDC at 6.25 km resolution). Each month (column) is based on a daily average on the 15th. Years are in rows. The region of Svalbard is highlighted by the red box. White and black ocean indicate significant sea-ice cover, while both shades of purple indicate open water

1.3.2. Ecology and importance of key Svalbard zooplankton species

As described in previous sections, the Svalbard region is a transition zone between warm and saline AtW and colder fresher ArW (Daase and Eiane 2007). The WSC carries AtW north along the western coast of Svalbard, giving the archipelago many sub-Arctic characteristics despite its high latitude (Hop et al. 2002; Willis et al. 2006). The different water masses are a major controlling factor on the distribution of zooplankton and the trophic structure of the marine ecosystem (Wassmann et al. 2006). At the high latitude of Svalbard, a pronounced phytoplankton spring bloom in close association with a receding ice edge produces large amounts of primary production which can be grazed by zooplankton (Søreide et al. 2008), leading to relatively high zooplankton abundances. Various sources of advection and transport of ice fauna into the region via melting sea ice also bring zooplankton into the Svalbard archipelago (Wassmann 2001; Edvardsen et al. 2003). The intense seasonality of primary production means that food for grazing zooplankton is limited in winter (Søreide et al. 2003). Many species thus enter a non-feeding mode and overwinter at depth (diapause – Tande and Hendersen 1988; Hagen and Auel 2001). This pattern of feeding in the productive upper layers during spring and summer followed by over-wintering in deeper and colder waters is known as seasonal vertical migration (SVM) (Falk-Petersen et al. 2007).

Zooplankton in the waters of the Svalbard archipelago can either be of Atlantic, Arctic or shelf origin. Zooplankton species of Atlantic origin carried northwards into the Svalbard archipelago via the WSC include *Calanus finmarchicus*, *Thysanoessa inermis*, *Thysanoessa longicaudata* and *Themisto abyssorum*. This influx of Atlantic species is significant (Slagstad and McClimans 2005; Wassmann et al. 2006). In fact, Pedersen (1995) calculated a total biomass of *C. finmarchicus* advected into the Barents Sea during spring/summer which was similar to the endemic production. Species of Arctic origin include *Calanus glacialis*, *Themisto libellula*, *Pseudocalanus minutus*, *Oithona similis*, *Mertensia ovum*, *Clione limacina* and *Limacina helicina* (Falk-Petersen et al. 1999; Søreide et al. 2003). Advection can also bring deep-dwelling zooplankton species onto the shallow shelf regions of the Svalbard archipelago. For example, a branch of the EGC which hits the Svalbard slope likely carries with it *Calanus hyperboreus* from

1. General Introduction

deeper Arctic waters (Wassmann et al. 2006). A further source of zooplankton in the Svalbard region are the ice-associated allochthonous macrozooplankton dominated by four ice amphipod species – *Apherusa glacialis*, *Gammarus wilkitzkii*, *Onisimus glacialis* and *Onisimus nansenii* (Lønne and Gulliksen 1991; Polterman 1997; Hop et al. 2000). The zooplankton community of Svalbard experiences large seasonal and interannual variations which can be related to changes in advective flux, primary production and local environmental conditions (Skjoldal et al. 1987; Tande 1991; Pedersen et al. 1995; Arashkevich et al. 2002; Wassmann et al. 2006).

Within this zooplankton community, herbivorous copepods comprise up to 70-90% of the mesozooplankton biomass (Wassmann et al. 2006). Of these, the most abundant species belong to the genus *Calanus*, and these copepods are the dominant herbivores throughout sub-Arctic and Arctic seas (Kwasniewski et al. 2003). These copepods are rich in lipids and represent an important food source for other zooplankton, pelagic fish such as polar cod and capelin (Lønne and Gulliksen 1989; Jensen et al. 1991; Hopkins and Nilssen 1991) and also some seabirds such as the Little Auk (Weslawski et al. 1999; Karnovsky et al. 2003) (Fig 1.10).

1. General Introduction

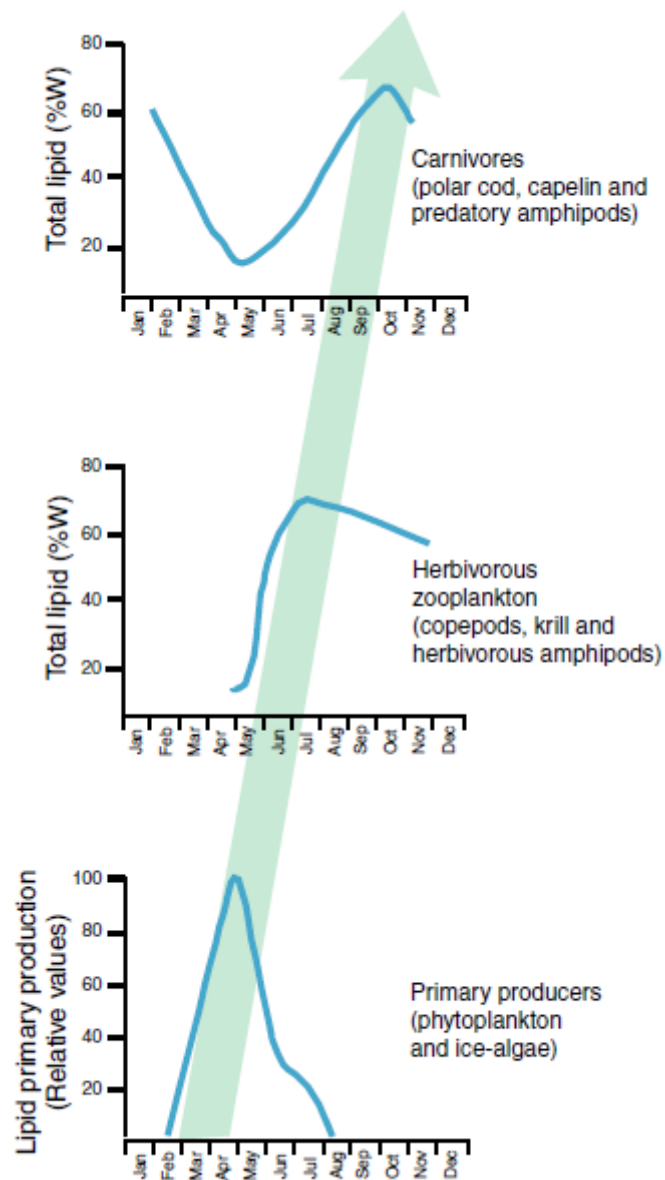


Fig 1.10) Energy flow (represented as lipid flow – changes in total lipid content (% dry weight) over the year) through Arctic food chains, from primary production via herbivorous zooplankton to carnivores. (Adapted from Falk-Petersen et al. 1990 by Wassmann et al. 2006)

The distribution of zooplankton from polar regions can be a very good indicator for ocean climate variability (Greene and Pershing 2000; Hays et al. 2005) due to this close association with water masses. Of the various zooplankton candidates to use as measures of this variability, *Calanus* as a genus is a robust indicator of the predominant water masses due to its reproductive cycle being strongly influenced by temperature and food availability (Conover and Huntley 1991; Falk-Petersen et al. 1999). *Calanus*

1. General Introduction

finmarchicus (Gunnerus 1770) is a boreal species with a centre of distribution in the Norwegian Sea south of Svalbard (Østvedt 1955; Wiborg 1955). However, the northward flowing North Atlantic Current (NAC – which is named the WSC as it flows northwards along the west coast of Svalbard) carries *C. finmarchicus* with it into the Arctic Ocean (Jaschnov 1970; Conover and Huntley 1991; Hirche and Mumm 1992). *Calanus glacialis* (Jaschnov 1955) is the only true Arctic species and is limited to shelf seas of the Arctic Ocean (Kwasniewski et al. 2003). This species dominates among *Calanus* north of the polar front (Unstad and Tande 1991), but is not found very far south of the front (Conover 1988). *Calanus hyperboreus* (Krøyer 1838) is an Arctic species associated with deep-water seas (Richter 1994; Hirche 1997). In the Barents Sea, this species coexists with *C. glacialis* but is less abundant (Conover and Huntley 1991; Thibault et al. 1999). The presence of all three *Calanus* species has been documented in the Svalbard archipelago (Kwasniewski et al. 2003), and their expected distributions can be summarised as follows: *C. finmarchicus* dominates in AtW, *C. glacialis* is associated with Arctic shelf waters and *C. hyperboreus* is a high-Arctic oceanic species (Daase and Eiane 2007; Daase et al. 2007; Blachowiak-Samolyk et al. 2008). For a detailed description of the life cycles of the *Calanus* copepods and further references, see Wassmann et al. (2006).

The onset of the phytoplankton bloom varies in the Svalbard region primarily due to differences in prevailing sea-ice conditions throughout the region (Søreide et al. 2008). Along the west coast where little sea-ice occurs due to the heavy influence of AtW, the bloom starts in April/May (Leu et al. 2006). However, in the northern and eastern archipelago, the bloom starts only when the sea-ice breaks up and this may not occur before June/July or as late as August (Hegseth 1998; Falk-Petersen et al. 2000b; Hegseth and Sundfjord 2008). Under such conditions of sea-ice cover however, ice algae may be an equally important food source for copepods (Søreide et al. 2006). The peak in ice algal biomass may precede the pelagic bloom by up to 2 months (Michel et al. 1996), and this production comprises approximately 20% of the total primary production in the seasonally ice covered regions of the Barents Sea (Hegseth 1998) and > 50% in the high Arctic Ocean itself (Legendre et al 1992; Gosselin et al. 1997). These variations in the timing of primary production affect the life cycle and behaviour of

grazing zooplankton, and a warming Arctic will have important implications for zooplankton. One such behaviour influenced by this variation in sea-ice cover and primary production is vertical migration which will be investigated in this thesis and is discussed briefly in the following section.

1.3.3. Vertical migration of zooplankton in the High Arctic

The pelagic realm provides a highly diverse habitat for the organisms that dwell within it, and this habitat is characteristically along a gradient in which light, temperature, food availability and predation risk all change with depth (Williamson et al. 1996). Diel vertical migration (DVM) of zooplankton is ubiquitous across most aquatic environments (Ringelberg 1995). In the most commonly observed behavioural migration pattern (synchronised DVM), animals feed in comparatively food-rich surface waters during the night but remain in deeper waters during the day (Forward 1988). This ‘classic’ pattern of vertical migration involves a dusk ascent of zooplankton and a dawn descent (Fig 1.11).

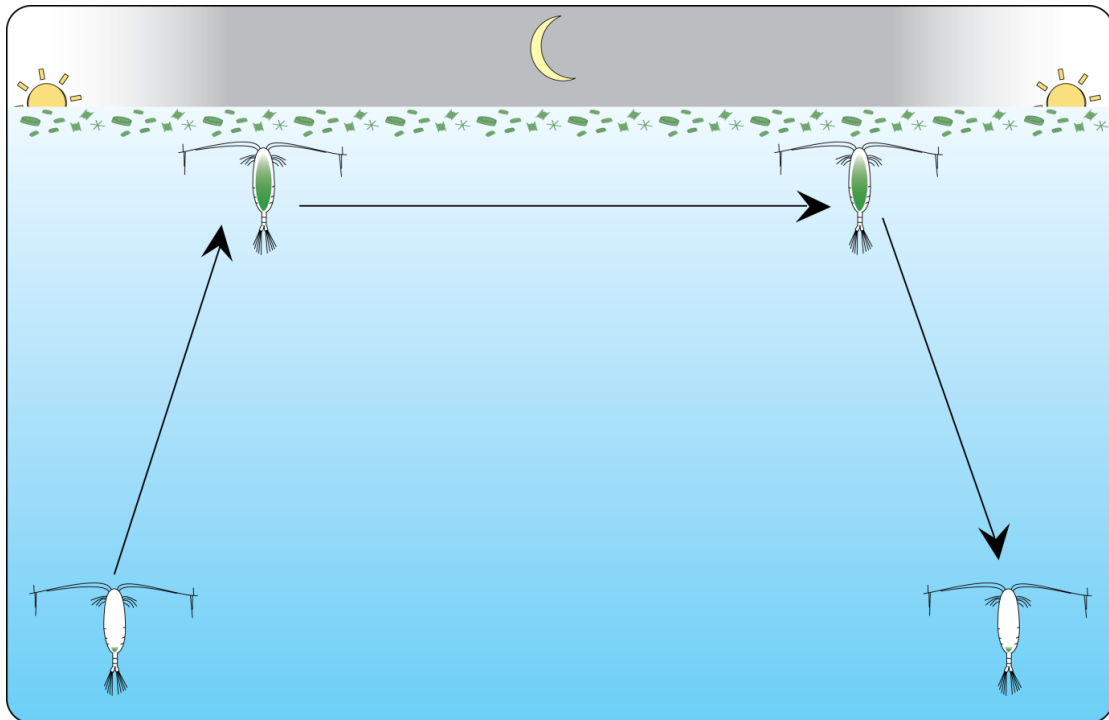


Fig 1.11) Illustration of classic diel vertical migration (DVM) under a diel light cycle. Copepods ascend into the productive surface waters at dusk to feed (food material in the gut represented in green within the copepod), and then descend at dawn to avoid visual predation. [Fig from Pierson 2008 online materials]

The accepted primary cost of daily vertical movements is a reduced feeding rate i.e. individuals at depth during the day being separated from their near-surface phytoplankton and microzooplankton food supply (Hays 2001). As a trade-off for this cost, the accepted ultimate function of classic DVM is to minimise the predation risk from visual predators – the predator evasion hypothesis (Zaret and Suffern 1976). Classic DVM has been shown to be more prominent in larger/more highly pigmented zooplankton species (i.e. making them more susceptible to visual predation) (Hays 1995), and also in conditions where planktivorous fish are more abundant (i.e. greater visual predation risk) (Bollens and Frost 1989).

Predator avoidance does not necessarily mean surface avoidance however, as described by reverse DVM. Reverse DVM is essentially the inverse of classic DVM, with zooplankton populations found near the better lit surface waters during the day and a descent to the deeper waters at night. This behaviour can be prompted by normally migrating predators (Neill 1990), and as many pelagic communities contain many

1. General Introduction

varied predators with different behaviours (e.g. carnivorous invertebrates alongside planktivorous fish), the migration responses by zooplankton prey may become highly complicated.

In general, one other broad category (apart from predator avoidance) of ultimate causative factors for DVM can be described (Lampert 1989). Residing in colder waters during the day and then ascending to feed in warmer waters at night when they are comparatively cooler may provide a metabolic (energetic) advantage for migrants (McLaren 1963). However, laboratory experiments (Orcutt and Porter 1983) and field studies (Stich and Lampert 1981) have both failed to demonstrate any metabolic advantage for migrating zooplankton.

DVM usually refers to the synchronised movements of zooplankton as a whole throughout the water column. However, zooplankton populations in the marine ecosystem are often highly diverse, and only a portion of individuals may migrate on a schedule. Parts of the population may instead remain at depth throughout the diel cycle (Dagg et al. 1998). This mode of migration in which certain members of the zooplankton population migrate when others do not is known as unsynchronised migration (as compared to the synchronised mass movements of classic DVM). Thus, within the predator avoidance hypothesis, DVM should be more pronounced for individuals/species that are most susceptible to visual predators (Hays 2003). Extensive evidence for this effect has been collected, describing how larger and more heavily pigmented species display DVM with larger amplitudes (Wiebe et al. 1992) and how smaller zooplankton arrive at the surface earlier and leave later (De Robertis et al. 2000) thereby increasing their surface residency period. Within this context, DVM should also vary between individuals of the same species depending on their nutritional state (Hays 2003). Lipid rich individuals are known to exhibit less pronounced DVM behaviour (Sekino and Yamamura 1999), as they have less need to expose themselves to the risk of predation in order to forage and gain energy. Furthermore, individuals with greater lipid stores have been shown to spend less time at the surface (Sekino and Yoshioka 1995).

1. General Introduction

In order to carry out vertical migration behaviour many species of zooplankton use external cues to coordinate their vertical migrations in response to the diel cycle (Cottier et al. 2006). The primary cue has often been identified as the rate of change in light at a specified depth (Fortier et al. 2001), or the changing location of an isolume (Frank and Widder 1997). In the field however, it is often very difficult to separate the proximate from the ultimate causes of DVM, as changing light levels are fundamental to both (Cottier et al. 2006). However, high latitude marine ecosystems are unique as the sun does not set during midsummer (midnight sun) or rise during midwinter (polar night), and so relative light levels do not change as markedly throughout the diel cycle. These conditions mean that essentially, during the midnight sun and the polar night, there may be no optimal time for zooplankton to ascend to the surface layers. Studying zooplankton vertical migrations under these conditions thus make it possible to better identify which external cues are responsible for their movements (if any), and the Svalbard archipelago at its high latitude is perfectly suited to this task.

Previous studies on zooplankton in Arctic regions have largely failed to demonstrate any coordinated vertical migration during summer i.e. when there is little change in the insolation levels through the diel cycle (Blachowiak-Samolyk et al. 2006). Thus DVM is often considered less important at high latitudes than seasonal migration patterns (Kosobokova 1978; Longhurst et al. 1984; Falkenhaug et al. 1997). Coordinated vertical migrations (i.e. classic DVM) then tend to resume towards autumn when a more marked diel cycle develops (Fischer and Visbeck 1993). The traditional paradigm is that DVM behaviour also ceases completely during the winter period in the high Arctic due to low food availability in the water column (Smetacek and Nicol 2005) and the over-wintering strategies of the copepods (Falk-Petersen et al. 2008). However, the ultimate causes for vertical migration still exist, as light attenuation with depth will still create a safer environment from visual predators within deeper waters (Fiksen and Carlotti 1998), and zooplankton food supply (phytoplankton) is still highly stratified with depth and occurs mainly towards the sunlit surface (Fortier et al. 2001).

Considering the continuing ultimate driving force behind zooplankton vertical migration, modern observation techniques have since been used to discover two modes

1. General Introduction

of vertical migration in the high Arctic. Cottier et al. (2006) used an Acoustic Doppler Current Profiler (ADCP) to identify unsynchronised vertical migrations of individuals at Kongsfjorden, with different species of copepod assuming different migration rhythms which gained increasing synchronicity (i.e. towards classic DVM) as the diel cycle became more marked.

In 2004, Falk-Petersen et al. (2008) took advantage of a record northward position of the Arctic polar ice edge (Vinje 1999) to study zooplankton migration in waters that were usually inaccessible due to ice cover. They found varying migration patterns between the different copepod species at different locations, and linked their migration patterns to the timing of the Arctic spring phytoplankton bloom that provides them with the majority of their food. The zooplankton were driven to gain as much energy as possible during the comparatively short bloom before overwintering in deeper and safer waters, and at locations where the bloom was in effect, classic DVM was detected.

In a further study using a moored ADCP, zooplankton vertical migration was analysed at both a seasonally ice covered location and an ice free location (Rijpfjorden and Kongsfjorden – see section 1.3.1 for hydrology) throughout the polar night. A DVM signal was observed at both locations (Berge et al. 2009). DVM (albeit at varying amplitudes) occurred regardless of variations in ice cover and changes in irradiance. Although the DVM signal was observed to be strongest during marked diel changes in irradiance, DVM continued when no apparent changes in illumination occurred. However, very minimal changes in irradiance which are impossible to determine with the human eye may still be driving DVM, as illustrated by a shift in DVM periodicity during the full moon during the Berge et al. study.

More recently, Wallace et al. (2010) analysed two years of moored ADCP data from Kongsfjorden and Rijpfjorden and observed unsynchronised vertical migration at both locations during summertime. These studies are putting forward a growing body of evidence that both a synchronised and unsynchronised vertical migration signal exists at all points in the annual cycle. The number of studies carried out using moored observations in fjords of the Svalbard archipelago is also highlighted by the number of

these publications, and so our research will add evidence both to the debate surrounding DVM at high latitude and also to the spatial validity of the conclusions drawn from moored observations.

1.4. Summary of climate change impacts on zooplankton in the high Arctic with implications for carbon flux

The widely accepted paradigm of polar marine biology is that the seasonal changes in sea-ice cover have a dramatic influence on ecosystem processes (Cisewski et al. 2009; Søreide et al. 2010; Leu et al. 2011). Within the current regime of a warming Arctic, the total area of sea-ice cover, its annual duration and thickness will all decrease. The major effects of ice on the Arctic marine ecosystem have long been understood (McGhee 1996), and any change in the distribution/abundance of ice cover has the potential to dramatically modify the system on a trophic level either through bottom-up reconfiguring of the food web or through top-down regulation (see Macdonald et al. 2005 for details). Ice cover limits wind mixing and attenuates light (which is known as a proximate cue for DVM), and can decrease stratification in winter which in turn heavily impacts primary production through the water column (Macdonald et al 2005).

Although such ice effects reduce pelagic production, algal communities that grow on the underside of the ice can support an entire system of their own, including autochthonous species that spend their entire life cycles among the ice, and allochthonous species that visit the ice at some point during their life cycle (Gulliksen and Lønne 1989). Ice thickness and snow cover can influence the types/abundances of ice algae within these sympagic systems, and the trophic links between algal production and the pelagic system (Niebauer and Alexander 1985). This ice algal food supply can be a valuable energy source to pelagic zooplankton in the Arctic (Søreide et al. 2006). Ice algae begins to grow in early March (Engelsen et al. 2002), and so peak ice algal biomass may precede the pelagic phytoplankton bloom by up to 2 months (Michel et al. 1996). The proportional importance of this food supply to the pelagic zone compared to

1. General Introduction

the phytoplankton bloom increases with latitude, the availability of which can affect the timing of zooplankton seasonal vertical migrations, as they decide when to ascend from overwintering at depth (Søreide et al. 2008).

Although the proposed loss of ice over the Arctic Ocean in the future ‘should’ increase pelagic primary production by allowing greater mixing and irradiation of the water column, the loss of this sympagic ecosystem may affect the vertical migrations of zooplankton. Fortier et al. (2001) suggest that interspecific differences in the pattern and extent of copepod DVM can be related in part to the vertical distribution of potential food, and this food distribution will be dramatically influenced by the loss of ice. Although this food source will essentially be lost with predicted climate warming, Berge et al. (2009) suggest an increase in DVM activity in Arctic waters in response to any thinning/loss of winter ice cover. As the observed synchronised classic DVM was strongest during periods of a marked diel light cycle during their study, any loss of ice cover should in theory increase the amplitude and synchronicity of zooplankton vertical migrations. Such an increase may have important implications for carbon flux in the Arctic Ocean (Hays 2003).

Primary producers, both in the water column (as seen during the Arctic spring phytoplankton bloom) and on the underside of ice (ice algal communities) may be grazed upon to support the pelagic food web, or descend together with faecal pellets and zooplankton carcasses to feed the benthos (Grebmeier and Dunton 2000) (Fig 1.12). The large spatial and seasonal variability observed in primary production in the Arctic strongly affects both this energy transfer through the food web and vertical flux (carbon flux) (Wassmann et al. 2006), and is driven largely by ice processes. As sea ice begins to melt in summer, a stratified and nutrified surface layer is exposed which rapidly prompts a bloom of phytoplankton with the increased irradiation (Reigstad et al. 2002). As this layer becomes less stratified due to wind-induced mixing, the bloom extends deeper until the nutrients have been depleted. Within this highly seasonal Arctic system, copepods play a keystone role as the link between primary production and the higher trophic levels, and so have a large effect on energy flux through the system (Tande 1991). Much of the phytoplankton biomass is retained in the pelagic system by

zooplankton grazing (Riser et al. 2008) (Fig 1.12). However, zooplankton faecal pellets also sink faster than ‘unprocessed’ organic matter and are thus more efficient transporters of organic material to the benthos. With a warming climate and changes in sea-ice cover affecting both the levels of primary production and associated zooplankton behaviour such as DVM, carbon flux through the has the potential to be significantly modified.

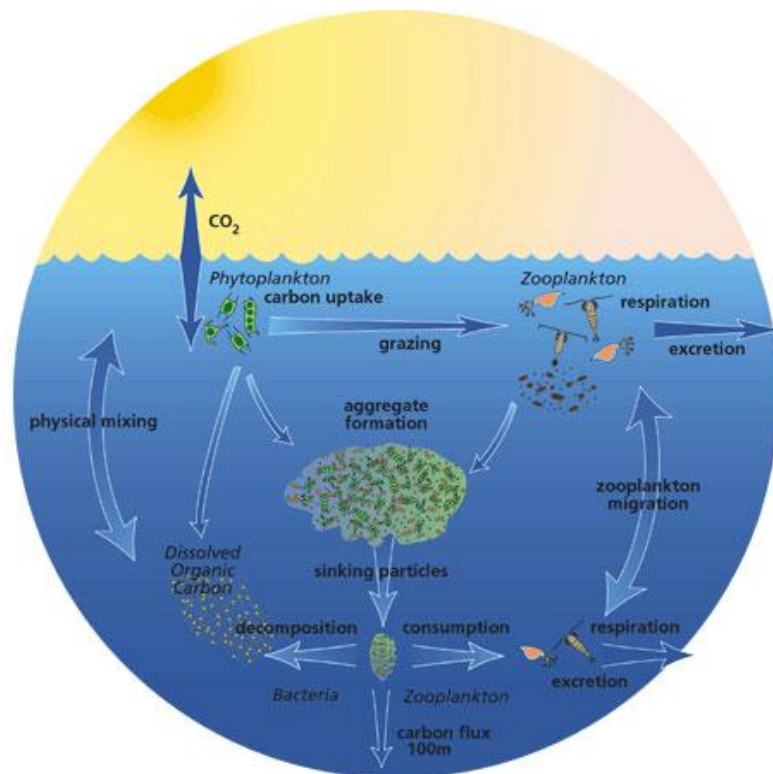


Fig 1.12) A simplified ‘biological pump’ illustrating the input of biological processes (grazing, zooplankton migration [investigated in this thesis], faecal pellet excretion) to the flow of carbon through the pelagic system. Arrows indicate the flow of carbon through the system. Abiotic uptake is illustrated on the left of the diagram, with biological process in the centre and right. Water column depth portrayed here is ~100 m. [Image from US Joint Global Ocean Flux Study – online 2012]

The pelagic ecosystems over Arctic shelves have been shown to be more tightly coupled to their benthic counterparts than warmer seas (Piepenburg 2005), and many factors enhance this effect including a reduced microbial loop, high seasonality, low temperatures and more rapid sinking of pelagic/sympagic algae due to mismatches between zooplankton grazer and phytoplankton population cycles (Wassmann et al. 2003). Many of these factors will be affected by climate change (Renaud et al. 2008),

1. General Introduction

and as the benthos plays a key role in carbon cycling and nutrient regeneration (Renaud et al. 2007), climate change in the Arctic may have severe impacts on atmospheric carbon dioxide levels. Up to 48% of fossil fuel derived carbon dioxide is now stored in the ocean (Sabine et al. 2004), and the Arctic Ocean is considered a good 'sink' for atmospheric carbon dioxide due to its cold and relatively fresh surface waters having huge potential for uptake (Takahashi et al. 1997). Thus, irrespective of any biological pump (i.e. biological processes such as DVM that add to the intake and flux of carbon through the pelagic system from the surface euphotic zone to deeper waters – Fig 1.12), warming of the Arctic could decrease this uptake ability and hence increase the potential levels of atmospheric carbon dioxide (Semiletov et al. 2007). These abiotic effects may outweigh the effects of proposed increased DVM (Berge et al. 2009), but the overall effects on carbon flux are still relatively unknown.

One biological phenomenon that has clearly been correlated to a loss of ice cover as a result of temperature increases however (the two changes predicted across the Arctic) is the proliferation of jellyfish, as observed in the Bering Sea during the 1990's (Brodeur et al. 1999). Jellyfish, as tactile predators, are able to track their prey equally well in darkness as compared to daylight (Hays 2003). Since visual predators (which are currently key components in the Arctic pelagic system - Falk-Petersen et al. 2008) have a reduced foraging rate in ice covered waters due to the drop in light (Bouchard and Fortier 2008), any increase in DVM during the dark period as proposed by Berge et al. (2009) should create a competitive advantage for tactile predators in the system. Instances where zooplankton exhibit reverse DVM patterns have been associated with higher levels of tactile predation (Hays 2003), and changing patterns in vertical movements of zooplankton will affect carbon flux through the system.

1.5. Zooplankton patchiness with implications for moored observations

Oceanic plankton is distributed unevenly, and the importance of this spatial heterogeneity to plankton ecology (influencing species interactions, modelling of population dynamics and assessment of community function) is well known (Folt and Burns 1999). Within highly dynamic systems (such as the Arctic fjords investigated in this thesis), plankton aggregations or ‘patches’ may influence the reliability of information gathered using moored observations, net hauls and any other sampling method based on a single point in space. High levels of advection have been described within Svalbard’s fjords (Basedow et al. 2004; Willis et al. 2006), and population growth rates and water mass residence times can influence spatial distributions of zooplankton by modifying patch formations and durations (Monsen et al. 2002). Dramatic environmental variability, as is characteristic of many high Arctic fjords (Hop et al. 2006) is known to be a major factor in determining spatial and patterns of zooplankton distribution (Rios-Jara 1998), and this environmental variability can change depending on the sampling location. Within coastal zones, zooplankton patch-formation can be impeded by intermittent wind forcing (Resgalla et al. 2001), making point sampling more representative of the system as a whole. However, oceanic frontal areas that are characterised by stronger horizontal gradients of temperature and density create complex hydrographic structures and a contrasting zooplankton distribution characterised by dramatic changes over relatively short spatial scales (Molinero et al. 2008). Long term oceanic moorings however are very useful for sampling in remote locations characterised by adverse weather conditions such as the high Arctic. As this thesis and a large body of research uses moored observations from fixed points in space to investigate changes in zooplankton, the conclusions from these observations must be validated on a broader spatial scale. One aim of this thesis is to put forward evidence of the spatial relevance of moored observations within Svalbard fjords in terms of the fjord length and the archipelago as a whole.

1.5.1. Currents at Kongsfjorden and Rijpfjorden

In order to discuss advection in this thesis and assess its influence on observations of patchiness and vertical migration, we must first describe the magnitude and direction of currents. Wallace et al. (2010) described depth-averaged horizontal current velocities up to approximately 15 cm/s at Kongsfjorden 2006/07, 30 cm/s at Kongsfjorden 2007/08 and 30 cm/s at Rijpfjorden (2006/07, 2007/08). In July 1999, the surface currents at approximately mid Kongsfjorden were measured at 10 – 30 cm/s (Svendsen et al. 2002). These velocities can be compared to the boundary flow of AtW over the southern margin of the Eurasian Basin reported in 1995 – 1996 as 1 – 5 cm/s (Woodgate et al. 2001). For this thesis, moored ADCP observations (including horizontal water velocities) were available from Kongsfjorden 2006/07 and 2008/09 and Rijpfjorden 2006/07, 2007/08, 2009/10 and 2010/11 (Fig 1.13). These observations were made from upward looking ADCP's attached to the moorings at approximately 100 m depth, and allowed the quantification of northward and eastward water velocities relative to the mooring positions. Data were collected continuously throughout the deployments at 20 min x 4 m depth resolution (Figs 1.14, 1.15, 1.16, 1.17, 1.18 and 1.19). Monthly means of horizontal current velocities binned vertically to match standard zooplankton multinet depths as closely as possible (15 – 20 m, 20 – 50 m, 50 – 95 m) at Kongsfjorden and Rijpfjorden over all deployments are displayed in Table 1.2 (a – d) in mm/s. These depth bins were chosen to allow discussion of advective influences on depth stratified net collected zooplankton samples. It is important to note that observations from the surface 0 - 15 m are excluded due to interference from surface reflection, and mm/s are used to add greater resolution to the current velocities.

Horizontal current velocities observed by our deployments at Kongsfjorden and Rijpfjorden were similar in magnitude to those reported by Wallace et al. (2010 - using some of the same deployments) and Svendsen et al. (2002) – i.e. 0 – 30 cm/s. The fastest mean (monthly mean) eastward velocity observed at Kongsfjorden (i.e. primarily into the fjord) was 44.4 mm/s at 20-50 m depth in February 2007, while the most negative value (i.e. primarily westward leaving the fjord) was -69.5 mm/s at 15-20 m in

1. General Introduction

April 2007 (Table 1.2a). The fastest mean northward velocity observed at Kongsfjorden (i.e. primarily leaving the fjord) was 52.2 mm/s at 15-20 m in April 2007, while the most negative value (i.e. primarily southward entering the fjord) was -39.4 mm/s at 15-20 m in August 2006 (Table 1.2c). All these fastest mean observations were between 39 – 70 mm/s in magnitude, and fastest current velocities appeared to be towards the surface in the 15-20 m layer at Kongsfjorden. The fastest mean eastward velocity observed at Rijpfjorden was 60.7 mm/s at 15-20 m in September 2007, while the most negative value was -36.7 mm/s at 15-20 m in October 2007 (Table 1.2b). The fastest northward velocity observed at Rijpfjorden (i.e. primarily leaving the fjord) was 51.8 mm/s at 15-20 m in July 2010, while the most negative value (i.e. primarily southward entering the fjord) was -76.1 mm/s at 15-20 m in September 2007 (Table 1.2d). These fastest mean velocities were similar in magnitude to those observed at Kongsfjorden, and were all observed in the surface-most 15-20 m layer. A dominant regime within our current velocity observations was variation, with high levels of temporal and vertical variation in current velocities described by high standard deviations about the monthly means (Tables 1.2a - d).

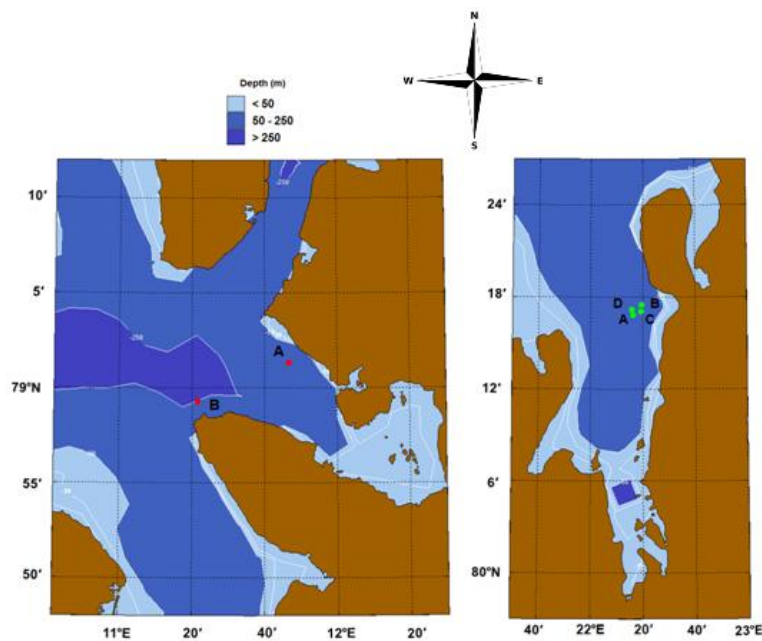


Fig 1.13) Left – map of Kongsfjorden with 2006/07 (A) and 2008/09 (B) mooring locations. Right – map of Rijpfjorden with 2006/07 (A), 2007/08 (B), 2009/10 (C) and 2010/11 (D) mooring locations.

1. General Introduction

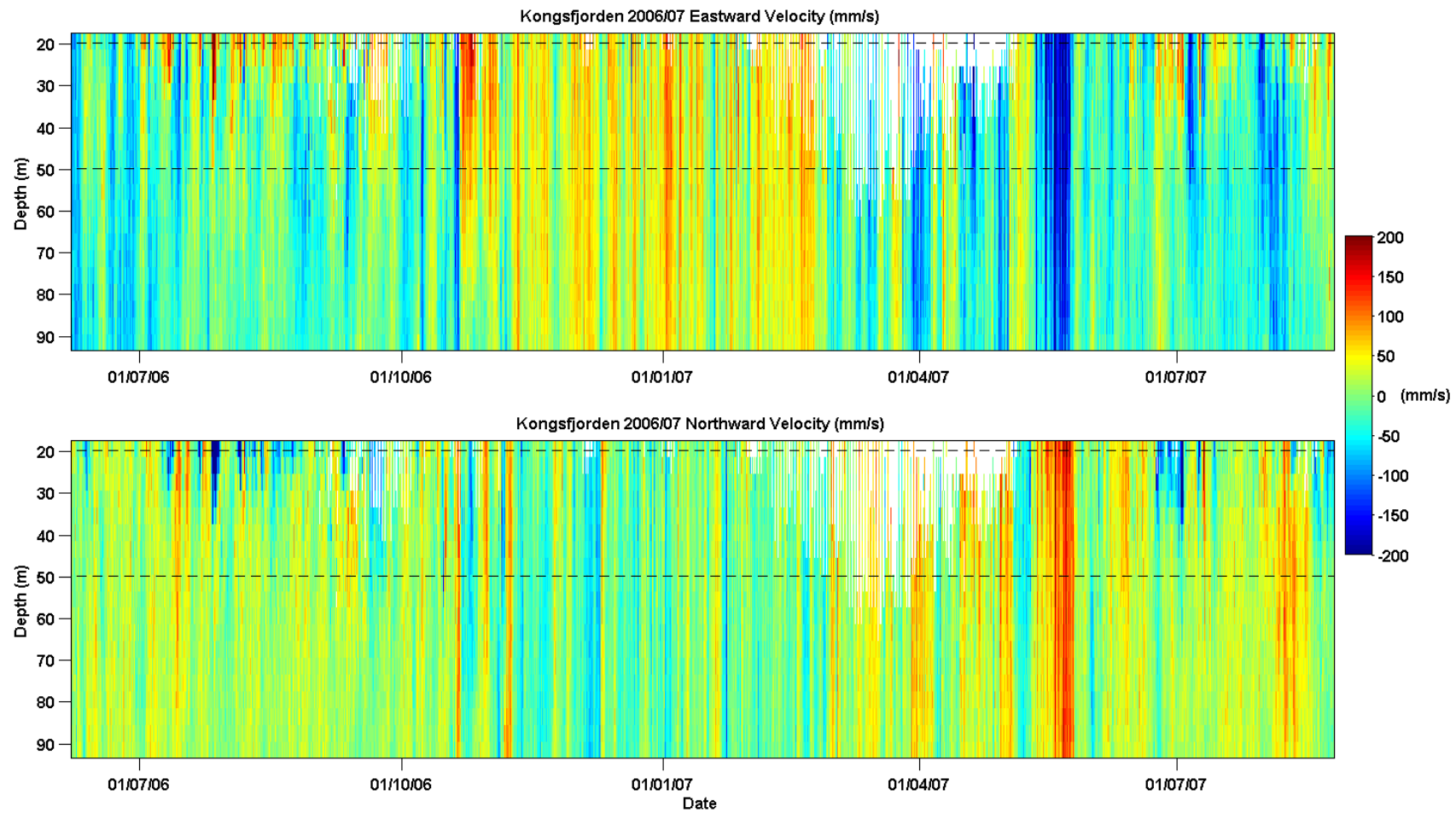


Fig 1.14) Kongsfjorden eastward horizontal current velocity (mm/s - above) and northward horizontal current velocity (mm/s – below) collected at 20 min x 4 m depth resolution by the upward looking ADCP attached to the mooring at approximately 100 m depth during the 2006/07 deployment. 15 – 95 m depth sampled. Dashed horizontal lines represent standard multinet zooplankton sample depths. White sections = no/bad data.

1. General Introduction

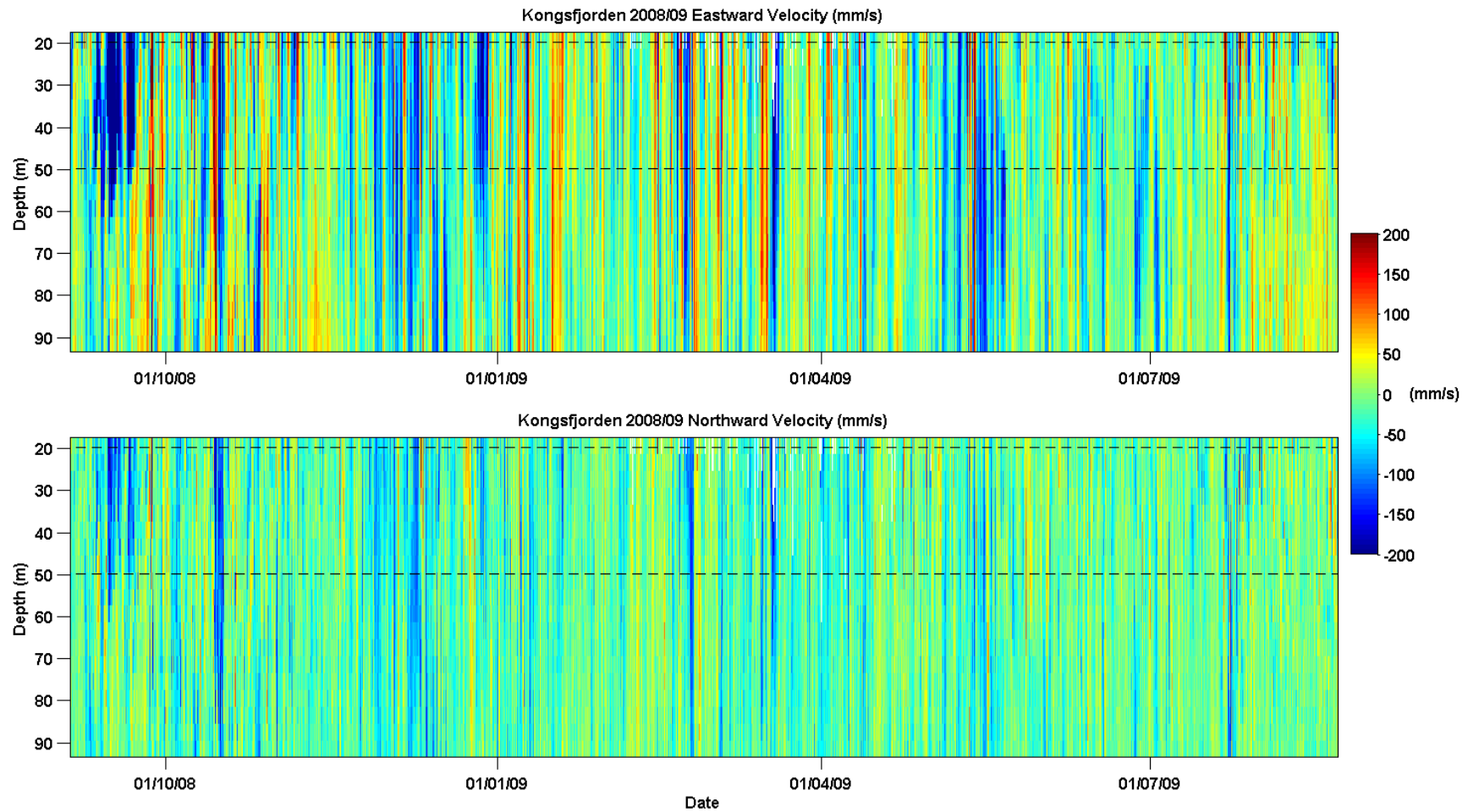


Fig 1.15) Kongsfjorden eastward horizontal current velocity (mm/s - above) and northward horizontal current velocity (mm/s – below) collected at 20 min x 4 m depth resolution by the upward looking ADCP attached to the mooring at approximately 100 m depth during the 2008/09 deployment. 15 – 95 m depth sampled. Dashed horizontal lines represent standard multinet zooplankton sample depths. White sections = no/bad data.

1. General Introduction

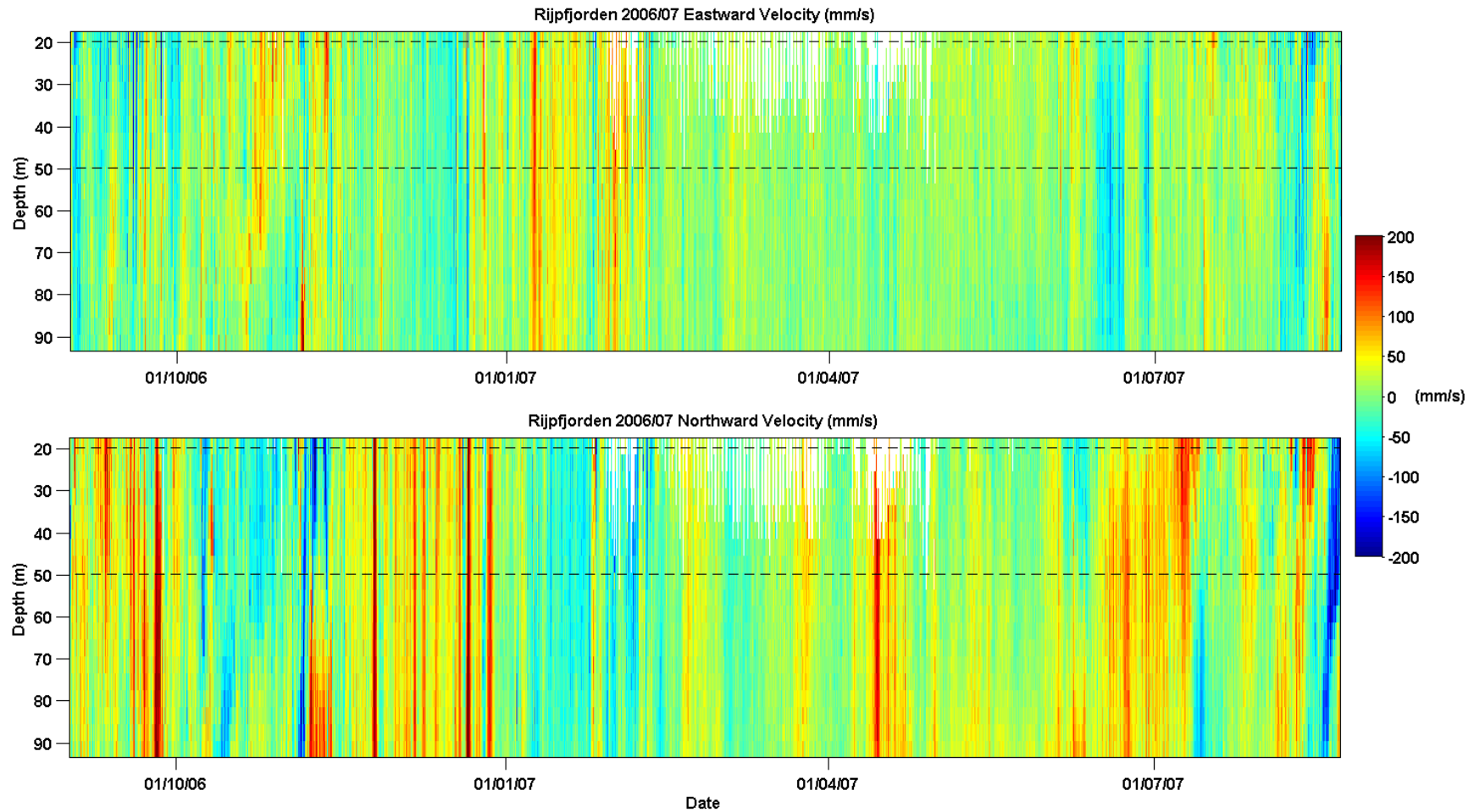


Fig 1.16) Rijpfjorden eastward horizontal current velocity (mm/s - above) and northward horizontal current velocity (mm/s – below) collected at 20 min x 4 m depth resolution by the upward looking ADCP attached to the mooring at approximately 100 m depth during the 2006/07 deployment. 15 – 95 m depth sampled. Dashed horizontal lines represent standard multinet zooplankton sample depths. White sections = no/bad data.

1. General Introduction

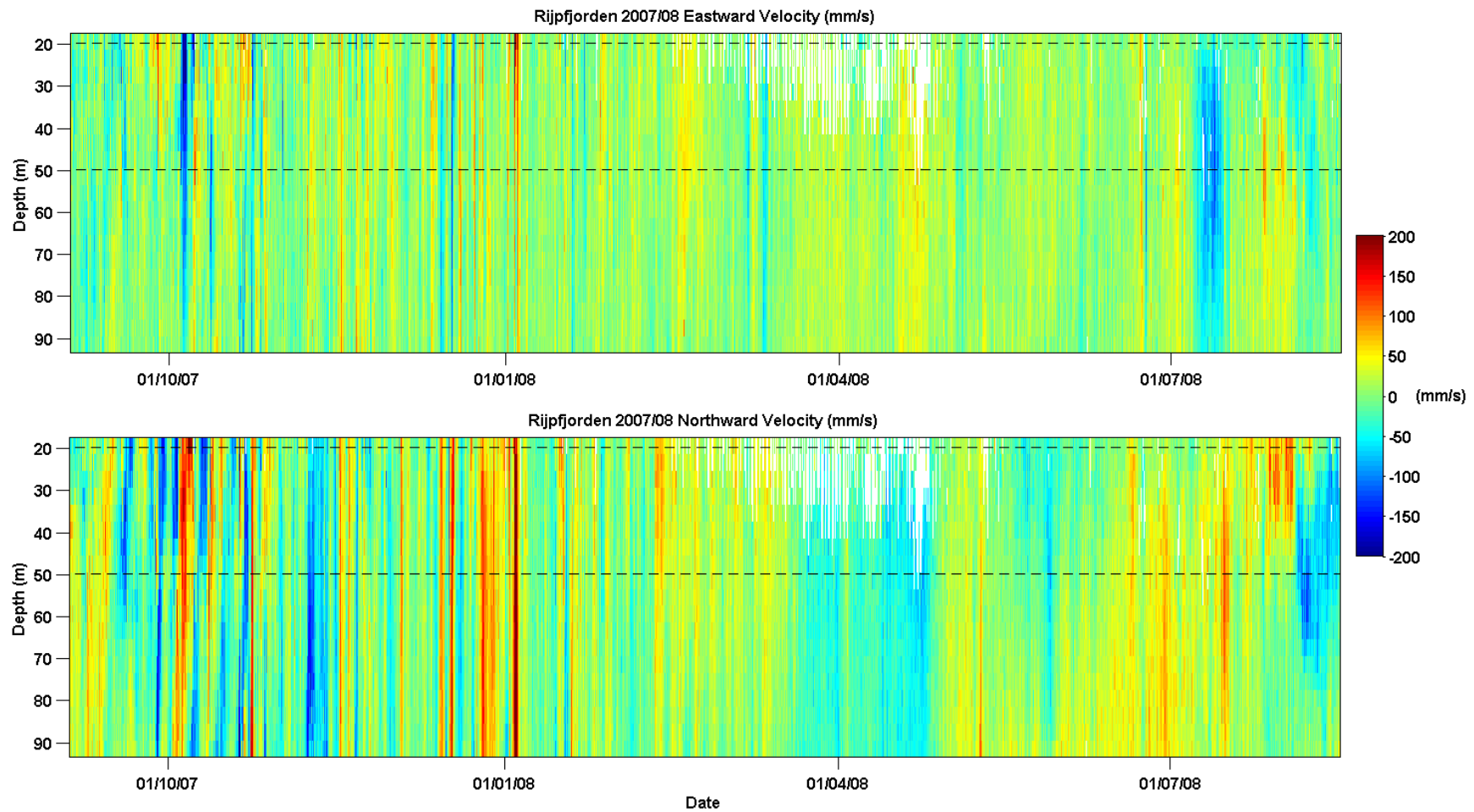


Fig 1.17) Rijpfjorden eastward horizontal current velocity (mm/s - above) and northward horizontal current velocity (mm/s – below) collected at 20 min x 4 m depth resolution by the upward looking ADCP attached to the mooring at approximately 100 m depth during the 2007/08 deployment. 15 – 95 m depth sampled. Dashed horizontal lines represent standard multinet zooplankton sample depths. White sections = no/bad data.

1. General Introduction

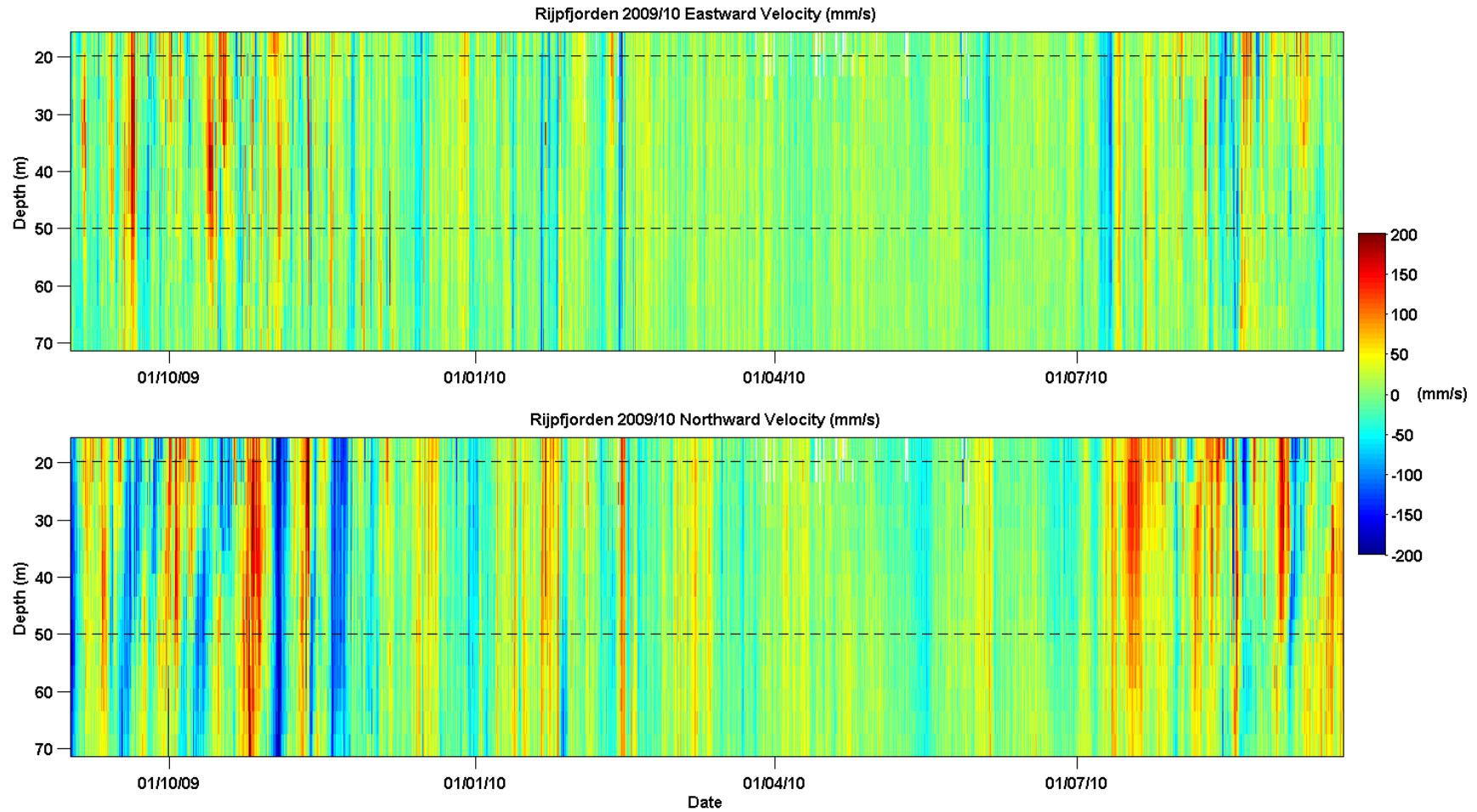


Fig 1.18) Rijpfjorden eastward horizontal current velocity (mm/s - above) and northward horizontal current velocity (mm/s – below) collected at 20 min x 4 m depth resolution by the upward looking ADCP attached to the mooring at approximately 100 m depth during the 2009/10 deployment. 15 – 73 m depth sampled. Dashed horizontal lines represent standard multinet zooplankton sample depths. White sections = no/bad data.

1. General Introduction

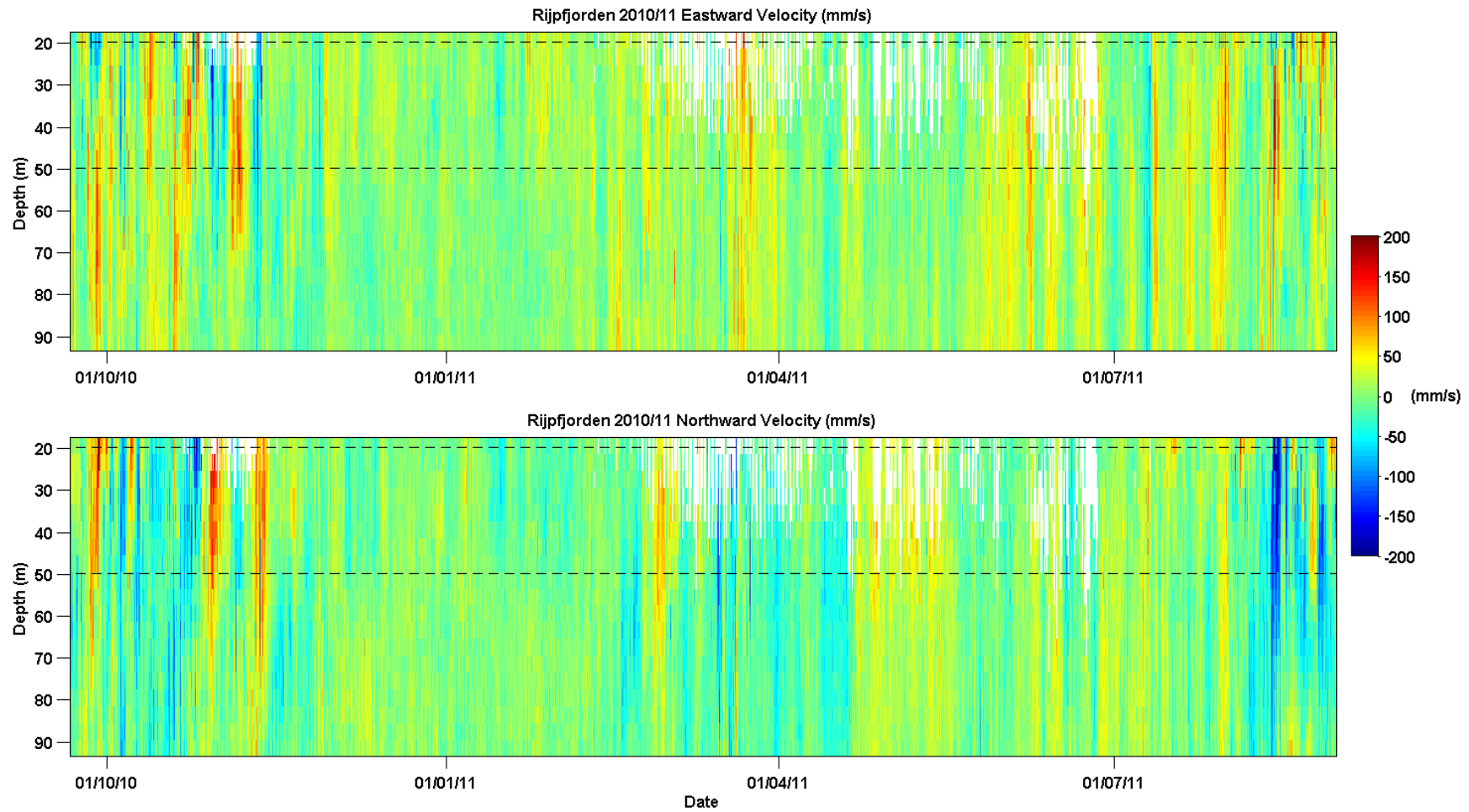


Fig 1.19) Rijpfjorden eastward horizontal current velocity (mm/s - above) and northward horizontal current velocity (mm/s – below) collected at 20 min x 4 m depth resolution by the upward looking ADCP attached to the mooring at approximately 100 m depth during the 2010/11 deployment. 15 – 95 m depth sampled. Dashed horizontal lines represent standard multinet zooplankton sample depths. White sections = no/bad data.

1. General Introduction

Table 1.2a) Kongsfjorden monthly mean (mean of all 20 min samples) eastward horizontal current velocities (mm/s) and associated standard deviations (in brackets). Velocities are binned vertically to match standard multinet sample depths as closely as possible (min depth 15 m, max depth 95 m – samples collected at 4 m vertical resolution). Location codes (A,B) refer to positions on Fig 1.13.

Location	Year	Depth (m)	Mean monthly eastward horizontal velocity (mm/s) and sd												
			Jan	Feb	Mar	Apr	May	Jun	Jul	Aug	Sep	Oct	Nov	Dec	
Kongsfjorden (A)	2006	15-20						-32.7(49)	19.0(62)	43.3(69)	16.8(56)	17.8(79)	23.9(50)	29.8(52)	
		20-50						-34.3(40)	-7.0(47)	0.3(37)	4.5(38)	0.1(68)	33.3(41)	39.3(34)	
		50-95						-47.6(29)	-22.4(24)	-20.6(23)	-14.7(23)	-17.6(44)	22.5(33)	34.7(29)	
Kongsfjorden (A)	2007	15-20	20.0(60)	35.4(44)	-29.1(77)	-69.5(70)	-62.5(85)	-10.8(52)	-12.4(65)	6.0(51)					
		20-50	32.8(44)	44.4(32)	-36.2(51)	-41.5(55)	-58.3(83)	-13.4(40)	-31.7(54)	-14.5(43)					
		50-95	27.3(34)	37.5(25)	-26.9(42)	-32.9(43)	-49.1(65)	-20.8(24)	-38.4(18)	-36.1(34)					
Kongsfjorden (B)	2008	15-20										-67.3(117)	-11.6(93)	-19.7(90)	-38.2(99)
		20-50										-66.6(122)	-7.4(74)	-18.9(61)	-48.7(74)
		50-95										-6.3(53)	-10.1(61)	-3.8(43)	-38.0(54)
Kongsfjorden (B)	2009	15-20	6.4(70)	-10.0(89)	-4.9(72)	-1.5(69)	-16.7(72)	-8.2(49)	-12.6(75)	-30.0(84)					
		20-50	7.9(57)	-8.3(71)	-1.5(70)	-5.0(60)	-29.5(64)	-20.6(43)	-7.4(49)	-2.3(49)					
		50-95	5.4(49)	-7.5(50)	-1.3(55)	-8.6(42)	-36.6(55)	-21.1(41)	-8.5(40)	18.7(25)					

1. General Introduction

Table 1.2b) Rijpfjorden monthly mean (mean of all 20 min samples) eastward horizontal current velocities (mm/s) and associated standard deviations (in brackets). Velocities are binned vertically to match standard multinet sample depths as closely as possible (min depth 15 m, max depth 95 m – samples collected at 4 m vertical resolution). Location codes (A,B,C,D) refer to positions on Fig 1.13. Velocities in italics are calculated to a max depth of 73 m.

Location	Year	Depth (m)	Mean monthly eastward horizontal velocity (mm/s) and sd												
			Jan	Feb	Mar	Apr	May	Jun	Jul	Aug	Sep	Oct	Nov	Dec	
Rijpfjorden (A)	2006	15-20										-25.4(50)	18.7(39)	10.9(50)	-6.9(44)
		20-50										-17.3(37)	18.9(30)	8.9(31)	-5.0(34)
		50-95										-4.8(28)	9.1(20)	5.6(30)	-8.0(28)
Rijpfjorden (A,B)	2007	15-20	23.5(44)	2.7(34)	7.5(17)	2.0(19)	11.9(15)	-0.4(22)	11.0(31)	-28.2(57)	60.7(152)	-36.7(154)	-25.0(116)	29.2(134)	
		20-50	31.8(33)	12.5(31)	8.1(15)	1.3(18)	13.0(10)	-5.8(31)	14.0(17)	-11.7(33)	-1.3(26)	-4.4(52)	12.2(26)	2.8(36)	
		50-95	30.8(31)	10.4(21)	6.1(11)	-0.2(13)	1.4(8)	-13.9(29)	7.8(16)	-8.5(34)	-5.5(18)	-4.3(34)	10.1(23)	3.2(30)	
Rijpfjorden (B)	2008	15-20	3.2(107)	5.3(21)	-0.6(24)	2.7(30)	2.9(16)	2.8(14)	-7.4(16)	3.2(58)					
		20-50	8.0(28)	14.1(20)	2.9(24)	14.8(20)	6.0(15)	8.3(17)	-12.7(31)	-15.4(22)					
		50-95	5.5(21)	9.4(15)	4.8(19)	18.4(15)	8.0(12)	5.5(17)	-2.9(38)	-3.8(19)					
Rijpfjorden (C)	2009	15-20									7.2(50)	19.1(59)	18.3(44)	-0.7(34)	
		20-50									11.8(48)	19.9(43)	10.0(37)	0.3(29)	
		50-73									-2.8(38)	6.0(31)	2.9(35)	-1.2(29)	
Rijpfjorden (C,D)	2010	15-20	-2.6(44)	1.2(41)	4.6(20)	1.3(22)	1.5(21)	-0.5(21)	8.8(43)	13.1(65)	16.9(41)	9.0(59)	1.0(35)	9.6(14)	
		20-50	-3.8(34)	0.5(34)	6.5(18)	0.6(16)	4.3(17)	0.4(21)	2.7(38)	0.4(45)	9.7(25)	16.2(47)	2.6(41)	7.8(15)	
		50-73/95	-6.1(29)	-3.8(30)	6.6(17)	1.3(15)	3.9(11)	0.9(19)	-0.3(33)	3.1(29)	-8.9(19)	14.5(25)	-3.2(25)	-0.7(11)	
Rijpfjorden (D)	2011	15-20	7.5(18)	6.3(14)	5.2(38)	-3.8(19)	-7.3(22)	9.9(20)	-2.9(34)	21.9(59)					
		20-50	4.4(19)	10.2(15)	18.9(30)	0.3(18)	-1.0(18)	20.8(24)	12.2(28)	15.4(34)					
		50-95	-1.6(8)	10.0(18)	13.9(22)	2.4(17)	7.6(16)	20.5(22)	15.6(28)	5.8(25)					

1. General Introduction

Table 1.2c) Kongsfjorden monthly mean (mean of all 20 min samples) northward horizontal current velocities (mm/s) and associated standard deviations (in brackets). Velocities are binned vertically to match standard multinet sample depths as closely as possible (min depth 15 m, max depth 95 m – samples collected at 4 m vertical resolution). Location codes (A,B) refer to positions on Fig 1.13.

Location	Year	Depth (m)	Mean monthly northward horizontal velocity (mm/s) and sd													
			Jan	Feb	Mar	Apr	May	Jun	Jul	Aug	Sep	Oct	Nov	Dec		
Kongsfjorden (A)	2006	15-20						10.0(47)	-9.0(82)	-39.4(82)	-3.1(55)	20.1(48)	6.3(43)	-8.8(48)		
		20-50						9.0(22)	10.6(43)	-1.2(26)	-1.1(33)	11.8(45)	-5.0(38)	-17.8(35)		
		50-95						14.8(17)	16.5(20)	14.4(13)	8.7(15)	11.5(30)	-10.7(34)	-21.7(28)		
Kongsfjorden (A)	2007	15-20	7.8(45)	-0.7(38)	46.0(64)	52.2(57)	50.2(71)	17.6(51)	1.1(52)	6.8(55)						
		20-50	-1.1(36)	-12.2(27)	34.8(40)	31.0(43)	41.9(66)	10.0(41)	9.1(41)	17.5(42)						
		50-95	-5.5(31)	-13.8(24)	26.3(29)	24.1(33)	37.2(54)	13.2(22)	19.9(12)	31.1(28)						
Kongsfjorden (B)	2008	15-20										-29.0(60)	-23.3(49)	-25.6(51)	-24.8(56)	
		20-50										-38.9(50)	-26.4(45)	-24.9(38)	-30.7(43)	
		50-95										-17.4(27)	-25.0(35)	-21.8(24)	-31.2(35)	
Kongsfjorden (B)	2009	15-20	-18.8(52)	-11.9(52)	-29.1(55)	-15.1(44)	-5.1(40)	-8.6(30)	-12.2(49)	-8.8(41)						
		20-50	-21.8(38)	-15.4(43)	-29.0(39)	-19.6(37)	-14.3(36)	-13.2(26)	-21.3(37)	-5.5(26)						
		50-95	-19.8(28)	-10.4(32)	-26.4(28)	-16.0(27)	-23.0(29)	-15.1(26)	-14.8(27)	-10.3(14)						

1. General Introduction

Table 1.2d) Rijpfjorden monthly mean (mean of all 20 min samples) northward horizontal current velocities (mm/s) and associated standard deviations (in brackets). Velocities are binned vertically to match standard multinet sample depths as closely as possible (min depth 15 m, max depth 95 m – samples collected at 4 m vertical resolution). Location codes (A,B,C,D) refer to positions on Fig 1.13. Velocities in italics are calculated to a max depth of 73 m.

Location	Year	Depth (m)	Mean monthly northward horizontal velocity (mm/s) and sd												
			Jan	Feb	Mar	Apr	May	Jun	Jul	Aug	Sep	Oct	Nov	Dec	
Rijpfjorden (A)	2006	15-20										39.5(64)	-23.5(45)	1.8(77)	49.4(57)
		20-50										44.8(47)	-25.3(35)	5.3(60)	49.1(55)
		50-95										42.9(45)	-8.7(26)	25.2(55)	49.7(55)
Rijpfjorden (A,B)	2007	15-20	-17.9(50)	-3.8(44)	4.8(27)	2.0(29)	-2.9(18)	8.1(36)	45.0(52)	35.3(89)	-76.1(174)	-33.7(152)	22.2(143)	26.8(132)	
		20-50	-22.4(36)	-4.8(39)	8.3(28)	28.6(42)	3.5(17)	26.6(39)	35.5(40)	-1.3(63)	-15.2(46)	5.5(71)	-12.9(42)	23.7(52)	
		50-95	-21.4(29)	-0.6(30)	6.2(24)	32.2(38)	17.0(15)	44.1(27)	15.4(37)	0.8(52)	-2.4(35)	-4.6(48)	-19.8(45)	17.7(49)	
Rijpfjorden (B)	2008	15-20	14.2(100)	10.3(22)	4.1(24)	-0.7(31)	-7.4(19)	-3.9(16)	16.2(25)	31.6(119)					
		20-50	15.0(51)	20.0(29)	1.6(31)	-29.8(26)	-8.6(25)	10.0(24)	32.0(26)	-26.0(48)					
		50-95	11.3(53)	7.0(24)	-5.6(25)	-30.0(22)	8.1(22)	30.2(19)	19.7(25)	-29.7(20)					
Rijpfjorden (C)	2009	15-20										-8.1(83)	14.8(76)	-23.1(100)	12.0(45)
		20-50										-15.9(63)	22.2(65)	-33.3(75)	3.3(38)
		50-73										-7.8(51)	10.2(58)	-34.7(62)	-1.3(33)
Rijpfjorden (C,D)	2010	15-20	20.8(50)	-4.1(43)	6.7(28)	4.2(23)	-15.0(25)	-11.7(26)	51.8(51)	23.1(84)	-22.9(67)	-15.9(68)	8.3(33)	-3.9(18)	
		20-50	16.4(43)	-7.4(38)	4.8(29)	8.5(17)	-11.5(24)	-7.1(24)	38.7(45)	26.5(54)	10.4(49)	-16.1(55)	10.3(38)	-2.6(18)	
		50-73/95	9.5(42)	-3.1(33)	5.5(27)	11.6(17)	-5.4(20)	3.8(20)	26.2(30)	10.1(36)	28.1(38)	-16.7(27)	-4.0(28)	3.3(11)	
Rijpfjorden (D)	2011	15-20	-10.7(16)	-3.1(17)	0.2(29)	1.0(21)	7.8(27)	-8.3(18)	25.1(35)	13.3(77)					
		20-50	-10.9(18)	-2.6(23)	-14.1(34)	-3.9(29)	10.9(27)	-6.4(23)	11.4(20)	-29.9(49)					
		50-95	-1.7(9)	-4.9(21)	-17.9(23)	-11.0(26)	5.9(17)	3.4(23)	5.2(22)	-30.1(29)					

1.6. Data chapter summary

Chapter 3 – Moored observations (hydrographic and sediment trap collected zooplankton) from Kongsfjorden (2 years) and Rijpfjorden (4 years) were used to investigate the seasonal changes in zooplankton community and compare an Atlantic influenced fjord to an Arctic dominated fjord. Current knowledge centres on information from Kongsfjorden only collected in 2002 (Willis et al. 2006) and 2005/06 (Willis et al. 2008). This thesis extends our knowledge both geographically by including Rijpfjorden and temporally.

Chapter 4 – Net hauls and multi-frequency acoustic observations from Kongsfjorden, Rijpfjorden and Billefjorden were made in close proximity to the moorings within 1 nautical mile of each other. These observations were used to assess the small scale spatial variation in zooplankton community around the moorings and compare this variability between locations of contrasting hydrology. No study of zooplankton spatial variation around the archipelago at this scale or around moorings has previously been carried out.

Chapter 5 – Net hauls and multi-frequency acoustic observations were made on a broad scale around the Svalbard archipelago over five years (2006 – 2010). These observations were used to assess spatial and interannual variation in zooplankton on a broad scale and investigate the spatial relevance of moored observations. Current knowledge on large scale variations in zooplankton community around the archipelago are based on a number of studies carried out at different locations, but none have covered the broad pan-Svalbard scope of this study and thus this is the first pan-Svalbard analysis. This study is also the first to determine characteristic spatial scales around the archipelago.

Chapter 6 – Net hauls and multi-frequency acoustic observations were made at extremes of the diel cycle (midday and midnight) at number of locations of contrasting hydrology and stages of primary production around the Svalbard archipelago in summer. These observations were used to assess the magnitude of vertical migration behaviour and to determine which species were responsible. The existence of DVM at

1. General Introduction

high latitude is currently debated, and many prior studies (e.g. Blachowiak-Samolyk et al. 2006; Daase et al. 2008) did not use higher resolution acoustic data. Thus the broad spatial scope of this study and the use of higher resolution sampling brings new evidence to this debate.

Chapter 7 - Net hauls and multi-frequency acoustic observations were made at extremes of the diel cycle (midday and midnight) at high latitude ice-covered locations to the north of the Svalbard archipelago in summer. These observations were used to assess the magnitude of vertical migration behaviour and to determine which species were responsible under these conditions. Although ice cover influenced certain locations in chapter 6, none of the conditions were truly ice-covered. During this study, the research vessel was anchored to sea-ice with net samples collected through spaces created by use of the vessels thrusters. This latitude and these conditions have rarely been investigated to date.

2. General Methods

2.1. Moored observations

The Scottish Association for Marine Science (SAMS) and Norwegian Polar Institute (NPI) have been deploying and maintaining a number of autonomous marine observation platforms (moorings) in the Svalbard archipelago since 2002. These moorings have been primarily deployed in AtW influenced Kongsfjorden (2009 configuration illustrated in Fig 2.1) and ArW dominated Rijpfjorden (2009 configuration illustrated in Fig 2.2), two fjords of contrasting hydrology.

2. General Methods

Kongsfjorden 2009 (10th Deployment).

LAT: 78° 57.754'N
LON: 011° 45.556'E
DEPTH: 221m
DEPLOYED: 1400Z 05.09.2009
CALM CLOUDY DAY

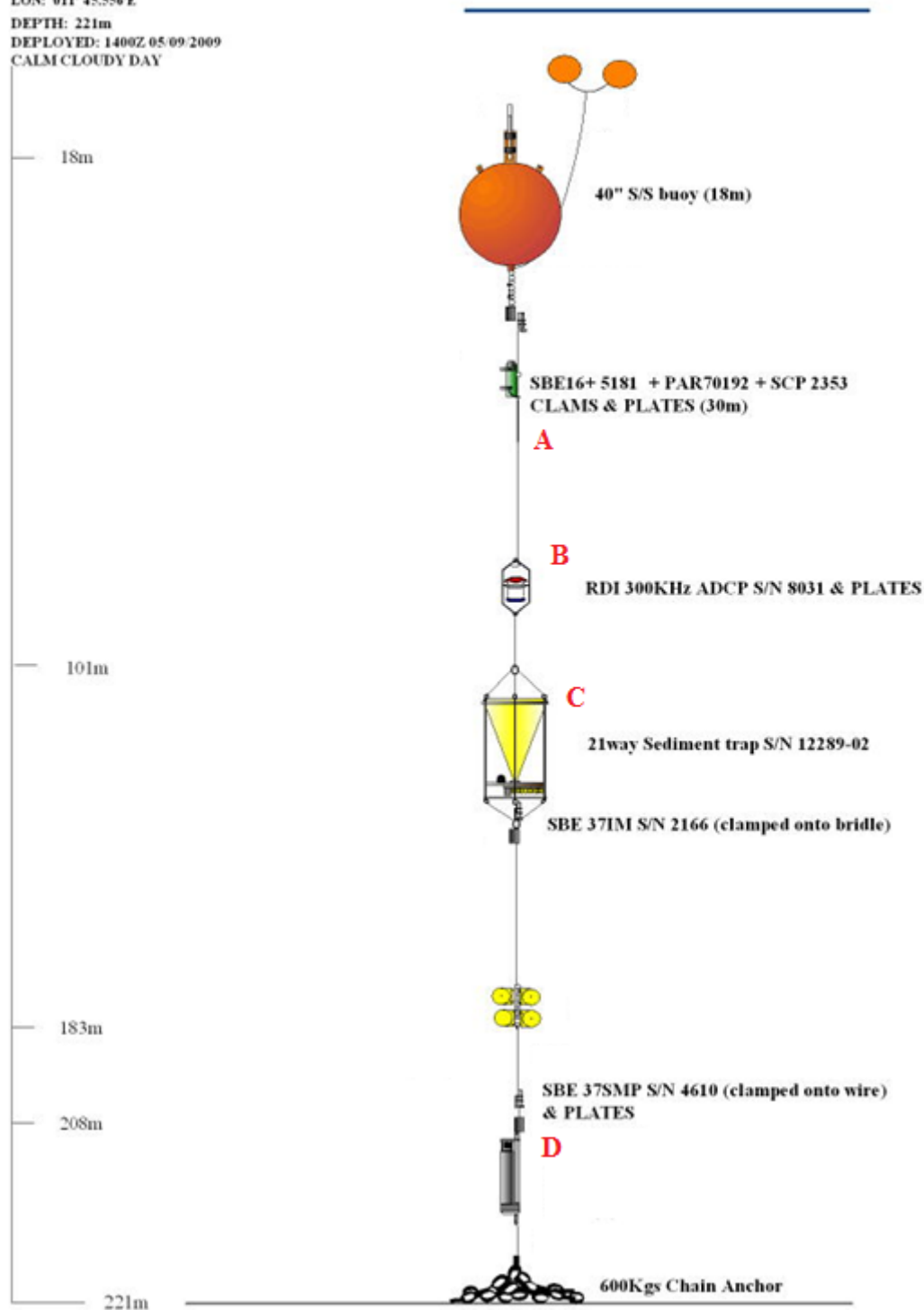


Fig 2.1) Basic configuration of SAMS mooring deployed in Kongsfjorden (2009). Water depth is displayed on the left (blue line indicates surface and black line indicates bottom).

2. General Methods

Rijpfjorden 2009

LAT: 58° 17.034'N
LON: 022° 18.149'E
DEPTH: 218m
DEPLOYED: 1310Z 31 08 2009

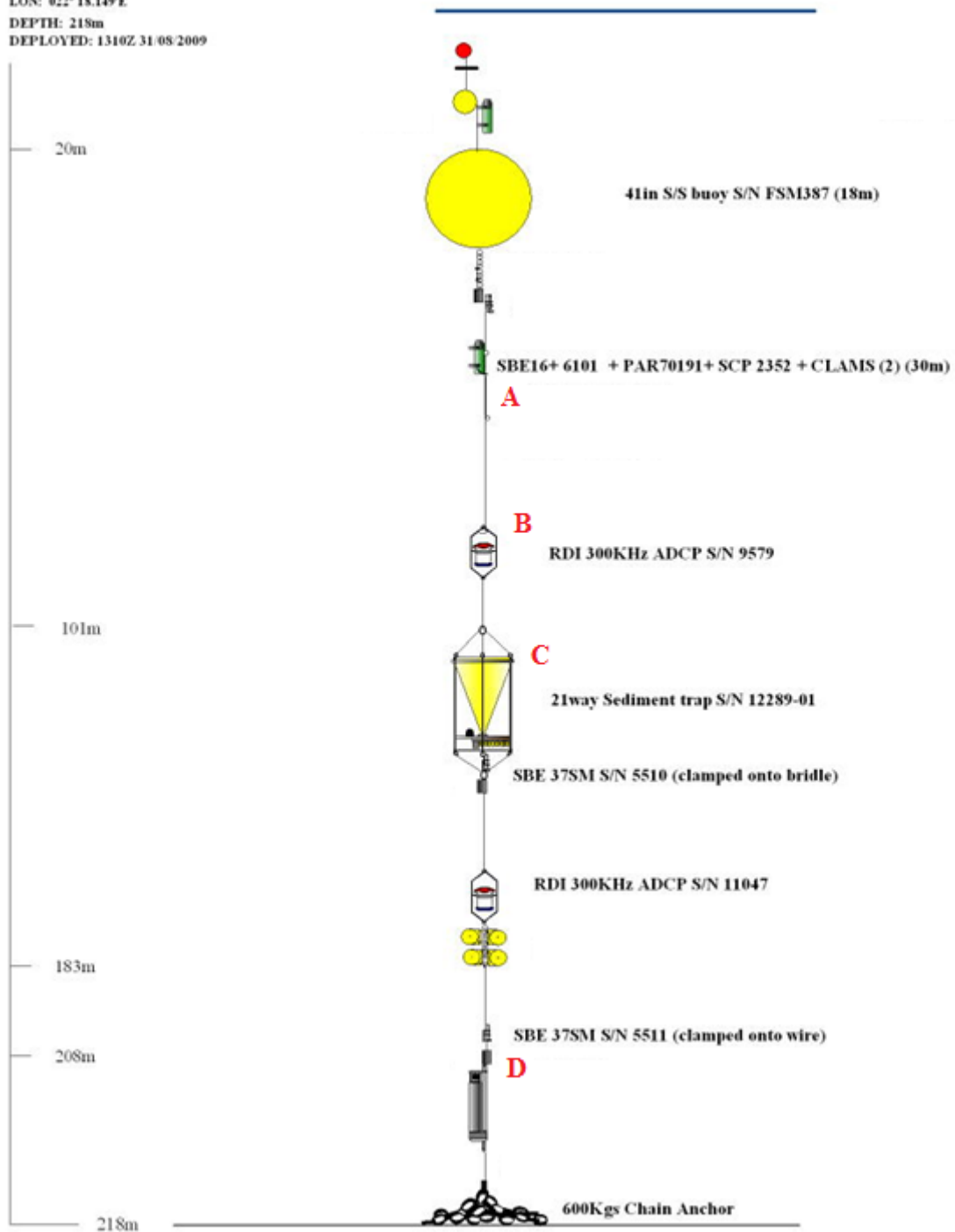


Fig 2.2) Basic configuration of SAMS mooring deployed in Rijpfjorden (2009). Water depth is displayed on the left (blue line indicates surface and black line indicates bottom).

2. General Methods

The set of instruments and the depth they are deployed at on each mooring can vary slightly, but the observations used in this thesis comprise of the following:

- 1) Temperature and salinity observations from the surface euphotic zone (A in Figs 2.1 and 2.2).
- 2) Upward looking ADCP horizontal current velocity observations from approximately 95 m depth (B in Figs 2.1 and 2.2).
- 3) Sequential sediment trap collection (using bottles which rotate on a programmed schedule to collect temporally distinct samples) from approximately 100-125 m depth (C in Figs 2.1 and 2.2).
- 4) Temperature and salinity observations from the bottom water (D in Figs 2.1 and 2.2).

For details on each sediment trap deployment, including all co-ordinates and equipment used, please see the SAMS website at [<http://martech.sams.ac.uk/arctictimeseries/>].

Biological observations of zooplankton are made by the sediment trap, and in this thesis the sediment trap collected zooplankton will be used to investigate temporal changes in the zooplankton community over lengthy periods of time in the two contrasting fjords (chapter 3). By comparing the two locations, we can investigate the likely changes that will occur in a warming Arctic.

Sediment traps have been used for many years, with the first use of a sediment collector in 1900 (Heim 1900). Although the technique is largely used in studies of carbon flux through the marine food web (example Wassmann et al. 2006), sediment trap collected material can also be used to investigate zooplankton. Although sequential sediment traps are not specifically designed to sample zooplankton in this manner, they have been used to monitor zooplankton communities in regions where it is not practical to use other forms of sampling to collect lengthy time series (Hargrave et al. 1989; Forbes et al. 1992; Willis et al. 2006; Willis et al. 2008). However, several factors discussed by Willis et al. (2006) must be considered when using sediment traps in this manner to study zooplankton communities. Firstly, only completely intact animals captured in the trap bottles showing no signs of decomposition should be considered for analysis. This

2. General Methods

indicates that the animals entered the trap actively and were killed by the preservative, and excludes detritus from the sample. Secondly, changes in the number of animals captured by the trap should largely be considered reflective of changes in community composition in water layers above the trap. In our case, this layer is approximately 0 – 100 m depth. The seasonal migration behaviour of zooplankton such as *Calanus* copepods (Kwasniewski et al. 2003) creates aggregations consisting of different stages at different depths throughout the annual season, and this will affect the numbers of each stage captured by the trap throughout the season (Willis et al. 2006). This generalisation is affected by zooplankton vertical migrations, which may increase the chances of certain vertically migrating species and stages of zooplankton encountering the sediment trap as they migrate between shallower and deeper waters. The presence of species and stages of zooplankton in the trap usually present in waters > 100 m depth during the sampling period should thus indicate vertical migration behaviour by these species/stages. However, using comparisons with net collected zooplankton at Kongsfjorden (Multinet system described in section 2.2), Willis et al. (2006) draw the conclusion that trends of animals captured in the sediment trap were consistent with trends observed in the net samples. As in their study, this thesis recommends that trends of animals captured using sediment traps should be discussed rather than quantitative abundances, and these trends are most likely to reflect a combination of physical processes (such as water mass advection through the sampled location especially in the 0 – 100 m depth layer), seasonal migratory behaviour and vertical migrations. As the volume of water sampled by sediment trap cannot be reliably quantified (owing to changes in advection above the trap and the fact that the trap is not hauled through a specific volume), quantitative conclusions should be treated with caution.

Using the deployments around the Svalbard archipelago, publications have used sediment trap collected zooplankton both qualitatively (Wallace et al. 2010) and quantitatively in terms of trends (Willis et al. 2006; Willis et al. 2008). Regardless of the complicating factors, these rare data sets are very useful when investigating temporal changes in zooplankton over annual seasons in remote locations.

2.2. Depth stratified vertical net hauls

Chapters 6 and 7 of this thesis investigate zooplankton vertical migration behaviour across a range of contrasting hydrographic conditions in the Svalbard region. The accepted method to gain irrefutable evidence for the migration patterns of zooplankton is considered to be depth stratified sampling (Hardy 1953). When such samples are collected at discrete depths over the entire water column, an increase in surface abundance at night and a corresponding decrease in abundance at depth are considered to be strong evidence of DVM (Cushing 1951). In this thesis, the Multinet Plankton Sampler (MPS), which is equipped with five nets (180 μm mesh size, 0.25 m^2 opening) that close in sequence at discrete depths was used to collect depth stratified zooplankton samples (Fig 2.3). However, a net of this opening size will only effectively sample smaller mesozooplankton due to avoidance by larger faster swimming macrozooplankton (Kasatkina et al. 2004). The smallest volume of water sampled throughout this thesis via net sampling is the 0 – 20 m layer, a volume of 5 m^3 . However, with observed zooplankton abundances well in excess of 500 individuals m^{-3} within this layer, these samples are considered representative of the mesozooplankton community.

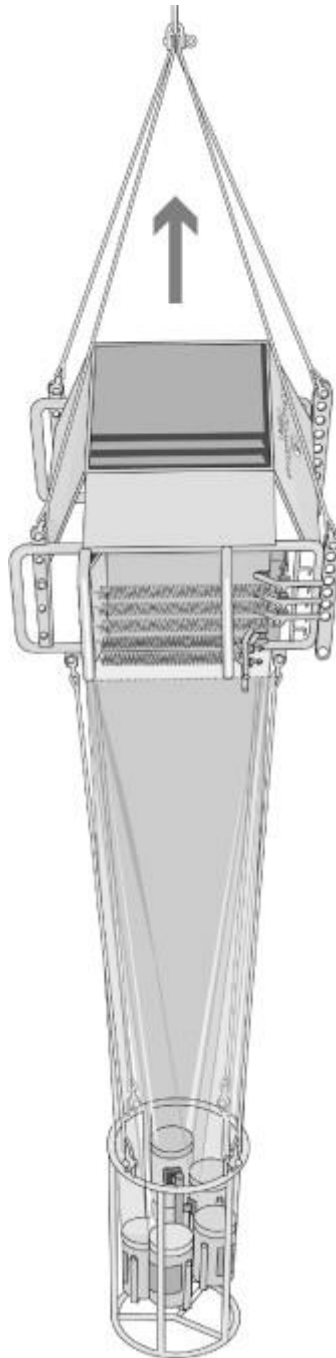


Fig 2.3) Sketch of the vertically hauled (signified by arrow) Multinet Plankton Sampler (MPS). Sample bottles hang in the rig below the net. [Figure from Wenneck et al. 2008, source HYDRO-BIOS Apparatebau GmbH].

2. General Methods

When required, the mean depth (Z_m) of mesozooplankton species and corresponding standard deviations (Z_s) were calculated from MPS determined abundances following the procedure described by Daase et al. (2008). Briefly:

$$Z_m = \frac{1}{2} \sum_{j=1}^n f_j d_j z_j / O$$

(2.1)

$$Z_s = \sqrt{\frac{1}{2} \sum_{j=1}^n f_j d_j z_j^2 / O - Z_m^2}$$

(2.2)

where n is the number of depth intervals, d_j = lower sample – upper sample depth (m) of sample interval j , z_j is the midstrata (m) of sample interval j , f_j is the density of individuals (per m^3) observed in depth interval j , and O corresponds to the area under the frequency curve (i.e. the estimated surface integrated abundance):

$$O = \frac{1}{2} \sum_{j=1}^n d_j f_j$$

(2.3)

2.3. Multi-frequency active acoustics

In order to observe zooplankton over a broader spatial scale at a higher resolution and avoid many of the biases surrounding point sampling, this research uses shipboard multi-frequency acoustic observation. Due to the ability of sound to travel large distances in the ocean and scatter off many organisms, it can be used as a rapid marine survey tool (Stanton et al. 1994). Multi-frequency techniques and acoustic modelling can then be used to identify which organisms are responsible for the acoustic backscatter collected (Stanton and Chu 2000). However, noise effects, especially near the surface (which is a critical area when studying zooplankton migrations) limit the accuracy of acoustic estimation, and smaller organisms tend to be lost amongst stronger echoes. These limitations, alongside difficulties in precisely identifying the scatterers themselves, make acoustic observations a very useful tool alongside net sampling, with net data being used to verify the acoustics (Pearre 2003). This approach is so powerful in gaining observations over broad spatial scales at high resolution that the use of multi-frequency acoustic scattering has become routine in the study of zooplankton (Brierley et al. 1998; Pieper et al. 2001; Lawson et al. 2004). Chapter 5 of this thesis especially uses shipboard multi-frequency acoustic observations collected over a number of years around the Svalbard archipelago and within the key fjords which contain the SAMS moorings to analyse the spatial distributions of zooplankton

For a detailed description of the propagation of sound waves through water with relevance to biological observation, see Horne (2000). The acoustic properties of different target species are known to vary with the operating frequency of the echosounder used, as animals scatter sound differently at different frequencies according to their morphology and material properties (Madureira et al. 1993). Thus, comparing echo levels at different frequencies from a particular target is likely to provide information on the size and type of that target, and this multi-frequency approach has been used for decades to observe marine animals (e.g. McNaught et al. 1975; Greenlaw 1979). This approach is known as the dB difference technique. As the wavelength of sound used to insonify targets increases above the size of the targets, the

2. General Methods

amplitude of the received echoes decreases rapidly (McNaught 1968; Greenlaw 1979; Horne and Clay 1998). Thus to observe zooplankton (the target organisms for this thesis), we need to use high frequency sound. Higher frequencies allow for maximisation of reflection from small zooplankton (Holliday and Pieper 1995). However, higher frequencies of sound are also more rapidly attenuated in sea water which limits their effective range. Observing marine zooplankton using hull-mounted echosounders thus tends to be an exercise in balancing range vs. small target identification. Due to the standardisation of echosounders, a combination of 18, 38, 120 and 200 kHz are often used in multi-frequency acoustic investigations (e.g. Brierley et al. 2001; Kloser et al. 2002; Madureira et al 1993; Watkins and Brierley 2002). In our case, the majority of the vessels available used 18, 38 and 120 kHz echosounders, and although the highest frequency of 120 kHz (approximate wavelength of 12 mm) does not return a high proportion of backscatter from small targets, the 120 kHz – 38 kHz dB difference method has been used in the past to classify zooplankton backscatter (Madureira et al. 1993). Thus, 120 kHz (which allows us a maximum effective observation depth of approximately 175 m) is a good compromise between maximal range and small target observation.

The calculation of likely backscatter from a target using theoretical backscatter models (reviews in Horne and Clay 1998; Stanton and Chu 2000) is known as forward modelling. Although target numerical density and biomass estimation (a primary use of forward modelling) is not a focus of this thesis, we still had to choose how to partition our backscatter and best separate zooplankton echoes from the rest. We can then use a zooplankton portion of the backscatter to assess patterns in zooplankton vertical and spatial distribution around the Svalbard archipelago. In order to determine the expected dB difference (120 kHz – 38 kHz) from zooplankton targets in our study area of the Svalbard archipelago, TS for these frequencies was modelled using simple models (as in Brierley et al. 2005) and length frequencies gathered from net sampled zooplankton in the archipelago. Although more modern higher resolution models exist, the simpler models used here are still applicable due to their ease of use under limited conditions (Stanton and Chu 2000). As in Brierley et al. (2005), the models used were the simplified fluid sphere for copepods (Greenlaw 1979), the randomly oriented fluid bent

2. General Methods

cylinder for euphausiids and chaetognaths (Stanton et al. 1994), and the straight fluid cylinder for amphipods (Trevorrow and Tanaka 1997) (Table 2.1). All these models required assumptions about the material properties of target organisms to be made. The two assumptions for parameterisation were g (density of organism : density of seawater ratio) and h (speed of sound in the organism : speed of sound in seawater ratio).

Following Brierley et al. (2005), we used median values for g and h gathered from the extensive literature (1.04 for both). All models were parameterised with a sound velocity in seawater of 1500 m s^{-1} , which is the generally accepted value. Table 2.1 outlines the models and zooplankton lengths used, while the 120 kHz – 38 kHz Mean Volume Backscattering Strength (when using a target density of $1 \text{ individual m}^{-3}$) is displayed in figure 2.4.

2. General Methods

Table 2.1) Zooplankton taxon sampled in the Svalbard archipelago (2009 and 2010 - length frequencies courtesy of the Norwegian Polar Institute). CI – CV = copepodite stages, AF = Adult Female. Models used to predict TS are the Simplified Fluid Sphere (SFS), Straight Fluid Cylinder (SFC) and randomly oriented Fluid Bent Cylinder (FBC). *¹ denotes body length to width ratio of 16 (Brierley et al. 2005) and *² denotes body length to width ratio of 8 (Stanton et al. 1994). TS models are parameterised using values specified in section 2.3. The euphausiid FBC model was used to predict backscatter from a range of lengths since no length frequency information was available.

Species / Stage	Taxon	Model Type	Size (mm) Mean (SD)	TS	TS	Source
				38 kHz (dB)	120 kHz (dB)	
<i>Calanus</i> CI	Copepod	SFS	0.69 (0.07)	-163.77	-143.79	Greenlaw (1979)
<i>Calanus</i> CII	Copepod	SFS	0.95 (0.08)	-155.43	-135.46	Greenlaw (1979)
<i>Calanus</i> CIII	Copepod	SFS	1.47 (0.18)	-144.07	-124.11	Greenlaw (1979)
<i>Calanus</i> CIV	Copepod	SFS	2.01 (0.30)	-135.90	-115.95	Greenlaw (1979)
<i>Calanus</i> CV	Copepod	SFS	2.84 (0.39)	-126.90	-107.03	Greenlaw (1979)
<i>Calanus</i> AF	Copepod	SFS	2.76 (0.26)	-127.63	-107.75	Greenlaw (1979)
<i>O. similis</i>	Copepod	SFS	0.45 (0.05)	-175.06	-155.09	Greenlaw (1979)
<i>O. atlantica</i>	Copepod	SFS	0.67 (0.07)	-164.47	-144.49	Greenlaw (1979)
<i>Pseudocalanus</i>	Copepod	SFS	0.80 (0.19)	-159.94	-139.97	Greenlaw (1979)
<i>Microcalanus</i>	Copepod	SFS	0.46 (0.06)	-174.45	-154.48	Greenlaw (1979)
<i>T. borealis</i>	Copepod	SFS	0.45 (0.04)	-174.91	-154.94	Greenlaw (1979)
<i>T. abyssorum</i>	Amphipod	SFC	4.52 (1.59)	-117.32	-98.08	Trevorrow and Tanaka (1997)
<i>T. libellula</i>	Amphipod	SFC	7.61 (3.97)	-103.87	-85.96	Trevorrow and Tanaka (1997)
<i>S. elegans</i>	Chaetognath	FBC * ¹	14.57 (4.61)	-110.55	-97.99	Stanton et al. (1994)
<i>E. hamata</i>	Chaetognath	FBC * ¹	9.54 (4.04)	-116.12	-104.94	Stanton et al. (1994)
	Euphausiid	FBC * ²				Stanton et al. (1994)

2. General Methods

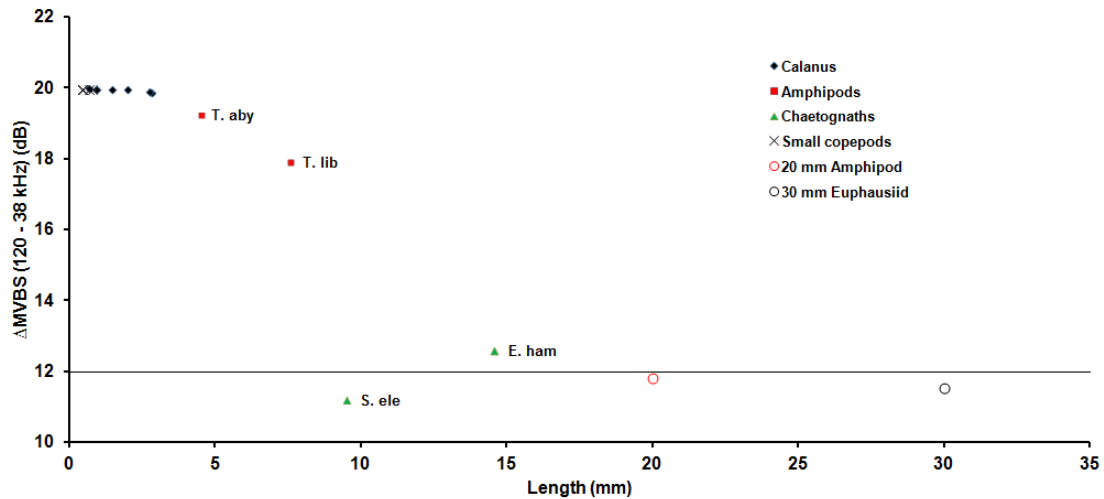


Fig 2.4) 120 kHz – 38 kHz MVBS (animal density of 1 individual m^{-3}) displayed for *Calanus* (stages CI – Adult Female), small copepods including *Oithona similis*, *Pseudocalanus* spp. and *Microcalanus* spp., amphipod species *Themisto libellula* and *Themisto abyssorum* and chaetognath species *Sagitta elegans* and *Eukrohnia hamata* sampled around the Svalbard archipelago in 2009/10 (models and lengths used outlined in Table 2). An amphipod of 20 mm length and a euphausiid of 30 mm length are included as reference. Black horizontal line at 12 dB Δ MVBS indicates upper limit of published 2 – 12 dB krill partition (Brierley et al. 1997; Brierley et al. 1998).

Madureira et al. (1993) have published one general method of partitioning backscatter based on 120 kHz – 38 kHz dB differences. In this method, they identify three distinct echo distributions belonging to three different groups of animal. Fish and squid (or nekton) have a Δ MVBS of < 2 dB, krill (or macrozooplankton) have the well established Δ MVBS of 2 – 12 dB, and zooplankton (or mesozooplankton) have a Δ MVBS > 12 dB. Δ MVBS values > 12 dB indicate higher echo intensity at 120 kHz than at 38 kHz, and this suggests that the targets are Rayleigh scatterers and so smaller than krill (i.e. acoustic cross section is equal to or less than the wavelength at 38 kHz, Clay and Medwin 1977).

When the measured lengths of copepods and amphipods around Svalbard (Table 2.1) were used in forward TS modelling, it became apparent that any differentiation between the small copepods would be impossible. The small amphipods were also too close to larger copepods in terms of their Δ MVBS values to be separated effectively using these two frequencies (Fig 2.4). However, the Madureira et al. (1993) classification system did largely remove backscatter due to chaetognaths (Fig 2.4) from the mesozooplankton

2. General Methods

portion, and also any macrozooplankton longer than approximately 2 – 3 cm. Since it is not possible to accurately separate purely copepod backscatter, or differentiate between mesozooplankton species using these frequencies, the Madureira et al. (1993) general backscatter classification system is used in this thesis. Thus, all acoustics will be discussed in terms of nekton, macrozooplankton and mesozooplankton backscatter, with net samples utilised whenever possible to better identify targets responsible for the backscatter within these partitions.

All data were logged using Echolog 60 (SonarData). Throughout most of the acoustic record, ship engine noise and surface disturbance produced noise spikes and bubble occlusions in the acoustic record, and these were removed in post-processing. The echosounder was calibrated at all frequencies prior to all cruises, and acoustic post-processing was conducted using Echoview (SonarData). Calibration-corrected acoustic data at each frequency were resampled onto a 12 ping (horizontal) X 2 m (vertical) grid to remove stochastic ping-to-ping variation (as in Brierley et al. 1998). With this resampled data, TVG (time varied gain) amplified noise was removed as per Watkins and Brierley (1996), and background noise was removed using the SNR (signal-to-noise ratio) technique as per De Robertis and Higginbottom (2007).

When reporting acoustic observations throughout this thesis, a number of measures of backscatter are used:

- 1) Volume backscattering strength in dB re 1 m^{-1} (S_v , which becomes Mean Volume Backscattering Strength – MVBS – when s_v is averaged over a finite volume).

$$S_v = 10 \log_{10}(s_v) \tag{2.4}$$

where s_v is the volume backscattering coefficient, the sum of all discrete targets in the sampled volume. For detailed explanation of all acoustic scattering equations, see MacLennan et al. (2002).

- 2) Nautical area scattering coefficient (NASC) in $\text{m}^2 \text{ nmi}^{-2}$, a measure of area scattering scaled using the nautical mile (1 nmi = 1852 m).

$$NASC = 4\pi(1852)^2 s_a \tag{2.5}$$

where s_a is the area scattering coefficient, the integral of s_v over a range interval (see MacLennan et al. 2002).

2.4. Multivariate analysis

Much of this section has been gleaned from the PhD thesis and methods of Saunders (2008). When focussing on trends, patterns and differences in community data comprising of numerous species/observations, it is useful to analyse the entire data set

2. General Methods

within the same test. This approach avoids breaking the data set into many single variables and allows the various variables to be ranked for significance inclusively. Thus when analysing DVM for example, multivariate analysis allows us to test all the observed species together and determine which are most responsible for the signal, rather than testing each one individually.

To analyse data from multiple samples and species together, the data need to be transformed to prevent the results being dominated by larger values. Transformations such as square root, fourth root and log transforms lower all data values, but lower larger values disproportionately more. With the ecological assumption that increasing numbers of a species become less significant the more they increase, transformation becomes very important for community data. Some accuracy is lost in any transformation, so the lowest level deemed sufficient must be used. Following numerous trials with various transformations and the associated draftsman plots, this thesis uses fourth root transformation across all community data (both net observed animal densities and acoustic backscatter observations) to ensure a standardised analysis between all communities and locations.

The draftsman plot is a method of determining the lowest required level of data transformation prior to multivariate analysis. With sufficient transformation, samples should be spread evenly from left to right and top to bottom on the plot. With abundance data (for this example the abundance of *Calanus finmarchicus* from chapter 4 of this thesis, Fig 2.5), square root transformation (B, Fig 2.5) appeared to be insufficient as many samples were clustered near the origin. Although log transformation (C, Fig 2.5) resulted in the most even spread of samples across the plot, the spread was similar to fourth root transformed data (A, Fig 2.5). Thus, the lowest level of sufficient transformation (fourth root) was selected.

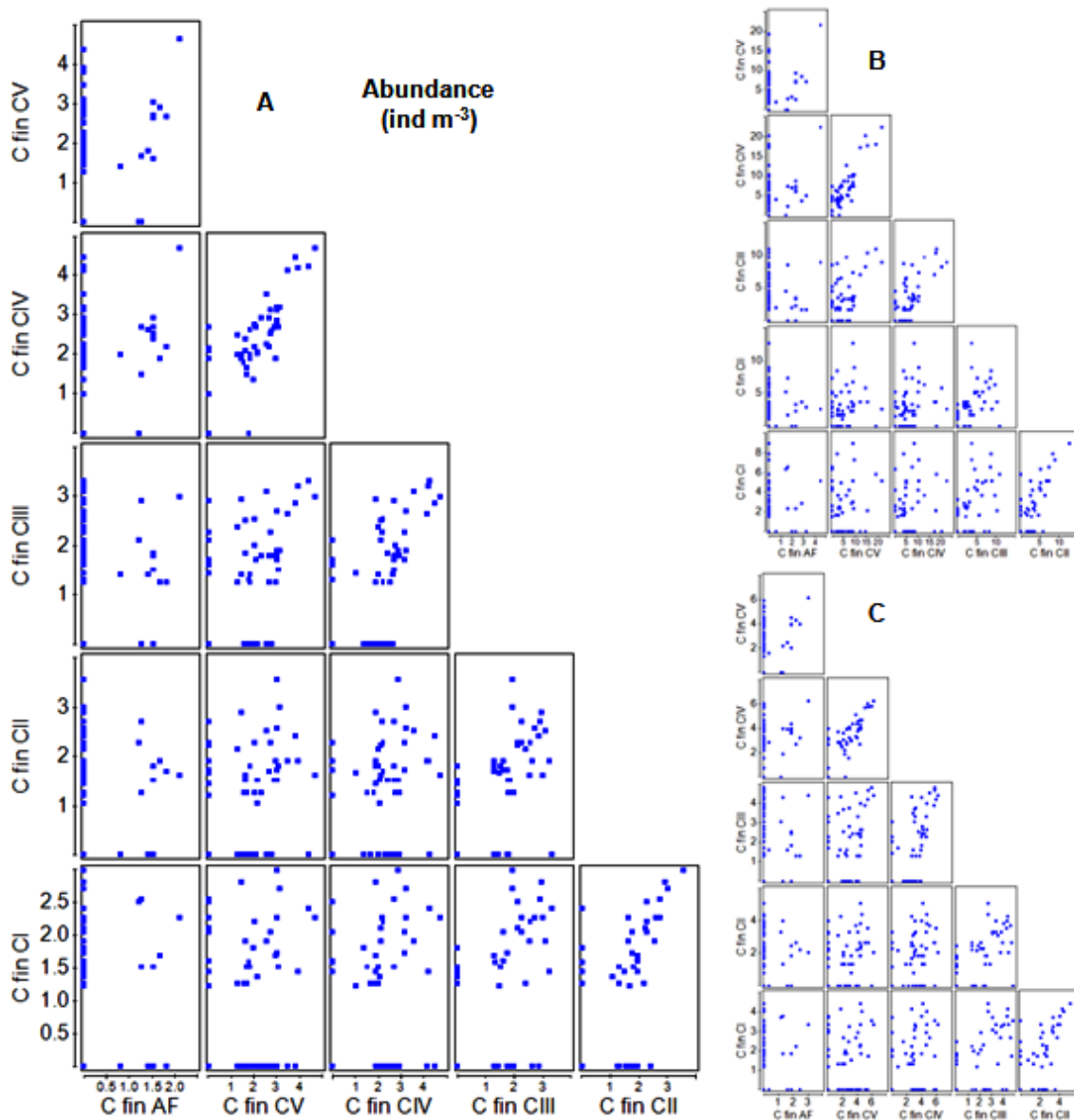


Fig 2.5) Draftsman plots of five stages of *Calanus finmarchicus* (C fin CI – AF, individuals m⁻³) collected by Multinet at KMT01, KMT02, KMT03, KMT04, KMT05, KMT06, BMT01, BMT02, BMT03, RMT01, RMT02, RMT03 (see chapter 4, Table 4.1 for station details). A = fourth root transformation, B = square root transformation, C = log(X + 1) transformation.

With s_v data (for this example s_v from mesozooplankton, macrozooplankton and nekton binned in 25 m vertical depth layers from chapter 4 of this thesis, Fig 2.6), square root transformation (B, Fig 2.6) again appeared to be insufficient as many samples were clustered near the origin. With s_v data however, log transformation (C, Fig 2.6) resulted

in the least spread of samples across the plot. With this data, fourth root transformation created the most even spread (A, Fig 2.6), and so was selected.

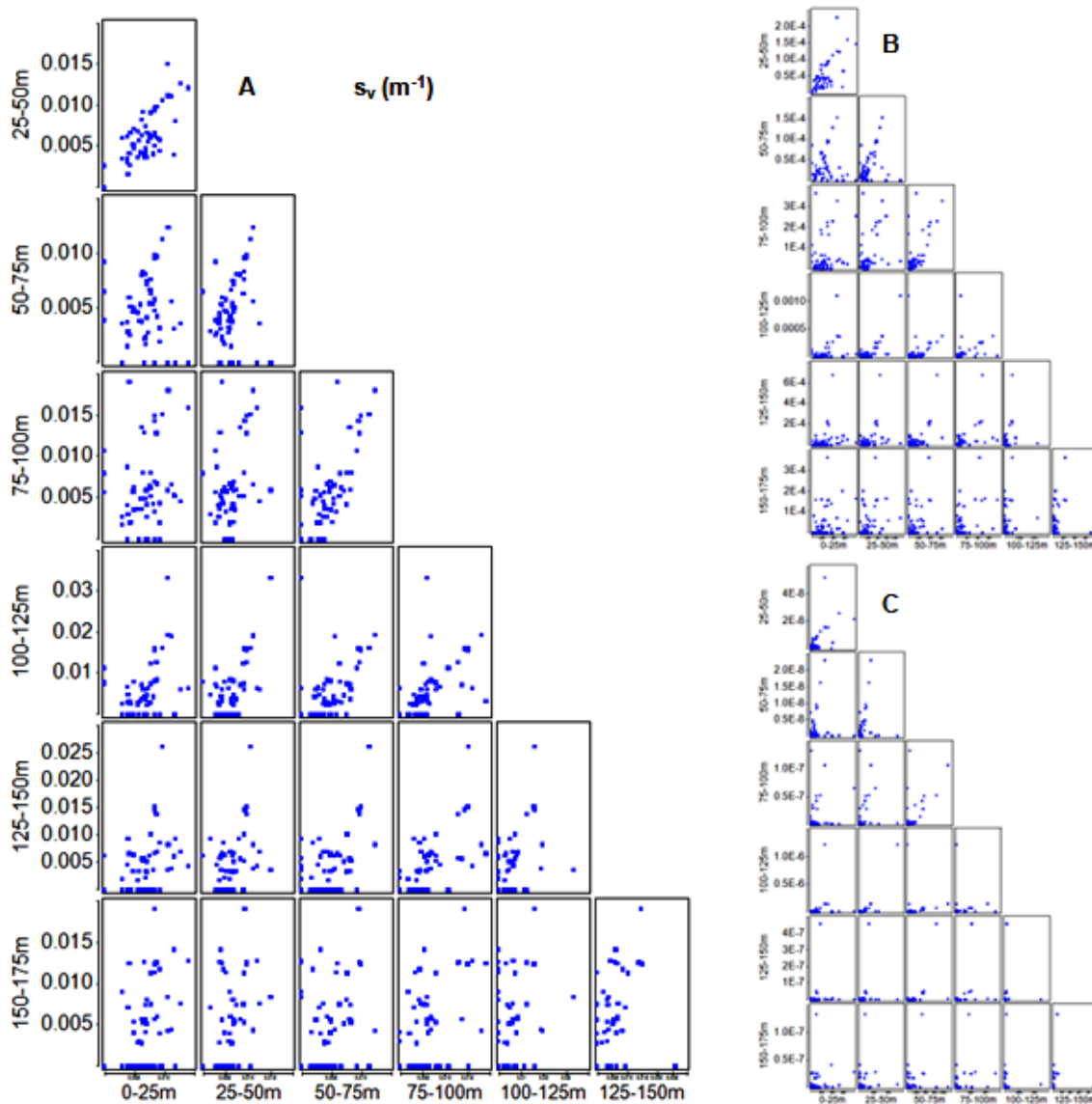


Fig 2.6) Draftsman plots of mesozooplankton, macrozooplankton and nekton s_v binned in 25 m vertical depth layers (m^{-1}) collected at 120 kHz at KMT01, KMT02, KMT03, KMT04, KMT05, KMT06, RMT01, RMT02, RMT03 (see chapter 4, Table 4.1 for station details). A = fourth root transformation, B = square root transformation, C = $\log(X + 1)$ transformation.

Finally, with NASC data (for this example NASC from mesozooplankton, macrozooplankton and nekton binned in 25 m vertical depth layers from chapter 7 of this thesis, Fig 2.7), the plots with square root transformed data (B, Fig 2.7) and log

2. General Methods

transformed data (C, Fig 2.7) followed a similar pattern to the plots using s_v , and again showed insufficient transformation. Fourth root transformation created the most even spread with NASC as with s_v (A, Fig 2.7), and so was selected for use.

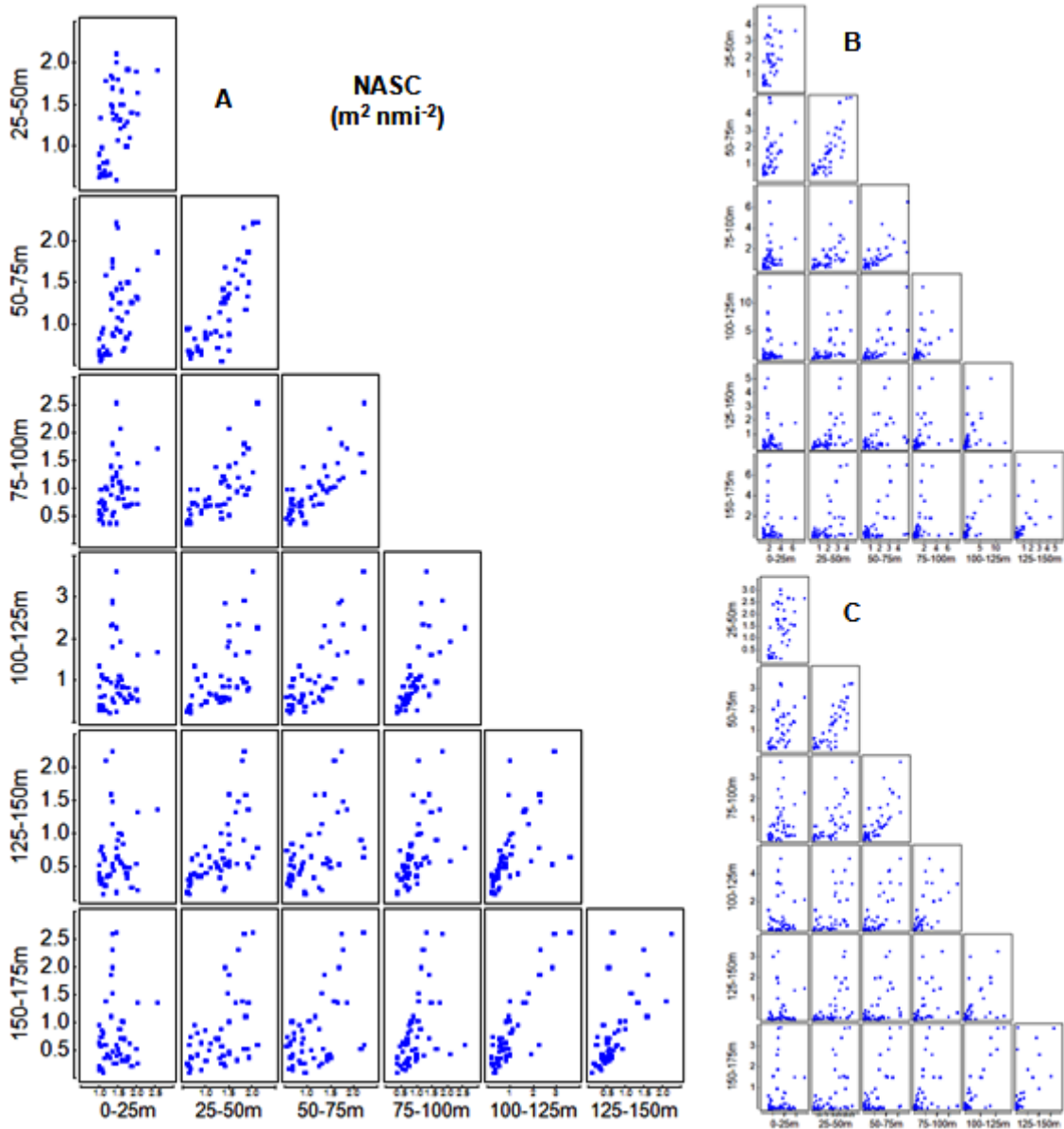


Fig 2.7) Draftsman plots of mesozooplankton, macrozooplankton and nekton NASC binned in 25 m vertical depth layers ($\text{m}^2 \text{nmi}^{-2}$) collected at 120 kHz at ICE19 and ICE22 (see chapter 7, Table 7.1 for station details). A = fourth root transformation, B = square root transformation, C = $\log(X + 1)$ transformation.

2. General Methods

In this thesis, PRIMER v 6.19 (Clarke and Gorley 2006) is used for all multivariate analysis. Nearly all analysis using this package is based on comparisons of distributions and distances between samples in multidimensional space. The number of dimensions depends on the number of variables. Euclidean distances between samples can be used with environmental data but are not appropriate for community data. This is due to the differences in comparing joint absences and equal abundances in the two types of data. In environmental data, a zero has equal significance to any other value. However, when comparing two communities there is a theoretically infinite number of species that do not occur in either sample. Within this framework, an equal non-zero abundance of any particular species should increase sample similarity but the infinite joint absences should not. To implement this, distances between community samples (A and B) are calculated using the Bray-Curtis Similarity Index (S):

$$S = 100 \times \left(1 - \left(\frac{\sum |A_x - B_x|}{\sum (A_x + B_x)} \right) \right) \quad (2.6)$$

where A_x and B_x are the abundance of x th species in samples A and B respectively.

2. General Methods

In order to visualise the distribution of samples in multidimensional space, a non-metric multidimensional scaling (MDS) plot is used. The plot contains no scale or axis, and the only important feature is the distance between samples, with closer samples being more similar to each other. To calculate statistical differences between groups of samples perceived on an MDS plot, Analysis of Similarity (ANOSIM) can be used. The test quantifies differences between groups (R) and gives it a significance value (p). The R value is calculated using the similarities within the Bray-Curtis similarity matrix in their ranked order, and compares average rank similarities of samples within groups to average rank similarities of samples between groups using:

$$R = X - Y / (0.5 \times (n(n - 1) / 2)) \quad (2.7)$$

where X = average ranked similarity between each sample in different groups, Y = average ranked similarity of samples in each group, and n = total number of samples. The ANOSIM R can be between -1 and 1, with negative numbers implying greater similarity between groups than within groups. 0 indicates no difference between groups, increasing to 1 for a complete difference. Taking this statistical test a step further, Similarity Percentage (SIMPER) analysis compares groups of samples on a species level, identifying how much each species accounts for the differences between groups. Finally, the BIO-ENV procedure performs a weighted Spearman rank correlation of the similarities between community samples (Bray-Curtis similarities) and the similarities in environmental data for the same samples (Euclidean distances). Results are between 0 and 1 for no correlation and complete correlation respectively.

3. Moored seasonal observations of zooplankton at Kongsfjorden and Rijpfjorden

3.1. Introduction

Continuous zooplankton time series are difficult to obtain in the Arctic over long periods of time due to the harsh and changeable environmental conditions. Locations may change between an ice-free and ice-covered state throughout the annual season, and winds and currents are changeable creating challenging conditions for repeat sampling. In order to gather observations over long periods of time in the Arctic, the Svalbard archipelago has been used as a study area which encompasses the wide variety of hydrological conditions found throughout the Arctic in an accessible area (see section 1.3.1 for detailed Svalbard hydrology). SAMS and NPI together maintain long-term oceanic moorings in two fjords of contrasting hydrology, Atlantic Water (AtW) dominated Kongsfjorden and Arctic Water (ArW) dominated Rijpfjorden. Alongside making hydrographic observations, these moorings include sediment traps deployed at a depth of approximately 100 – 125 m. Over a number of years since their first deployment in 2002, these sediment traps have been collecting a continuous time-series of zooplankton within these two fjords. Elements of this rare data set have been used in numerous publications to observe zooplankton vertical migration behaviour at high latitude (Wallace et al. 2010) and also discuss the influence of advection in Kongsfjorden (Willis et al. 2006; Willis et al. 2008).

The detailed hydrology Kongsfjorden and Rijpfjorden, the two contrasting fjords, have been outlined in detail in section 1.3.1 of this thesis. Briefly, Kongsfjorden is influenced by the dominant water masses found along the West Spitsbergen Shelf which include a mixture of Atlantic, Arctic and glacial water masses (Saloranta and Svendsen 2001). AtW influence at Kongsfjorden varies throughout the annual cycle, and Kongsfjorden

3. Moored seasonal observations of zooplankton at Kongsfjorden and Rijpfjorden

and the adjacent shelf switch from a state of Atlantic dominance in summer (warm and saline) to one of Arctic dominance in winter (cold and saline) (Svendsen et al. 2002; Cottier et al. 2005). ArW is also carried northward along the west coast of Svalbard to Kongsfjorden, but this time in a coastal current on the shelf itself (Willis et al. 2006). It is important to note that AtW entering Kongsfjorden mixes with ArW as it crosses the shelf to form Transformed Atlantic Water (TAtW), with temperatures and salinities distinct from the core of the WSC (Willis et al. 2006). For details on the well documented circulation regime within Kongsfjorden, please see Svendsen et al. 2002, Basedow et al. 2004 and Cottier et al. 2005. The zooplankton community in Kongsfjorden comprises co-occurring boreal and Arctic species which respond to changes in the dominant water masses along the western Svalbard coast (Kwasniewski et al. 2003). Zooplankton species associated with AtW masses include the copepods *Calanus finmarchicus* and *Oithona atlantica* (Kielhorn 1952; Brodsky 1967), the amphipod *Themisto abyssorum*, the appendicularian *Fritellaria borealis* (Arashkevich et al. 2002) and euphausiids of the genus *Thysanoessa* (Willis et al. 2006). Zooplankton species associated with ArW masses include the copepod *Calanus glacialis* (Unstand at Tande 1991), the chaetognath *Sagitta elegans*, the amphipod *Themisto libellula* (Dalpadado et al. 2001) and the pteropods *Clione limacina* and *Limacina helicina* (Willis et al. 2006). The co-occurring *Calanus* populations which dominate the zooplankton numerically within Kongsfjorden consist of local and advected individuals, with the relative proportions of each based on the volume of AtW and ArW intrusions into the fjord (Kwasniewski et al. 2003). *Calanus hyperboreus*, the oceanic deeper water species of *Calanus* (Hirche 1997), has also been identified as an expatriate in the fjord, with advection of ArW the sole supply of fresh individuals into the fjord (Kwasniewski et al. 2003). Advection is known to critically influence the zooplankton community within Kongsfjorden (Willis et al. 2006; Willis et al. 2008).

Contrastingly, Rijpfjorden is situated on the north coast of Nordaustlandet in the northeast of the archipelago at 80°N. Although AtW influence within the WSC may reach this area, Rijpfjorden is dominated by typically Arctic conditions (Berge et al. 2009; Wallace et al. 2010) and is covered by fast ice for 6 – 8 months a year. The three

3. Moored seasonal observations of zooplankton at Kongsfjorden and Rijpfjorden

Calanus copepods and the pteropod *Limacina helicina* are known to dominate the mesozooplankton community within Rijpfjorden, with the occurrence of ice associated macrozooplankton such as the amphipod *Gammarus wilkitzkii* (Lønne and Gulliksen 1991) far more likely than at Kongsfjorden.

Using sediment trap collected zooplankton from Kongsfjorden and Rijpfjorden, the aim of this chapter is to investigate changes through the annual season. Since we have collected zooplankton over a number of years within these fjords, we will also investigate interannual changes within each fjord under the varying influences of the dominant water masses. These relationships between the zooplankton community and the respective hydrographic conditions have implications within the current scenario of a warming Arctic. Although one may debate the accuracy of using sediment trap collected zooplankton to observe changes in the zooplankton community, a previous study in Kongsfjorden comparing net collected zooplankton communities from a location close to the mooring to the sediment trap collected community (Willis et al. 2006) throughout the annual season concluded that the trends observed in the sediment trap were representative of the net sampled zooplankton community. Their study also recommended using the trends within the sediment trap collected community over time rather than the numbers of animals caught in the trap when discussing the changes in zooplankton. Our study builds on this research by extending it geographically to Rijpfjorden and thus including an ArW site for comparison, and also temporally to investigate interannual variations.

3.2. Materials and methods

3.2.1. Sampling location

This investigation was carried out over approximately three years at Kongsfjorden (two mooring deployments between 2006 – 2009) and five years at Rijpfjorden (four mooring deployments between 2006 – 2011) (Table 3.1, Fig 3.1). The majority of the deployments lasted from approximately September to August of the following year.

3. Moored seasonal observations of zooplankton at Kongsfjorden and Rijpfjorden

Table 3.1) Details of each mooring deployment including location, start and end date, sediment trap depth, bottle sequence and Seabird microcat (recording temperature and salinity) depths

Location (year)	Latitude (N)	Longitude (E)	Deployment start Date	Deployment end Date	Trap depth (m)	Bottle start dates	Microcat depths (m)
Kongsfjorden (2006/07)	79°01.198	11°46.417	07/06/06	25/08/07	101	10/06/06 , 01/07/06, 01/08/06, 01/09/06, 01/10/06, 01/11/06, 01/12/06, 01/01/07, 01/02/07, 01/03/07, 01/04/07, 08/04/07, 15/04/07, 22/04/07, 01/05/07, 08/05/07, 15/05/07, 22/05/07, 01/06/07, 01/07/07, 01/08/07 05/09/08, 01/10/08, 01/11/08, 01/12/08, 01/01/09, 04/02/09, 18/02/09,	19, 198
Kongsfjorden (2008/09)	78°59.179	11°20.929	04/09/08	22/08/09	103	04/03/09, 18/03/09, 01/04/09, 08/04/09, 15/04/09, 22/04/09, 29/04/09, 06/05/09, 13/05/09, 20/05/09, 27/05/09, 03/06/09, 01/07/09, 29/07/09 02/09/06, 01/10/06, 01/11/06, 01/01/07, 01/03/07, 01/04/07, 29/04/07, 15/07/07, 22/07/07, 29/07/07, 05/08/07, 12/08/07	25, 201
Rijpfjorden (2006/07)	80°17.600	22°18.800	01/09/06	22/08/07	106	04/09/07, 01/10/07, 01/11/07, 01/12/07, 01/01/08, 04/02/08, 18/02/08, 03/03/08, 17/03/08, 31/03/08, 14/04/08, 28/04/08, 12/05/08, 26/05/08, 09/06/08, 23/06/08, 07/07/08, 14/07/08, 21/07/08, 28/07/08, 11/08/08	24, 203
Rijpfjorden (2007/08)	80°16.889	22°18.954	04/09/07	16/08/08	104	01/09/09, 01/10/09, 01/11/09, 01/12/09, 01/01/10, 01/02/10, 01/03/10, 15/03/10, 29/03/10, 12/04/10, 26/04/10, 10/05/10, 24/05/10, 07/06/10, 21/06/10, 28/06/10, 05/07/10, 12/07/10, 19/07/10, 26/07/10, 09/08/10	12, 198
Rijpfjorden (2009/10)	80°17.030	22°18.150	01/09/09	19/09/10	102	01/10/10, 01/11/10, 01/12/10, 01/01/11, 01/02/11, 01/03/11, 15/03/11, 29/03/11, 12/04/11, 26/04/11, 10/05/11, 24/05/11, 07/06/11, 21/06/11, 28/06/11, 05/07/11, 12/07/11, 19/07/11, 26/07/11, 09/08/11, 23/08/11	27, 211
Rijpfjorden (2010/11)	80°17.223	22°15.455	21/09/10	30/08/11	115		33, 222

3. Moored seasonal observations of zooplankton at Kongsfjorden and Rijpfjorden

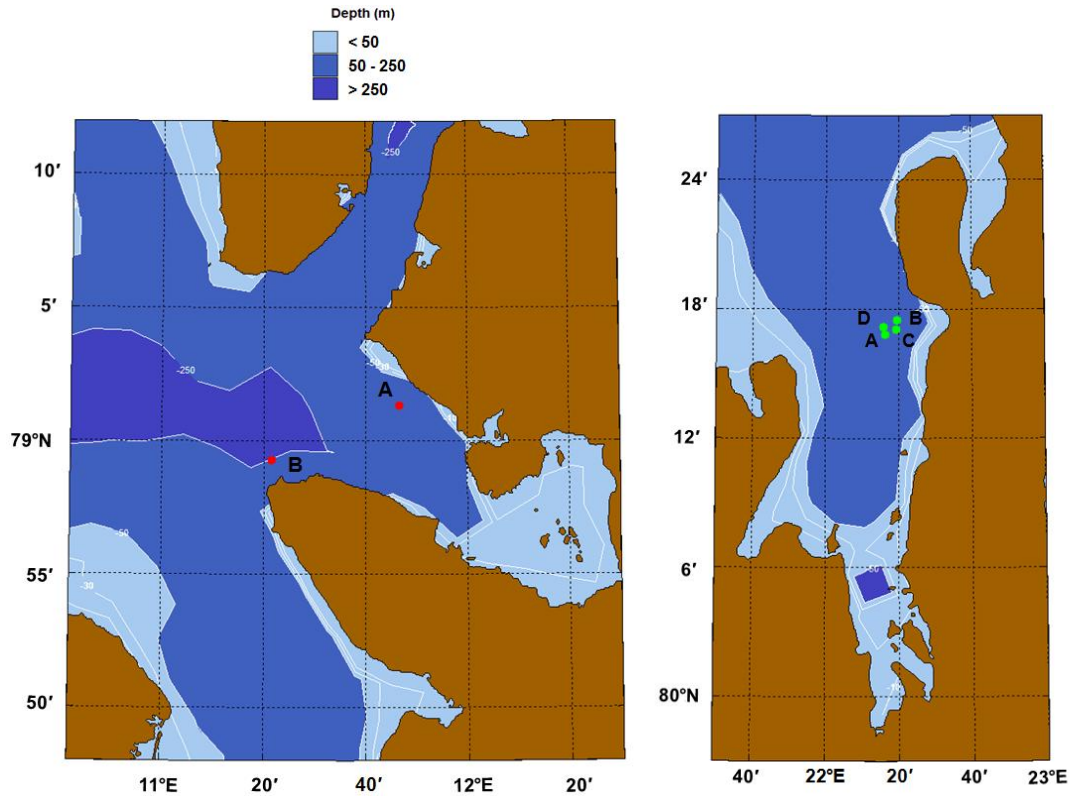


Fig 3.1) Left – map of Kongsfjorden with 2006/07 (A) and 2008/09 (B) mooring locations. Right – map of Rijpfjorden with 2006/07 (A), 2007/08 (B), 2009/10 (C) and 2010/11 (D) mooring locations. For broad scale Svalbard archipelago hydrology, see section 1.3.1.

In order to discuss the hydrography of the two fjords, we must first define the water masses. As used by Willis et al. (2006), our water mass definitions are gathered from the Svendsen et al. (2002) study of Kongsfjorden. In order to compare the two fjords consistently, the same water mass definitions are applied to Rijpfjorden. See section 1.3.1 for details.

3.2.2. Environmental parameters

Two Seabird 37 Microcats were deployed on each mooring at similar depths to continuously record both surface and bottom temperature and salinity above and below the sediment trap (Table 3.1). The surface microcat varied between 12 – 33 m depth

3. Moored seasonal observations of zooplankton at Kongsfjorden and Rijpfjorden

between deployments, and the bottom microcat between 198 – 222 m. Mean temperature (T) and salinity (S) were calculated over the entire duration of each sediment trap bottle sample (for bottle durations, see Table 3.1) in order to best compare the zooplankton community to the dominating hydrographic conditions. The Arctic sea-ice concentrations (observed by AMSR-E and projected using arctic grids from NSIDC at 6.25 km resolution by the University of Bremen) described in section 1.3.1 will be referred to when discussing prevailing ice conditions. An upward looking ADCP was deployed on each mooring at approximately 100 m depth, and observations of eastward and northward horizontal current velocities between 15 – 95 m were collected at 20 min x 4 m depth resolution. Negative eastward flow indicates westward flow while negative northward flow indicates southward flow. These current velocities and monthly averages are fully described in section 1.5.1, and referred to through this chapter.

3.2.3. Sediment trap zooplankton sampling

A sequential sediment trap (McLane Parflux 78H-21, 21 bottle carousel, 0.5 m² opening) was deployed on each mooring between 100 – 115 m water depth (Table 3.1). Mooring deployment and recovery was carried out mostly by RV *Jan Mayen*, with RV *Lance* used in Kongsfjorden to deploy the mooring in 2006. The sampling frequency for each bottle in the sequence was designed to most effectively sample the entire annual season with highest resolution during the productive period. Thus, at Kongsfjorden bottle durations were generally one month between June and March, decreasing to one week during the productive period in April/May (Table 3.1). Similarly at Rijpfjorden, bottle durations were generally approximately one - two months between September and March, decreasing to two weeks through March, April and May and one week between June and July/August. These differences in timing of the sequential sediment trap reflected the differences in timing of the ‘spring’ phytoplankton bloom and associated productivity in the two fjords (Zenkevitch 1963; Falk-Petersen et al. 2007; Søreide et al. 2008, Leu et al. 2011). Due to these differences in duration for each bottle in the sequence combined with the quasi-quantitative sampling manner of our sediment trap, comparisons of numerical abundance between bottles should be made with

3. Moored seasonal observations of zooplankton at Kongsfjorden and Rijpfjorden

caution, and rather the trends and patterns in community composition should be discussed.

The trap sample bottles were filled with filtered seawater containing NaCl to create a density gradient between the bottle and the surrounding seawater, and 2% formalin buffered with sodium borate to preserve any collected zooplankton. For each deployment, trap samples were passed through the smallest possible sieve in order to collect as much of the zooplankton community as possible while removing sediments from the sample. This mesh size differed based on the quantities of sediment in each deployment, and varied between 150 – 300 μm . Thus for certain deployments, smaller species such as *Microcalanus* and *Oithona* may not have been retained proportionally on the sieve. However, within each deployment, the results are comparable as the same mesh sieve was used in each case between samples. When comparing between deployments, the smaller species are excluded from analysis. All animals retained on the sieve were intact and showed no signs of decomposition. This suggests they entered the trap alive and were subsequently killed by the preservative. All zooplankton were sorted and identified as per Falk-Petersen et al. (1999) and Daase and Eiane (2007). *Calanus* were identified and staged by prosome length as per Kwasniewski et al. (2003). Zooplankton species are presented as numbers per trap sample in this study.

3.2.4. Multivariate analysis

Similarity matrices created in PRIMER were used to test for changes in zooplankton species composition over time (i.e. differences between the zooplankton communities in each bottle through each deployment). Bottles which were empty were excluded from the analysis as they will highly skew the grouping. Due to the use of varying bottle durations throughout each deployment (i.e. numerical abundances will vary based on the duration of each bottle), fourth root transformations were carried out on all zooplankton numerical data before Bray-Curtis analysis. This transformation disproportionately reduces larger values, and so trends in community composition

3. Moored seasonal observations of zooplankton at Kongsfjorden and Rijpfjorden

become more important through the data set rather than numerical abundances. For reference, a run of the analysis was carried out with the weekly trap samples pooled for comparison with the monthly samples, and similar trends in similarity between sample groups through time were obtained. Bray-Curtis similarity was used to compare samples in order to remove the effects of joint species absences between samples and focus on the species present through the time series (see section 2.4 for details on the multivariate techniques used here). Once the Bray-Curtis similarity matrix was created between all samples, hierarchical clustering was used to create a dendrogram of similarity between samples. This routine was carried out on:

- 1) Each deployment separately using all the identified zooplankton species. Similar samples were then grouped together to identify phases in zooplankton community over time. Empty bottles are displayed in their relevant phase chronologically although they were not included in the cluster analysis. These phases are displayed on time series plots of the dominant zooplankton species along with the mean surface and bottom temperature for each sample. In order to maintain temporal resolution, samples are not pooled to create equivalent time durations throughout each deployment.
- 2) Pooled deployments at each fjord (i.e. two deployments at Kongsfjorden and four at Rijpfjorden). When comparing between deployments, smaller zooplankton species were excluded from analysis due to interannual variations in sieve mesh size. This approach allowed interannual differences in zooplankton community to be assessed within each location

Similarity percentage analysis was carried out to determine which species were most responsible for the identified phases in zooplankton community composition at each deployment, and also for interannual differences within each location in terms of percentage contribution. Finally, a weighted Spearman rank correlation was carried out on similarities between community samples (Bray-Curtis similarity) and the similarities between mean temperature and salinity for each sample (Euclidean distance matrix). This correlation quantifies the degree to which changes in the community align with

3. Moored seasonal observations of zooplankton at Kongsfjorden and Rijpfjorden

changes in the physical environment, and the physical variables included were mean sample surface temperature and salinity and mean sample bottom temperature and salinity.

3.3. Results

3.3.1. Sediment trap zooplankton

Zooplankton taxa recorded in the samples included 35 species/genera (Table 3.2). At Kongsfjorden, *Calanus* copepods, *Pseudocalanus* spp., *Microcalanus* spp., *Metridia longa* and bivalve veligers were most numerous in trap samples, with copepods dominant across both deployments. At Rijpfjorden, *Oithona* spp., polychaete larvae, copepod nauplii and larger macrozooplankton species such as *Themisto libellula* and *Gammarus wilkitzkii* tended to dominate alongside the *Calanus* copepods (Table 3.2). In 2006/07, the only directly comparable season between Kongsfjorden and Rijpfjorden, over twice the number of animals overall were recorded in the samples at Kongsfjorden.

3. Moored seasonal observations of zooplankton at Kongsfjorden and Rjipfjorden

Table 3.2) Relative numerical abundance (% of total across the deployment) of the main species identified in the trap samples at each deployment. Total deployment numerical abundance and the mesh sized used to remove zooplankton also noted.

Deployment	KF	KF	RF	RF	RF	RF
	2006/07	2008/09	2006/07	2007/08	2009/10	2010/11
Mesh size (μm)	300	150	300	150	150	150
Total numerical abundance	2800	1676	1021	1401	5734	2523
Copepods	(%)	(%)	(%)	(%)	(%)	(%)
<i>Calanus finmarchicus</i>	33.6	9.7	6.5	17.0	0.6	1.2
<i>Calanus glacialis</i>	33.6	21.0	27.3	8.9	7.1	11.3
<i>Metridia longa</i>	10.2	2.7	3.6	1.6	2.2	4.4
<i>Calanus hyperboreus</i>	7.4	3.6	11.3	4.4	0.6	0.5
<i>Pareuchaeta</i> spp.	2.1		0.4	0.4		0.2
<i>Chiridius</i> spp.	0.3		1.0			
<i>Pseudocalanus</i> spp.	0.3	11.0	0.1	6.1	4.5	4.0
<i>Oithona</i> spp.	0.2	1.1		24.2	24.3	9.1
<i>Microcalanus</i> spp.		22.2		5.9	5.0	2.4
<i>Triconia/Oncea</i> spp.		1.0		1.7	0.1	0.2
Macrozooplankton						
<i>Sagitta elegans</i>	4.1	0.2	0.2	0.5	0.2	0.2
Polychaeta spp.	2.5	0.8	0.6	2.6		
<i>Eualus gaimardii</i>	0.9			0.1		
<i>Themisto libellula</i>	0.4	0.06	16.9	2.4	0.8	5.3
<i>Thysanoessa</i> spp.	0.4		0.6		0.1	0.3
<i>Eukrohnia hamata</i>	0.3		3.3	0.2	0.1	
<i>Meganyctiphanes norvegica</i>	0.3				0.1	
<i>Themisto abyssorum</i>	0.1		0.6	0.9	0.1	0.5
<i>Pandalus borealis</i>	0.05					
<i>Gammarus wilkitzkii</i>			13.8	1.7	1.1	24.2
Other						
<i>Fritellaria borealis</i>	0.4			1.7	2.0	1.0
Ostracoda spp.	0.3		0.2	0.1	0.2	0.2
<i>Limacina helicina</i>	0.1		0.5	4.1	0.1	
<i>Clione limacina</i>	0.1				0.1	
<i>Mertensia ovum</i>	0.1		0.1	1.5	0.5	0.6
<i>Aglantha digitale</i>	0.05		0.2	0.1		0.2
<i>Oikopleura</i> spp.		0.8	12.0	0.8	3.1	0.5
Juveniles						
Bivalve veliger		21.5		2.2	6.3	3.5
Echinoderm larvae		1.9		4.1	0.05	0.6
Isopod larvae		1.0		0.1		
Polychaeta larvae		0.8		1.2	22.0	1.3
Copepod nauplii		0.4		0.8	8.2	28.1
Cyprid larvae				0.3	9.8	0.1

3.3.2. Kongsfjorden

In 2006/07, when the larger mesh size of 300 μm was used, Bray-Curtis similarity analysis identified 3 groups of zooplankton community composition at 42 % similarity. These are labelled KA, KB and KC on Figs 3.2, 3.3a and 3.4, and the similarity clusters are displayed in Fig 3.4. It was apparent from this analysis that trap bottles were not clustering purely on bottle duration, as group KB included bottles varying between 7 and 31 days in duration. The more important dimension to the clustering was the trend in community composition between bottles. In phase KA between June 06 and January 07, *Calanus* numbers in trap samples was minimal (Fig 3.2), and *Metridia longa* and macrozooplankton species (dominated by euphausiids and *Eualus gaimardii*) were only recorded from November onwards (Fig 3.3a). However, the first few empty bottles were excluded from the cluster analysis, and so phase KA essentially began when animals were first recorded in November 06. In February 07, the community composition switched to phase KB, with CV of *Calanus finmarchicus* and adult females (AF) of *Calanus glacialis* dominant with some CIV *Calanus hyperboreus* present. This dominance of *Calanus* during phase KB compared to KA was reflected by similarity percentage analysis that identified *C. finmarchicus* AF, *C. glacialis* AF and *C. glacialis* CIV as most responsible for the difference between phase KA and KB (19 % responsible). In April 07, the community switched to phase KC, with AF the dominant stage in both the *C. finmarchicus* and *C. glacialis* populations, and no *C. hyperboreus* present. During this phase which lasted till mid May 07, minimal numbers of other copepods and macrozooplankton species were recorded compared to phase KB (Fig 3.3a). In mid May, the community then reverted back to phase KB until the end of August, but although the community compositions between these two KB phases were clearly similar, several differences were identified. Younger copepodid stages of all *Calanus* species were now prevalent in the samples, with the *C. glacialis* population containing especially few AF in this phase. Furthermore, highest numbers in of *Sagitta elegans* (peaking mid May), polychaetes (peaking July/August) and *Oikopleura* spp. (peaking June) were recorded in trap samples during this second phase KB.

3. Moored seasonal observations of zooplankton at Kongsfjorden and Rijpfjorden

In 2008/09, a smaller mesh size of 150 μm was used, and thus data were available for smaller animals (Fig 3.3b). During this deployment, Bray-Curtis similarity analysis again identified 3 groups of zooplankton community composition at 46 % similarity. These are labelled KD, KE and KF on Figs 3.2, 3.3a, 3.3b and 3.5, and the similarity clusters are displayed in Fig 3.5. However, as is immediately apparent from Figs 3.2, 3.3a and the large difference in similarity between KD and KE/KF in Fig 3.5, no larger zooplankton were recorded in the bottles after the first bottle in October 08, and so these three phases were based largely on the trends in smaller animals which were recorded in low numbers throughout the deployment (Fig 3.3b). The first bottle (KD) in October 08 (which coincided with phase KA from 2006 during which very few animals - especially *Calanus* - were recorded) contained a very high number of *C. finmarchicus* CIV – CV, *C. glacialis* CV and *C. hyperboreus* CIV – AF. A very high number of *Pseudocalanus* spp. and a range of smaller animals (including bivalve veligers and *Microcalanus* spp. in particular) were also recorded (Fig 3.2 and 3.3a,b). Throughout the remainder of the deployment, bivalve veligers were mostly all that was identified in the bottles, with the switch between phases KE and KF in mid February 09 at a very similar date to the switch between phases KA and KB from the 2006/07 deployment. This difference between phase KE and KF in 09 however was largely due to echinoderm larvae, copepod nauplii and bivalve veligers (71 % responsible), as no larger zooplankton were present.

3. Moored seasonal observations of zooplankton at Kongsfjorden and Rijpfjorden

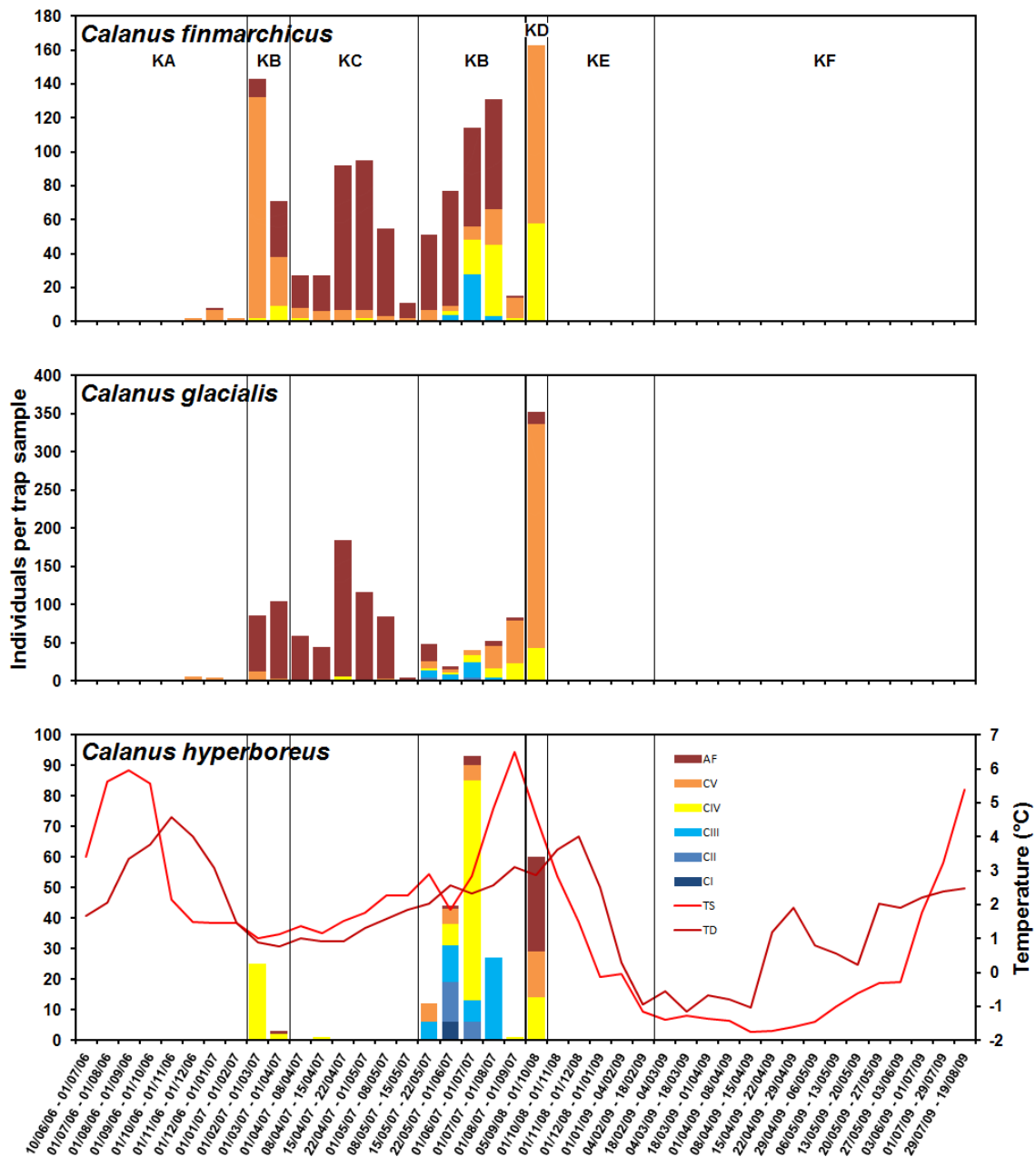


Fig 3.2) Numbers of *Calanus finmarchicus* (upper), *Calanus glacialis* (centre) and *Calanus hyperboreus* (lower) copepodid stages recorded in sediment trap bottles at Kongsfjorden 2006/07 (left) and 2008/09 (right). The break between deployments is indicated by the thick vertical line. Phases of similarity between samples are indicated by the vertical narrow lines and labelled on the upper plot KA, KB, KC, KD, KE and KF. On the lower series, surface mean temperature for each sample (TS) is displayed in light red, and bottom mean temperature for each sample (TD) in dark red. On all plots, AF = Adult Female, CV – CI = copepodite stages 1 – 5. Note y-axis scales differ and bottle durations vary.

3. Moored seasonal observations of zooplankton at Kongsfjorden and Rijpfjorden

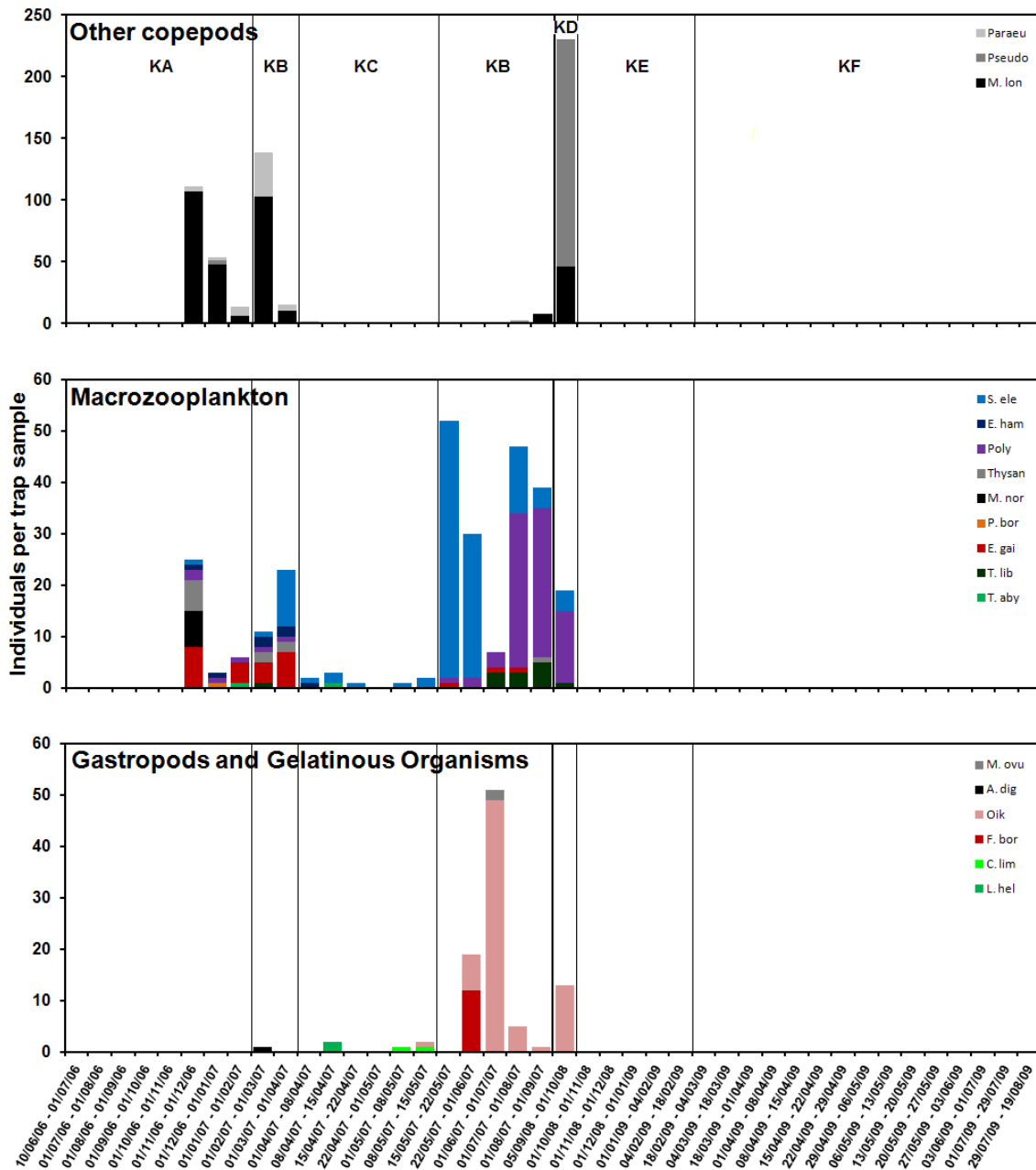


Fig 3.3a) Numbers of other copepods (*Pareuchaeta* spp., *Pseudocalanus* spp. and *Metridia longa* - upper), macrozooplankton (*Sagitta elegans*, *Eukrohnia hamata*, polychaeta spp., *Thysanoessa* spp., *Meganctiphanes norvegica*, *Pandalus borealis*, *Eualus gaimardii*, *Themisto libellula* and *Themisto abyssorum* – centre), and gastropods and various gelatinous organisms (*Mertensia ovum*, *Aglantha digitale*, *Oikopleura* spp., *Fritellaria borealis*, *Clione limacina* and *Limacina helicina* – lower) recorded in sediment trap bottles at Kongsfjorden 2006/07 (left) and 2008/09 (right). The break between deployments is indicated by the thick vertical line. Phases of similarity between samples are indicated by the vertical narrow lines and labelled on the upper plot KA, KB, KC, KD, KE and KF. Note y-axis scales differ and bottle durations vary.

3. Moored seasonal observations of zooplankton at Kongsfjorden and Rijpfjorden

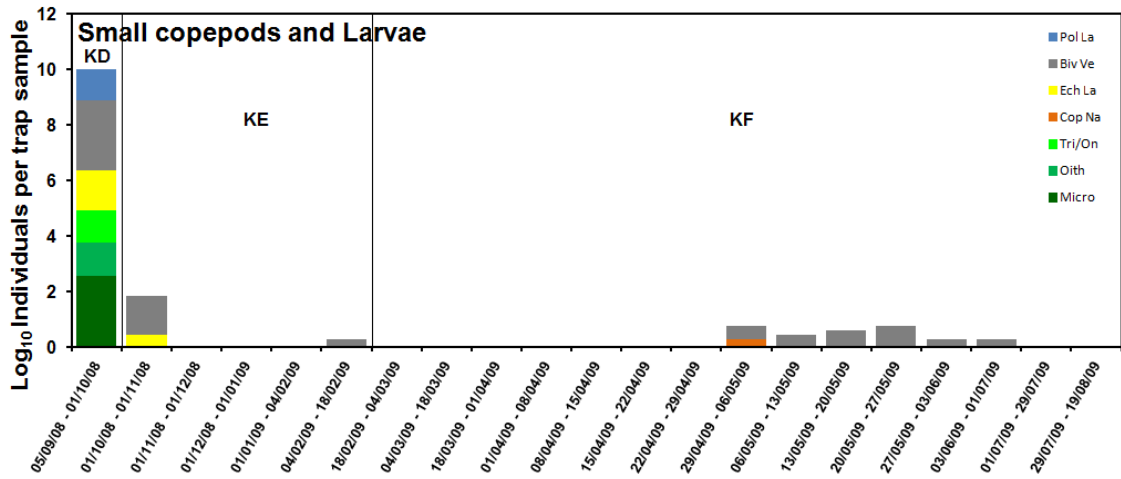


Fig 3.3b) Numbers of small copepods and larval stages (polychaete larvae, bivalve veligers, echinoderm larvae, copepod nauplii, *Triconia/Oncea* spp., *Oithona* spp. and *Microcalanus* spp.) recorded in sediment trap bottles at Kongsfjorden 2008/09. Phases of similarity between samples are indicated by the vertical narrow lines and labelled KD, KE and KF. Note y-axis scale is Log₁₀ scale and bottle durations vary.

3. Moored seasonal observations of zooplankton at Kongsfjorden and Rijpfjorden

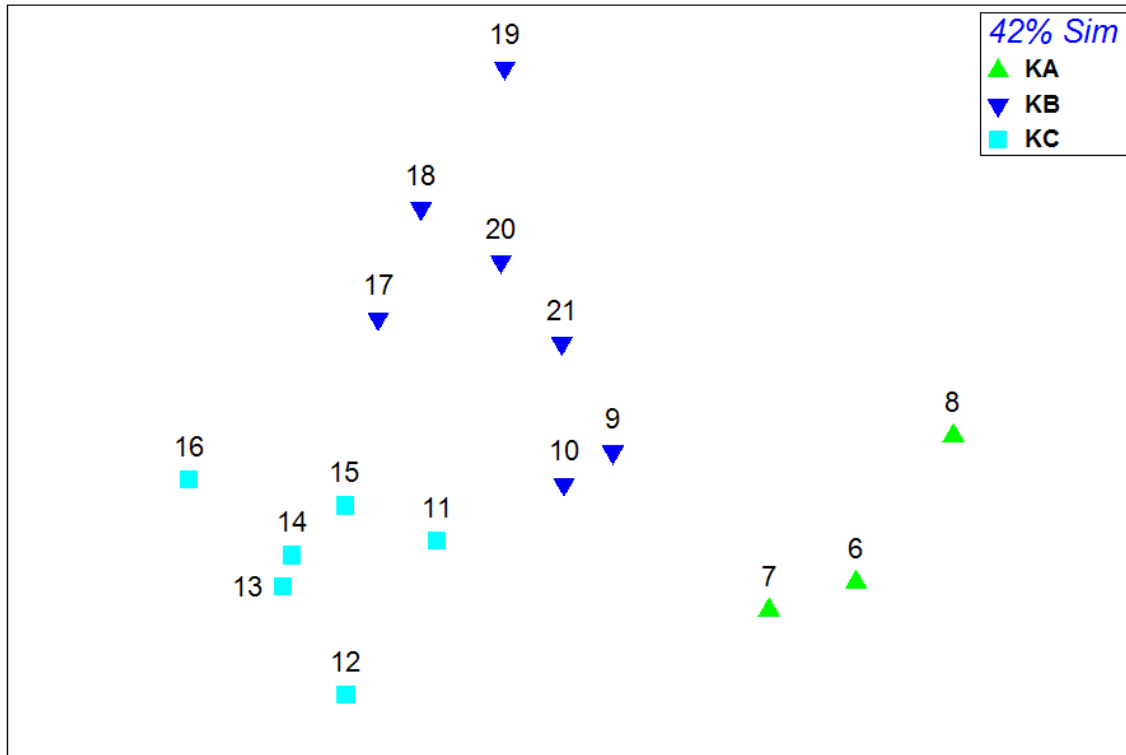


Fig 3.4) Multi Dimensional Scaling (MDS) Plot based on Bray Curtis Similarity analysis on fourth root transformed zooplankton numbers recorded in sediment trap bottles at Kongsfjorden 2006/07. Numbers are sequential sediment trap bottle number (see Table 3.1 for bottle start dates and durations), and each point represents the zooplankton community collected in each bottle. Empty bottles not included. Distances between points on the MDS represent similarity, with closer points being more similar. Groups KA, KB and KC cluster at 42% similarity and are the phases of similarity displayed on Figs 3.2 and 3.3a.

3. Moored seasonal observations of zooplankton at Kongsfjorden and Rijpfjorden

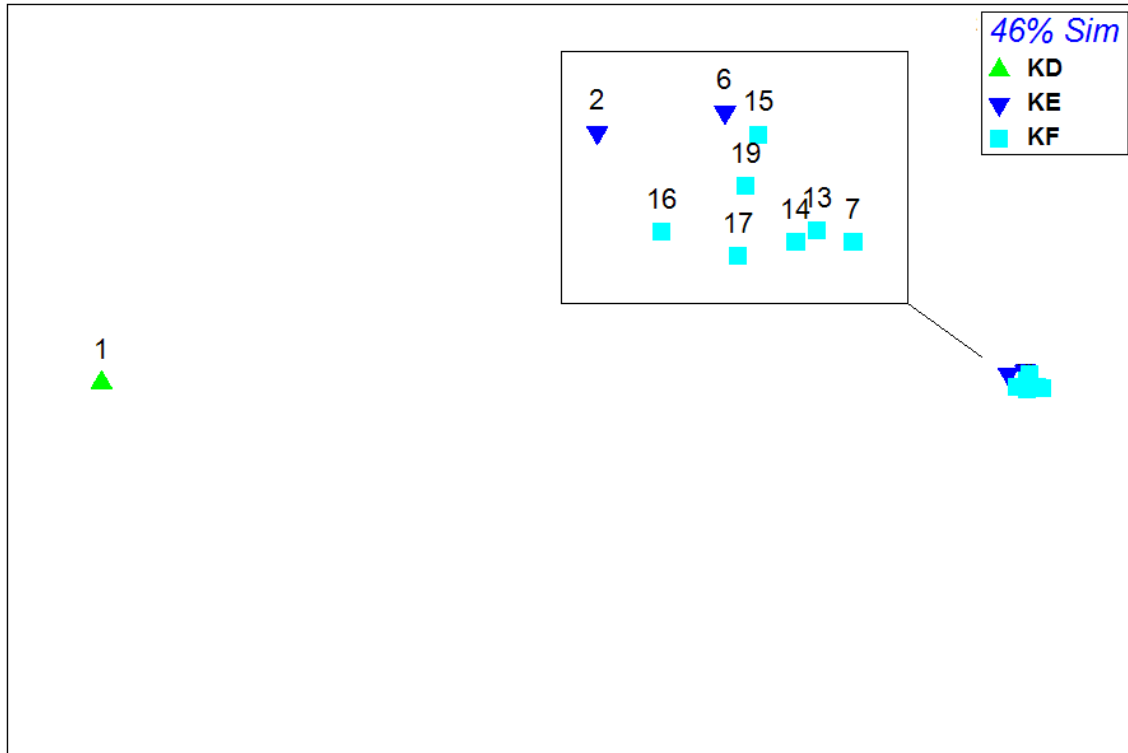


Fig 3.5) Multi Dimensional Scaling (MDS) Plot based on Bray Curtis Similarity analysis on fourth root transformed zooplankton numbers recorded in sediment trap bottles at Kongsfjorden 2008/09. Numbers are sequential sediment trap bottle number (see Table 3.1 for bottle start dates and durations), and each point represents the zooplankton community collected in each bottle. Empty bottles not included. Distances between points on the MDS represent similarity, with closer points being more similar. Groups KD, KE and KF cluster at 46% similarity and are the phases of similarity displayed on Figs 3.2, 3.3a and 3.3b. Inset shows zoom of groups KE and KF.

3.3.3. Kongsfjorden hydrography

In 2006/07 during zooplankton community phase KA, temperature and salinity at the surface varied significantly, and the period between June and October 06 during which very few animals were recorded in the trap samples was dominated by higher surface temperature (reaching above 6°C) and low surface salinity (Fig 3.6). These conditions for bottles 1 to 5 were largely indicative of SW (salinity < 34, temperature > 1°C) and IW (salinity 34 – 34.7, temperature > 1°C) conditions (Fig 3.7). It is interesting to note that bottom temperature appeared to largely follow surface variations in temperature after incorporating a lag of up to several weeks. Bottom temperature reached its highest

3. Moored seasonal observations of zooplankton at Kongsfjorden and Rijpfjorden

recorded level during 2006/07 during this initial phase ($> 4.5^{\circ}\text{C}$), while bottom salinity reached its lowest recorded level (approximately 33.8). When zooplankton began to appear in the bottles during phase KA, surface temperatures were lower (approximately 1°C) and salinities higher with much less variation (34.3 – 34.8), reflecting conditions much more indicative of TAtW (salinity > 34.7 , temperature $> 1^{\circ}\text{C}$) (Fig 3.7 – red). Eastward current velocity especially in the surface 50 m increased during this period and was more sustained over time, with velocities reaching > 100 mm/s (Fig 1.14). With the switch to phase KB in February 07, surface salinity increased marginally and temperature fell to the lowest recorded levels of the deployment (just below 1°C). Bottom temperature was also at its lowest. Although salinity remained similar, temperature began to rise with the switch to phase KC in April 07, with conditions especially during the end of this phase again indicative of TAtW (Fig 3.7 – green). With the final switch back to phase KB in zooplankton community in May 07, surface temperature began to rise dramatically to its highest recorded level ($> 7^{\circ}\text{C}$) in August. Salinity also fell dramatically, and these conditions in 2007 were similar to those in 2006 at the start of the deployment and were indicative of SW and IW (Fig 3.7 – blue). High eastward and northward current velocities throughout the sampled 15 – 95 m layer were recorded in May 07 alongside the final switch to phase KB (eastward $< - 150$ mm/s indicating primarily westward flow, northward > 150 mm/s).

3. Moored seasonal observations of zooplankton at Kongsfjorden and Rijpfjorden

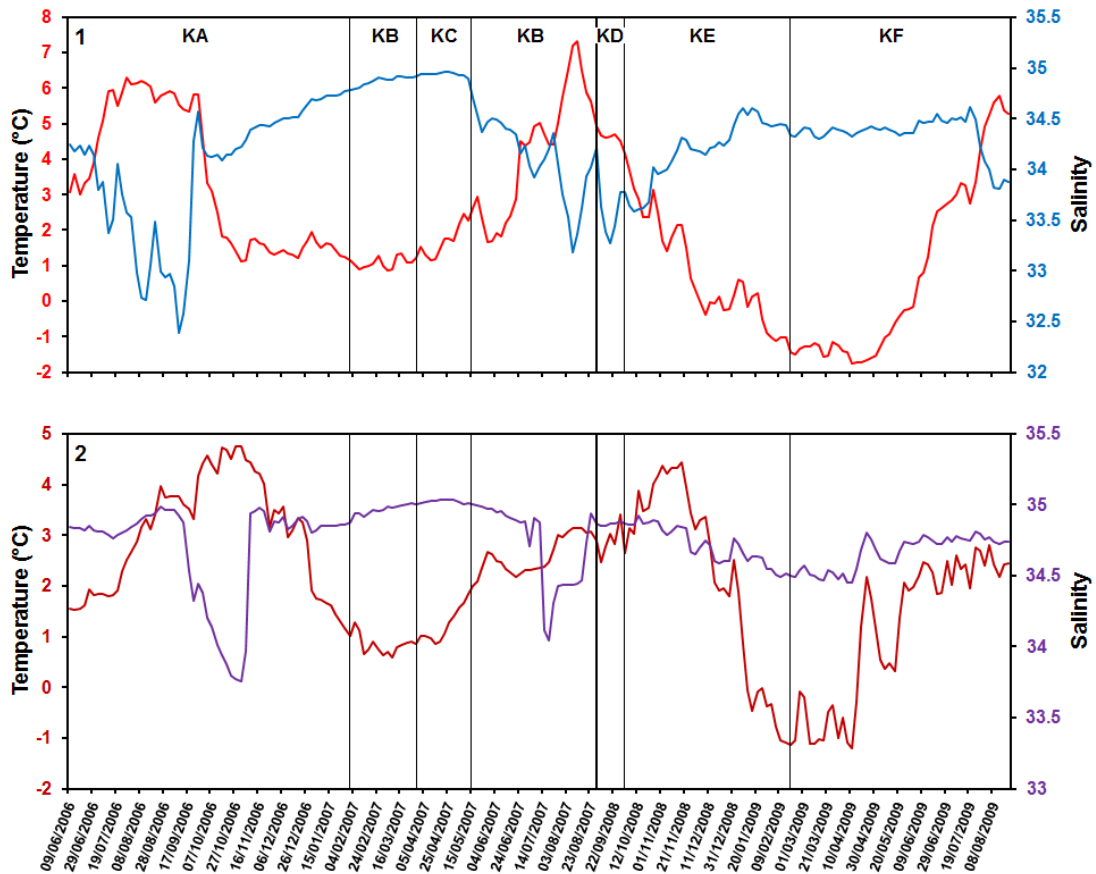


Fig 3.6) Time series of daily mean temperature and salinity from observations by the surface (19 m in 2006/07 and 25 m in 2008/09 – plot 1 upper, light red = temperature, light blue = salinity) and bottom (198 m in 2006/07 and 201 m in 2008/09 – plot 2 lower, dark red = temperature, purple = salinity) microcats deployed on the moorings in Kongsfjorden. The break between deployments is indicated by the thick vertical line. Phases of similarity between zooplankton samples are indicated by the vertical narrow lines and labelled on the upper plot KA, KB, KC, KD, KE and KF. Note y-axis scales differ.

3. Moored seasonal observations of zooplankton at Kongsfjorden and Rijpfjorden

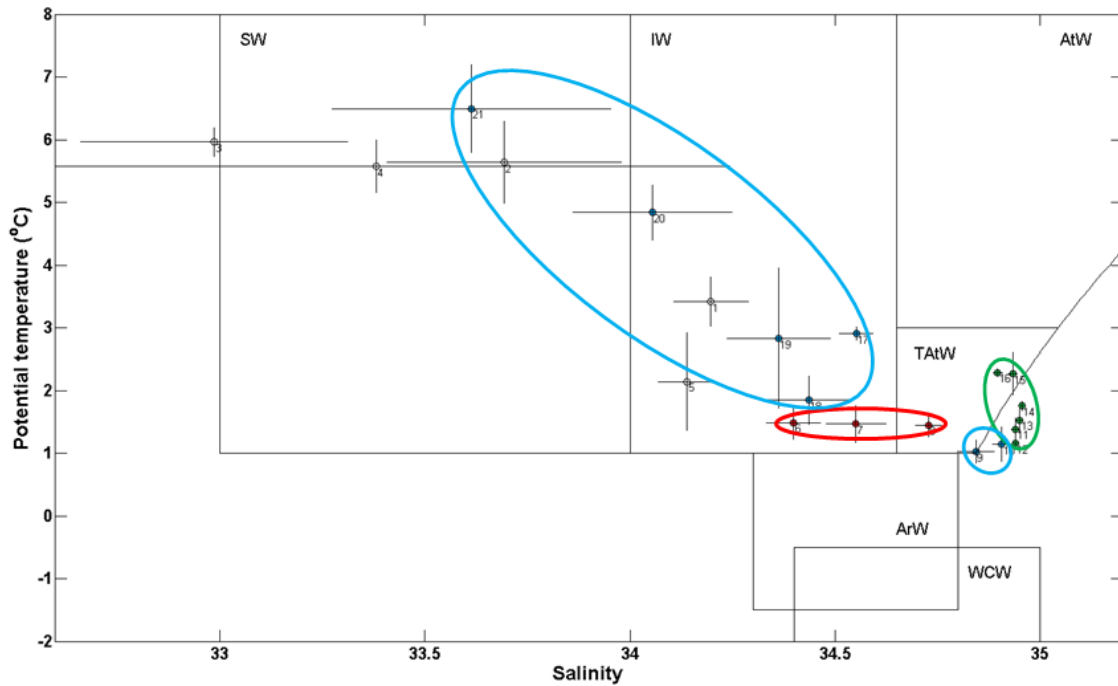


Fig 3.7) T-S diagram displaying temperature and salinity (means for each bottle calculated from daily averages during each bottle deployment with associated standard deviation) recorded at 19 m at Kongsfjorden 2006/07. The data are coloured and circled based on the three phases of zooplankton community composition (phase KA = red, phase KB = blue, phase KC = green). Empty bottles that contained no zooplankton are not coloured in. Bottle numbers are displayed from 1 to 21. Water mass definitions as per Svendsen et al. (2002).

In 2008/09, the deployment began in September 08 and phase KD hydrographic conditions were largely comparable to August 2007 and August/September 2006 with surface temperature and salinity indicative of SW (Fig 3.6, 3.8 – red). As in 2006, surface temperature began to drop dramatically around October 08 during the switch to zooplankton community phase KE, but in 2008/09 in contrast to 2006/07, temperatures dropped below 0°C during this phase and salinity remained comparatively low indicating transition to WCW (salinity > 34.4, temperature < - 0.5°C) by the end of phase KE in February 09 (Fig 3.8 – blue). Both surface and bottom temperature reached their lowest recorded values at Kongsfjorden during the 2008/09 deployment. This low surface temperature reached nearly -2°C in April 09 during phase KF, and the sample bottles in which some smaller zooplankton were recorded occurred in WCW, ArW (salinity 34.3 – 34.8, temperature < 1°C) and finally IW (Fig 3.8 – green) as

3.3.4. Rijpfjorden

In 2006/07, when the larger mesh size of 300 μm was used, Bray-Curtis similarity identified 3 groups of zooplankton community composition at 23 % similarity. These groups were far more distinct than found in Kongsfjorden (42% 2006/07 and 46% in 2008/09). They are labelled RA, RB and RC on Figs 3.9 and 3.10a, and the similarity clusters are displayed in Fig 3.11. In phase RA between September 06 and May 07, all three *Calanus* species were recorded in the trap samples, with highest numbers of *C. glacialis* and lowest numbers of *C. finmarchicus*. CV and AF dominated the *C. glacialis* and *C. finmarchicus* populations, while CIV dominated the *C. hyperboreus* population (Fig 3.9). This difference in copepodid composition between *C. glacialis* and *C. finmarchicus* vs. *C. hyperboreus* was similar to observations at Kongsfjorden in March/April 2006/07. Comparatively fewer other copepods were recorded during this phase, but high relative numbers of macrozooplankton (especially *Themisto libellula* and *Gammarus wilkitzkii*) were recorded which peaked between November 06 and January 07 (Fig 3.10a). In May 07, the zooplankton community composition switched to phase RB, with fewer *C. glacialis* and *C. finmarchicus* individuals dominated by AF, and no *C. hyperboreus* present. No other copepods were recorded during phase RB, and very few macrozooplankton also. This phase lasted till July 07 before the switch to phase RC, with younger stage CIII of *C. glacialis* and *C. hyperboreus* now recorded in the trap samples in low numbers. No other copepods and few macrozooplankton persisted from phase RB through phase RC, but a dramatic increase in *Oikopleura* spp. was recorded at the start of phase RC, peaking in mid July. This dominance of *Oikopleura* spp. in the zooplankton community composition of phase RC was highlighted by similarity percentage analysis that identified the species as most responsible (18 %) for the differences between phase RB and RC.

From 2007/08 onwards at Rijpfjorden, a smaller mesh size of 150 μm was used to separate zooplankton from the sediments, and so information on smaller animals became available (Fig 3.10b). In 2007/08, Bray-Curtis similarity analysis identified just 2 groups of zooplankton community composition at 21 % similarity. These groups are

3. Moored seasonal observations of zooplankton at Kongsfjorden and Rijpfjorden

labelled RD and RE, and the similarity clusters are displayed in Fig 3.12. In phase RD between September and the end of November 07, the three *Calanus* species were recorded in the trap samples in relatively high numbers (Fig 3.9). In contrast to 2006/07 though, *C. finmarchicus* was the most numerous *Calanus* species collected in sediment trap bottles at Rijpfjorden in 2007/08 during phase RD. CIV and CV dominated all *Calanus* populations during this phase, although CII and CIII were recorded for *C. finmarchicus* and CIII for *C. glacialis* and *C. hyperboreus* (Fig 3.9). *Pseudocalanus* spp. was recorded during this phase in relatively high numbers (Fig 3.10a), with a range of macrozooplankton species also recorded in the trap samples (especially *Onisimus* spp. and polychaetes which were recorded in their highest numbers throughout the entire Rijpfjorden deployments). *Limacina helicina*, *Fritellaria borealis* and *Mertensia ovum* were all recorded in comparatively high numbers, making this phase relatively diverse in species. High numbers of smaller zooplankton were also recorded (especially *Oithona* spp. and *Microcalanus* spp.) (Fig 3.10b). In December 07, zooplankton community composition switched to phase RE, with no *C. glacialis* and *C. hyperboreus*, and very few *C. finmarchicus* individuals recorded in the trap samples through the entire phase which lasted until August 08. Very few other animals were recorded during phase RE, with mostly smaller zooplankton species (*Oithona* spp., *Triconia/Oncea* spp., copepod nauplii and bivalve veligers) recorded in the trap samples. However, the presence of copepod nauplii in March and June/July 08 indicated spawning copepods somewhere in the vicinity of the mooring. The final switch back to phase RD in August 08 was largely due to the smaller species of *Oithona* spp. (15 %) and *Microcalanus* spp. (9 %), with very few other zooplankton present in the final trap sample.

In 2009/10, Bray-Curtis similarity again identified 2 groups of zooplankton community composition at 42 % similarity. These groups were far less distinct than those identified in the 2006/07 and 2007/08 Rijpfjorden deployments, and were similar in their percentage distinction to Kongsfjorden. This was likely due to the more even distribution of many species (especially smaller animals – Fig 3.10b) throughout the deployment. The two phases are labelled RF and RG on Figs 3.9 and 3.10a,b, and the similarity clusters are displayed in Fig 3.13. In phase RF between September 09 and the

3. Moored seasonal observations of zooplankton at Kongsfjorden and Rijpfjorden

end of February 10, all three *Calanus* species were recorded in the trap samples, with *C. glacialis* the most numerous. Only CIV and CV of *C. finmarchicus* were recorded, while the *C. glacialis* (CII – AF) and *C. hyperboreus* (CIII – AF) populations contained younger copepodids (Fig 3.9). Relatively high numbers of *Pseudocalanus* spp. and especially *M. longa* were recorded during this phase, with a range of macrozooplankton species dominated by *G. wilkitzkii* also recorded. *Oikopleura* spp. and a range of smaller species (especially *Oithona* spp.) were also recorded in the trap samples. It was immediately apparent that there was a transition period between the two phases between March and early July 10. During this period, zooplankton community composition oscillated between the two phases RF and RG, with *C. finmarchicus* nearly completely absent, and *C. glacialis* and *C. hyperboreus* recorded in comparatively low numbers in the trap bottles. Numbers of other copepods (especially *M. longa*) were comparatively lower during this transition period, and macrozooplankton was largely absent. When analysing the smaller zooplankton species during this transition period, it became apparent that copepod nauplii and polychaete larvae were only present in the trap samples during phase RG, and similarity percentage analysis highlighted copepod nauplii (8 %), polychaete larvae (7 %) and *M. longa* (5 %) as most responsible for the differences between phase RF and RG. By mid July 10 phase RG was fully established, and this phase continued to the end of the deployment in September 10. No *C. finmarchicus* or *C. hyperboreus* were recorded during this phase, but *C. glacialis* numbers increased to the highest levels recorded in trap bottles throughout the deployment. This *C. glacialis* population contained all stages, with CI recorded in June and July for the only time across all Rijpfjorden deployments. Dramatic spikes in the number of *Oikopleura* spp. (July) and *F. borealis* (August) to their highest recorded values were also observed during phase RG (Fig 3.10a). Copepod nauplii, polychaete larvae and bivalve veligers all continued in comparatively high numbers through this phase.

In 2010/11, Bray-Curtis similarity identified 3 groups of zooplankton community composition at 39 % similarity. These groups were again less distinct than those identified in the 2006/07 and 2007/08 Rijpfjorden deployments, and were similar in

3. Moored seasonal observations of zooplankton at Kongsfjorden and Rijpfjorden

their percentage distinction to Rijpfjorden 2009/10. The three phases are labelled RH, RI and RJ on Figs 3.9 and 3.10a,b, and the similarity clusters are displayed in Fig 3.14. In phase RH between October 10 and Mid June 11, all three *Calanus* species were recorded in the trap samples, although *C. glacialis* was by far the most dominant species (Fig 3.9). CIII – CV of *C. finmarchicus* and CIV – CV of *C. hyperboreus* were recorded in low numbers during this phase. The *C. glacialis* population was dominated mostly by CV, although CII – AF were recorded. Comparatively high numbers of *Pseudocalanus* spp. and especially *M. longa* were recorded in trap bottles during this phase between October 10 and mid April 11, with comparatively high numbers of *T. libellula* recorded between October 10 and the end of Dec 10 and very high number (highest recorded values across all deployments) of *G. wilkitzkii* in April 11. Very few animals were recorded towards the end of phase RH from May to early June 11. Towards the end of June 11, zooplankton community composition switched to phase RI, with the three *Calanus* species only recorded during this phase in very low numbers. *M. longa* was completely absent during phase RI, and macrozooplankton was also largely absent. *F. borealis* was recorded in the trap samples during phase RI for the first time in the deployment, and copepod nauplii especially were recorded throughout the phase in comparatively high numbers. The presence of copepod nauplii in phase RI was most responsible for the difference between phase RH and RI (14 %), while the absence of *G. wilkitzkii* in phase RI was also highly responsible (8 %). Toward the end of August 11, zooplankton community composition switched to phase RJ until the end of the deployment in early September 11. In phase RJ, *Calanus* numbers in the trap bottles remained low but marginally higher than recorded during phase RI, while copepod nauplii were completely absent and polychaete larvae and bivalve veligers were recorded in comparatively high numbers (Fig 3.10b). These changes in smaller zooplankton were most responsible for separating phase RJ from phase RI, with copepod nauplii (12 %), bivalve veligers (8 %) and polychaete larvae (7 %) the three most responsible taxa.

3. Moored seasonal observations of zooplankton at Kongsfjorden and Rijpfjorden

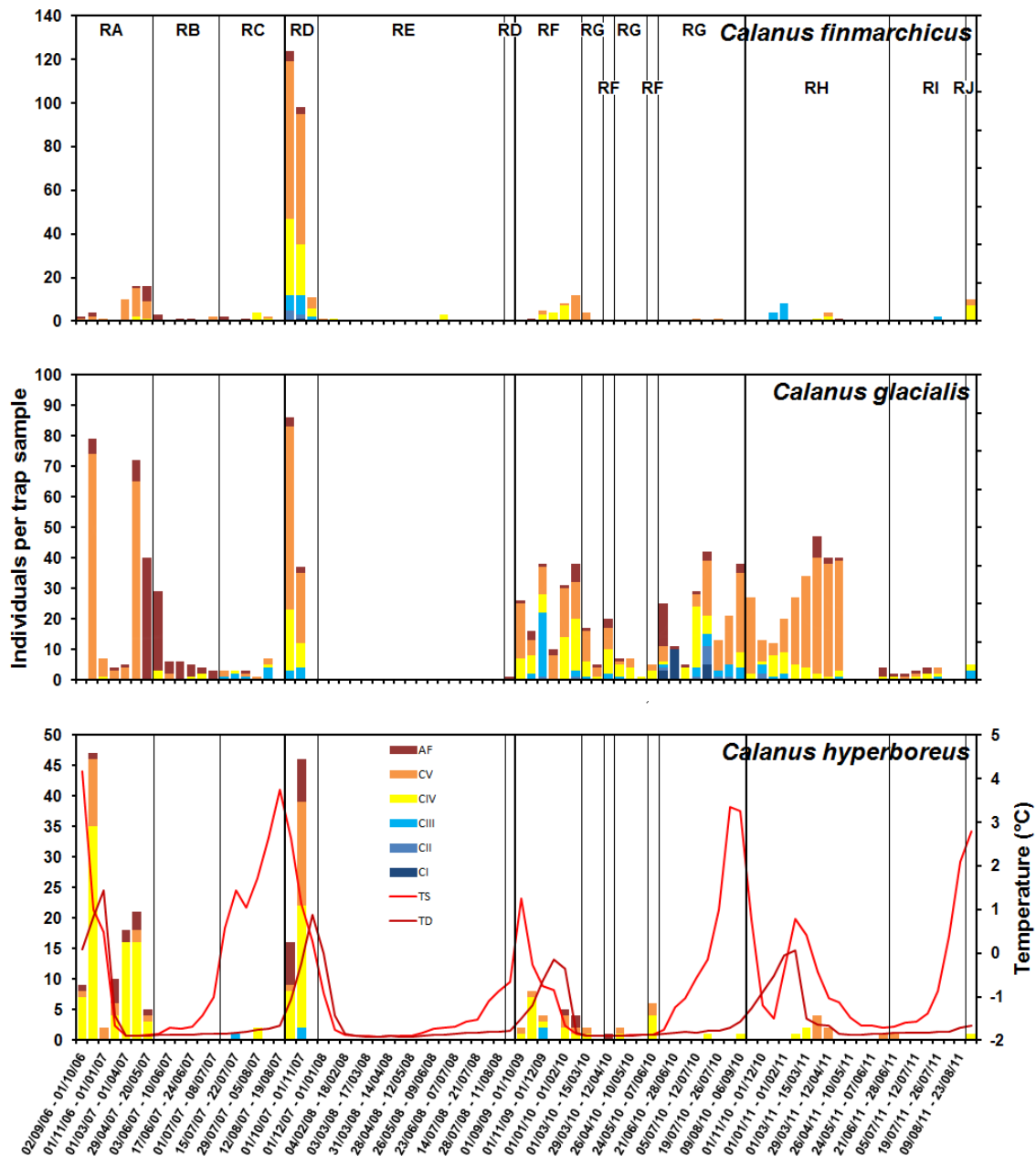


Fig 3.9) Numbers of *Calanus finmarchicus* (upper), *Calanus glacialis* (centre) and *Calanus hyperboreus* (lower) copepodid stages recorded in sediment trap bottles at Rijpfjorden 2006/07 (left), 2007/08 (centre-left), 2009/10 (centre-right) and 2010/11 (right). Breaks between deployments are indicated by thick vertical lines. Phases of similarity between samples are indicated by the vertical narrow lines and labelled on the upper plot RA, RB, RC, RD, RE, RF, RG, RH, RI and RJ. On the lower series, surface mean temperature for each sample (TS) is displayed in light red, and bottom mean temperature for each sample (TD) in dark red. On all plots, AF = Adult Female, CV – CI = copepodite stages 1 – 5. Note y-axis scales differ and bottle durations vary.

3. Moored seasonal observations of zooplankton at Kongsfjorden and Rijpfjorden

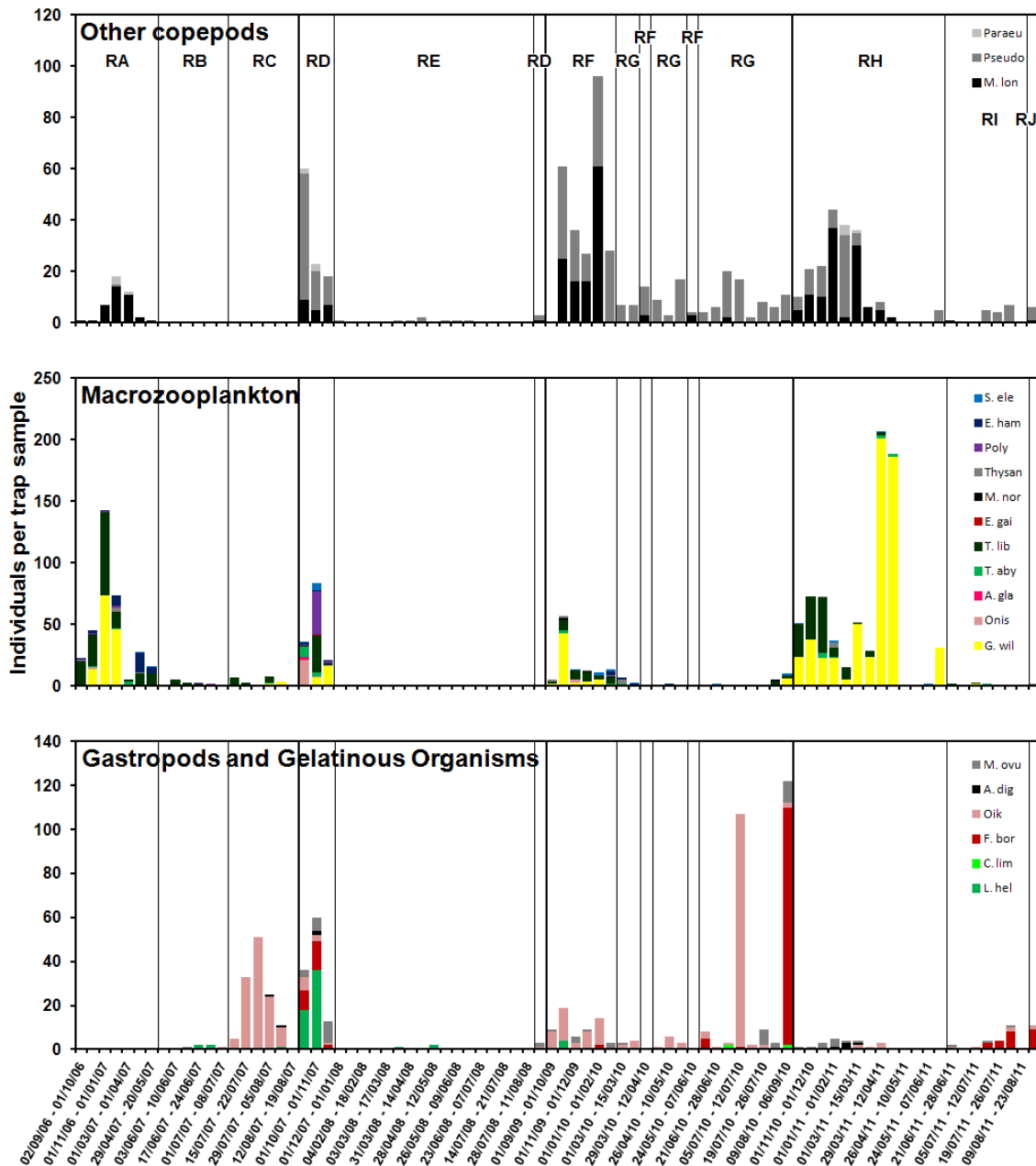


Fig 3.10a) Numbers of other copepods (*Pareuchaeta* spp., *Pseudocalanus* spp. and *Metridia longa* - upper), macrozooplankton (*Sagitta elegans*, *Eukrohnia hamata*, polychaeta spp., *Thysanoessa* spp., *Meganyctiphanes norvegica*, *Pandalus borealis*, *Eualus gaimardii*, *Themisto libellula*, *Themisto abyssorum*, *Apherusa glacialis*, *Onisimus* spp. and *Gammarus wilkitzkii* – centre), and gastropods and various gelatinous organisms (*Mertensia ovum*, *Aglantha digitale*, *Oikopleura* spp., *Fritellaria borealis*, *Clione limacina* and *Limacina helicina* – lower) recorded in sediment trap bottles at Rijpfjorden 2006/07 (left), 2007/08 (centre-left), 2009/10 (centre-right) and 2010/11 (right). Breaks between deployments are indicated by the thick vertical lines. Phases of similarity between samples are indicated by the vertical narrow lines and labelled on the upper plot RA, RB, RC, RD, RE, RF, RG, RH, RI and RJ. Note y-axis scales differ and bottle durations vary.

3. Moored seasonal observations of zooplankton at Kongsfjorden and Rjipfjorden

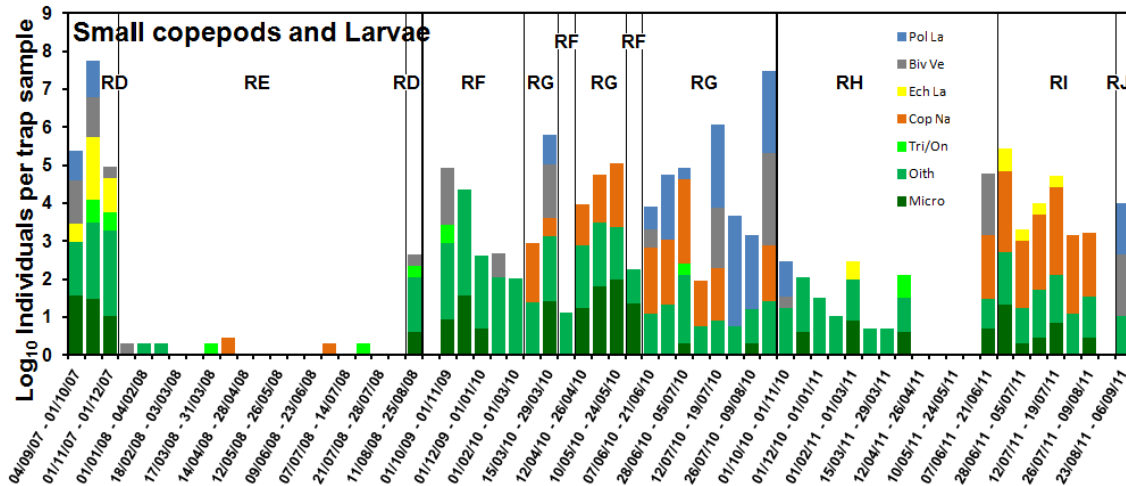


Fig 3.10b) Numbers of small copepods and larval stages (polychaete larvae, bivalve veligers, echinoderm larvae, copepod nauplii, *Triconia/Oncea* spp., *Oithona* spp. and *Microcalanus* spp.) recorded in sediment trap bottles at Rjipfjorden 2007/08 (left), 2009/10 (centre) and 2010/11 (right). Breaks between deployments are indicated by the thick vertical lines. Phases of similarity between samples are indicated by the vertical narrow lines and labelled RD, RE, RF, RG, RH, RI and RJ. Note y-axis scale is Log₁₀ and bottle durations vary.

3. Moored seasonal observations of zooplankton at Kongsfjorden and Rijpfjorden

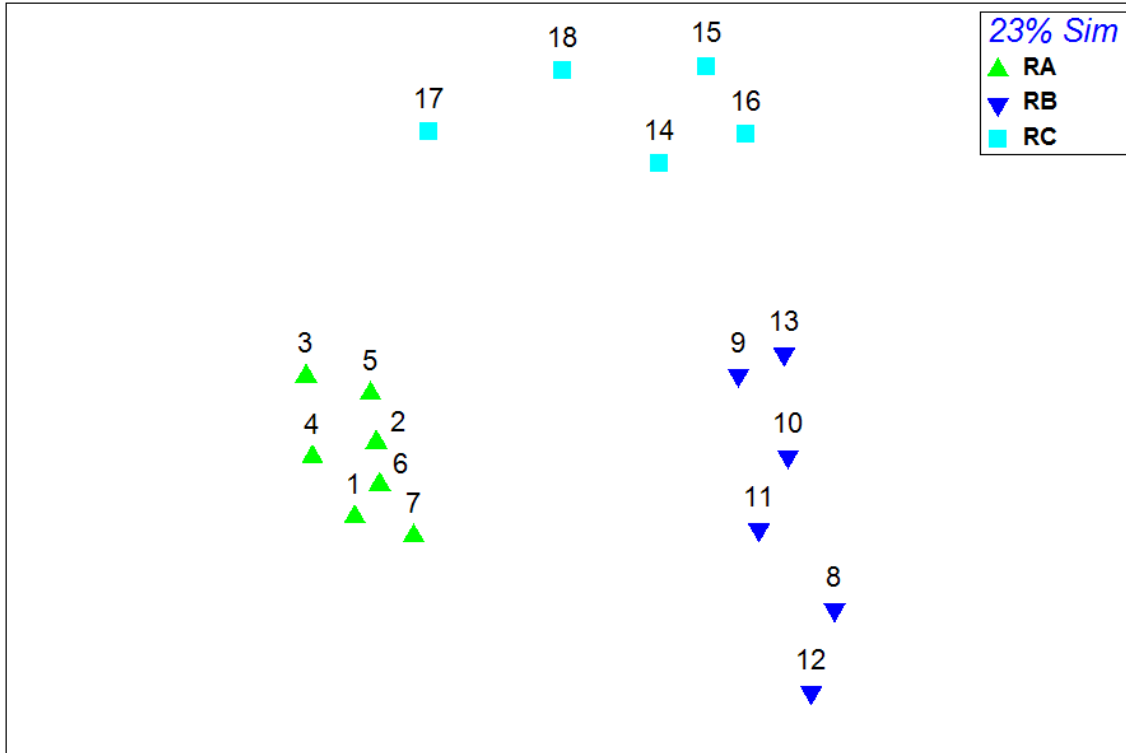


Fig 3.11) Multi Dimensional Scaling (MDS) Plot based on Bray Curtis Similarity analysis on fourth root transformed zooplankton numbers recorded in sediment trap bottles at Rijpfjorden 2006/07. Numbers are sequential sediment trap bottle number (see Table 3.1 for bottle start dates and durations), and each point represents the zooplankton community collected in each bottle. Empty bottles not included. Distances between points on the MDS represent similarity, with closer points being more similar. Groups RA, RB and RC cluster at 23% similarity and are the phases of similarity displayed on Figs 3.9 and 3.10a.

3. Moored seasonal observations of zooplankton at Kongsfjorden and Rijpfjorden

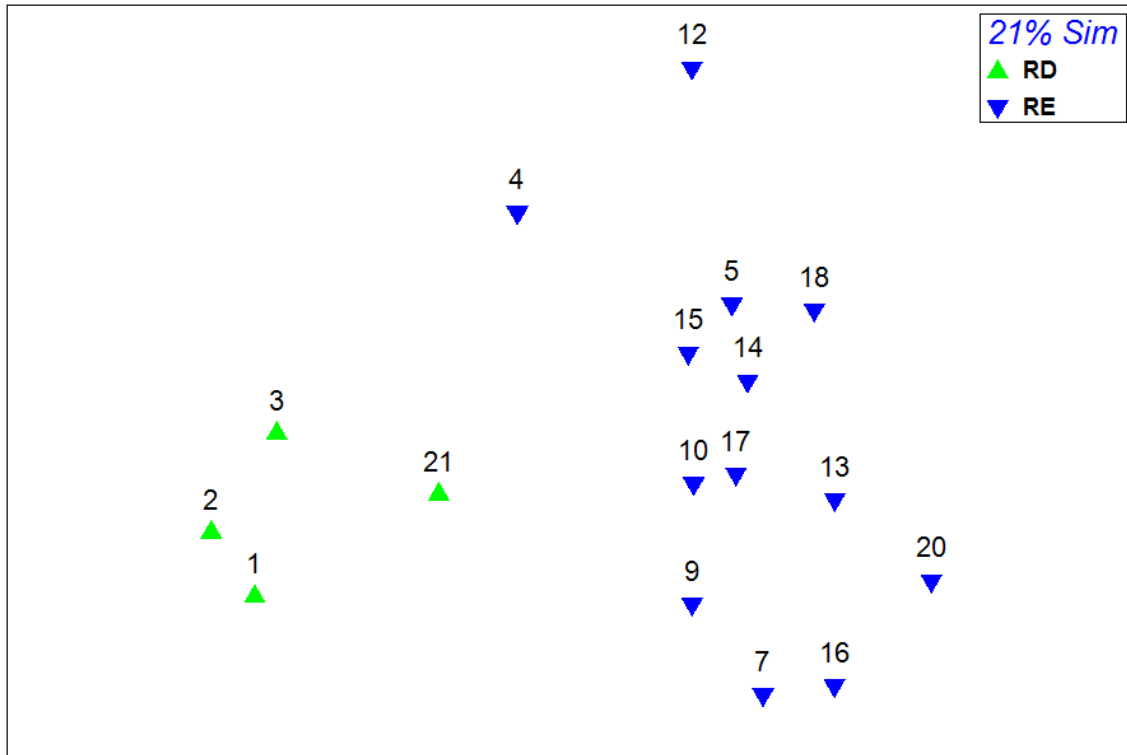


Fig 3.12) Multi Dimensional Scaling (MDS) Plot based on Bray Curtis Similarity analysis on fourth root transformed zooplankton numbers recorded in sediment trap bottles at Rijpfjorden 2007/08. Numbers are sequential sediment trap bottle number (see Table 3.1 for bottle start dates and durations), and each point represents the zooplankton community collected in each bottle. Empty bottles not included. Distances between points on the MDS represent similarity, with closer points being more similar. Groups RD and RE cluster at 21% similarity and are the phases of similarity displayed on Figs 3.9, 3.10a and 3.10b.

3. Moored seasonal observations of zooplankton at Kongsfjorden and Rijpfjorden

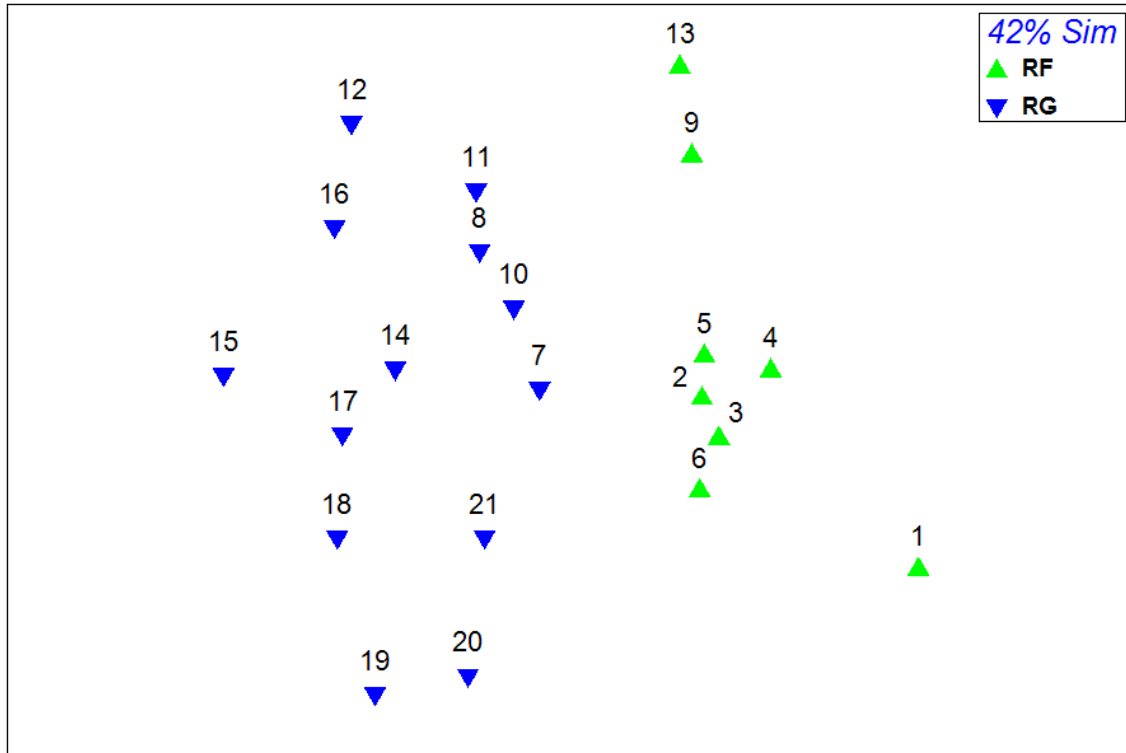


Fig 3.13) Multi Dimensional Scaling (MDS) Plot based on Bray Curtis Similarity analysis on fourth root transformed zooplankton numbers recorded in sediment trap bottles at Rijpfjorden 2009/10. Numbers are sequential sediment trap bottle number (see Table 3.1 for bottle start dates and durations), and each point represents the zooplankton community collected in each bottle. Empty bottles not included. Distances between points on the MDS represent similarity, with closer points being more similar. Groups RF and RG cluster at 42% similarity and are the phases of similarity displayed on Figs 3.9, 3.10a and 3.10b.

3. Moored seasonal observations of zooplankton at Kongsfjorden and Rijpfjorden

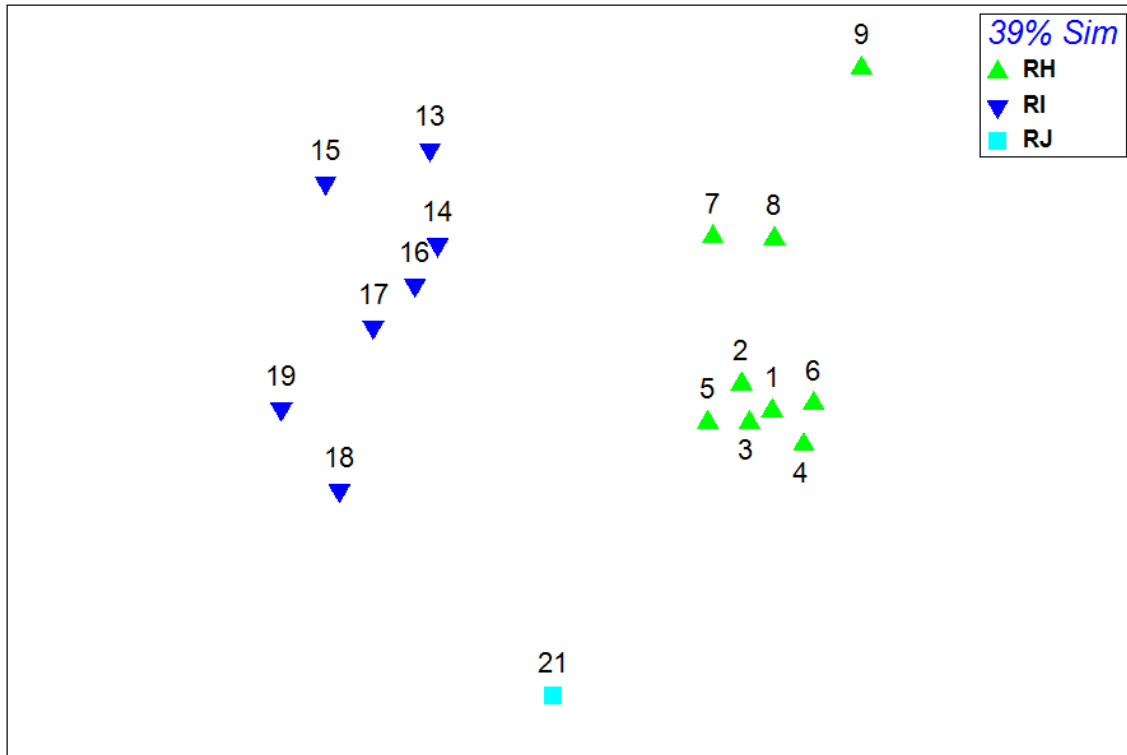


Fig 3.14) Multi Dimensional Scaling (MDS) Plot based on Bray Curtis Similarity analysis on fourth root transformed zooplankton numbers recorded in sediment trap bottles at Rijpfjorden 2010/11. Numbers are sequential sediment trap bottle number (see Table 3.1 for bottle start dates and durations), and each point represents the zooplankton community collected in each bottle. Empty bottles not included. Distances between points on the MDS represent similarity, with closer points being more similar. Groups RH, RI and RJ cluster at 39% similarity and are the phases of similarity displayed on Figs 3.9, 3.10a and 3.10b.

3.3.5. Rijpfjorden hydrography

In 2006/07 during zooplankton community phase RA, surface temperatures dropped from their highest recorded level at Rijpfjorden ($> 4.5^{\circ}\text{C}$) in early September 06 to nearly -2°C by mid January 07 (Fig 3.15). Salinity, although variable, remained relatively high during this period, and surface conditions changed from SW and IW dominance during the start of phase RA to WCW by mid January 07 (Fig 3.16 – red). Bottom temperature also reached its highest recorded value at Rijpfjorden during phase RA in 2006/07 (approximately 2.5°C). With the switch to phase RB in May 07, surface temperature began to rise and salinity to drop, indicating a change from WCW to ArW

3. Moored seasonal observations of zooplankton at Kongsfjorden and Rijpfjorden

(Fig 3.16 – blue). A very steep rise in surface temperature to $> 3^{\circ}\text{C}$ and fall in salinity in July 07 coincided with the switch to phase RC in zooplankton community (Fig 3.15), and this dramatic change switched the hydrographic conditions back to SW dominance during this phase (Fig 3.16 – green). Northward current velocities of up to 150 mm/s between 20 – 95 m were observed at Rijpfjorden as surface temperature began to rise during this switch to zooplankton phase RC (Fig 1.16). By the end of the deployment in August 07, conditions were similar to observations at the start of the deployment in September 06, although both surface and bottom temperatures and surface salinity were lower.

3. Moored seasonal observations of zooplankton at Kongsfjorden and Rijpfjorden

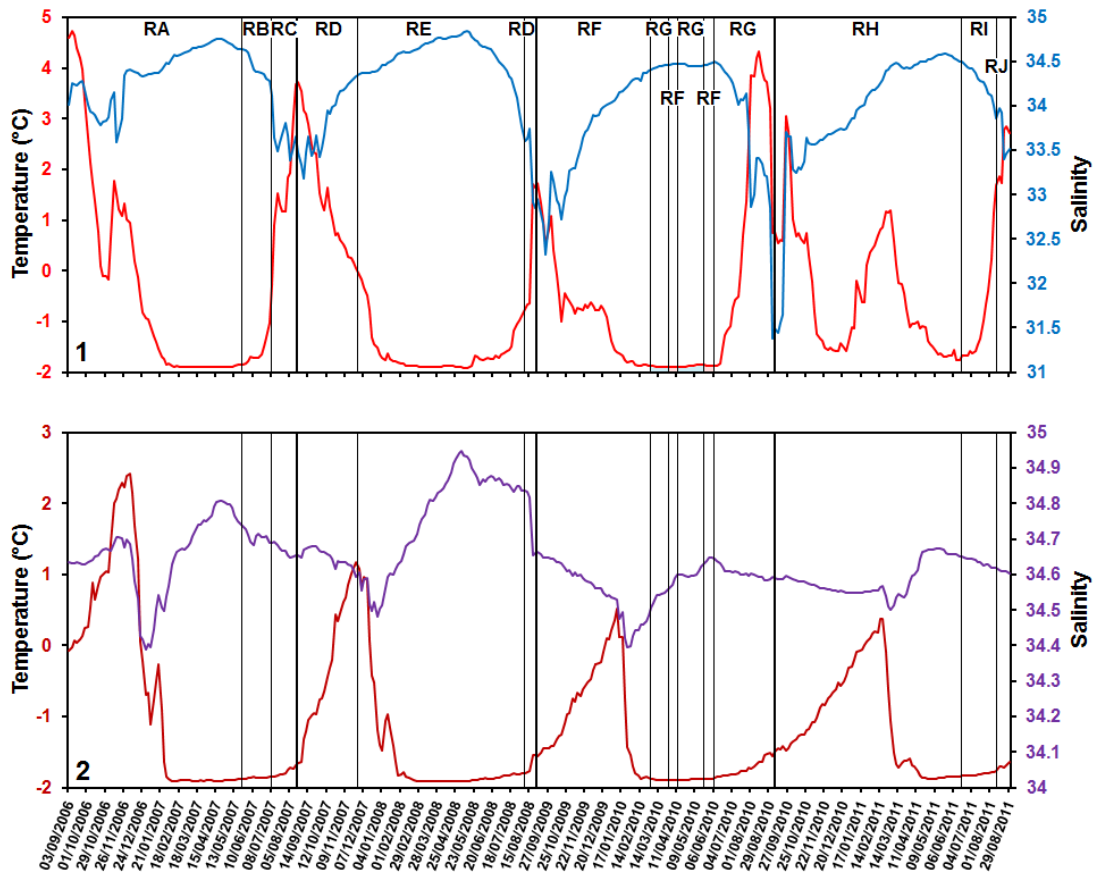


Fig 3.15) Time series of daily mean temperature and salinity from observations by the surface (24 m in 2006/07, 12 m in 2007/08, 27 m in 2009/10, 33 m in 2010/11 – plot 1 upper, light red = temperature, light blue = salinity) and bottom (203 m in 2006/07, 198 m in 2007/08, 211 m in 2009/10, 222 m in 2010/11 – plot 2 lower, dark red = temperature, purple = salinity) microcats deployed on the moorings in Rijpfjorden. Breaks between deployments are indicated by thick vertical lines. Phases of similarity between zooplankton samples are indicated by the vertical lines and labelled on the upper plot RA, RB, RC, RD, RE, RF, RG, RH, RI and RJ. Note y-axis scales differ.

3. Moored seasonal observations of zooplankton at Kongsfjorden and Rijpfjorden

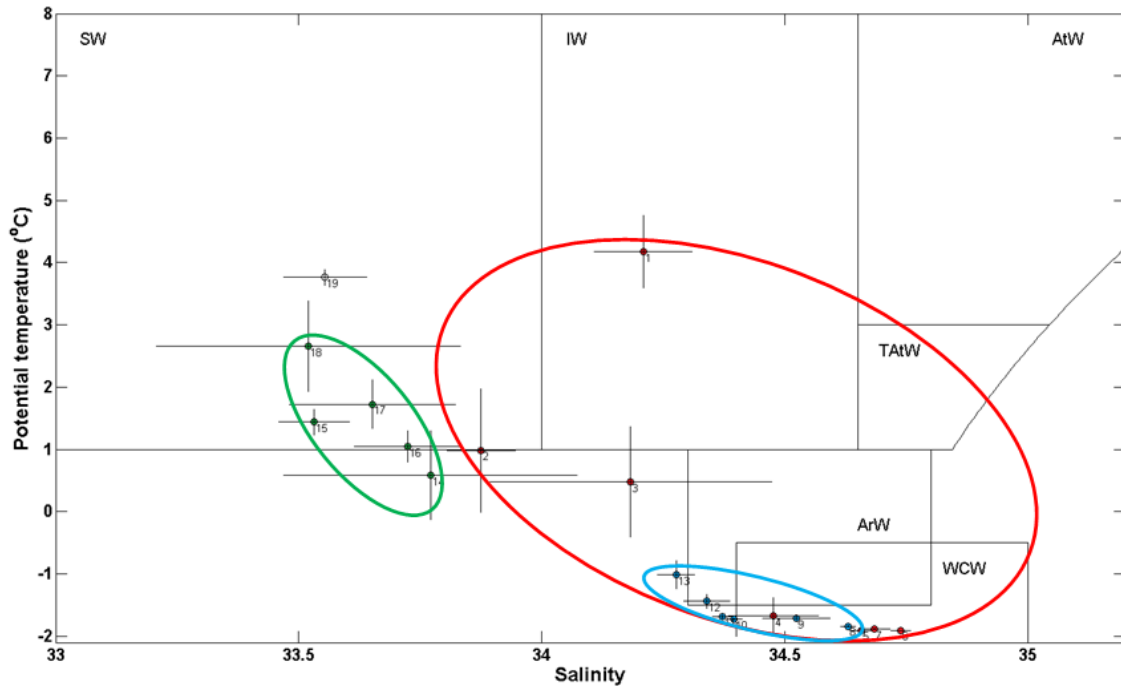


Fig 3.16) T-S diagram displaying temperature and salinity (means for each bottle calculated from daily averages during each bottle deployment with associated standard deviation) recorded at 24 m at Rijpfjorden 2006/07. The data are coloured and circled based on the three phases of zooplankton community composition (phase RA = red, phase RB = blue, phase RC = green). Empty bottles that contained no zooplankton are not coloured in. Bottle numbers are displayed from 1 to 19. Water mass definitions as per Svendsen et al. (2002).

In 2007/08, the mooring deployment began very soon after the end of the 2006/07 deployment in September 07, and surface temperature (highest of the deployment > 3.5°C) and salinity indicated SW (Fig 3.17). Similarly to the pattern recorded in 2006/07, surface temperature fell throughout phase RD to approximately 0°C by December 07, indicating a shift towards ArW by the end of phase RD. Bottom temperatures during this phase however rose from approximately -2°C to > 1°C, a significant rise. The switch to zooplankton community phase RE in 2007/08 occurred at the start of December 07 while surface temperature was still falling and salinity still rising. Surface temperature then reached minimal values around -2°C by February 08, indicating WCW dominance through most of phase RE (Fig 3.17 – blue). However, the recorded trend in bottom temperature changed from rising in phase RD to falling in phase RE, and bottom temperature also reached minimal values around -2°C with the

3. Moored seasonal observations of zooplankton at Kongsfjorden and Rijpfjorden

highest bottom salinities recorded at Rijpfjorden (> 34.9) during phase RE. Surface temperature began to rise and salinity to fall towards the end of phase RE from April 08 onwards, but this trend increased sharply with the final switch back to phase RD in zooplankton community. During the two week final phase RD in August 08, surface temperature rose by $> 2^{\circ}\text{C}$ to $> 1.5^{\circ}\text{C}$ and salinity fell sharply. This sharp change in hydrography returned the system towards conditions more similar to SW recorded during the first zooplankton phase RD as highlighted by bottle 21 on Fig 3.17. High northward current velocities (both positive > 100 mm/s, and negative indicating primarily southward flow < -100 mm/s) accompanied this sharp change in hydrography in August 08, especially in the surface 0 – 50 m layer (Fig 1.17).

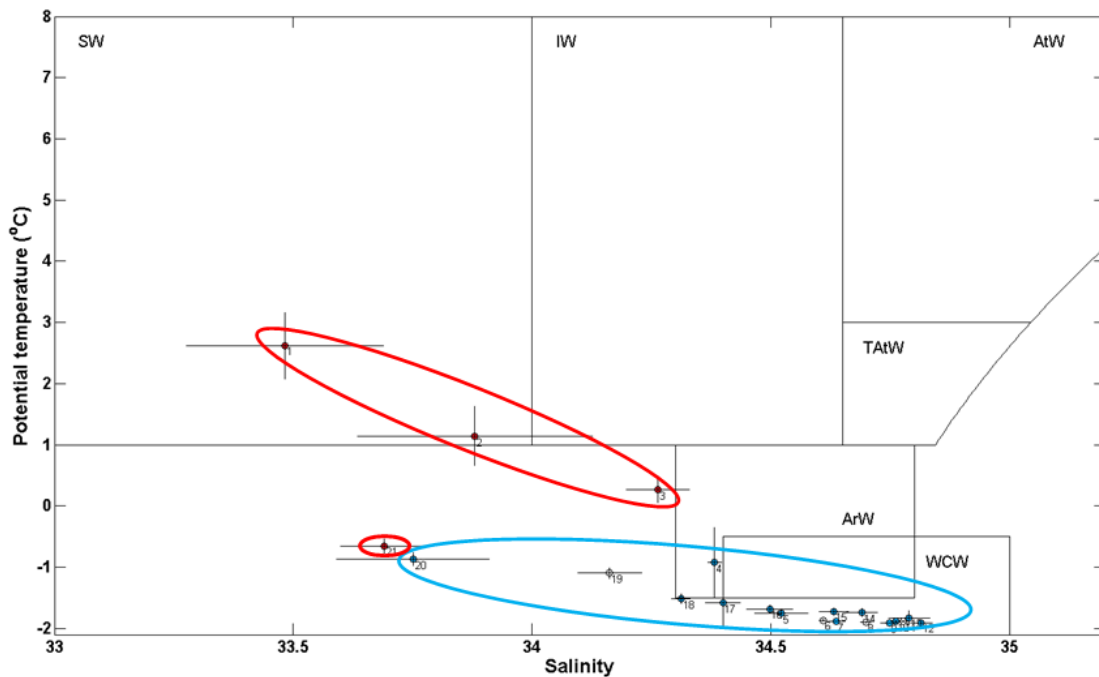


Fig 3.17) T-S diagram displaying temperature and salinity (means for each bottle calculated from daily averages during each bottle deployment with associated standard deviation) recorded at 12 m at Rijpfjorden 2007/08. The data are coloured and circled based on the two phases of zooplankton community composition (phase RD = red, phase RE = blue). Empty bottles that contained no zooplankton are not coloured in. Bottle numbers are displayed from 1 to 21. Water mass definitions as per Svendsen et al. (2002).

3. Moored seasonal observations of zooplankton at Kongsfjorden and Rijpfjorden

In 2009/10, the mooring deployment began at the start of September 09, and surface temperature ($< 2^{\circ}\text{C}$) and salinity (< 32.8) were low compared to September 06 and 07. Surface temperature fell to minimal values (approximately -2°C) by January 10 during phase RF, and bottom temperature rose from near -2°C to $> 0^{\circ}\text{C}$ during this period, before falling sharply towards the end of phase RF back to minimal values. Surface hydrography during phase RF thus initially indicated low salinity cold SW (Fig 3.18), moving towards WCW by the end of phase RF. High northward current velocities oscillating in direction (i.e. between positive – up to 200 mm/s – and negative – down to -200 mm/s – values) were observed from the start of the deployment in September 09 to approximately mid November 09 during phase RF (Fig 1.18). With the onset of the transition period between phase RF and RG in March 10, both surface and bottom temperatures were minimal and stable (Fig 3.15), indicating WCW (Fig 3.18). With the onset of a fully established zooplankton community phase RG in June 10, surface temperature began to rise dramatically (by over 6°C to $> 4^{\circ}\text{C}$ before August 10), and salinity also fell sharply indicating a change to SW by the end of the deployment in September 10 which was similar to the conditions recorded at the start of the deployment in September 09. High northward current velocities (up to 180 mm/s) were observed during this final phase RG from approximately July 10 onwards, especially in the surface 0 – 50 m layer (Fig 1.18).

3. Moored seasonal observations of zooplankton at Kongsfjorden and Rijpfjorden

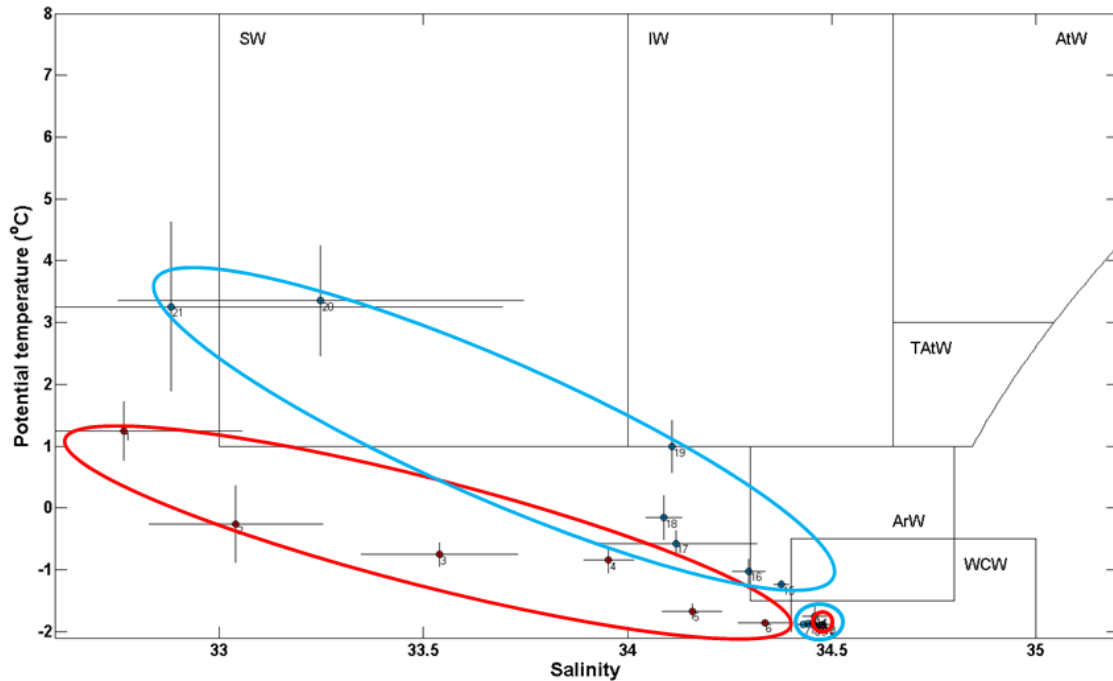


Fig 3.18) T-S diagram displaying temperature and salinity (means for each bottle calculated from daily averages during each bottle deployment with associated standard deviation) recorded at 27 m at Rijpfjorden 2009/10. The data are coloured and circled based on the two phases of zooplankton community composition (phase RF = red, phase RG = blue). Bottle numbers are displayed from 1 to 21. Water mass definitions as per Svendsen et al. (2002).

In 2010/11, the mooring deployment began in September 10, with surface temperature and salinity again lower than during this period in 2006 and 2007 and more similar to conditions in 2009. Surface salinity was at its lowest recorded level at the start of the deployment in September 10 (< 31.5), although this value increased dramatically before the first trap bottle was initiated on October 10. Similarly to the other Rijpfjorden deployments, surface temperature initially decreased through phase RH until approximately mid December 10 when temperature began to rise from < -1.5°C to > 1°C by February/March 11 (Fig 3.15). Surface temperature had dropped back to minimal values by the end of phase RH in June 11, with salinity reaching its highest recorded value for the deployment at approximately 34.5. Thus, phase RH in 2010/11 was influenced by SW, ArW and WCW conditions (Fig 3.19 – red). As in 2006/07 and 2009/10, the switch to zooplankton phase RI coincided with a dramatic increase in surface temperature, although this change was not sufficient to move the water mass

3. Moored seasonal observations of zooplankton at Kongsfjorden and Rjipfjorden

classification from one of WCW/ArW dominance (Fig 3.19 – blue). With the switch to zooplankton phase RJ in mid August 11 however, temperature had increased sufficiently (to $> 1.5^{\circ}\text{C}$) and salinity fallen (to < 34) to indicate SW dominance (Fig 3.19 – green). This SW dominance was similar to the conditions recorded during phase RC in July 2007 (Fig 3.16 – green). Highly negative northward current velocities indicating primarily southward flow were observed during phase RJ from mid August 11 onwards (down to -200 mm/s), especially within the surface 0 – 50 m layer (Fig 1.19).

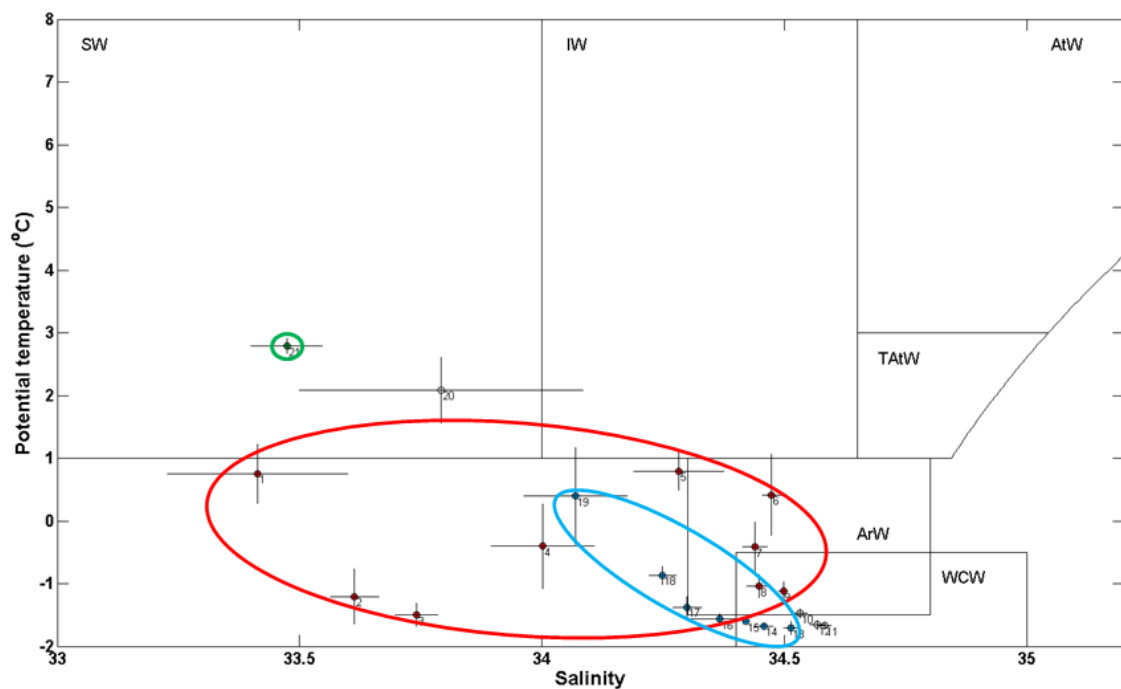


Fig 3.19) T-S diagram displaying temperature and salinity (means for each bottle calculated from daily averages during each bottle deployment with associated standard deviation) recorded at 33 m at Rjipfjorden 2010/11. The data are coloured and circled based on the three phases of zooplankton community composition (phase RH = red, phase RI = blue, phase RJ = green). Empty bottles that contained no zooplankton are not coloured in. Bottle numbers are displayed from 1 to 21. Water mass definitions as per Svendsen et al. (2002).

3.3.6. Correlations between hydrography and sediment trap zooplankton

At Kongsfjorden across the two deployments and Rijpfjorden across the four deployments, Spearman rank correlation between the trends in zooplankton community recorded in trap bottles and the trends in surface (22 m mean at Kongsfjorden and 24 m mean at Rijpfjorden) and bottom (200 m mean at Kongsfjorden and 209 m mean at Rijpfjorden) temperature and salinity (mean values for each trap bottle with associated standard deviations - sd) resulted in a highest correlation at Kongsfjorden of 0.431 (possible maximum correlation of 1 and minimum of 0) between zooplankton community and a combination of mean bottom temperature and sd. Correlations between zooplankton community and mean bottom temperature alone (0.379) and between zooplankton community and mean surface salinity and sd (0.320) were also comparatively high at Kongsfjorden (Table 3.3 – only five highest correlations at each location and depth displayed). At Rijpfjorden, correlation values were lower than at Kongsfjorden, with a highest correlation of 0.266 between zooplankton community and mean bottom salinity. The highest correlation at Rijpfjorden between surface hydrographic observations and zooplankton community was 0.047 (between zooplankton community and mean temperature and sd) (Table 3.3).

3. Moored seasonal observations of zooplankton at Kongsfjorden and Rijpfjorden

Table 3.3) Spearman rank correlations (possible maximum correlation of 1 and minimum of 0) between trends in sediment trap zooplankton community at Kongsfjorden and Rijpfjorden and any combination of trends in mean temperature (mean temp. over each bottle deployment [variable (1)], associated sd [variable (2)]) and salinity (mean sal. over each bottle deployment [variable (3)], associated sd [variable (4)]) both at the surface (22 m mean over the 2 Kongsfjorden deployments, 24 m mean over the 4 Rijpfjorden deployments) and bottom (200 m mean at Kongsfjorden, 209 m mean at Rijpfjorden). Only five highest correlations at each depth from each location are displayed. Columns 6 – 12 display correlations with combinations of variables (1), (2), (3) and (4) from columns 2 – 5. Highest correlations at each depth from each location are highlighted in bold.

Location (depth – m)	Correlation between zooplankton community and:										
	(1) Mean temp. (°C)	(2) Temp. sd	(3) Mean sal.	(4) Sal. sd	(1) (2)	(1) (2)	(1) (2)	(1) (3)	(2) (3)	(2) (3)	(3) (4)
Kongsfjorden (22)			0.312	0.304					0.269	0.274	0.320
Kongsfjorden (200)		0.379			0.431	0.324	0.323		0.323		
Rijpfjorden (24)	0.044				0.047	0.029	0.022	0.018			
Rijpfjorden (209)			0.266					0.239	0.251	0.231	0.236

3.4. Discussion

3.4.1. Hydrodynamic control on zooplankton community composition

Although there is an increasing amount of information outlining the physical changes of the Arctic environment in response to climate warming, there is less information available on the associated changes in biotic communities (Willis et al. 2008). These changes in community composition within a warming Arctic can have significant ecological effects, such as the lack of suitable prey items for planktivorous seabirds (Stempniewicz 2001). As highlighted in chapters 6 and 7 of this thesis, different zooplankton species associated with the different dominant water masses also maintain different diel vertical migration (DVM) patterns. These patterns can have important implications for carbon flux through the pelagic system, and have been related to levels of sea-ice cover and consequent primary production (Fortier et al. 2001; Hays 2003; Berge et al. 2009) which are all changing during the current regime of warming. Although relatively recent studies by Willis et al. (2006; 2008) have described long term time series of zooplankton community composition in Kongsfjorden, this study is the first to describe long term time series of zooplankton from Rijpfjorden, and does so over a number of years. It is important to note that sequential sediment traps may not collect zooplankton samples which are quantitatively representative of the zooplankton community, although a prior study at Kongsfjorden has shown that trends in zooplankton collected via sediment trap were consistent with trends observed via net sampling (Willis et al. 2006 – see section 2.1). Thus the term ‘abundance’ shall not be used through this discussion, but rather the observed trends discussed.

Plankton communities are known to form assemblages which are closely related to hydrography, and this phenomenon has been widely reported across the Arctic (e.g. Søreide et al. 2003; Daase and Eiane 2007; Blachowiak-Samolyk et al. 2008; Trudnowska et al. 2012). Physical processes such as advection have been reported to

3. Moored seasonal observations of zooplankton at Kongsfjorden and Rijpfjorden

influence productivity, community composition and age structure of zooplankton in fjords (Matthews and Heimdal 1980; Aksnes et al. 1989; Basedow et al. 2004). In their studies of Kongsfjorden, Willis et al. (2006; 2008) highlighted the importance of advection into the fjord on the structure of the zooplankton community, and it has been well reported that zooplankton remain closely associated with the different water masses found around the Svalbard archipelago (Hop et al. 2002; Kwasniewski et al. 2003). In this study, the concurrent long term zooplankton and hydrographic time series clearly highlights the close association between the zooplankton community and hydrographic changes in both Kongsfjorden and Rijpfjorden.

In Kongsfjorden in 2007, *Calanus* copepods were first recorded in the sediment trap in relatively high numbers from February onwards (phases KB and KC) when water mass conditions were most indicative of TAtW compared to the largely SW conditions before in phase KA. SW is locally produced by glacial melting and solar heating, while TAtW is known to be advected into the fjord from the West Spitsbergen Shelf. This advected water mass can penetrate far into the fjord (Berge et al. 2005; Cottier et al. 2005; Svendsen et al. 2002) and zooplankton carried with it are retained within the fjord (Basedow et al. 2004). It is thus most likely that the *Calanus* copepods were advected into the fjord from the shelf waters outside, and the highest peak in *C. finmarchicus* during this influx (an AtW associated species) supports this. The timing of the TAtW influx and its associated peak in *Calanus* numbers agreed closely with observations from Kongsfjorden in 2006 (Willis et al. 2008). Monthly mean eastward current velocities between 15 – 95 m observed by the mooring at Kongsfjorden changed from positive values between November 2006 and February 2007 to negative values (indicating primarily westward flow and water leaving the fjord) between March and July 2007. Kwasniewski et al. (2003) described how the Coriolis effect creates up-fjord flow along the southern coast, and down-fjord outflow along the northern coast of Kongsfjorden. Thus, our observed increase in outflow along the northern coast where the 2006/07 mooring was positioned during phases KB and KC indicated an increase in advection into the fjord along the southern coast, and subsequent flushing of the fjord along the northern coast. This flow brought with it zooplankton from within the fjord

3. Moored seasonal observations of zooplankton at Kongsfjorden and Rijpfjorden

which were collected in the sediment trap. Both 2006 and 2007 were comparatively ‘warm’ years around the Svalbard archipelago as described by prevailing sea ice conditions in July, August and September (Fig 1.9). This increased influx of AtW to the archipelago further explains the dominance of AtW masses and their associated zooplankton in Kongsfjorden. *Pareuchaeta norvegica* also peaked in numbers as phase KB began with the February influx of TAtW, and this was also aligned with observations in 2006 by Willis et al.

Just prior to the dominance by *Calanus* copepods, between approximately November 2006 and January 2007, conditions were less saline and more indicative of IW, a mixture of TAtW and SW. During these conditions in phase KA, *M. longa* and macrozooplankton such as euphausiids dominated in the fjord. *M. longa* especially is known as a boreo-Arctic copepod species (Willis et al. 2008) that remains active during the autumn and winter (Båmstedt et al. 1985) and peaks in abundance around December (Barthel 1995), and so this species was unlikely to be closely associated with the advected TAtW mass and was more likely resident in the fjord. It was unlikely that a dramatic increase in DVM behaviour after the Arctic winter prompted the observed increases in trap numbers, as DVM behaviour has been shown to continue through winter by prior studies (Cottier et al. 2006; Berge et al. 2009). With the final switch in zooplankton phase (back to phase KB) in May 2007, surface temperature increased dramatically and salinity fell, indicating a shift from TAtW dominance back to one of locally produced SW heated by solar radiation by the end of the deployment in September 2007 through an intermediate period of a mixture of the two (IW). However, such a dramatic increase in temperature also indicated a further influx of TAtW, with salinity kept low by mixing with meltwater. This influx in May would align closely with a similar influx observed in Kongsfjorden in 2002 (Willis et al. 2006). The influx was closely associated with peak trap numbers of *Sagitta elegans*, polychaetes, *Oikopleura* spp., *C. hyperboreus* and also the first recordings of younger stages of all three *Calanus* species. The fluorescence data recorded by the mooring at 19 m depth indicated peak fluorescence levels in May/June 2007, indicating that peak phytoplankton bloom conditions coincided with the occurrence of immature stages of *Calanus*. The large number of *C. finmarchicus* and *C. glacialis* adult females recorded just prior to this

3. Moored seasonal observations of zooplankton at Kongsfjorden and Rijpfjorden

through April 2007, followed by the appearance of young copepodid stages all indicated synchronised spawning of the two species in time with the phytoplankton bloom. It has been hypothesised that the different life histories of *C. finmarchicus* and *C. glacialis* result in segregated spawning in Kongsfjorden (Tande 1982; Smith 1990; Scott et al. 2000). However, our observations from 2007 and the observations of Willis et al. from 2002 both indicate synchronised spawning within the fjord.

Kongsfjorden in 2008/09 was generally much colder than in 2007/08. The prevailing sea ice conditions around the archipelago between July and September illustrated this difference well (Fig 1.9). During phase KD in September 2008, comparatively high temperature and low salinity indicated SW, although the high temperature was likely due to some TAtW influence as in 2007/08. These warmer conditions coincided with peak trap numbers of *Calanus*, *Pseudocalanus* spp., polychaetes and *Oikopleura* spp. No large zooplankton were recorded subsequently during the entire trap deployment, and phases KE and KF were distinct purely based on the numbers of smaller zooplankton species captured in the trap. However, phases KE and KF were also distinguishable by their contrasting hydrology to each other and to conditions in 2007, lessening the possibility that the trap failed to function properly during this deployment. From October 2008 onwards with the onset of phase KE, temperature dropped dramatically to below -1°C , far lower than in 2007, and the numbers of bivalve veligers and echinoderm larvae fell with it. Phase KF then began with minimal temperatures indicative of WCW which was never classified at the surface during the 2006/07 deployment, and at these temperatures the formation of sea ice was likely in the fjord. During this period between January 2009 and April 2009, monthly mean eastward current velocities recorded by the mooring were far lower than the same time period in 2007. Although the two mooring deployments were in different positions influencing current direction, the observed difference in current velocity indicated less fjord-shelf exchange in 2009 during the colder conditions compared to 2007. This difference in advection helps explain the absence of large zooplankton in the sediment trap during this period in 2009. As temperatures began to rise from May 09 onwards, so did the number of bivalve veligers recorded in the trap samples. These observations from 2009 with very little AtW influence through the winter and spring period reinforce prior

3. Moored seasonal observations of zooplankton at Kongsfjorden and Rijpfjorden

observations that advection maintains the populations of various species in the fjord (Kwasniewski et al. 2003; Willis et al. 2006; 2008), and suggests that resident populations in this case were not able to maintain themselves without this advection.

When correlating surface temperature and salinity (means with associated standard deviations (sd) for each trap sample) with zooplankton community composition, a combination of mean salinity and sd generated the highest correlation (0.320 with a possible maximum of 1 and a minimum of 0) at Kongsfjorden across the two deployments. Correlation with temperature was lower. However, a higher correlation was identified with a combination of bottom mean temperature and sd (0.431), with salinity at this depth less correlated to zooplankton community composition. As the advection of TAtW has been so strongly linked to zooplankton community composition both by this study and others, these results indicate that surface salinity may be a better indication of the presence of AtW influenced water masses than surface temperature. The higher correlation of zooplankton community composition with bottom (approximately 200 m) temperature indicates one of two possibilities. Firstly, zooplankton species may be advected into Kongsfjorden at greater depths, and TAtW intrusions may be reflected more accurately at 200 m than at 20 m. This is plausible as AtW is known to be found generally below 200 m depth in the open ocean as the Atlantic layer (Schlosser et al. 1995). Vertical migrations of the zooplankton may then bring them into contact with the sediment trap at 100 m depth. However, Willis et al. (2006) closely linked surface temperatures to zooplankton community composition at Kongsfjorden in 2002, so the dominance of this deeper advection is unlikely. Secondly, zooplankton advected into the fjord may take some time to come into contact with the sediment trap, and the lag between surface and deeper temperature which is noticeable in the data may create a situation where bottom temperatures actually correlate more closely with zooplankton recorded by the sediment trap.

The new results from Rijpfjorden include a number of interesting observations. Throughout all the deployments, the oscillating pattern between warmer and less saline conditions in August/September (indicative generally of locally produced SW heated by solar radiation) and very cold conditions through a homogenous water column between

3. Moored seasonal observations of zooplankton at Kongsfjorden and Rijpfjorden

approximately January and June (indicative of WCW) persisted. These cold winter conditions were dominated by sea ice cover at Rijpfjorden, and current velocities were generally lower. Zooplankton community composition was closely aligned to this cycle in hydrography, with the first phase (from September to anywhere between January and early June) generally containing higher numbers of *Calanus*, *M. longa*, *Pseudocalanus* spp., *G. wilkitzkii* and *T. libellula* and displaying close alignment with the warmer conditions. The subsequent winter period and zooplankton phases generally contained far fewer of these species, with high numbers of *Oikopleura* spp. and *Fritellaria borealis* indicating the rise in temperature around July/August. Various interannual changes in hydrography were observed however, and these had implications for zooplankton community composition.

In September 2006, although surface temperature was the highest recorded at Rijpfjorden ($> 4.5^{\circ}\text{C}$) and most indicative of IW (a mixture of TAtW and SW), the numbers of AtW associated *C. finmarchicus* remained comparatively low. Comparatively high numbers of ArW associated *C. glacialis* (Unstad and Tande 1991), *C. hyperboreus*, *T. libellula* (Dalpadado et al. 2001) and *G. wilkitzkii* (Lønne and Gulliksen 1991) however were recorded under these conditions in phase RA. It is possible that the warmer conditions prompted greater levels of ice-melt which dislodged the ice associated *G. wilkitzkii* and resulted in higher numbers entering the trap. With the change to phase RB and temperatures at a minimum, copepod and macrozooplankton numbers dropped to minimal values, and as temperatures rose again in phase RC, the only animal that appeared to respond was *Oikopleura* spp. as its numbers peaked during phase RC. During this switch to phase RC in July 2007, monthly mean northward current velocity in the 15 – 20 m layer (45 mm/s) increased dramatically compared to the prior January – June 2007 period (mean of -1.6 mm/s), and so it is likely that the *Oikopleura* spp. recorded in the trap were advected individuals. In September 2007, although temperatures were colder than 2006 ($< 3^{\circ}\text{C}$), *C. finmarchicus* trap numbers in phase RD were the highest recorded at Rijpfjorden and higher than *C. glacialis* and *C. hyperboreus* which were similar in numbers to 2006. This result is intriguing, as the close association of *C. finmarchicus* with AtW is well established. This observation thus indicates that a water mass definition of temperature

3. Moored seasonal observations of zooplankton at Kongsfjorden and Rijpfjorden

< 3°C and salinity < 33.5 can still suggest the influence of AtW heavily modified by mixing with locally produced cold fresh water. The highest monthly mean current velocity across all Rijpfjorden deployments was observed in September 2007 in the 15 – 20 m layer (-76.1 mm/s), and this negative value indicated southward flow into the fjord. This advection during September 2007 explains the peak trap numbers of *C. finmarchicus*, and identifies them as advected individuals. Comparatively high numbers of the ArW associated *Limacina helicina* (Willis et al. 2006), but also the presence of AtW associated *Themisto abyssorum* (Arashkevich et al. 2002) during this phase further confirmed the presence of mixed water masses. During this deployment as temperatures dropped to a minimum during phase RE, surface and bottom salinity both reached their highest recorded levels. This indicated greatest ice formation during the winter of 2007/08 (as highlighted by far more sea ice at this latitude in 2008 compared to 2007 – Fig 1.9), and nearly all zooplankton species were absent from the trap samples.

In September 2009, surface temperature was lower than in the previous two deployments. The number of *C. finmarchicus* was again low as in 2006, and numbers of *C. glacialis* and *C. hyperboreus* were also lower. The lower temperature indicated little advection of TAtW into the fjord, and the fewer *Calanus* individuals recorded at this period in the annual cycle appeared to support this. Monthly mean northward current velocity in the 15 – 20 m layer was -8.1 mm/s in September 2009 compared to -76.1 mm/s in September 2007, reinforcing the difference in advection between these two deployments. During this phase RF in 2009, *M. longa* and *Pseudocalanus* spp. were recorded in comparatively high numbers in the trap. As mentioned before, *M. longa* is known as a boreo-Arctic species that remains active during the autumn and winter, and the lower temperatures in 2009 helps explain its higher numbers. As temperatures began to rise again in phase RG, spikes in numbers of *Oikopleura* spp. and the AtW associated *F. borealis* (Arashkevich et al. 2002) were recorded, indicating the possible influence of advected TAtW into the fjord. As in July 2007, monthly mean northward current velocity increased dramatically during this period in phase RG (51.8 mm/s in July 2010) compared to the months before. Copepod nauplii, bivalve veligers and polychaete larvae in particular were also recorded in comparatively high numbers during this phase of increasing temperature, and more younger copepodids of *C. glacialis* were recorded

3. Moored seasonal observations of zooplankton at Kongsfjorden and Rijpfjorden

compared to phase RF. Although an increase in northward flow over the mooring indicated water primarily leaving the fjord, the observed increasing temperature suggests that *C. glacialis* had spawned outside Rijpfjorden on the adjacent shelf, and younger copepodids and nauplii had been advected into the fjord in warmer water and then flushed northwards over the mooring in outflow water (due to the Coriolis effect and the moorings position on the eastern coast of Rijpfjorden). In September 2010 during the final deployment, the lowest surface temperature and salinity were recorded (indicating the least influence of advection into the fjord), and phase RH lasted the longest (till the end of June 11). The number of *C. glacialis* was similar to 2009, but *C. finmarchicus* and *C. hyperboreus* were recorded in lower numbers suggesting their numbers are more affected by advection into Rijpfjorden during this period.

Interestingly, a significant warming event was recorded during phase RH between approximately February and May 11, with water mass characteristics approaching IW and indicating an influx of TAtW into the fjord. It appears that this influx brought with it sufficient zooplankton (especially *C. glacialis* and *Pseudocalanus* spp.) to maintain phase RH in zooplankton community for this lengthy period. This warming event (when temperatures reached well above 0°C) also closely coincided with the highest numbers of *G. wilkitzkii* recorded in the trap samples, supporting our suggestion that the melting of sea-ice dislodges this species which then enters the trap. As in 2010, rising temperatures during phase RI in 2011 again coincided with higher numbers of copepod nauplii recorded from July onwards, suggesting copepods are spawning during this period on the adjacent shelf and the nauplii are being advected into the fjord.

When correlating surface temperature and salinity with zooplankton community composition at Rijpfjorden across the four deployments, a combination of mean temperature and sd generated the highest correlation (0.047), but this correlation value was far lower than at Kongsfjorden. This indicates that advection of warmer water into the fjord which would affect temperature more strongly is less important at Rijpfjorden across all our deployments, and suggests Kongsfjorden was more strongly influenced by the advection of AtW influenced water masses. The comparative location of Rijpfjorden on the northeast coast at the maximum extent of AtW influence makes this highly likely. A higher correlation was identified with bottom mean salinity (0.266) at

3. Moored seasonal observations of zooplankton at Kongsfjorden and Rijpfjorden

Rijpfjorden. Bottom salinity is strongly influenced by sea-ice formation and the sinking of dense brine, and this result suggests sea-ice cover exerts a strong influence on zooplankton community composition at Rijpfjorden.

In terms of the current regime of climate change and a warming Arctic, our results show that ArW associated *Calanus* species of *C. glacialis* and *C. hyperboreus* and other ArW associated species such as *S. elegans* persisted at Kongsfjorden although the fjord was influenced by TAtW. In fact, the numbers of *C. glacialis* collected by the trap tended to be higher than *C. finmarchicus* at Kongsfjorden. Furthermore, although Rijpfjorden can be influenced by high numbers of *C. finmarchicus* in warmer years (e.g. 2007/08) indicating AtW influence reaches its location, the fjord was still largely dominated by ArW associated species with larger numbers of macrozooplankton such as *T. libellula* and *G. wilkitzkii*. Interestingly, large numbers of *Oithona* spp. were also found in Rijpfjorden and appeared to be largely persistent through the annual cycle. This small copepod is usually significantly underestimated in net hauls, and is known to be more flexible in terms of its reproduction and trophic interactions (Ashjian et al. 2003; Hagen and Auel 2001). Although this copepod is not responsible for the major energy flow through the pelagic system, it may play a key role in ecosystem function and its flexibility may allow it to dominate more in a warming Arctic (Hansen et al. 2003).

3.4.2. Conclusion

The high resolution time series of zooplankton and associated hydrographic data have clearly demonstrated the close association between dominant hydrographic conditions and zooplankton community composition at both Kongsfjorden and Rijpfjorden. Kongsfjorden is identified as more strongly influenced by Atlantic water advection into the fjord, but Arctic water associated species still persist there. Rijpfjorden is less influenced by advection of Atlantic water, but is more strongly influenced by sea-ice formation and cold Arctic conditions and dominated by Arctic water associated species. Warm years at Rijpfjorden do however bring Atlantic water influence and an influx of Atlantic water associated species.

4. Small scale spatial variation in zooplankton around moorings at Kongsfjorden, Rijpfjorden and Billefjorden

4.1. Introduction

Oceanic plankton is distributed unevenly, and the importance of this spatial heterogeneity to plankton ecology is well known (Folt and Burns 1999). In fact, this phenomenon in phytoplankton is one of the oldest oceanographic observations (Bainbridge 1957). Plankton aggregations or ‘patches’ are likely to influence diversity (Hobson 1989; Bracco et al. 2000), species interactions and community function (Folt and Burns 1999; Brentnall et al. 2003) and productivity (Martin et al. 2002). Zooplankton are generally sparsely distributed through much of the water column except for a few high-density aggregations where abundances may reach 10^3 times the median value (Folt et al. 1993; Megard et al. 1997). A large body of work has shown that zooplankton patchiness may be non-random (Hardy 1936; Cassie 1963; Wiebe 1970; Fasham et al. 1974) and also looked at the relationship between zooplankton and phytoplankton spatial structure along a range of scales (Horwood 1981; Levin et al. 1988; Piontkovski et al. 1995). Zooplankton have been traditionally considered passive members of patches that were the product of large-scale physical processes (Pinel-Alloul 1995). However, more recent research has incorporated biological processes as at least partially responsible for plankton patchiness (Zhou et al. 1994; Wiafe and Frid, 1996; Strutton et al. 1997). Much of this shift in opinion is due to more modern approaches in biological sampling which allow smaller scale biological processes in zooplankton to be observed (Fields and Yen 1997; Strickler 1998; Tiselius 1998). Strickler (1998) observed cyclopoid copepods mating in a 1-litre vessel, and noted how males could perceive females in the vessel and follow their movements 2 – 3 mm behind. Furthermore, animals of only 0.3 mm in size could swim up to 90 mm in 20

4. Small scale spatial variation in zooplankton around moorings at Kongsfjorden, Rijpfjorden and Billefjorden

seconds, behavioural capability which may allow them to influence their aggregations. Fields and Yen (1997) observed the escape behaviour of marine copepods in relation to fluid disturbances around them, and found that in some species the threshold of disturbance to initiate an escape response was very low. This suggested that their natural marine environments were hydrodynamically quiet, allowing them to swim actively through the environment. Amongst a number of apparatus (optical and electronic plankton counters, high frequency echosounders deployed on undulating CTD frames, video techniques etc), the Acoustic Doppler Current Profiler (ADCP) has been used increasingly to observe zooplankton (Smith et al. 1989; Greene et al. 1998; Berge et al. 2009; Wallace et al. 2010).

Four biological mechanisms are consistently cited as potential drivers of zooplankton patchiness: diel vertical migration (DVM), predator avoidance, finding food and mating (Folt and Burns 1999). Chapters of this thesis alongside other published research (Cottier et al. 2006; Falk-Petersen et al. 2008; Berge et al. 2009; Wallace et al. 2010) have shown DVM to occur in Arctic waters throughout the annual cycle. Various zooplankton predators have also been shown to inhabit these Arctic waters in chapters of this thesis. This thesis and numerous publications (e.g. Falk-Petersen et al. 2008; Blachowiak-Samolyk et al. 2008; Kwasniewski et al. 2012) have used the waters surrounding the Svalbard archipelago (including its numerous fjords) as a proxy for the Arctic marine system. Two fjords in particular, Atlantic water influenced Kongsfjorden and Arctic water dominated Rijpfjorden, have been compared and contrasted as the two oceanographic extremes found throughout the Arctic (Berge et al. 2009). However, these fjords exhibit environmental gradients along their length. In Kongsfjorden, this is largely due to the inputs from large tidal glaciers in the inner fjord (Hop et al. 2002). For a full review of the physical environment in Kongsfjorden, see Svendsen et al. (2002). In addition to this spatial gradient, these fjords are also influenced by a strong annual cycle highlighted in the previous chapter. Density fronts at the fjord entrance during winter and spring (Cottier et al. 2005) can limit exchange between the fjord and the adjacent shelf, which in turn affects the advection of zooplankton into the fjord (Willis et al. 2006). The combination of these factors suggests a high likelihood of

4. Small scale spatial variation in zooplankton around moorings at Kongsfjorden, Rijpfjorden and Billefjorden

zooplankton patchiness within the fjords. However, although much useful information has been gathered and published on zooplankton phenomenon from data collected by ADCP and sediment trap apparatus attached to fixed moorings within these fjords (e.g. Willis et al. 2006; Berge et al. 2009; Wallace et al. 2010), most studies on zooplankton spatial distribution around Svalbard and the Arctic have been carried out on relatively large spatial scales (e.g. Daase and Eiane 2007; Blachowiak-Samolyk et al. 2008). When Kongsfjorden was investigated along its length in terms of zooplankton distribution at a smaller spatial scale, Hop et al. (2002) found significant differences between stations in the inner and outer fjord. Another recent study using high resolution Laser Optical Plankton Counter measurements on the northern West Spitsbergen shelf described differences in zooplankton patches across frontal systems outside the fjords, and also between zooplankton patches within the fjords and outside them (Trudnowska et al. 2012). These findings of variations and patchiness make it important to assess how representative the moored observations within each fjord are compared to the rest of the fjords length and the pan-Arctic system.

To begin this assessment, the aim of this study was to investigate zooplankton spatial distribution on a small scale (~1 nautical mile) within three high latitude fjords of the Svalbard archipelago (Kongsfjorden, Rijpfjorden and Billefjorden). These fjords all contain long term fixed moorings from which important data on zooplankton have been collected and published, and so assessing the spatial relevance of these moored observations is important. Although spatial variability in plankton has long been discussed (e.g. Bigelow 1926; Hardy and Gunther 1935; Cassie 1959; Haury et al 1978), most studies have been concerned with variations at a larger scale (100-1000 km - Haury 1976). However, a study carried out in the Great South Channel of Georges Bank by Gallagher et al. (1996) using a Video Plankton Recorder has described how smaller scale distributions appear related to the planktons ability to aggregate in relation to background mixing intensity. Here, stronger swimmers such as *Calanus finmarchicus* (a species found in high abundances in Kongsfjorden) formed dense clusters in regions of high static water column stability, but were randomly distributed in more mixed water masses. Considering this variation, the contrasting fjord conditions and stability

4. Small scale spatial variation in zooplankton around moorings at Kongsfjorden, Rijpfjorden and Billefjorden

of Kongsfjorden, Rijpfjorden and Billefjorden may influence the spatial relevance of moored observations within each fjord to a differing degree. In order to best assess the spatial variation of zooplankton around the three moorings, a multi-disciplinary approach using a higher resolution multi-frequency echosounder and traditional depth-stratified net sampling was used in close proximity to the mooring itself. Along with its higher vertical and horizontal resolution, the echosounder also samples larger fast-moving macrozooplankton more effectively than any single net due to net avoidance and selectivity (Kasatkina et al. 2004).

4.2. Materials and methods

4.2.1. Sampling locations

This investigation was carried out over two years (2008/09) aboard RV *Jan Mayen* (Cruises AB320 and AB321), with all samples collected between 31 August – 7 September i.e. towards the end of the ‘midnight sun’ period on the Svalbard archipelago. Samples were collected from within three Svalbard fjords containing oceanic moorings, in triangular positions as close to the mooring as feasible (Table 4.1, Fig 4.1). The stations in this investigation were: Kongsfjorden in 2008 (KF 08 – KMT01/02/03), Kongsfjorden in 2009 (KF 09 – KMT04/05/06), Billefjorden in 2008 (BF 08 – BMT01/02/03) and Rijpfjorden in 2009 (RF 09 – RMT01/02/03).

4. Small scale spatial variation in zooplankton around moorings at Kongsfjorden, Rijpfjorden and Billefjorden

Table 4.1) Sampling station details including start date and time, station location and maximum water depth. Y (yes) and N (no) signify whether relevant data are available or not.

Station	Date	Start time (UTC)	Latitude (N)	Longitude (E)	Depth (m)	MPS depth strata (m)	MPS sampling time (UTC)	Acoustic data	CTD data
KMT01	04/09/08	00:40	78°59.433	11°22.832	319	300-200, 200-100, 100-50, 50-20, 20-0	00:55	Y	Y
KMT02	04/09/08	01:30	78°59.920	11°20.518	329	300-200, 200-100, 100-50, 50-20, 20-0	01:50	Y	N
KMT03	04/09/08	03:20	78°59.273	11°14.368	318	300-200, 200-100, 100-50, 50-20, 20-0	03:20	Y	N
KMT04	05/09/09	16:50	78°57.690	11°47.826	192	150-100, 100-50, 50-20, 20-0	16:50	Y	Y
KMT05	05/09/09	17:30	78°58.156	11°47.215	257	200-100, 100-50, 50-20, 20-0	17:40	Y	Y
KMT06	05/09/09	18:20	78°57.962	11°43.049	252	200-100, 100-50, 50-20, 20-0	18:40	Y	Y
BMT01	07/09/08	13:20	78°39.595	16°41.708	195	185-100, 100-50, 50-20, 20-0	13:20	N	Y
BMT02	07/09/08	14:00	78°39.834	16°41.287	189	175-100, 100-50, 50-20, 20-0	14:00	N	N
BMT03	07/09/08	14:40	78°39.618	16°40.484	189	175-100, 100-50, 50-20, 20-0	14:40	N	N
RMT01	31/08/09	22:50	80°16.463	22°18.071	169	150-100, 100-50, 50-20, 20-0	22:50	Y	Y
RMT02	31/08/09	23:20	80°17.004	22°15.488	200	150-100, 100-50, 50-20, 20-0	23:25	Y	N
RMT03	31/08/09	23:40	80°17.502	22°18.749	217	150-100, 100-50, 50-20, 20-0	23:55	Y	Y

4. Small scale spatial variation in zooplankton around moorings at Kongsfjorden, Rijpfjorden and Billefjorden

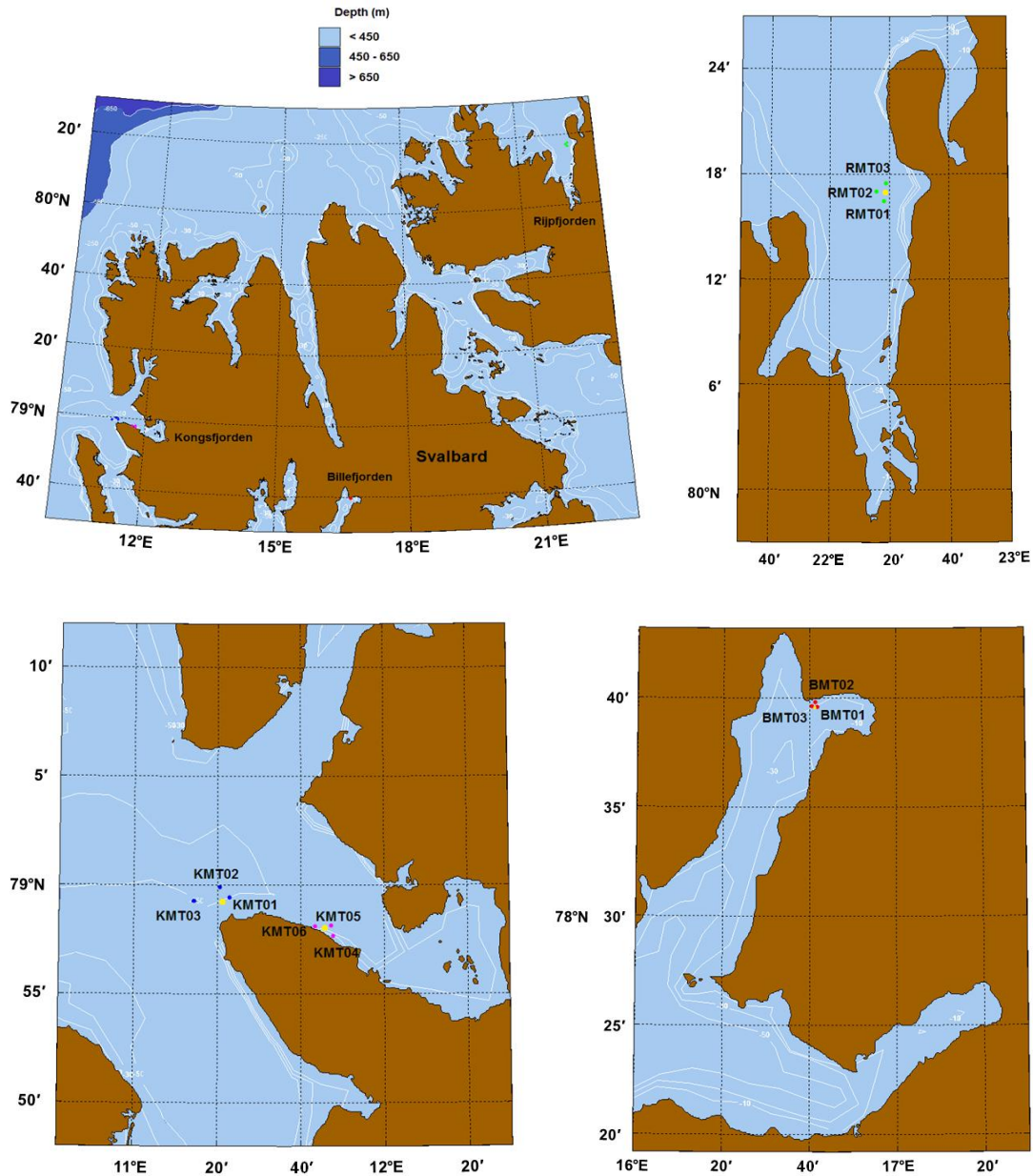


Fig 4.1) Top left – Broad scale map of the fjords sampled around the Svalbard archipelago (Rijpfjorden, Billefjorden and Kongsfjorden). Top right – expanded view of Rijpfjorden with the three sampling stations in green (RMT01/02/03). Bottom right – expanded view of Billefjorden with the three sampling stations in red (BMT01/02/03). Bottom left – expanded view of Kongsfjorden with the six sampling stations (KMT01/02/03 in blue and KMT04/05/06 in pink). Yellow dots in each expanded view represent the position of the mooring in each case. All stations are detailed in Table 4.1.

Please see thesis section 1.3.1 for detailed hydrology of the Svalbard archipelago and the three fjords investigated here. Briefly, Kongsfjorden opens onto the West

4. Small scale spatial variation in zooplankton around moorings at Kongsfjorden, Rijpfjorden and Billefjorden

Spitsbergen Shelf (WSS), and is heavily influenced by the convergence and mixing of AtW carried northward in the WSC (Svendsen et al., 2002; Basedow et al., 2004; Willis et al., 2006). Rijpfjorden in contrast is known to be more strongly influenced by ArW (Søreide et al., 2010) and, as a seasonally ice covered fjord, can be subject to high influxes of meltwater (Falk-Petersen et al., 2008). Billefjorden is separated from the AtW dominated system of Isfjorden by a number of sills and so it also dominated by Arctic conditions with seasonal ice cover and influxes of meltwater (Arnkvaern et al. 2005; Nilsen et al. 2008).

4.2.2. Environmental parameters

Salinity, temperature, depth and fluorescence were measured by Seabird CTD and processed following standard Sea Bird Electronics (SBE) data processing procedures by the Norwegian Polar Institute. CTD profiles were taken immediately prior to mesozooplankton sampling when possible, depending on time constraints at each station. Unfortunately due to these constraints, CTD profiles could not be collected at KMT02/03, BMT02/03 or RMT02 (Table 4.1). At these stations, the spatially closest CTD profile is used as a measure of the physical environment. An upward looking ADCP was deployed on each mooring at 70 - 100 m depth, and observations of eastward and northward horizontal current velocities between 15 – ~95 m were collected at 20 min x 4 m depth resolution. Negative eastward flow indicates westward flow while negative northward flow indicates southward flow. As mooring instrumentation was switched on after our net sampling in each case to avoid interference, current velocity observations were only available a day after sampling. Observations are thus used from the day after sampling in each case at times as close as possible to net sampling periods (one hour average binned vertically to match our multinet net sampling depths as closely as possible – i.e. 15 – 20, 20 – 50, 50 – 95 m). Although these current observations do not allow a measure of spatial variability in horizontal flow (as they are all collected by fixed moorings), they allow us to assess the temporal changes in currents during net sampling around each mooring.

4.2.3. Zooplankton sampling

Mesozooplankton sampling was conducted with a Multinet Plankton Sampler (MPS, Hydro-Bios, Kiel – see section 2.2 for details). Sample times and depths are detailed in Table 4.1. The depths of each sequential net were chosen at each station in order to allow comparable surface (i.e. 0-100 m) resolution while still sampling the entire water column. Filtered water volume was derived from measurements made by flowmeters attached to the MPS. All samples were fixed in 4% formalin/seawater solution and analysed for species composition post cruise as per Falk-Petersen et al. (1999) and Daase and Eiane (2007). The prosome lengths of all *Calanus* and *Metridia longa* were also measured. The mean depth (Z_m) of mesozooplankton species and corresponding standard deviations (Z_s) were calculated following the procedure described by Daase et al. (2008) (see 2.2. for equations).

4.2.4. Acoustic observations

A downward facing, hull-mounted Simrad EK60 echosounder operating at frequencies of 18, 38 and 120 kHz and a ping rate of 0.5 pings s^{-1} was used to gather backscatter information from the water column (12 m to near seabed). At all stations the ship attempted to remain stationary during data collection. Unfortunately due to a data logging error, data were not logged at Billefjorden (BMT01/02/03 – Table 4.1). Only data from the upper 175 m of the water column were used in the analysis due to range limitations at 120 kHz. The near field of 0-12 m (0-12 m at 38 kHz and 0-6.5 m at 120 kHz) was also excluded from analysis. Thus, data from 12-175 m were used in the acoustic analysis. To separate the backscatter into mesozooplankton, macrozooplankton and nekton echoes, 120 kHz – 38 kHz MVBS differentiations were used as per Madureira et al. (1993) (see 2.3. for calibration, noise removal and dB differencing details).

4. Small scale spatial variation in zooplankton around moorings at Kongsfjorden, Rijpfjorden and Billefjorden

In order to combine and compare the partitioned acoustic data and mesozooplankton net hauls, acoustic data were chosen from each station to match the mesozooplankton net sampling times as closely as possible. At all locations (KF 08, KF 09 and RF 09), one hour of acoustic data were collected in total; 20 minutes of acoustic data at each station that matched the net hauls as closely as possible (i.e. at KMT01/02/03/04/05/06, RMT01/02/03) were then used to calculate a Mean Volume Backscattering Strength ($MVBS = 10 \log_{10} [\text{mean}(S_v)]$, where S_v is the volume backscattering strength) for each net sampling event using echo integration on a 25 m X 10 min grid. For relevant equations and definitions, see Maclellan et al. (2002). Due to vessel drift and movement between stations, each 20 minutes of acoustic data that matched net hauls as closely as possible included both nominally stationary portions at each station and some vessel movement. Thus, these acoustic observations integrate a larger spatial area than the corresponding net samples. Using logged acoustic data at all available stations (i.e. no data from Billefjorden) and corresponding GPS fixes, the drift and movement of the ship during each 20 min observation period was plotted (Figs 4.4, 4.5 and 4.6).

The mean depth (Z_m) of mesozooplankton, macrozooplankton and nekton MVBS and corresponding standard deviations (Z_s) were calculated following the procedure described by Daase et al. (2008) and using our 25 m X 10 min grid and 12-175 m sampling depth (see equations in 2.2, with f_j being MVBS (dB) in this case).

4.2.5. Multivariate and Wilcoxon signed-rank analysis

Similarity matrices created in PRIMER were used to test for differences between the stations based on 1) hydrography, 2) mesozooplankton community composition, and 3) mesozooplankton vertical distribution.

4. Small scale spatial variation in zooplankton around moorings at Kongsfjorden, Rijpfjorden and Billefjorden

1) 10-m averages of temperature, salinity and fluorescence were calculated over the upper 180 m at each station and normalised (ranges converted to numerical values with a grand mean of zero and standard deviation of one) in order to summarise the hydrographic conditions. These data were then compared using a Euclidean distance similarity matrix and presented using a hierarchical cluster dendrogram.

2) Fourth-root transformed MPS-determined abundances of mesozooplankton were compared using a Bray-Curtis similarity matrix. The differences between locations (Kongsfjorden, Billefjorden and Rijpfjorden), stations (e.g. KMT01, KMT02 etc) and different depth strata were quantified using Analysis of Similarity (ANOSIM – see section 2.4). Similarity Percentage (SIMPER) analysis was also carried out to determine which species were most responsible for the observed differences in community structure between samples. Mesozooplankton abundances were also combined over the entire sampled depth (Table 4.1) at each sampling event and analysed using ANOSIM to assess the differences between samples irrespective of depth stratification.

3) Fourth-root transformed partitioned 120 kHz MVBS data (dB) were compared between locations, stations and taxa (mesozooplankton/macrozooplankton/nekton) using a Bray-Curtis similarity matrix and Analysis of similarity (as above). Similarity percentage analysis was carried out to determine which depth strata were most responsible for the observed differences in MVBS from the three taxonomic groups between samples. Mean depth information (Z_m) for each species (calculated from net abundances and depth stratified MVBS) was also standardised using a fourth-root transformation and compared between stations using Bray-Curtis similarity. The resulting Z_m dendrogram allows us to visualise the differences between the depth stratified samples.

4. Small scale spatial variation in zooplankton around moorings at Kongsfjorden, Rijpfjorden and Billefjorden

All these methods were used to quantify and assess spatial differences within locations (i.e. between samples within the same location) compared to the differences between the sampled locations (i.e. Kongsfjorden, Billefjorden and Rijpfjorden). In order to further quantify and assess the significance of differences between MPS abundance and MVBS data at each station (i.e. splitting the data set into constituent stations and making pairwise comparisons between stations), analysis by Wilcoxon signed-rank test was carried out.

4.3. Results

4.3.1. Environmental conditions

During our study, none of the sampled stations were directly affected by sea-ice cover and sampling occurred in open water. At Kongsfjorden, although glacial MW influenced the fjord, temperatures and salinities indicated AtW dominance during our sampling in 2008 and 2009 (Fig 4.2). Temperatures in the upper 25 – 50 m were approximately 5°C, with salinity as low as 33 at the surface and rising to nearly 35 by 75 m depth. This indicated fresh MW heated by solar radiation at the surface and mixed with AtW, with a layer of AtW beneath. At KF 09, the profiles displayed an intrusion of warmer water at approximately 75 – 100 m depth, while this was largely absent at KF 08. The fluorescence maximum was more pronounced at KF 08, and was located between 25 – 50 m depth, while at KF 09 this maximum was far less pronounced and was shallower.

At Billefjorden (2008), temperatures and salinities were similar to those found at Kongsfjorden at the surface, again indicating a layer of MW heated by radiation at the

4. Small scale spatial variation in zooplankton around moorings at Kongsfjorden, Rijpfjorden and Billefjorden

surface. Here however the thermocline was much steeper, with temperatures falling below zero at approximately 50 m depth. This colder water mass with a salinity close to 35 indicated ArW, with very cold Bottom Water (temperature < -1.7) below 100 m depth. The fluorescence maximum was more pronounced here than at any other location, and was located at approximately 20 m depth. The depth of this pronounced fluorescence maximum at Billefjorden corresponded to the boundary between surface MW and deeper ArW.

At Rijpfjorden (2009), surface temperatures were near zero, with salinity as low as 30.6. This very cold fresh surface layer was likely to be MW which has not been transformed by mixing with AtW or solar heating. Here the salinity rose steeply to 33.5 by 20 m and > 34 below 50 m, while temperatures increased above 1°C at approximately 20 m, before gradually dropping back below zero below 75 m. As at Billefjorden, these deeper waters indicated ArW with colder Bottom Water beneath. The fluorescence maximum was least pronounced at Rijpfjorden (Fig 4.2).

4. Small scale spatial variation in zooplankton around moorings at Kongsfjorden, Rijpfjorden and Billefjorden

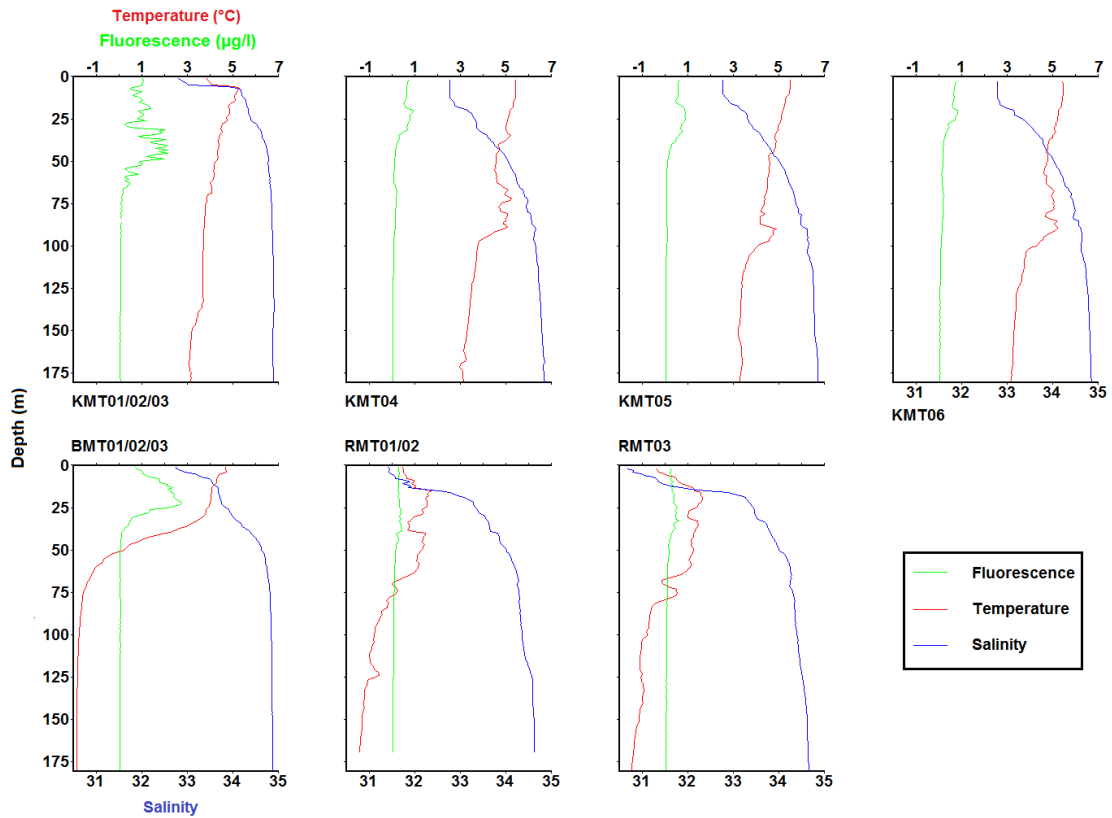


Fig 4.2) Vertical profiles of temperature (°C), salinity and fluorescence (µg/l) collected at Kongsfjorden (KMT - top), Billefjorden (BMT - bottom left) and Rijpfjorden (RMT - bottom right). ‘/’ between station numbers indicate the same profile is used for multiple stations. Station details in Table 4.1.

Analysis of similarity on 10-m averages of temperature, salinity and fluorescence over the upper 180 m resulted in a significant difference between the three locations ($R = 0.653$, $p = 0.029$) and also between the two years of sampling ($R = 0.782$, $p = 0.048$). The corresponding dendrogram from a cluster analysis of the same data illustrates these results (Fig 4.3). Kongsfjorden in 2008 (KF 08) was the least similar to all other stations, but interestingly was more similar to Billefjorden in 2008 (BF 08) than it was to Kongsfjorden in 2009 (KF 09). The greater similarity between KF 09 and RF 09 than between KF 09 and KF 08 is likely due to the more similar fluorescence profiles at KF 09 and RF 09 (Fig 4.2). For the locations with numerous profiles collected in the same year (i.e. KF 09 and RF 09), the differences within locations were far less than the differences between locations (Fig 4.3).

4. Small scale spatial variation in zooplankton around moorings at Kongsfjorden, Rijpfjorden and Billefjorden

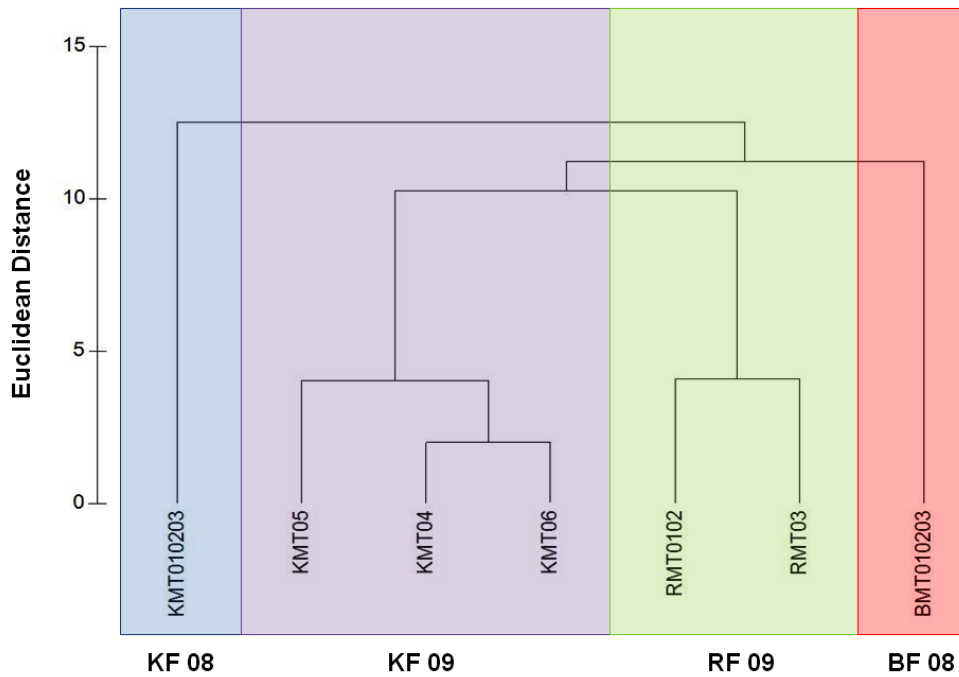


Fig 4.3) Dendrogram displaying the Euclidean distance grouping between normalised CTD data (10 m averages of temperature, salinity and fluorescence calculated from the surface to 180 m depth at each station) at all sampled stations. Only one CTD cast was available at KF 08 and BF 08, and at RF 09 the cast at RMT01 is used for RMT02 also. Colours outline different locations and years of sampling. Station details in Table 4.1.

Mean (mean of 3 x 20 min samples to create an hourly mean) horizontal current velocities observed the day after net sampling by upward looking ADCP's deployed on each mooring and binned vertically to match our net sampling depth strata are displayed in Table 4.2. Although these current velocities were not simultaneous with net sampling events, they give use the closest possible observations of currents at the same phases in the 24 hour tidal cycle. The zooplankton station which each current observation is linked to is described in Table 4.2. For full zooplankton sampling station details, see Table 4.1.

4. Small scale spatial variation in zooplankton around moorings at Kongsfjorden, Rijpfjorden and Billefjorden

Highest mean horizontal velocities were observed at Rijpfjorden, especially in the 20 – 50 m layer (-143.2 mm/s northward flow at 22:00 – 23:00 indicating primarily southward flow into the fjord – Table 4.2). Current velocities at Kongsfjorden and Billefjorden were generally lower, although associated standard deviations highlighted a regime of variation in currents through time and depth at all locations. These variations at Kongsfjorden and Rijpfjorden can be observed on Figs 1.14 – 1.19. Highest standard deviation was calculated about the mean horizontal velocity at Kongsfjorden (sd of 39.6 at 00:20 – 01:20 in the 20 – 50 m layer), and in general highest levels of variation as indicated by $sd > 30$ were observed through various depth layers and times at Kongsfjorden (Table 4.2).

4. Small scale spatial variation in zooplankton around moorings at Kongsfjorden, Rijpfjorden and Billefjorden

Table 4.2) Mean (mean of 3 x 20 min samples to create an hourly mean) eastward and northward horizontal current velocities (mm/s) and associated standard deviations observed the day after net sampling (at times which match net sampling times as closely as possible) by upward looking ADCP's deployed on each mooring. Standard deviations are displayed in brackets after each mean. Velocities are binned vertically to match net sampling depth strata as closely as possible. For full zooplankton net sampling station details, see Table 4.1.

Location	ADCP date	ADCP time (UTC)	Linked to station	Mean eastward horizontal velocity (mm/s) and sd			Mean northward horizontal velocity (mm/s) and sd.		
				Horizontal current velocity depth bins (m)					
				50 - 95	20 - 50	15 - 20	50 - 95	20 - 50	15 - 20
Kongsfjorden	05/09/08	00:20 - 01:20	KMT01	-27.1 (24.6)	-82.6 (29.3)	-30.7 (20.7)	5.6 (20.0)	8.5 (39.6)	40.2 (13.5)
		01:20 - 02:20	KMT02	-25.6 (34.1)	-102.4 (31.2)	-75.3 (20.7)	4.1 (13.8)	-10.8 (29.6)	41.3 (17.9)
		03:00 - 04:00	KMT03	-15.7 (19.1)	-95.0 (38.5)	-126.5 (28.0)	-15.9 (8.6)	-23.9 (11.4)	1.7 (10.9)
Kongsfjorden	06/09/09	16:20 - 17:20	KMT04	6.8 (24.6)	37.5 (17.3)	-30.3 (17.5)	-5.9 (15.8)	-15.0 (13.0)	-10.7 (8.4)
		17:20 - 18:20	KMT05	1.4 (28.5)	41.4 (17.4)	-30.5 (11.2)	0.9 (13.2)	-20.6 (13.8)	-19.5 (9.1)
		18:20 - 19:20	KMT06	4.9 (37.7)	38.6 (14.5)	-10.3 (21.7)	4.4 (14.1)	-30.8 (13.8)	-28.8 (14.6)
Billefjorden	08/09/08	12:40 - 13:40	BMT01	-10.3 (10.9)	-2.7 (17.7)	11.5 (10.2)	-12.0 (9.8)	-5.8 (17.0)	-29.5 (14.2)
		13:40 - 14:40	BMT02	-13.3 (8.4)	-4.9 (12.1)	11.3 (16.2)	-12.8 (12.6)	-6.5 (14.0)	-15.0 (15.2)
		14:40 - 15:40	BMT03	-9.5 (12.0)	-2.1 (14.6)	6.7 (6.9)	-3.0 (13.6)	-16.4 (9.3)	-12.3 (18.7)
Rijpfjorden	01/09/09	22:00 - 23:00	RMT01	-18.4 (9.3)	2.7 (23.6)	21.8 (10.3)	-127.4 (22.4)	-143.2 (17.9)	-123.2 (13.2)
		23:00 - 00:00	RMT02	-28.5 (8.7)	5.7 (32.7)	15.3 (6.0)	-124.4 (24.3)	-133.2 (18.7)	-119.2 (10.5)
	02/09/09	00:00 - 01:00	RMT03	-25.4 (8.1)	1.2 (30.6)	12.0 (3.9)	-119.6 (26.9)	-118.9 (24.2)	-113.0 (18.1)

4. Small scale spatial variation in zooplankton around moorings at Kongsfjorden, Rijpfjorden and Billefjorden

The plots of vessel position during each of the 20 minute acoustic observations indicated drift and highlighted the variable regime of surface currents throughout our sampling (Figs 4.4, 4.5, 4.6). At Kongsfjorden in 2008, the ship drifted > 800 m at KMT01 during acoustic data collection (Fig 4.4). The 20 minutes of acoustic observation which matched KMT02 as closely as possible included some active movement between stations and also considerable drift once at KMT02, and the 20 minutes integrated a distance of > 1000 m. Once the net sample was collected at KMT03, the 20 minutes of acoustic data were collected over the greatest distance at Kongsfjorden in 2008, a distance > 1500 m (Fig 4.4).

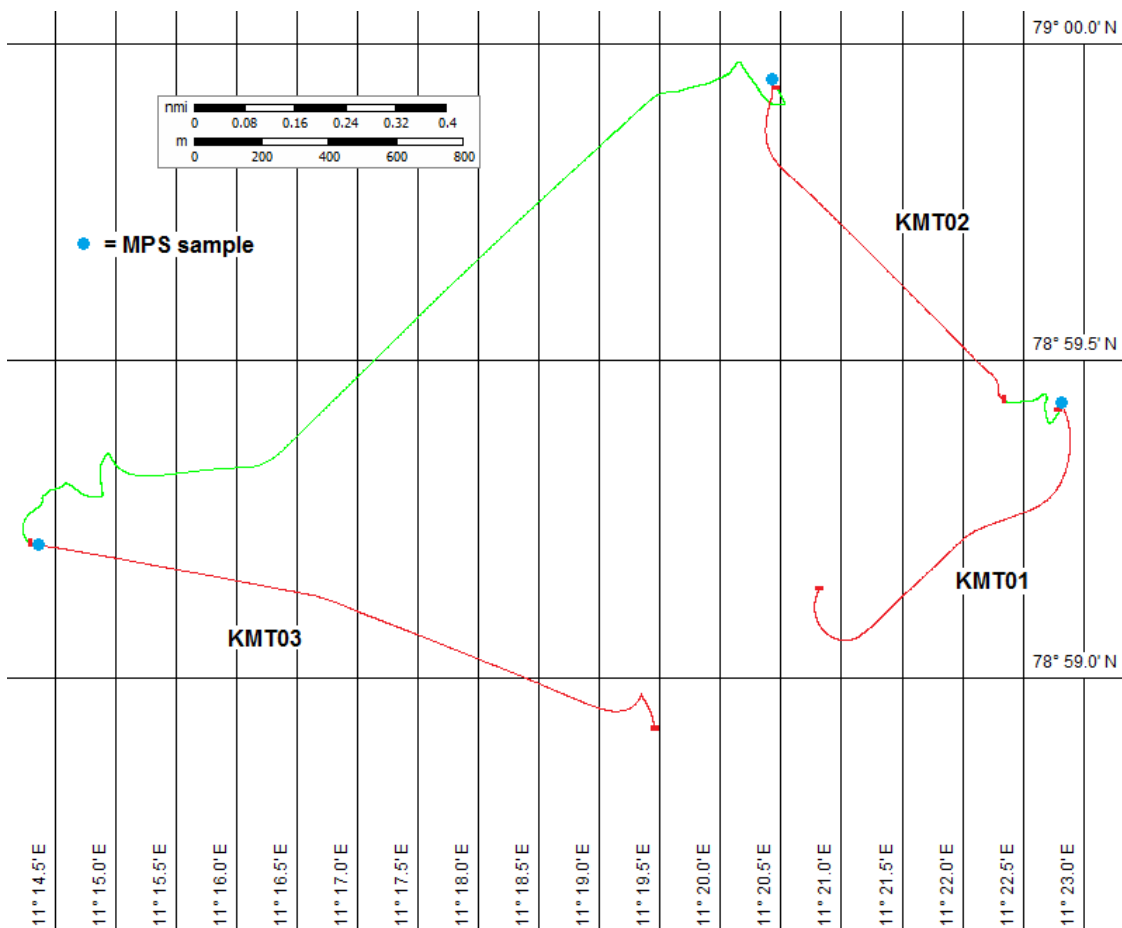


Fig 4.4) Cruise track plotted from GPS fixes during sampling at Kongsfjorden in 2008 (stations KMT01, KMT02 and KMT03 – see Table 4.1. for details). Blue circles represent multinet (MPS) zooplankton net samples collected at each station. Red dashes and red track signify the start and end of each 20 min acoustic observation.

4. Small scale spatial variation in zooplankton around moorings at Kongsfjorden, Rijpfjorden and Billefjorden

At Kongsfjorden in 2009, the 20 minutes of acoustic observation which matched KMT04 as closely as possible included some drift and active movement towards KMT05 over a distance of approximately 1000 m (Fig 4.5). The 20 minutes at KMT05 however included no active movement, and as the drift was circular, the start and end of acoustic data collection were approximately 100 m apart (Fig 4.5). The drift was similar at KMT06 (100 m), and the 20 mins of acoustic observation included no active movement between the stations.

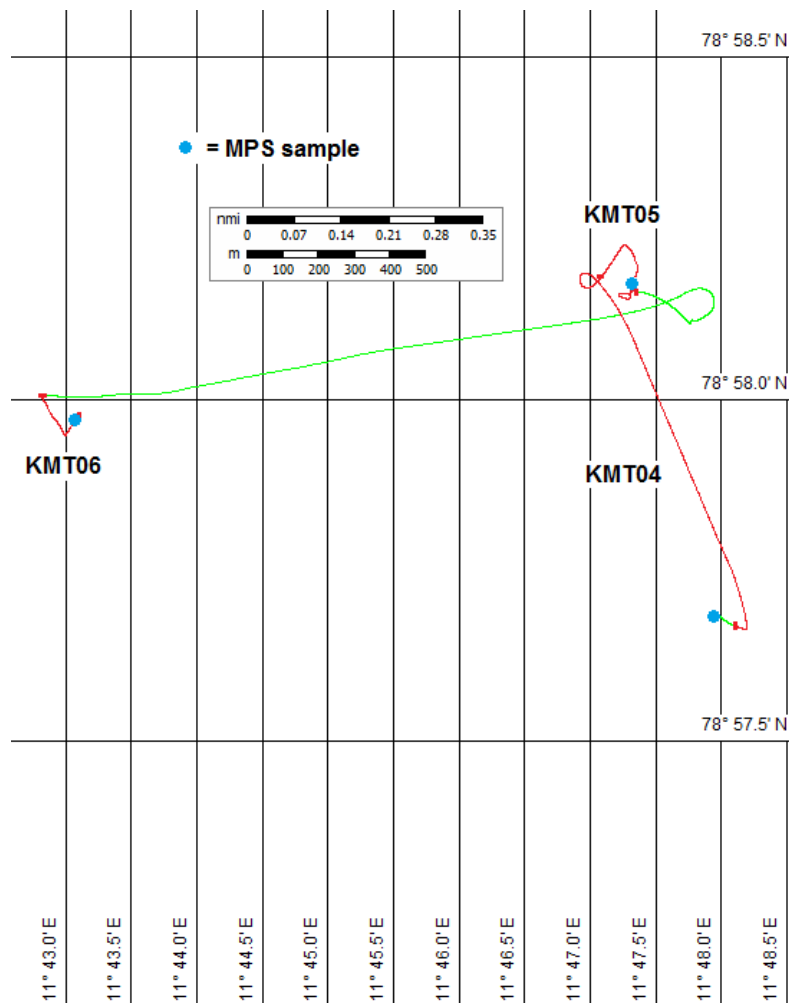


Fig 4.5) Cruise track plotted from GPS fixes during sampling at Kongsfjorden in 2009 (stations KMT04, KMT05 and KMT06 – see Table 4.1. for details). Blue circles represent multinet (MPS) zooplankton net samples collected at each station. Red dashes and red track signify the start and end of each 20 min acoustic observation.

4. Small scale spatial variation in zooplankton around moorings at Kongsfjorden, Rjippfjorden and Billefjorden

At Rjippfjorden in 2009, time constraints at all stations meant that each 20 minutes of acoustic observation which matched net samples as closely as possible needed to include movement between stations (Fig 4.6). However, it must be noted that drift at RMT01 after the net sample was significant before the vessel began to move towards RMT02, and the 20 minutes at RMT01 included approximately 500 m of drift and 800 m of active vessel movement (Fig 4.6). At RMT02, vessel drift was approximately 250 m, and the acoustic observations also integrated approximately 400 m of active movement. The 20 minutes of acoustic data that matched the net sample at RMT03 as closely as possible included mostly active movement between stations, and data were collected over the largest distance in this study (> 2000 m, Fig 4.6).

4. Small scale spatial variation in zooplankton around moorings at Kongsfjorden, Rijpfjorden and Billefjorden

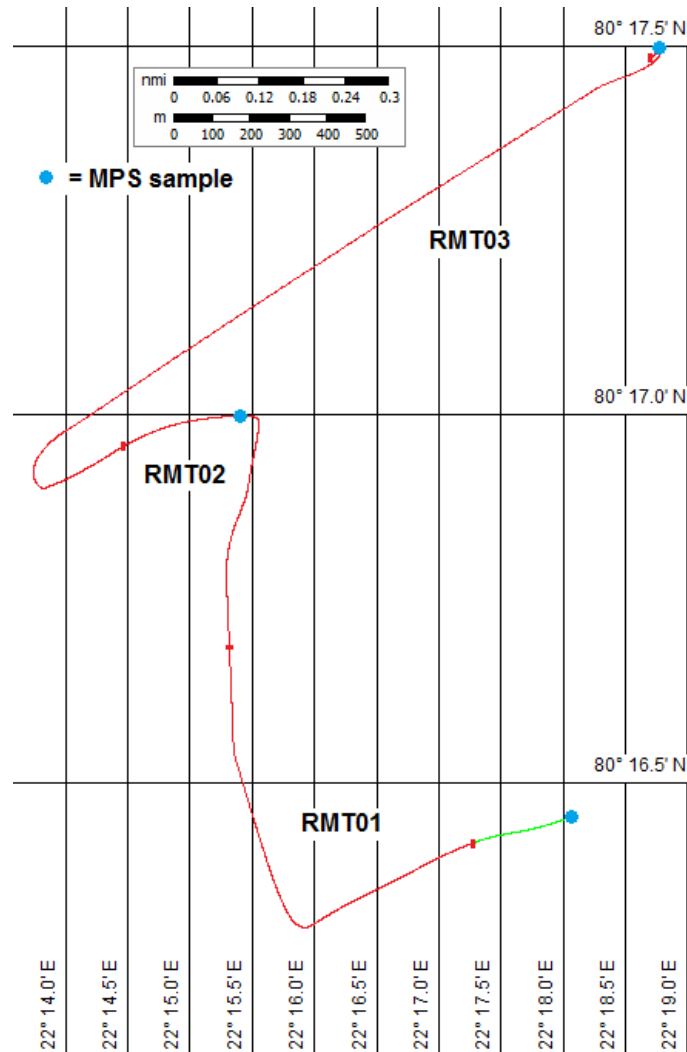


Fig 4.6) Cruise track plotted from GPS fixes during sampling at Rijpfjorden in 2009 (stations RMT01, RMT02 and RMT03 – see Table 4.1. for details). Blue circles represent multinet (MPS) zooplankton net samples collected at each station. Red dashes and red track signify the start and end of each 20 min acoustic observation.

4.3.2. Copepod populations and vertical distribution of *Calanus* and *Metridia longa*

To abbreviate species name for the remainder of this chapter, we will use the following codes: C. fin – *Calanus finmarchicus*, C. gla – *Calanus glacialis*, C. hyp – *Calanus hyperboreus*, M. long – *Metridia longa*, O. sim – *Oithona similis*, O. atl – *Oithona*

4. Small scale spatial variation in zooplankton around moorings at Kongsfjorden, Rijpfjorden and Billefjorden

atlantica, Pseudo – *Pseudocalanus* spp., Micro – *Microcalanus* spp., T. bor – *Triconia borealis*, Cop. nau – copepod nauplii, L. hel – *Limacina helicina*, Ech. lar – Echinoderm larvae, Biv. vel – Bivalve veliger, F. bor – *Fritellaria borealis*, Oik – *Oikopleura* spp, S. min – *Scolocithricella minor*, A. long – *Acartia longiremis*, T. abys – *Themisto abyssorum*, T. lib – *Themisto libellula*, E. ham – *Eukrohnia hamata*, S. ele – *Sagitta elegans*.

Copepods dominated numerically in all MPS samples (Fig 4.7). The small copepod *O. sim* was the most abundant species and on average accounted for > 53 % of the total number of individuals recorded in all samples (Table 4.3).

4. Small scale spatial variation in zooplankton around moorings at Kongsfjorden, Rijpfjorden and Billefjorden

Table 4.3) Integrated (integrated abundances over the total sampled depth summed for all 3 MPS hauls) and relative abundance (%) of the 10 most abundant species sampled at KF 08, KF 09, BF 08 and RF 09 using combined MPS hauls at each station (details in Table 4.1). For species abbreviations, see start of section 4.3.2.

KF 08 integrated abundance ind. m⁻³, (%)	KF 09 integrated abundance ind. m⁻³, (%)	BF 08 integrated abundance ind. m⁻³, (%)	RF 09 integrated abundance ind. m⁻³, (%)
O. sim 3663.1 , (58.11)	O. sim 2497.0 , (54.66)	O. sim 2583.2 , (38.95)	O. sim 1757.0 , (60.01)
Pseudo 433.8 , (6.88)	C. fin 648.8 , (14.20)	Micro 1167.3 , (17.60)	C. fin 332.6 , (11.35)
C. fin 389.3 , (6.18)	Pseudo 573.7 , (12.55)	Pseudo 864.4 , (13.03)	C. gla 279.1 , (9.53)
T. bor 280.9 , (4.46)	Micro 217.2 , (4.75)	F. bor 439.6 , (6.63)	Pseudo 172.6 , (5.89)
Micro 275.6 , (4.37)	C. gla 183.2 , (4.01)	A. long 424.1 , (6.39)	F. bor 157.2 , (5.37)
Biv. vel 249.8 , (3.96)	O. atl 100.3 , (2.20)	C. gla 386.0 , (5.82)	Cop. nau 70.7 , (2.41)
C. gla 217.8 , (3.45)	L. hel 64.6 , (1.41)	L. hel 342.9 , (5.16)	Micro 43.3 , (1.48)
L. hel 179.6 , (2.85)	A. long 53.8 , (1.18)	Ech. lar 108.8 , (1.64)	L. hel 26.1 , (0.89)
A. long 143.1 , (2.27)	Biv. vel 49.8 , (1.09)	C. fin 76.6 , (1.16)	Ech. lar 20.4 , (0.70)
Oik. 129.8 , (2.06)	S. min 48.2 , (1.06)	Biv. vel 62.6 , (0.94)	S. min 14.7 , (0.50)

4. Small scale spatial variation in zooplankton around moorings at Kongsfjorden, Rijpfjorden and Billefjorden

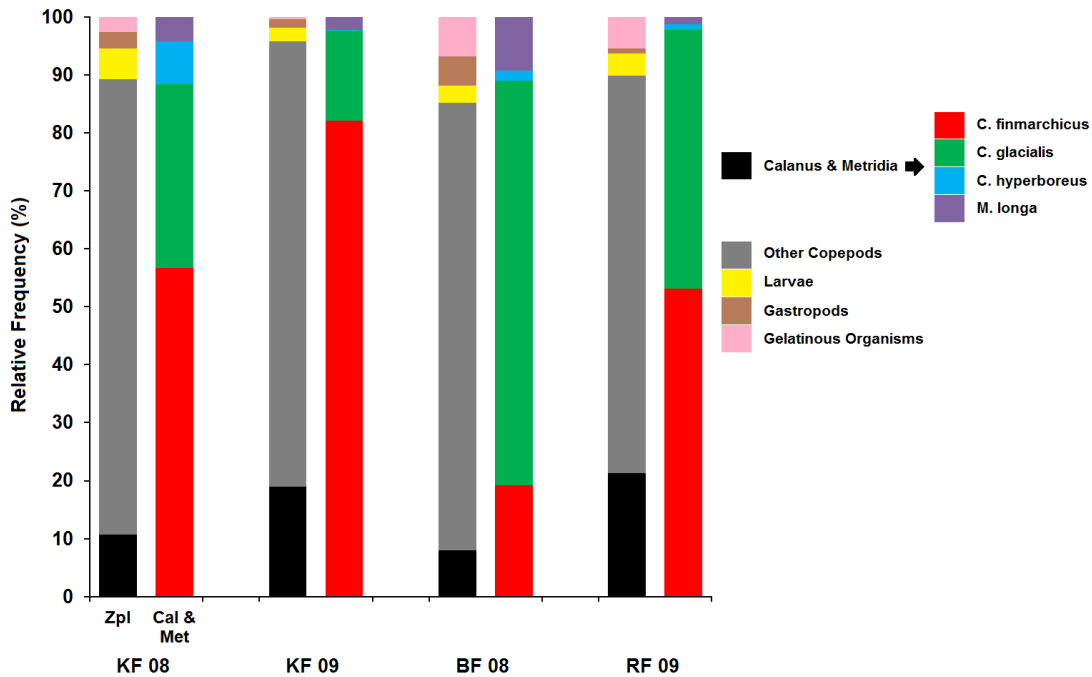


Fig 4.7) Relative frequencies (% abundance) of animals in combined MPS hauls at KF 08, KF 09, BF 08 and RF 09 (station details in Table 4.1). At each location, the *Calanus* and *Metridia longa* population is expanded to illustrate the proportion of species within this subset. Other copepods (grey) includes *Microcalanus* spp., *Pseudocalanus* spp., *Oithona similis*, *Oithona atlantica*, *Triconia borealis*, *Scolocithricella minor*, *Acartia longiremis*, *Microsetella norvegica*, *Bradyidius similis*, *Neoscolocithrix farrani*, *Harpacticus uniremis*, *Harpacticus superflexus* and *Oncea* spp. Larvae (yellow) includes copepod nauplii, echinoderm larvae, bivalve veligers, polychaete larvae, cyprid larvae, scyphozoa ephyra, bryozoan cyphonautes, isopod larvae and cnidaria cerinulas. Gastropods (brown) include *Limacina helicina* and *Limacina retroversa*. Gelatinous organisms (pink) include *Eukrohnia hamata*, *Sagitta elegans*, *Fritellaria borealis*, *Oikopleura* spp., *Aglantha digitale* and *Mertensia ovum*.

Apart from *O. sim*, the most abundant species were *Pseudo* spp. and *C. fin* across the three locations, accounting together on average for 17.8 % of the total number of individuals recorded in all samples (Table 4.3). *C. hyp* (0.23 % on average) and *M. long* (0.56 % on average) both had very low abundances across the study area. In terms of total integrated abundance (i.e. all animal abundances integrated over the total sampled depth for each MPS haul and summed within a location – 3 MPS hauls each), the two 2008 locations, KF 08 and BF 08 had the highest abundances which were similar between the two locations (6304 and 6633 ind. m⁻³ respectively). RF 09 had the lowest total integrated abundance (2928 ind. m⁻³), while KF 09 had a significantly lower

4. Small scale spatial variation in zooplankton around moorings at Kongsfjorden, Rijpfjorden and Billefjorden

abundance than KF 08 (4568 ind. m⁻³). Although the total integrated abundances were lower across all species, the percentage abundance of *Calanus* was higher at the 2009 stations (approximately 20% vs. approximately 10% in 2008 – Fig 4.7).

When comparing KF 08 and KF 09, a number of similarities and differences were identified. *O. sim*, *Pseudo*, *C. fin* and *Micro* were the dominant species in both years (Table 4.3). However, in KF 09, the relative frequency of *Calanus* (18.22 %) was greater than in KF 08 (10.25 %), mainly due to a rising proportion of *C. fin* (Fig 4.7). KF 09 also displayed virtually no *C. hyp* while KF 08 contained a small proportion of this species. In terms of its *Calanus* population, BF 08 had the highest relative abundance of *C. gla* (81.98 %) of all the locations, but the lowest relative abundance of *Calanus* vs. other species (7.10 %) (Fig 4.7). BF 08 also displayed the highest relative frequencies of *M. long* and gelatinous organisms across all locations. RF 09 displayed the highest relative frequency of *Calanus* across all stations (21.06 %), and high relative frequencies of *O. sim* and *C. fin* which were comparable to Kongsfjorden. The relative frequency of *C. gla* compared to all other species was also highest in Rijpfjorden (9.53 %) (Table 4.3).

The differences in proportions of the three *Calanus* species and *M. long* were reflected in the mean length frequencies at each location. In figure 4.8, the relative frequencies of mean lengths (lengths of *C. fin*, *C. gla*, *C. hyp* and *M. long* combined at each station and a mean and corresponding standard deviation calculated from the three stations at each location) are displayed. KF 09 and RF 09 shared the lowest mean length class (1.5 – 2 mm) mainly due to their high relative proportion of *C. fin* with proportionally less larger *C. hyp* and *M. long*. KF 08 had a slightly higher mean length class (2 – 2.5 mm), and a much greater range of lengths due to the higher proportional abundance of larger *C. hyp* (Fig 4.8). At BF 08, the lowest proportion of smaller *C. fin* and the highest proportion of larger *C. gla* combined to create the highest mean length class (3 – 3.5 mm). The high relative frequency of this size class indicated further that individuals of this *C. gla* population at BF 08 were of very similar size.

4. Small scale spatial variation in zooplankton around moorings at Kongsfjorden, Rijpfjorden and Billefjorden

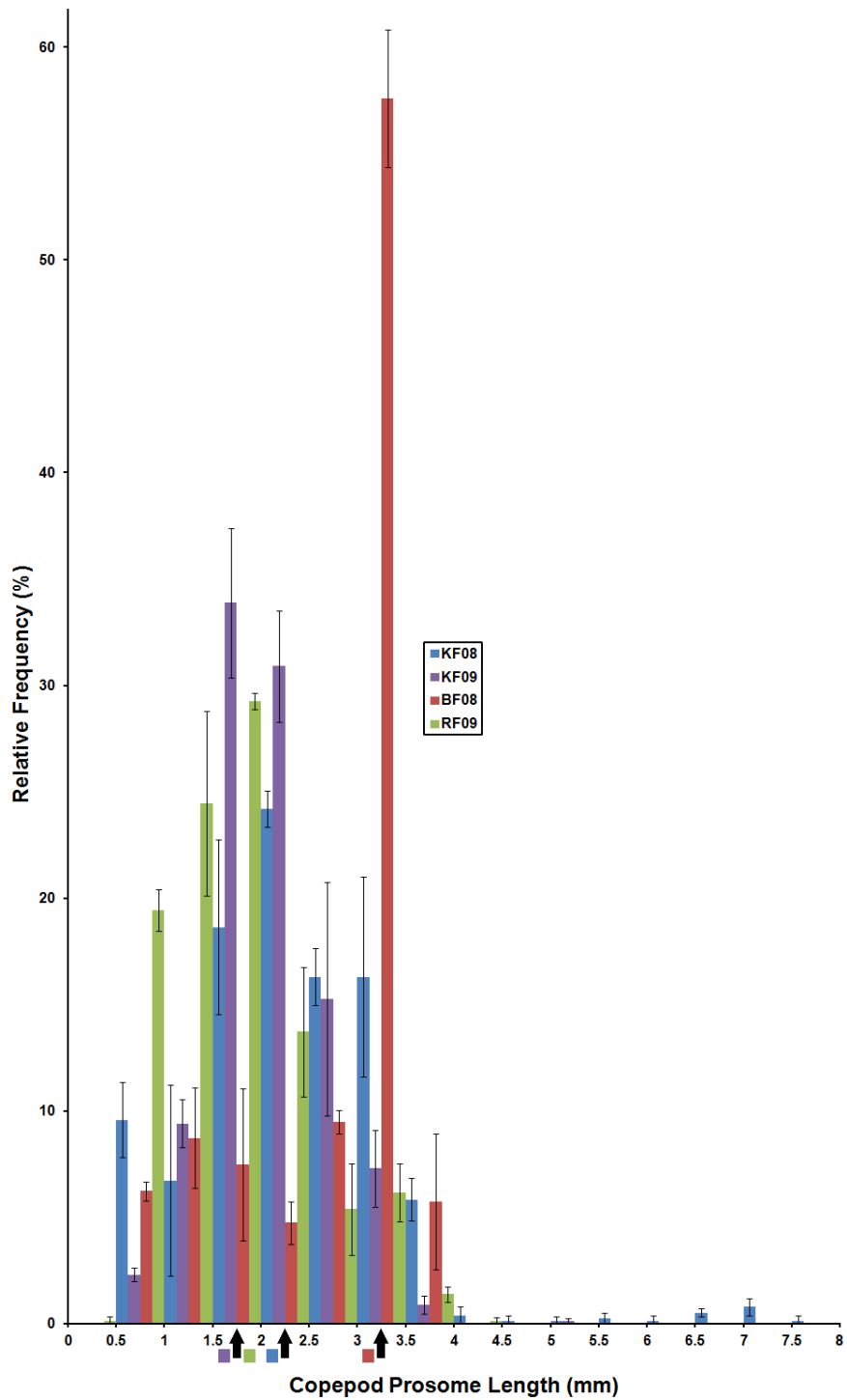


Fig 4.8) Prosome length distributions of *Calanus* and *Metridia longa* combined at each location with their corresponding standard deviations. KF 08 (blue) = mean of KMT01/02/03, KF 09 (purple) = mean of KMT04/05/06, BF 08 (red) = mean of BMT01/02/03, RF 09 (green) = mean of RMT01/02/03. Black arrows indicate the mean size class for each location.

4. Small scale spatial variation in zooplankton around moorings at Kongsfjorden, Rijpfjorden and Billefjorden

In order to determine variation within locations, the depth stratified MPS abundances of all species at each station (i.e. three stations at each location detailed in Table 4.1) were compared to each other within each location using Wilcoxon signed-rank analysis ($n = 290$ at each station). No significant differences were found between KMT01/02/03 at KF 08. However at KF 09, the depth stratified community at KMT06 was significantly different from KMT04 ($V = 979.5$, $p = 0.000$) and KMT05 ($V = 1678.5$, $p = 0.005$). At BF 08, differences were found between BMT01 and BMT02 ($V = 1269$, $p = 0.001$) and between BMT02 and BMT03 ($V = 3019$, $p = 0.021$), and at RF 09 all stations were significantly different from each other in terms of their depth stratified abundances (RMT01 vs. RMT02 $V = 3122$, $p = 0.007$, RMT01 vs. RMT03 $V = 3915.5$, $p = 0.000$, RMT02 vs. RMT03 $V = 3093$, $p = 0.000$). As the samples at each location were collected at different times of day, MPS abundances were integrated over the entire sampled depth and the same comparisons carried out ($n = 58$ at each station). This approach of removing depth stratification from the samples should reduce the effects of DVM on creating differences between samples. Significant differences were still identified between the same stations using this approach, although they were of lesser magnitudes.

In order to display the vertical distributions and abundances of *Calanus* and *M. long* most concisely, the 3 MPS hauls at each location were combined (mean and standard deviation calculated for abundances of each stage at each depth). The resulting depth distributions are displayed with corresponding standard deviations which represent the summed standard deviations across all stages at each depth (Fig 4.9). When reporting these results, 'total abundance' is not an integrated value across depth layers, but rather a sum of all mean abundances generated from the 3 MPS hauls at each location. For integrated abundances of dominant species, see Table 4.3.

4. Small scale spatial variation in zooplankton around moorings at Kongsfjorden, Rijpfjorden and Billefjorden

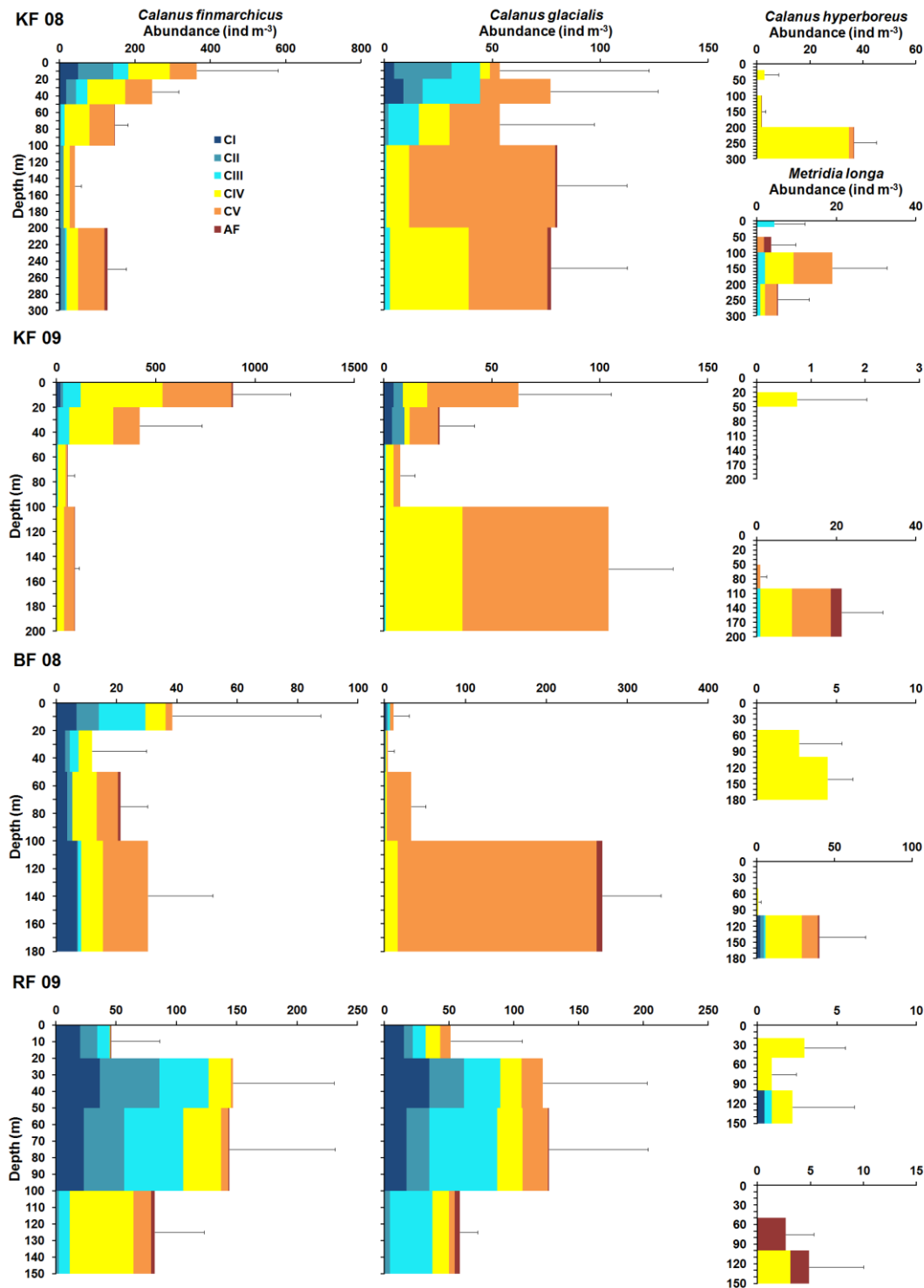


Fig 4.9) Vertical profiles of *Calanus finmarchicus* (left), *Calanus glacialis* (centre), *Calanus hyperboreus* and *Metridia longa* (right) collected by MPS (mean of 3 hauls) at Kongsfjorden 2008 (KF 08 top), Kongsfjorden 2009 (KF 09 upper centre), Billefjorden 2008 (BF 08 centre lower) and Rijpfjorden 2009 (RF 09 bottom). Error bars display cumulative standard deviation across all stages at each depth. Note that sampled depths vary between locations.

4. Small scale spatial variation in zooplankton around moorings at Kongsfjorden, Rijpfjorden and Billefjorden

At KF 08, 81.8 % of the *C. fin* population were situated in the upper 100 m. The upper 50 m contained most of the CI, CII and CIII at KF 08 (256.3 ind. m⁻³, 85.2 %) (Fig 4.9). CIV and CV dominated overall, accounting for 66.5 % of the total population. The *C. fin* layer which varied the most between stations at KF 08 was the 0 – 20 m layer, with a total standard deviation 4 times as much as any other layer (± 215.4). In contrast, the *C. gla* population was spread more evenly through the water column (Fig 4.9). CI, CII and CIII dominated the upper 50 m, constituting 68.2 % of this layer. High relative abundances of CV were observed below 100 m (67.6 ind. m⁻³ between 100 – 200 m), although total abundances were less than *C. fin* (Figs 4.7, 4.9). Again, CIV and CV dominated overall, accounting for 67.4 % of the total population. The variation in *C. gla* between stations at KF 08 was approximately the same at all depths, with the highest variation in the 0 – 20 m layer (± 69.3). The highest total abundance at all locations of *C. hyp* was recorded at KF 08 (41.2 ind. m⁻³), although this abundance was much lower than *C. fin* and *C. gla*. This population was almost entirely comprised of CIV below 200 m. The total *M. long* abundance at KF 08 was also low (33.2 ind. m⁻³), and most individuals were located below 100 m (Fig 4.9). Levels of variation between stations at KF 08 for *M. long* were higher than for *C. hyp*, with the highest variation between 100 – 200 m (± 13.7).

Total abundances of *C. fin* were higher at KF 09 compared to KF 08 (1454.9 and 926.8 ind. m⁻³ respectively (Fig 4.9). The relative abundance of younger stages at the surface and throughout the water column was also far lower at KF 09 compared to KF 08. Here CIV and CV dominated by a greater margin at all depths, accounting for 85.9 % of the total population. At KF 09, variation in *C. fin* between stations was greatest between 20 – 50 m (± 314.3), and although variation was higher between 0 – 20 m than at KF 08, variation relative to *C. fin* abundance was lower at this depth. As with *C. fin*, the *C. gla* population at KF 09 contained proportionally less juvenile stages than at KF 08, with CIV and CV constituting 89.5 % of the total *C. gla* population. Both *C. gla* abundance and relative frequency compared to *C. fin* was also less at KF 09 (Figs 4.7, 4.9). The *C. gla* population was less evenly distributed through the water column at KF 09 compared to KF 08, with most individuals in the surface layer or deeper water. Although *C. gla*

4. Small scale spatial variation in zooplankton around moorings at Kongsfjorden, Rijpfjorden and Billefjorden

abundances were slightly higher in these surface and deep layers at KF 09 (62.2 ind. m⁻³ at 0 – 20 m and 104.0 ind. m⁻³ at 100 – 200 m) compared to KF 08 (53.3 ind. m⁻³ at 0 – 20 m and 77.3 ind. m⁻³ at 200 – 300 m), variation between stations at these depths was lower (average standard deviation of 36.45 at KF 09 and 52.25 at KF 08). *C. hyp* was almost entirely absent at KF 09, while the low total abundance of *M. long* (24.9 ind m⁻³) was dominated by CIV, CV and adults below 100 m depth (Fig 4.9).

At BF 08, total abundance of *C. fin* was the lowest recorded in this study (102.1 ind. m⁻³). CI, CII and CIII accounted for 49.6 % of this smaller population however, a higher proportion than at either of the years at Kongsfjorden (Fig 4.9). CI, CII and CIII dominated the upper 50 m (73.5 % abundance in this layer), while CIV and CV accounted for 72.0 % of *C. fin* below 50 m depth. Variation in *C. fin* between stations at BF 08 was highest between 0 – 20 m (± 49.1). In contrast to *C. fin* at this location, a high abundance of *C. gla* was observed below 100 m (301.9 ind. m⁻³), and this population was almost entirely dominated by CV (Fig 4.9). Very few *C. gla* individuals were observed shallower than 50 m depth (15.6 ind. m⁻³). *C. hyp* abundances were again very low at BF 08 (total abundance of 7.1 ind. m⁻³), and only CIV were recorded below 50 m depth. At BF 08, a mixed population containing all developmental stages of *M. long* was observed at the highest total abundances and relative frequencies recorded in this study (42.2 ind. m⁻³) (Figs 4.7, 4.9). This population of *M. long* was dominated by CIV and CV (accounting for 81.6 % of the *M. long* population), and recorded almost entirely below 100 m depth.

At RF 09, *C. fin* was relatively abundant (total abundance of 251.9 ind. m⁻³), although numbers here were far less than at Kongsfjorden. In contrast to Kongsfjorden however, the population at RF 09 was heavily dominated by CI, CII and CIII which accounted for 71.2 % of the *C. fin* population. A further contrast was identified in the depth distribution of *C. fin* between Rijpfjorden and Kongsfjorden, with most individuals located below 20 m (84.2 %) (Fig 4.9). The majority of the *C. fin* population at RF 09 was located between 20 – 100 m, and this layer accounted for 68.1 % of the total

4. Small scale spatial variation in zooplankton around moorings at Kongsfjorden, Rijpfjorden and Billefjorden

number of individuals. Although the abundance of *C. fin* between 50 – 100 m was fairly similar at RF 09 and KF 08/KF 09, the variation between stations within RF 09 was significantly higher at this depth (± 87.6 compared to an average of ± 35.7 at Kongsfjorden). The lower abundances of *C. fin* between 0 – 20 m were comprised almost entirely of CI, CII and CIII, while the deeper 100 – 150 m layer was dominated by CIV and CV (76.0 %). *C. gla* at RF 09 followed a very similar pattern to *C. fin* at RF 09 in terms of total abundance, stage composition, depth stratification and variation between stations (Fig 4.9). As can be noted from Fig 4.7, the relative frequencies of these two species were very similar at RF 09. A very low total abundance of *C. hyp* was again observed (6.1 ind. m^{-3}), and this population was again dominated by CIV. At RF 09, although the total abundance of *M. long* was very low (7.6 ind m^{-3}), it consisted mostly of adults (58.8 %) which was in contrast to all other locations.

In order to remove the influence of differing abundances of species/stages and assess only the differences in depth distribution between stations at the same location (i.e. three stations at each location detailed in Table 4.1), mean depths (Z_m) were calculated for each species/stage and stations were compared to each other within each location using Wilcoxon signed-rank analysis ($n = 58$ at each station). Again, no significant differences were identified between KMT01/02/03 at KF 08 using Z_m . At KF 09, KMT04 was identified as being significantly different from KMT05 ($V = 196.5$, $p = 0.020$) and KMT06 ($V = 197.5$, $p = 0.007$). This differed slightly to the results gathered using depth stratified abundances, where KMT06 was found to be significantly different from the other two stations at KF 09. At BF 08 and RF 09, none of the stations were identified as being significantly different from the others at the same location when using Z_m .

4.3.3. Multivariate analysis of net samples

When all stations were tested together, significant differences in depth-stratified MPS abundances were found between stations (ANOSIM $R = 0.328$, $p = 0.001$) and locations (i.e. Kongsfjorden, Billefjorden and Rijpfjorden – $R = 0.460$, $p = 0.001$). However, pairwise comparisons on the Bray-Curtis similarity matrix resulted in no significant differences between stations at the same location (i.e. within KF 08, KF 09, BF 08 and RF 09) and also no significant differences between any of the stations at KF 08 vs. any of the stations at KF 09. The largest pairwise differences were between stations in Kongsfjorden (2008) and Rijpfjorden, with KMT01 vs. RMT02/03 ($R = 0.735$, $p = 0.008$), KMT02 vs. RMT03 ($R = 0.644$, $p = 0.008$) and KMT03 vs. RMT01/02/03 ($R = 0.638$, $p = 0.008$). Pairwise comparisons between locations overall highlighted the largest difference between Billefjorden and Rijpfjorden ($R = 0.746$, $p = 0.001$), and the smallest between Kongsfjorden and Billefjorden ($R = 0.294$, $p = 0.001$). The sampled depths at all stations were grouped as follows (0 – 50, 50 – 100, 100 – 200 and 200 – 300 m) in order to test for differences between depths at all the stations combined. A significant difference was found between the depth strata ($R = 0.321$, $p = 0.001$), and pairwise tests highlighted the largest differences between the surface layer and deepest layers (0 – 50 vs. 100 – 200 m $R = 0.576$, $p = 0.001$, 0 – 50 vs. 200 – 300 m $R = 0.574$, $p = 0.003$). There was no significant difference between 0 – 50 and 50 – 100 m, or between 100 – 200 and 200 – 300 m.

As Wilcoxon signed-rank tests had found differences between communities within KF 09, BF 08 and RF 09, SIMPER (see section 2.4 for details) was used to identify which species were most responsible for differences between the stations highlighted by Wilcoxon signed-rank differences. The species most responsible for community differences between KMT06 and KMT04/05 were *Oik* (5.54 % responsible), *O. sim* (5.15 %), and *Biv. vel* (4.76 %). The species most responsible for differences between BMT01 and BMT02 and between BMT02 and BMT03 were *F. bor* (7.26 %), *C. gla CV*

4. Small scale spatial variation in zooplankton around moorings at Kongsfjorden, Rijpfjorden and Billefjorden

(5.90 %) and *O. sim* (4.88 %). The species most responsible for the differences between RMT01/02/03 were *C. fin CI* (4.69 %), *F. bor* (4.63 %) and polychaete larvae (4.10 %).

To remove the influence of differences between sampled depths and changes in depth stratification between stations, the MPS abundances were integrated over the entire sampled depth and tested again. A significant difference was found again between all locations together ($R = 0.998$, $p = 0.001$), although with this integrated data no significant difference was found between Billefjorden and Rijpfjorden. This is probably due to the smaller sample size when using integrated abundances (Kongsfjorden contained KF 08 and KF 09 and so had a larger sample size than Billefjorden or Rijpfjorden). The largest significant difference was identified between Kongsfjorden and Rijpfjorden ($R = 1.000$, $p = 0.012$). The corresponding dendrogram (water column integrated abundance) is displayed on figure 4.10. Finally, to remove the influence of varying abundances between stations and test just for changes in depth stratification, mean depth (Z_m) was calculated for each species/stage and the Z_m data were tested again. A significant difference in Z_m was found between all locations ($R = 0.793$, $p = 0.001$), and as with the integrated abundances, pairwise tests identified the largest difference between Kongsfjorden and Rijpfjorden ($R = 0.796$, $p = 0.012$) and no difference between Billefjorden and Rijpfjorden. The corresponding dendrogram (mean zooplankton depth) is displayed on figure 4.10.

Both dendrograms (Fig 4.10) illustrate that within location similarity was much higher than between location similarity. Both dendrograms also illustrate that the differences between stations at KF 08 and KF 09 were less than the differences between Kongsfjorden and the other two locations. When considering integrated abundance (Fig 4.10 bottom), KF 08 and KF 09 shared approximately 80 % similarity compared to approximately 75 % similarity between Kongsfjorden and Billefjorden, and approximately 70 % similarity between Kongsfjorden and Rijpfjorden which were the most distant locations. Although much of the branching pattern remained the same

4. Small scale spatial variation in zooplankton around moorings at Kongsfjorden, Rijpfjorden and Billefjorden

when considering mean depths (Fig 4.10 top), KF 08 and KF 09 were less similar to each other in terms of zooplankton mean depths (approximately 75 % similarity).

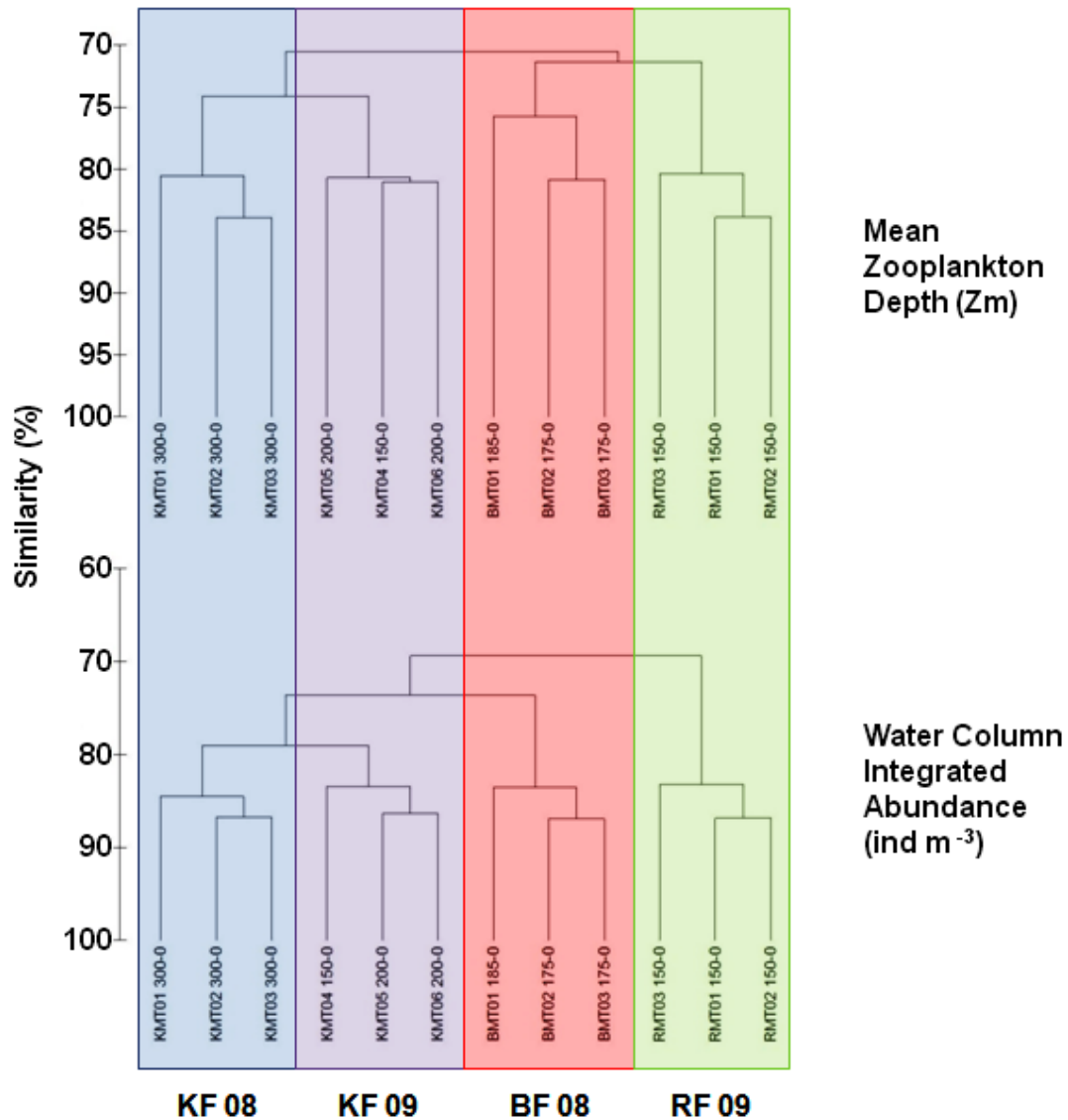


Fig 4.10) Hierarchical cluster dendrograms based on Bray-Curtis similarity analysis of fourth-root transformed zooplankton mean depth (Z_m - top) and integrated abundance over the total sampled depth (bottom). Similarity scale on cluster dendrograms represents percentage similarity between samples. Sampling depths from which Z_m is calculated and over which abundances are integrated are displayed in the sample names (station details in Table 4.1). Shaded areas represent sampling locations and years labelled below.

4. Small scale spatial variation in zooplankton around moorings at Kongsfjorden, Rippfjorden and Billefjorden

4.3.4. Acoustic observations

For this section, Mean Volume Backscattering Strength (MVBS - dB) values reported are based on echo integrations carried out on partitioned acoustic data (mesozooplankton [ME], macrozooplankton [MA] and nekton [NE]) using a 25 m X 10 min grid at each station. MVBS from each of the two ten minute periods at each station are averaged (by converting S_v to s_v , calculating a mean s_v then converting back to S_v – for equations and definitions see Maclennan et al. 2002) and displayed for each category on figure 4.11. MVBS was generally low at all Kongsfjorden stations (-90.4 dB mean across all size categories and depths - Figs 4.11, 4.12).

4. Small scale spatial variation in zooplankton around moorings at Kongsfjorden, Rijpfjorden and Billefjorden

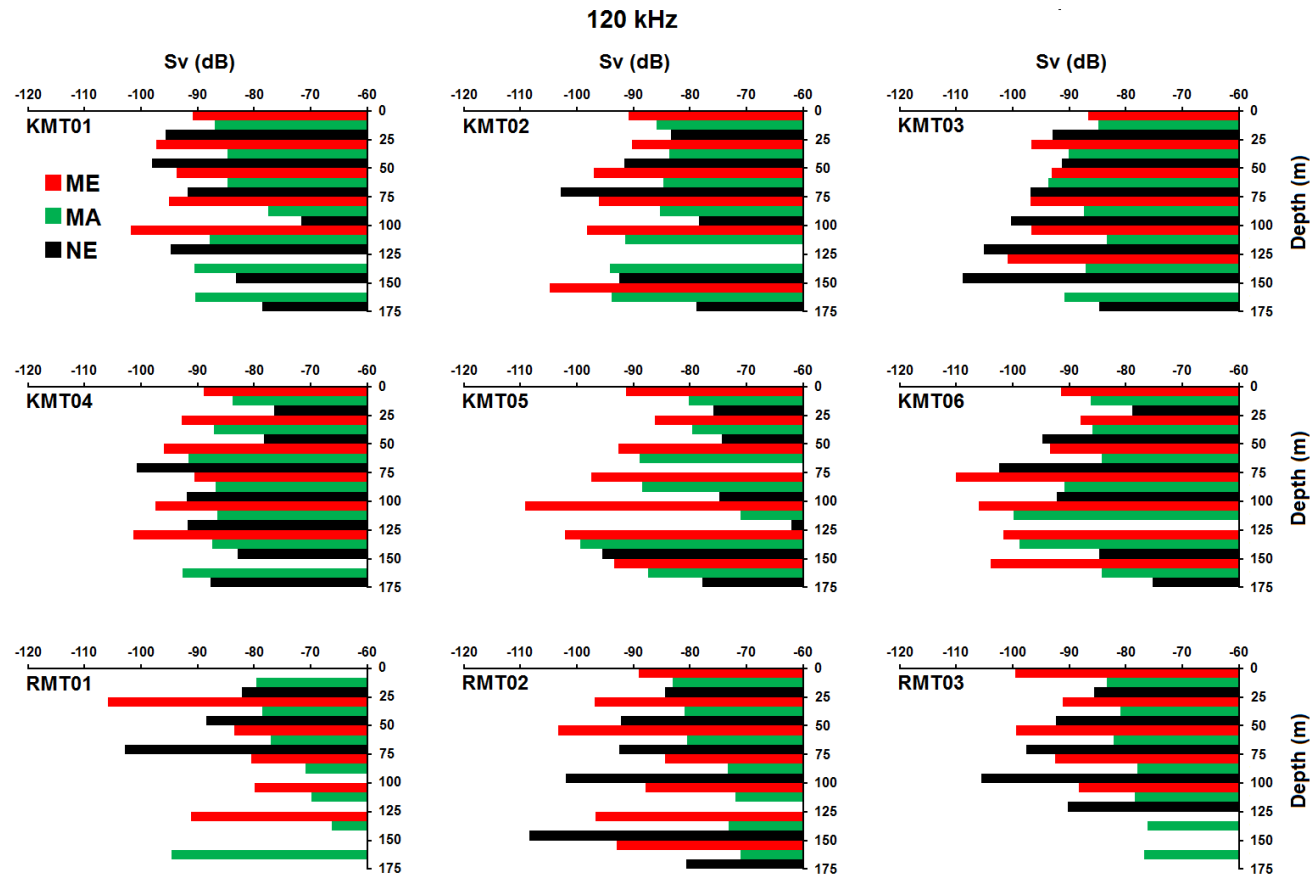


Fig 4.11) Mean values of 120 kHz S_v (dB) from each category (for backscatter partitioning details, see section 2.3) integrated on a 25 m X 10 min grid at KF 08 (top), KF 09 (centre) and RF 09 (bottom). Data was not collected at BF 08 (for station details, see Table 4.1). Data are integrated over 20 mins at each station between 12 – 175 m (i.e. surface 0 – 25 m values are based on 12 – 25 m integrations). ME (red) = mesozooplankton category ($\Delta MVBS > 12$ dB), MA (green) = macrozooplankton category ($\Delta MVBS 2 - 12$ dB, NE (black) = nekton category ($\Delta MVBS < 2$ dB). These colours for each category are similar to the colours expected on a $\Delta MVBS$ echogram (Fig 4.12).

4. Small scale spatial variation in zooplankton around moorings at Kongsfjorden, Rijpfjorden and Billefjorden

At KF 08 (KMT01/02/03), ME backscatter was observed primarily above 100 m depth with highest values in the 0 – 25 m layer (Fig 4.11). ME echo intensity was highest at KMT03 (-83.7 dB) between 0 – 25 m. The highest echo intensities were recorded for MA between 75 – 125 m depth (mean of -85.6 dB at KMT01 and -85.4 at KMT03), and NE backscatter was identified largely below 125 m (mean of -84.5 dB) at KMT01 and KMT02 (Figs 4.11, 4.12). The visible low intensity scattering layer below approximately 100 m at KMT03 (Fig 4.12) appeared to be dominated by MA echoes (mean of -87.5 dB) with some ME backscatter between 100 – 150 m. A dense high intensity patch between 75 – 100 m at KMT01 (at approximately 00:41 – Fig 4.12) created the highest echo intensity recorded at KF 08 and was largely attributable to NE (-68.7 dB) and MA (-74.6 dB).

At KF 09 in contrast to KF 08, NE echoes were identified in a scattering layer above 50 m depth primarily at KMT04 (mean of -78.1 dB) and KMT05 (mean of -75.7 dB) (Fig 4.12). NE traces were also recorded below 125 m depth at KMT05 and KMT06 (Fig 4.12). ME echoes were again of highest intensity above 50 m depth, although overall ME backscatter was lower than at KF 08 (highest value of -86.9 dB recorded between 0 – 25 m at KMT04). At KF 09 MA backscatter was also generally highest above 50 m depth (mean of -84.1 dB between 0 – 50 m across KMT04/05/06). As at KF 08, a high intensity patch between 100 – 125 m at KMT05 (at approximately 17:40 – Fig 4.12) created the highest echo intensity recorded at KF 09 and was largely attributable to NE (-59.1 dB) and MA (-68.8 dB).

At RF 09, it was apparent that the vessel moved significantly during sampling, as bottom intrusions illustrate (Fig 4.12). Here, MVBS was significantly higher than at Kongsfjorden (-85.7 dB mean across all taxa and depths - Figs 4.11, 4.12). Across all Rijpfjorden stations, no significant patches of high intensity NE backscatter were observed (Fig 4.11). At RMT01, NE backscatter was only observed above 75 m depth (Fig 4.11). ME backscatter was also lower between 0 – 50 m than at Kongsfjorden (mean of -96.1 dB). The dominant scattering layer between 50 – 150 m (Fig 4.12) was

4. Small scale spatial variation in zooplankton around moorings at Kongsfjorden, Rjipfjorden and Billefjorden

attributable to MA (mean of -72.9 dB) and ME echoes (mean of -83.0 dB), with highest echo intensities between 75 – 125 m. The same scattering layer continued at RMT02, and deeper water here allowed the scattering layer to continue down to the maximum sampling depth of 175 m (Fig 4.12). Again highest echo intensities were recorded between 75 – 125 m (MA mean of -72.6 dB, ME mean of -86.8 dB), although MA backscatter continued at high intensity down to 175 m depth (Fig 4.11). At RMT03, the vessel moved to a location where the scattering layer no longer existed (at approximately 23:55 – Fig 4.12). However, although values were lower due to this, the backscatter profile shows a similar pattern to RMT01/02, with highest intensity ME and MA echoes recorded below 75 m depth (Fig 4.11).

In order to determine variation within locations, the depth stratified MVBS of all taxa at each station were compared to each other within each location using Wilcoxon signed-rank analysis ($n = 42$ at each station). As with the same test using MPS abundances, no significant differences were found between KMT01/02/03 at KF 08. However, similarly to the result found using MPS abundances at KF 09, MVBS at KMT06 was significantly different from KMT05 ($V = 544$, $p = 0.032$), and KMT05 was also found to be significantly different from KMT04 ($V = 235$, $p = 0.019$). In a further similar result to that found using MPS abundances at RF 09, RMT03 was found to be different from both RMT02 ($V = 604$, $p = 0.003$) and RMT01 ($V = 481$, $p = 0.007$). To remove the influence of varying echo intensities between stations and test just for changes in the depth distribution of MVBS, mean depth (Z_m) was calculated for the MVBS of each taxon and the Z_m at each station were compared again within locations by Wilcoxon signed-rank. However, with the smaller sample size of 6 at each station, no significant differences were found between stations within KF 08, KF 09 or RF 09. The only difference between stations to pass a 10% significance test was between KMT04 and KMT05 ($V = 2$, $p = 0.094$), and these two stations also displayed the most significant (i.e. lowest) p value when their zooplankton community Z_m were compared.

4. Small scale spatial variation in zooplankton around moorings at Kongsfjorden, Rijpfjorden and Billefjorden

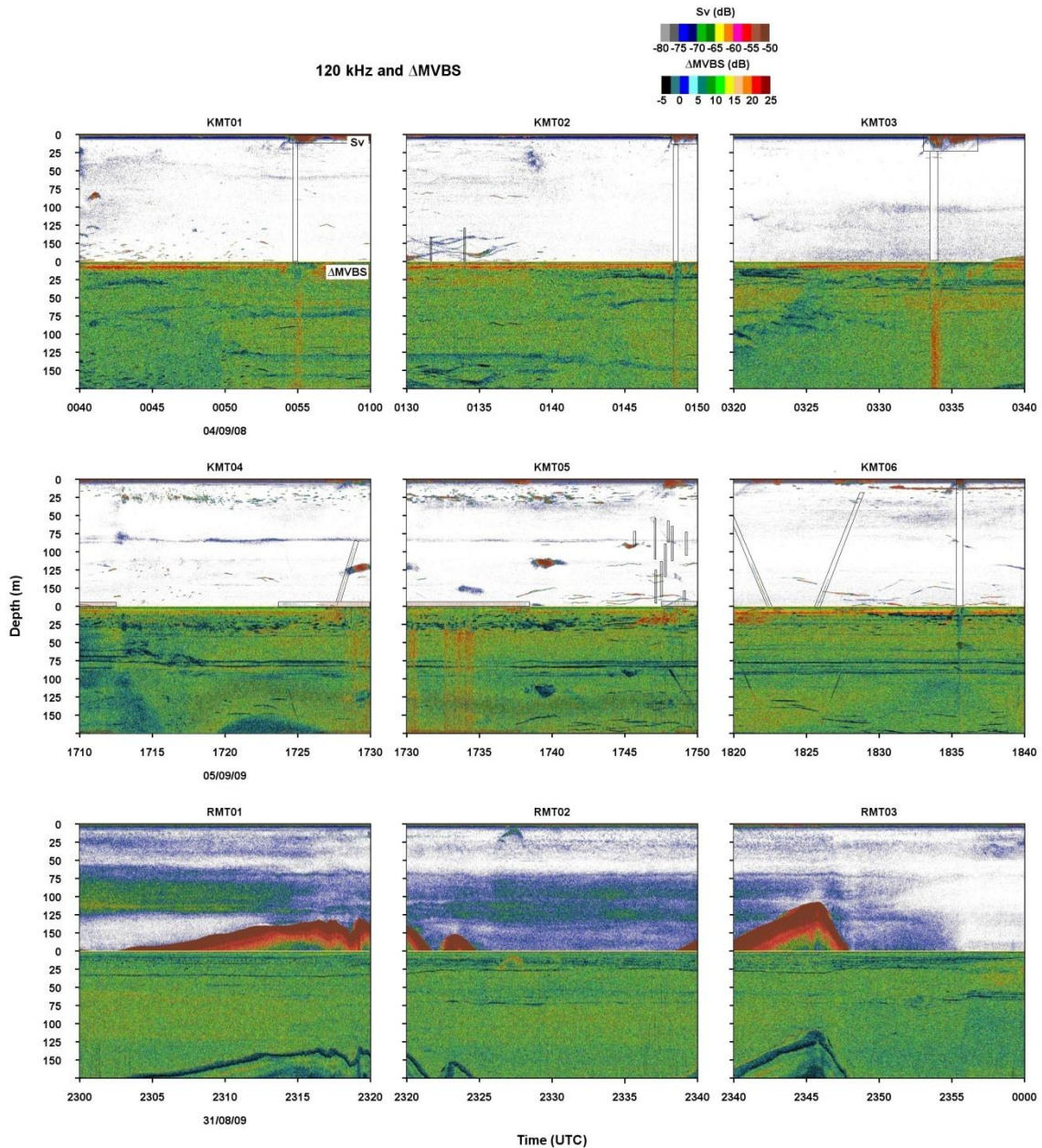


Fig 4.12) 120 kHz backscatter (dB – above) and Δ MVBS (120 kHz – 38 kHz, dB – below) from each sampled station (KF 08 – top, KF 09 – centre, RF 09 – bottom). Echograms display 0 – 175 m backscatter, but the 0 – 12 m layer is excluded from echo integration due to the visible nearfield effect. Volume backscatter (S_v) is expressed using a colour scale between -80 and -50 decibels (dB). Δ MVBS is expressed using a colour scale between -5 and 25 dB. Δ MVBS echoes with yellow-red shades represent stronger scattering at 120 kHz (i.e. smaller targets), while Δ MVBS echoes with grey-black shades represent stronger scattering at 38 kHz (i.e. larger targets). Black outlined shapes include areas of interference (e.g. due to net deployment, acoustic interference, surface noise and missed pings) which were discarded from echo integration. Brown layers at RF 09 are bottom intrusions.

4.3.5. Multivariate analysis of acoustic observations

When all acoustic stations were tested together (i.e. no Billefjorden observations), a significant difference in depth-stratified MVBS (25 m X 10 min grid, $n = 378$) was found between locations (i.e. Kongsfjorden and Rijpfjorden – $R = 0.222$, $p = 0.001$). However, no difference was identified between stations (i.e. KMT01/02/03/04/05/06 and RMT01/02/03 treated individually), indicating no significant difference between stations at KF 08 and KF 09. Pairwise comparisons on the Bray-Curtis similarity matrix supported this conclusion, with no significant differences between stations at KF 08 vs. stations at KF 09. The only pairwise comparison which was significant was between KMT06 and RMT01 ($R = 0.291$, $p = 0.039$). A significant difference was also identified between MVBS of the three different taxa ($R = 0.345$, $p = 0.001$). Pairwise comparisons between taxa highlighted the largest difference between ME and MA MVBS ($R = 0.481$, $p = 0.001$). As the three taxa displayed differences in MVBS between stations, the three taxa were compared between stations individually. ME MVBS displayed no significant difference between locations, while MA MVBS ($R = 0.310$, $p = 0.001$) and NE MVBS ($R = 0.472$, $p = 0.004$) did. This results indicated that MA and NE backscatter were more responsible for differences between locations than ME backscatter.

To remove the influence of varying echo intensities between stations and test just for changes in depth stratification with all the stations together, mean depth (Z_m) was calculated for each taxa and the Z_m data were tested again. A significant difference in Z_m was again found between Kongsfjorden and Rijpfjorden ($R = 0.580$, $p = 0.001$). This difference was of greater magnitude than the difference identified with MVBS values indicating a stronger difference in depth stratification between locations compared to echo intensity. As found when using MVBS values, there was no significant difference between the sampled stations when each station was treated individually, indicating less difference between KF 08 and KF 09 than between Kongsfjorden and Rijpfjorden.

4.4. Discussion

4.4.1. Variations in zooplankton between locations

When discussing any observed differences in zooplankton between locations and especially any differences in depth distribution, one phenomenon which may affect our conclusions is diel vertical migration (DVM). In their study across northern Svalbard waters, Daase and Eiane (2007) identified a relationship between abundance in the upper 50 m and time of sampling for three species – *M. longa*, *C. finmarchicus* and *Microcalanus* spp. They suggested that different mechanisms were responsible for the differences in vertical distributions observed for different species (for example meroplankton are less likely to be affected by water mass distribution since they spend relatively short periods of time in the pelagic zone). Other prior studies on spatial distributions of zooplankton in the Arctic have chosen to largely ignore DVM at high latitude, and Blachowiak-Samolyk et al. (2008) stated that a ‘comprehensive literature survey’ on Arctic zooplankton diel vertical migration revealed that dominant zooplankton taxa did not carry out DVM under midnight sun conditions (Blachowiak-Samolyk et al. 2008). In terms of the diel cycle, KF 08 and RF 09 were sampled during approximately the same phase (around midnight), while KF 09 and BF 08 were also sampled during the same diel phase (between noon and dusk – Table 4.1). Multivariate analysis and clustering did not highlight these pairs of locations as being more similar to each other vs. differences between regions of contrasting hydrology (Fig 4.10), indicating that DVM effects were outweighed in our analysis. However, although the overall similarity clustering of zooplankton communities remained the same irrespective of depth stratification (Fig 4.10), the difference between KF 08 and KF 09 (which were sampled at different diel phases) increased by approximately 5% when zooplankton mean depth were analysed compared to abundance irrespective of depth distribution. Thus, although DVM behaviour may be affecting the depth distribution of zooplankton

4. Small scale spatial variation in zooplankton around moorings at Kongsfjorden, Rijpfjorden and Billefjorden

communities sampled at different times, the evidence put forward by this study appears sufficient to suggest that water masses and dominant hydrography were more responsible for differences in zooplankton community structure between our locations. When discussing differences within our locations (e.g. KMT01, KMT02 and KMT03 within KF 08), zooplankton sampling events were within a couple of hours of each other during the same diel phase, and so significant DVM effects were unlikely.

Plankton communities often form assemblages which are closely related to hydrographic variability, and such regional patterns in zooplankton distribution have been reported by a number of studies across North Atlantic and Arctic regions (Huntley et al. 1983; Hirche and Mumm 1992; Clark et al. 2001; Harvey et al. 2001; Head et al. 2003; Daase and Eiane 2007; Blachowiak-Samolyk et al. 2008; Trudnowska et al. 2012). Zooplankton communities in the Barents Sea and around the Svalbard archipelago are often found in assemblages with a close relationship to specific water masses (Pedersen et al. 1995; Søreide et al. 2003). Furthermore, Daase and Eiane (2007) reported zooplankton communities being grouped together on intermediate spatial scales (ca. 90 km) in waters North of Svalbard, with differences between groups being based more on changing species densities than changing species composition. As our three locations were further than 90 km apart, we would expect them to show differences between species abundances at each location. Zooplankton biomass is also known to be higher on the shelf than in deeper waters (Blachowiak-Samolyk et al. 2008), with some species being closely linked to deeper waters (e.g. *Metridia longa*, *Oncea* spp.). However, all three of our locations were on the shelf and had approximately similar depths, largely removing this as a factor that could create differences between the locations. This study puts forward evidence that links specific zooplankton species to certain depths however, with multivariate analysis highlighting significant differences between MPS sampled depths across all stations, especially between the surface waters and deepest sampled depths.

4. Small scale spatial variation in zooplankton around moorings at Kongsfjorden, Rijpfjorden and Billefjorden

Our three study locations, Kongsfjorden, Billefjorden and Rijpfjorden represented contrasting hydrology and the dominance of different water masses, and were all sampled during the same point in the annual season. AtW dominated the Kongsfjorden stations during both years of sampling (Fig 4.2), while ArW and Bottom Water dominated at Billefjorden. Temperatures and salinities at Rijpfjorden indicated a combination of ArW and Melt Water, and also possible mixing with AtW as temperatures rose to almost 3°C. Thus, Atlantic-associated species (*Calanus finmarchicus*, *Oithona atlantica* (Kielhorn 1952; Brodsky 1967), *Themisto abyssorum* and *Fritellaria borealis* (Arashkevich et al. 2002)) would be expected in greatest abundances at Kongsfjorden. Abundances of *Calanus finmarchicus* were highest at both Kongsfjorden stations (Table 4.3), while abundances of *Oithona atlantica* at KF 08 and KF 09 accounted for 91.4 % of the total abundance across all three locations. Although abundances were low due to the use of MPS hauls, *Themisto abyssorum* was only identified at Kongsfjorden (both KF 08 and KF 09). *Fritellaria borealis* however was found to be far more abundant at Billefjorden and Rijpfjorden (Table 4.3), challenging previous observations by Blachowiak-Samolyk et al. (2008) and Arashkevich et al. (2002) that linked this species to AtW.

Arctic-associated species (*Calanus glacialis* (Unstad and Tande 1991), *Sagitta elegans* and *Themisto libellula* (Dalpadado et al. 2001)) would be expected in greatest abundances at Billefjorden and Rijpfjorden. *Calanus glacialis* abundance (both proportionally – Fig 4.7 - and in magnitude – Table 4.3) was highest at Billefjorden followed by Rijpfjorden. *Sagitta elegans* abundance at Billefjorden and Rijpfjorden accounted for 93.8% of the total sampled abundance, while *Themisto libellula* was only identified at Rijpfjorden. Statistical differences were also identified between the communities in this study, with no significant differences in either integrated abundances or mean depths between KF 08 and KF 09 (both AtW dominated) or between BF 08 and RF 09 (both ArW dominated). The largest significant differences were found however between Kongsfjorden and Rijpfjorden using these two measures, followed by significant differences also between Kongsfjorden and Billefjorden (clustering displayed in Fig 4.10). This difference between AtW dominated regions and

4. Small scale spatial variation in zooplankton around moorings at Kongsfjorden, Rijpfjorden and Billefjorden

ArW dominated regions did not appear to be limited to the mesozooplankton species most effectively sampled by MPS. Acoustic backscatter (which unfortunately could not be collected at Billefjorden) further illustrated significant statistical differences between Kongsfjorden and Rijpfjorden (Fig 4.12). Furthermore, this data set included backscatter from larger animals (macrozooplankton and nekton), and these two taxa were shown to be more responsible for differences between Kongsfjorden and Rijpfjorden than mesozooplankton backscatter. Abundances of faster swimming euphausiids, amphipods and fish were thus also linked closely to the dominant water masses, with higher nekton traces apparent in Kongsfjorden and higher macrozooplankton backscatter observed in Rijpfjorden (Fig 4.11). Thus, our study puts forward further evidence that species abundances and distributions are closely linked to the distribution of water masses over broad spatial scales.

In order to better assess which environmental variables were most responsible for zooplankton community structuring, a correlation analysis between physical variables (any combination of temperature, salinity, fluorescence and bottom depth) and zooplankton abundances was carried out at KF 09 (i.e. the only location with a CTD profile for every MPS sample). The physical measure most correlated with zooplankton abundances was a combination of temperature and fluorescence (0.631), with the highest correlation from a single variable coming from fluorescence (0.583). This result indicated that the availability of primary production was a dominant factor influencing zooplankton distribution. The lowest correlation was found with bottom depth, as the sampled locations did not vary greatly in depth.

Differences between the two ArW dominated systems (Billefjorden (2008) and Rijpfjorden (2009)) were also apparent in this study although no MVBS was available from Billefjorden. No significant differences between Billefjorden and Rijpfjorden were identified using zooplankton integrated abundances and mean depths, but a significant difference was identified when using depth stratified abundances. In terms of hierarchical clustering, Billefjorden lay between Rijpfjorden and Kongsfjorden (Fig

4. Small scale spatial variation in zooplankton around moorings at Kongsfjorden, Rijpfjorden and Billefjorden

4.10), and so the zooplankton community appeared to be a combination of the two. This effect was most likely due to the relative abundance of *Oithona similis*, the most dominant zooplankton species in the study, with an integrated abundance of 2583 ind. m⁻³ at Billefjorden compared to 1757 ind. m⁻³ at Rijpfjorden and a mean value of 3080 ind. m⁻³ at Kongsfjorden. Interestingly however, RF 09 contained more *Calanus finmarchicus* and less *Calanus glacialis* than BF 08. Although total zooplankton abundance was far lower at RF 09 compared to BF 08 and the Kongsfjorden stations, RF 09 contained abundances of *Calanus finmarchicus* that were comparable with Kongsfjorden. This substantial abundance of a typically AtW associated species in Rijpfjorden is noteworthy. The CTD profiles displayed a prominent warm water intrusion between approximately 75 – 100 m at KF 09 that was absent at KF 08 (Fig 4.2). This indicated a greater influence of AtW in Kongsfjorden in 2009 at these depths compared to 2008, and such interannual differences in AtW influence at Kongsfjorden have been reported before (e.g. Cottier et al. 2005). This difference in hydrography at Kongsfjorden would suggest an increased northward flow of AtW between 75 – 100 m, and this AtW may have been carried northwards then eastwards around the Svalbard archipelago by the West Spitsbergen Current. Temperatures nearing 2°C with salinities over 34 (Fig 4.2) below 50 m at Rijpfjorden indicated the possible influence of a mixture of AtW and ArW (TAtW), and these ‘warmer’ conditions below the surface layers in 2009 appear to have carried *Calanus finmarchicus* to Rijpfjorden. As our Billefjorden stations in 2008 were in the inner basin which has a shallow sill separating it from the AtW influenced system outside, any warm water intrusions would not have been able to enter the fjord. This would explain why Rijpfjorden in 2009 had a far higher abundance of *Calanus finmarchicus*. A high proportional abundance of *Calanus glacialis* has been described before in Billefjorden at approximately the same annual period as this study (Arnkværn et al. 2005). *Calanus glacialis* is closely associated with colder ArW masses (Unstad and Tande 1991), and apart from at the surface, temperatures below approximately 50 m were far colder at BF 08 than RF 09 (Fig 4.2). 95 % of all *Calanus glacialis* were located below 50 m (mean across all three stations - Fig 4.9), and this was further evidence of the close association of *Calanus glacialis* with ArW and explains why Billefjorden contained so much more *Calanus glacialis* than Rijpfjorden in this study.

4. Small scale spatial variation in zooplankton around moorings at Kongsfjorden, Rijpfjorden and Billefjorden

The *Calanus finmarchicus* and especially the *Calanus glacialis* community at RF 09 also consisted of far more younger copepodid stages (CI – CIII) than were found at BF 08 (Fig 4.9), although BF 08 did contain a relatively large number of *Calanus finmarchicus* CI - CIII. BF 08 displayed a far more pronounced fluorescence maximum than RF 09 (Fig 4.2) indicating the presence of pelagic primary production, but *Calanus glacialis* is known to begin reproduction in February/March in Billefjorden which is well before the spring phytoplankton bloom (Arnkværn et al. 2005). Subsequent development creates a dominance of stages CIII – CV during summer/autumn (Ashjian et al. 2003) which is when our study took place. Our observations support this life history of *Calanus glacialis* at Billefjorden. *Calanus finmarchicus* however in contrast relies on external food resources (i.e. primary production) for reproduction and development, and so they tend to spawn after the spring bloom (Diel and Tande 1992). The younger copepodid stages of *Calanus finmarchicus* are thus likely to be using the pelagic food source identified at BF 08 to develop following later spawning closer to our study period. This difference in life history helps explain the greater number of younger copepodids of *Calanus finmarchicus* at Billefjorden compared to *Calanus glacialis*. Sea-ice break-up and the onset of the ‘spring’ phytoplankton bloom however may be up to 4 months later in the northeast at Rijpfjorden (Reigstad et al. 2002; Søreide et al. 2008). Although favourable development conditions at Rijpfjorden for *Calanus glacialis* have been recorded in prior studies despite this later bloom (with most individuals developing to CV by the end of August - Søreide et al. 2008), it would appear that *Calanus glacialis* in our study at Rijpfjorden could not reach stages CIV and CV as effectively by early September as at Billefjorden. The lack of pelagic primary production available for development is highlighted by the lack of any noticeable fluorescence maximum at RF 09.

Interestingly, typically deep water associated species such as *Metridia longa* (Mumm 1993; Head et al. 2003) and *Microcalanus* spp. (Daase and Eiane 2007) were far more abundant at BF 08 than at any other station (Table 4.3, Fig 4.7) although the sampling depth on average was the shallowest. The deep Bottom Water which these species are typically associated with maintains a temperature below -1.7°C and salinity greater than

4. Small scale spatial variation in zooplankton around moorings at Kongsfjorden, Rijpfjorden and Billefjorden

35. The CTD profile at Billefjorden (Fig 4.2) displays just these conditions below 75 m which explains the high abundances of these species at BF 08.

In the central Arctic, regional differences in zooplankton communities have been reported to be lower than the differences in vertical distribution patterns that match respective water column stratification (Mumm 1993; Auel and Hagen 2002). Along with our evidence that links specific zooplankton species to certain depths and also highlights significant differences in overall community composition between different depth strata across all stations, hierarchical clustering based on all MPS sampled species showed that differences between stations based on their zooplankton mean depths (Z_m) were slightly greater than differences between the same stations based on their integrated abundances (Fig 4.10). Although the two indices were largely similar and the difference was slight, this may be further evidence that differences in depth stratification between locations are more important in Arctic systems than differences in zooplankton abundances. However, this conclusion must be treated with caution as differences in depth distributions between locations in this study could be due to either water column hydrographic stratification or DVM behaviour (as the samples were collected at different times of day). The result appears to be similar when using backscatter, with a far higher test statistic when testing for differences in MVBS Z_m between locations vs. testing for differences in MVBS between locations. This is an indication that depth distributions of macrozooplankton and nekton were also different between locations, and were more important than the overall differences in echo intensity between locations.

At KF 08 and KF 09, we collected two sets of samples at Kongsfjorden in subsequent years at slightly different locations (Fig 4.1). This allowed us an opportunity to observe interannual variation in zooplankton at Kongsfjorden. Although all multivariate analysis considering abundances, mean depths and MVBS resulted in no significant differences identified between KF 08 and KF 09, and similarities between these stations were also greater in hierarchical clustering than between Kongsfjorden and other locations (Fig

4. Small scale spatial variation in zooplankton around moorings at Kongsfjorden, Rijpfjorden and Billefjorden

4.10), a number of observable differences between KF 08 and KF 09 did exist. In terms of the physical environment, when the temperature recorded by the two oceanic moorings in Kongsfjorden (average of 27 m depth) around which our samples were based were analysed, average temperatures at 27 m in May 2008 were 1.5°C compared to -0.7°C in May 2009. Furthermore, although temperatures recorded at 27 m were very similar in the first weeks of September (i.e. when our study occurred), temperature dropped to below 3°C in 2009 by the third week of September while it stayed above 4°C till the end of September in 2008. These observations indicate warmer conditions at Kongsfjorden in 2008 compared to 2009.

KF 09 had lower total zooplankton abundance than KF 08 (Table 4.3) which is to be expected during colder conditions, but interestingly a higher abundance of *Calanus* largely due to a higher abundance of AtW associated *Calanus finmarchicus*. However, almost no *Calanus hyperboreus* were recorded at KF 09, compared to significantly more at KF 08 (Fig 4.7). The lack of *Calanus hyperboreus* at KF 09 may be explained by the relative positions of the stations sampled in 2009 compared to those sampled in 2008 (Fig 4.1). As KF 09 is further within the fjord and in shallower water (approximately 100 m shallower - Table 4.1), the oceanic deeper water species of *Calanus hyperboreus* (Hirche 1997) is less likely to be found here. As *Calanus finmarchicus* is advected into the fjord within AtW (Willis et al. 2006), higher abundances of this species may be expected at KF 08 during the warmer conditions, rather than at KF 09 as observed in these data.

However, CTD profiles collected at KF 09 displayed a warm water intrusion at approximately 75 – 100 m depth which was not present at KF 08, indicating that AtW influence was stronger at this depth in 2009, bringing with it the AtW associated species *Calanus finmarchicus* and *Oithona atlantica*. Thus, AtW influx at deeper depths (75 – 100 m) brought AtW associated species into Kongsfjorden in 2009 during an overall ‘cold’ period. This provides evidence that advection which is important in shaping the structure of fjordic pelagic systems (Basedow et al. 2004; Willis et al. 2006;

4. Small scale spatial variation in zooplankton around moorings at Kongsfjorden, Rijpfjorden and Billefjorden

Kwasniewski et al. 2012) can vary significantly between depths, and ‘colder’ years at Kongsfjorden do not necessarily mean less AtW influence.

When analysing the stage composition and depth distribution of *Calanus* between years (Fig 4.9), it became apparent that there were many more immature copepodid stages (CI – CIII) of *Calanus finmarchicus* and *Calanus glacialis* in surface waters at KF 08 than there were at KF 09. KF 08 displayed a far more significant fluorescence maximum between 25 – 50 m than KF 09, indicating higher levels of primary production during the warmer conditions. A prior thorough evaluation of mesozooplankton dynamics in relation to food availability within Kongsfjorden (Kwasniewski et al. 2012) has described how *Calanus* species (especially *Calanus finmarchicus* and *Calanus glacialis*) make efficient use of pelagic primary production when reproducing and developing through copepodid stages. The higher numbers of young copepodid stages found at KF 08 with the presence of a pronounced fluorescence maximum compared to KF 09 without one provides evidence that younger copepodids were still in the process of utilising the food supply to develop in 2008. Mean horizontal current velocities observed at KF 08 the day after zooplankton sampling were also higher at 15 – 20 m depth (mean eastward velocity = -77.5 mm/s, mean northward velocity = 27.7 mm/s) than at KF 09 the day after zooplankton sampling (mean eastward velocity = -23.7 mm/s, mean northward velocity = -19.7 mm/s) (Table 4.2). These stronger surface currents at KF 08 may have advected the immature copepodid stages of *Calanus* into the sampling area, influencing their numbers collected during net sampling.

4.4.2. Variations in zooplankton within locations

Although much of the reported zooplankton dynamics and structure between locations identified in this study have been documented before, our approach of collecting three MPS and backscatter observations within 1 nautical mile of each other and assessing differences between them is novel within Svalbard fjords. Unfortunately, replicates could not be collected at each station due to time constraints, and this is a limitation of our investigation. However, such singular net deployments are regularly used when assessing the distribution of zooplankton (Daase and Eiane 2007; Blachowiak-Samolyk et al. 2008; Kwasniewski et al. 2012), largely due to the time required to collect further samples and analyse them for species composition. These prior mentioned studies have all either assessed zooplankton distributions over larger spatial scales, or assessed temporal dynamics within point locations.

Our first result when considering small scale variation was the difference between KF 08 and KF 09. None of our indices (species abundance, mean depth, MVBS etc) indicated any significant differences between the three stations sampled at KF 08. However, at KF 09, KMT06 was identified as significantly different from the others in terms of species abundances, and KMT04 was identified as significantly different from the others in terms of species mean depth. Significant differences were also found between stations at KF 09 using MVBS, with KMT05 being significantly different from the others. These results clearly indicated greater spatial variation in zooplankton distribution and abundance at KF 09 over small scales. The species most responsible for community differences on average between KMT06 and the other two stations at KF 09 (in order of magnitude) were *Oikopleura* spp., *Oithona similis* and bivalve veligers. These species were all found in similar or higher relative abundances at KF 08 (Table 4.3), so appear to have been structured differently between stations at KF 09 to create our observed differences. In fact, KMT06 contained all the sampled *Oikopleura* spp. at KF 09, while this species was spread more or less evenly across stations at KF 08.

4. Small scale spatial variation in zooplankton around moorings at Kongsfjorden, Rijpfjorden and Billefjorden

KMT06 also contained 57 % of all *Oithona similis* at KF 09, while the percentage abundance of this species in the three KF 08 stations was evenly spread 38 % : 30 % : 32 %. Furthermore, the evenness of the depth distributions of these species between stations differed between KF 08 and KF 09. At KMT06, 76 % of *Oikopleura* spp. were located between 0 – 20 m, while at KF 08 across all stations, mean *Oikopleura* spp. percentage abundance between 0 – 20 m was 55 %. Similarly across KF 09, mean bivalve veliger percentage abundance between 0 – 20 m was 97 %, while across KF 08 the value was 68 %. These observations indicated that not only were these species more horizontally aggregated over small scales at KF 09, but they were also more densely aggregated in surface waters.

Gallager et al. (1996) demonstrated how plankton communities were closely associated with water mass structure on scales of < 1 m – 70 km. Their study described how the extent at which a water mass acts as a boundary to plankton is species specific, with greater constraints imposed on less active organisms. The three species identified as being most aggregated between stations at KF 09 (*Oikopleura* spp., *Oithona similis* and bivalve veligers) are all comparatively weak swimmers. Gallager et al. (1996) suggested that weak swimmers tend to be concentrated in regions of high vertical stability (i.e. edges of water masses or density gradients). At KF 08, the CTD profile suggested a steep gradient in temperature and salinity at the very surface (shallower than 10 m – Fig 4.2), but then a very gradual cline below which may be preventing weak swimmers from aggregating in the surface 20 m. At KF 09, the gradient was less steep but began at approximately 20 m depth and was more continuous between 25 – 75 m. This gradient may have been sufficient to create the vertical stability required to aggregate weak swimmers between 0 – 20 m, and helps to explain the differences in vertical distribution between KF 08 and KF 09. When considering the differences in spatial aggregation, KF 08 was just outside Kongsfjorden (Fig 4.1), and was subjected to a different current regime than the location at KF 09 (Table 4.2). Horizontal current velocities collected by ADCP's attached to the moorings a day after net sampling at both KF 08 and KF 09 describe significantly faster current velocities at KF 08, especially towards the surface (Table 4.2 – negative current velocities indicate direction not magnitude). For example,

4. Small scale spatial variation in zooplankton around moorings at Kongsfjorden, Rijpfjorden and Billefjorden

mean eastward horizontal velocity was -77.5 and -93.3 mm/s at 15 – 20 m depth and 20 – 50 m depth respectively at KF 08, and just 27.7 and -8.7 mm/s at the same depths at KF 09. The faster currents at KF 08 may have had a dispersing effect on weaker swimmers which were less aggregated between stations at KF 08 compared to KF 09. Such dispersal of small zooplankton throughout the surface layer with stronger advection has been described before (Tiselius 1998). Vessel drift during acoustic data collection was also greater at KF 08 compared to KF 09 (Figs 4.4 and 4.5), confirming the difference in current regimes.

As we have mentioned before, 2009 appeared to be a ‘colder’ year at Kongsfjorden than 2008, but with an influx of AtW below 75 m. This greater influx of AtW at KF 09 below 75 m may have reinforced the pycnocline at KF, allowing the stratified water column to aggregate weak swimmers in the layers above it. Advective effects in the surface layers were not just observed for the three weaker swimming species that were most responsible for differences within KF 09 mentioned already. When the standard deviations of *Calanus finmarchicus* and *Calanus glacialis* abundance (across the 3 MPS samples) were assessed at Kongsfjorden (Fig 4.9), it was apparent that the greatest variation between samples within each sampled year (KF 08 and KF 09) was in the upper 50 m, and especially the 0 – 20 m layer. Thus spatial differences appear to be greatest within this layer for *Calanus* also, indicating greater advective effects towards the surface.

KMT04 was significantly different from the other stations at KF 09 based on zooplankton mean depths. This would indicate that although KMT06 was most different in terms of a combination of abundance and depth stratification (as explained above), KMT04 was most different purely based on differences in zooplankton depth stratification. To ascertain which species had the largest differences in mean depth between KMT04 and the other stations, an average mean depth was calculated from Z_m at KMT05 and KMT06, and the difference between this mean and the value at KMT04 was calculated. Only species and stages with combined abundance $> 50 \text{ ind. m}^{-3}$ across

4. Small scale spatial variation in zooplankton around moorings at Kongsfjorden, Rijpfjorden and Billefjorden

KF 09 were considered. *Calanus glacialis* CIV (difference of 60.5 m), CV (difference of 42.5 m), copepod nauplii (difference of 41.6 m) and *Calanus finmarchicus* CII (difference of 26.9 m) were all shallower at KMT04 by over 25 m, while echinoderm larvae were the only zooplankton deeper at KMT04 by over 25 m (difference of -41.0 m). These differences in mean depth however were created largely by differences in the 0 – 20 m layer, which has been identified as the layer most likely to be affected by advection. Echinoderm larvae in particular have been reported to be more affected by advection than other larval forms (Schluter and Rachor 2001; Daase and Eiane 2007). It would appear then that advection and circulation within the 0 – 20 m layer was most responsible for creating the observed differences in mean depths between stations at KF 09. Differences within KF 09 were also highlighted by MVBS, with KMT05 significantly different from the other stations. In this case, the echogram and extracted MVBS (Figs 4.11, 4.12) indicated that patches of high intensity macrozooplankton and nekton backscatter between 75 – 100 m were largely responsible for the difference between KMT05 and the other stations. This depth corresponds to the inflow of AtW identified by our CTD profiles, and so these taxa were likely being advected into the fjord in 2009. Plots of vessel drift at KF 09 (Fig 4.5) indicated that the 20 minutes of acoustic data at KMT05 integrated less vessel movement (approximately 100 – 200 m) than KMT04 (approximately 1000 m), and yet more patches of high intensity macrozooplankton and nekton backscatter were observed at KMT05. This indicates that either the patches observed at KMT05 were small, or they were moving across underneath the nominally stationary ship either actively (as they are likely to be active swimmers) or passively with the currents.

At Billefjorden, significant differences in MPS abundances were also identified between BMT02 and the other two stations. In this case, the species most responsible on average for the differences (in order of magnitude) were *Fritellaria borealis*, *Calanus glacialis* CV, and *Oithona similis*. These were also the species found in highest abundance at BF 08 compared to all other stations, and so were responsible both for separating Billefjorden from the other locations, and also for separating locations within Billefjorden. BMT02 contained 50 % of all recorded *Fritellaria borealis* at Billefjorden,

4. Small scale spatial variation in zooplankton around moorings at Kongsfjorden, Rijpfjorden and Billefjorden

although depth distributions of the species were similar across all stations within Billefjorden. Relative abundance and depth distributions of *Oithona similis* also appeared fairly similar between stations at Billefjorden, and so it is likely that the high relative abundance of this species compared to any other (Table 4.3) makes it responsible for differences between BMT02 and the other stations. These results, and the lack of any significant differences between stations at Billefjorden in terms of their zooplankton mean depths indicate that differences in species abundances dominated more at Billefjorden compared to differences in depth distributions within these species. Horizontal current velocities across all depth layers observed (15 – 78 m) were generally slowest at Billefjorden the day after net sampling (Table 4.2), and as at KF 09 compared to KF 08, this lower level of advection would help explain why weak swimmers such as *Fritellaria borealis* were more aggregated spatially.

Rijpfjorden displayed the most differences between stations of any location, with all three stations being identified as significantly different from each other using depth stratified MPS abundances, and RMT03 identified as significantly different from the other two stations in terms of MVBS. The species most responsible on average for the differences in MPS abundances (in order of magnitude) were *Calanus finmarchicus* CI, *Fritellaria borealis* and polychaete larvae. The prevalence of AtW associated species in this list again highlights their importance within Rijpfjorden during our sampling period, and both *Calanus finmarchicus* (especially CI, Table 4.3, Fig 4.9) and *Fritellaria borealis* had high relative abundances at Rijpfjorden compared to other species. Although the overall abundance of polychaete larvae at Rijpfjorden was low (summed total abundance across all layers and stations of 53.6 ind. m⁻³), Rijpfjorden contained 68.3 % of all sampled polychaete larvae in this study. *Fritellaria borealis* was recorded mostly at RMT01 (46.6 % of all recorded abundance at RF 09), while polychaete larvae were recorded mostly at RMT02 (73.4 % of all recorded abundance at RF 09). The mean depths of these two taxa where they were most abundant were also different from the other stations, with *Fritellaria borealis* being 15.5 m shallower at RMT01 and polychaete larvae being 22.1 m deeper at RMT02. *Calanus finmarchicus* CI abundance was distributed unevenly across all three stations (60.8 % at RMT01, 22.2

4. Small scale spatial variation in zooplankton around moorings at Kongsfjorden, Rijpfjorden and Billefjorden

% at RMT02 and 17 % at RMT03), and depth distributions of this stage were also different at all three stations (mean depth of 48.6 m at RMT01, 57.9 m at RMT02 and 31.7 m at RMT03). Other species with a similar pattern of differing abundances at each station and differences in mean depth between each station of at least 10 m included *Microcalanus* spp., *Limacina helicina* and bivalve veligers. These animals/stages did not have particularly high abundances at Rijpfjorden (Table 4.3), but were clearly patchy both vertically and horizontally and are all relatively small weak swimmers. Mean horizontal current velocities observed at Rijpfjorden the day after net sampling were the highest observed across all locations (up to -143 mm/s) in a southerly direction across all depths observed (15 – 73 m) (Table 4.2). In contrast to Kongsfjorden, where weaker currents in 2009 appear to have aided the formation of patches of weak swimmers compared to 2008, spatial variability was observed under a regime of comparatively strong currents at Rijpfjorden. Our sampling location in Rijpfjorden is towards the eastern coast of the fjord and is somewhat sheltered to the north by a peninsula of land (Fig 4.1). Alldredge and Hamner (1980) observed high zooplankton densities in the lee of a small point protruding into a strong tidal current, and suggested that transport of zooplankton by fine-scale current patterns may be a major cause of aggregation in some near-shore locations. At Rijpfjorden in our study, strong southward flow may be diverted by the shoreline near our sampling location, leading to zooplankton aggregation.

RMT03 was also identified as significantly different in terms of MVBS (Figs 4.11, 4.12), and it was clear from the echograms that the dominant scattering layer observed at Rijpfjorden between approximately 50 – 175 m ended at approximately 23:55 at RMT03 (Fig 4.12). Plots of vessel movement at Rijpfjorden (Fig 4.6) describe how each 20 minute portion of acoustic data at all stations included significant vessel movement, both passive drift and active steaming. During the acoustic data collection period that matched the net sample at RMT03 as closely as possible, the vessel moved to a location which no longer contained the scattering layer observed at all other Rijpfjorden stations. Inspection of the GPS plot shows northward vessel movement during data collection for RMT03. RMT03 is the northern most station at Rijpfjorden (towards the mouth of the

4. Small scale spatial variation in zooplankton around moorings at Kongsfjorden, Rijpfjorden and Billefjorden

fjord - Fig 4.1), and since both the more southerly stations display the scattering layer, it is likely the latitude of RMT03 is where this scattering layer ended, with more southerly locations containing the layer and more northerly locations without it. The large amounts of vessel drift at Rijpfjorden (also visible in a primarily south westerly direction) helps further explain the greater spatial variation within the fjord in terms of advective influence, as clearly there were strong surface currents in Rijpfjorden when it was sampled. The two CTD profiles available at Rijpfjorden did not display any significant differences (Fig 4.2), and so dominant hydrography appears to have been similar across the sampled area. Thus advection appears to be the most likely explanation for the observed spatial differences within Rijpfjorden.

4.4.3. Conclusion

Across a broader scale, zooplankton distributions and abundances were closely linked to the dominant water masses, with ArW species found to be more dominant in Billefjorden and Rijpfjorden, and AtW species dominating in Kongsfjorden. However, evidence is put forward suggesting Rijpfjorden is influenced by advected AtW species during summer/autumn, and that this traditionally Arctic marine system may not always be as 'Arctic dominated' as assumed. The observed regional differences include marked differences in zooplankton depth stratification, putting forward further evidence that zooplankton species align themselves in the water column differently under differing environmental conditions. Furthermore, interannual variations in zooplankton at Kongsfjorden between 2008 and 2009 have been identified and related to the advection of AtW into the fjord, and this difference in hydrology may have brought about variations in the intensity and timing of primary production with subsequent effects on the abundance and stage composition of *Calanus*. It is proposed that advection is the most prominent factor influencing small scale zooplankton spatial variation within the fjords of Svalbard, especially in the surface waters containing weaker swimmers which tend to be more susceptible to high levels of advection. Significant variation in both

4. Small scale spatial variation in zooplankton around moorings at Kongsfjorden, Rjipfjorden and Billefjorden

zooplankton abundance and depth stratification have been identified over scales < 1 nautical mile, especially at Rjipfjorden compared to Kongsfjorden.

5. Broad scale spatial variation in zooplankton around the Svalbard archipelago

5.1. Introduction

The current trend of warming in the Arctic continues with the announcement in September 2012 of a record minimum Arctic sea-ice extent since the satellite record began in 1979 (NSIDC 2012). The Atlantic sector of the Arctic (in which the Svalbard archipelago is found) has experienced the greatest effects of this climate change (Marshall et al. 2001; Moline et al., 2008). As highlighted in chapter 3 of this thesis, an increasing volume of Atlantic water flowing into the Arctic causes shifts in the dominant water masses (Walczowski and Piechura 2007), with subsequent effects on zooplankton communities (Beaugrand et al. 2002; Hays et al. 2005; Willis et al. 2006). The West Spitsbergen Shelf (WSS) is characterised by an unstable balance between Arctic and Atlantic regimes (Saloranta and Svendsen 2001), and a good example of this dynamic between changing water masses and zooplankton that has been highlighted throughout this thesis is the *Calanus* complex. Within this dynamic system, researchers attempt to monitor the changes occurring in the Arctic through a variety of means, and long term time series are most useful when determining trends.

This thesis focuses on zooplankton, a key component of the pelagic ecosystem that links primary production with higher trophic levels. Hays et al. (2005) describe how zooplankton can be particularly good indicators of climate change due to their tight coupling with environmental change. The non-linear responses of zooplankton to change can make them even better indicators than the physical changes in the system, as they can amplify subtle environmental changes. Taylor et al. (2002) describe how plankton populations respond to climatic signals other than those that dominate the driving variables, allowing them to integrate many changes beyond those observed by

researchers amongst the physical environment. This thesis and numerous publications (e.g. Willis et al. 2006; Berge et al. 2009; Wallace et al. 2010) have used fixed oceanic moorings to observe both physical and biological changes in the fjords of Svalbard, and have made inferences and drawn conclusions regarding change in the Arctic from these point samples. However, as discussed in the previous chapter, the variability and patchiness of zooplankton around the archipelago make it important to assess how representative the moored observations are on a broader spatial scale. The previous chapter of this thesis began our spatial assessment of the moorings on a small scale (~ 1 nautical mile), and identified significant spatial variations on this scale. This chapter will continue the assessment on a larger pan-Svalbard scale. In order to best assess the spatial variation of zooplankton on a medium to large scale, high resolution multi-frequency echosounding was used to gain backscatter observations of zooplankton through the water column. Traditional depth-stratified net samples were used to determine which species were most prevalent amongst the backscatter. Although a number of studies have investigated large scale zooplankton distributions around the archipelago (e.g. Daase and Eiane 2007; Blachowiak-Samolyk et al. 2008; Kwasniewski et al. 2010; Trudnowska et al. 2012), none have so far had the pan Svalbard coverage that we put forward here.

The concept of scale which is widely used in ecology (Schneider 2001) includes the measurement of spatial scales when describing the biological diversity of ecosystems (e.g. Beever et al. 2006). For this chapter, characteristic scale is defined as per Powell (1989) and Legendre and Legendre (1998) as the distance before the quantity of interest changes (i.e. the distance over which statistically similar observations are made). This definition of characteristic scale is dependent on the sampling resolution, and is applicable over a wide range of spatial scales (Legendre and Legendre 1998). For this chapter, our observations were backscatter from animals in the water column.

5.2. Materials and methods

5.2.1. Sampling location

This investigation was carried out over five years (2006 – 2010) and nine research cruises, with acoustic observations carried out from a number of research vessels (RV *Lance*, RV *Jan Mayen* and RRS *James Clark Ross*). Unfortunately, fully designated sampling was not possible on many of the cruises, and so transects were collected on an opportunistic basis. For this reason, transect length was limited to 10 nautical miles (nm) with no change in direction in order to generate the greatest number of comparable transects in all visited locations. Observations were also collected over 1 hour periods when the vessels were stationary at all possible locations. The visited locations are outlined in Table 5.1a,b and Fig 5.1. All sampling occurred between May and early September, with the vast majority of data collected in a narrower period from mid-July to early September. Only one cruise was carried out in May in 2010. Thus, although temporal variations may affect our data, the collection period largely during the Arctic summer should lessen this effect, and all data collected within each year are considered seasonally comparable.

5. Broad scale spatial variation in zooplankton around the Svalbard archipelago

Table 5.1a) Sampling locations including date, time and bottom depth. All acoustic stations and transects and their relevant times are not included for brevity. Net samples for 2009 and 2010 continue on Table 5.1b.

Year	Date Start	Date End	Date	Time (UTC)	Latitude (N)	Longitude (E)	Depth (m)
Acoustic							
2006	13/07/06	18/07/06			78.00 – 79.06	07.88 – 15.46	
2007	23/07/07	29/07/07			77.96 – 79.08	07.68 – 15.76	
2008	16/08/08	06/09/08			78.12 – 81.10	07.95 – 22.28	
2009	16/07/09	06/09/09			78.12 – 81.23	04.23 – 18.42	
2010	04/05/10	02/09/10			76.05 – 81.57	08.20 – 32.07	
Net							
2008			02/08/2008	15:00	79.72	08.83	454
			02/08/2008	23:00	79.72	08.83	452
			08/08/2008	12:00	80.35	16.27	386
			08/08/2008	22:00	80.35	16.27	386
			12/08/2008	16:30	80.50	11.25	788
			12/08/2008	22:30	80.50	11.25	777
			14/08/2008	20:45	80.30	22.32	225
			15/08/2008	09:30	80.28	22.30	225
			16/08/2008	14:55	80.13	22.17	202
			16/08/2008	20:40	80.17	22.17	177
			17/08/2008	05:55	80.60	22.13	174
			18/08/2008	21:00	78.97	11.93	339
			19/08/2008	06:00	78.97	11.93	340
			19/08/2008	22:45	79.20	11.42	344
			20/08/2008	00:55	79.50	11.13	326
			20/08/2008	04:15	78.98	09.50	321
			25/08/2008	23:20	78.39	16.43	192
			26/08/2008	05:00	78.39	16.43	195
			26/08/2008	11:05	78.39	16.43	191
			26/08/2008	17:10	78.39	16.42	194
			27/08/2008	21:55	78.58	11.34	317
			28/08/2008	05:00	78.58	11.34	308
			28/08/2008	09:45	78.58	11.34	318
			28/08/2008	17:05	78.58	11.33	317
			04/09/2008	10:00	78.59	11.24	318
			04/09/2008	16:15	78.59	11.23	309
			04/09/2008	22:00	78.59	11.24	319
			06/09/2008	11:15	78.40	16.42	193
			06/09/2008	23:30	78.40	16.42	195

5. Broad scale spatial variation in zooplankton around the Svalbard archipelago

Table 5.1b) Sampling locations including date, time and bottom depth. All acoustic stations and transects and their relevant times are not included for brevity.

Year	Date Start	Date End	Date	Time (UTC)	Latitude (N)	Longitude (E)	Depth (m)
Net							
2009			17/07/2009	22:30	79.01	11.41	315
			17/07/2009	19:15	78.99	11.66	249
			17/07/2009	11:00	78.96	11.94	321
			18/07/2009	03:45	79.04	11.13	320
			18/07/2009	14:30	78.98	08.54	278
			18/07/2009	11:30	78.98	09.50	217
			19/07/2009	01:30	78.90	07.77	1116
			19/07/2009	13:30	79.05	07.00	1306
			20/07/2009	10:30	79.06	04.18	2404
2010			06/05/2010	07:45	76.40	19.85	1937
			11/05/2010	08:00	77.75	10.77	247
			20/07/2010	14:30	78.95	11.95	333
			22/07/2010	02:00	79.05	07.00	1316
			24/07/2010	06:35	78.23	08.92	1249
			18/08/2010	00:15	80.13	22.15	194
			18/08/2010	19:15	80.29	22.28	274
			19/08/2010	08:25	80.61	22.12	187
			19/08/2010	09:05	80.61	22.12	187
			20/08/2010	04:30	81.14	22.76	236
			21/08/2010	03:30	81.35	21.96	368
			21/08/2010	14:30	81.39	22.35	508
			22/08/2010	18:30	81.55	22.69	889
			23/08/2010	17:40	81.72	23.18	2798
			27/08/2010	11:00	81.57	30.96	1303
			27/08/2010	23:00	81.54	30.41	832
			27/08/2010	12:20	81.61	30.84	1944
			28/08/2010	11:00	81.50	32.09	581
			29/08/2010	23:00	81.44	30.79	401
			29/08/2010	11:45	81.51	30.14	860
		30/08/2010	00:00	81.44	30.85	401	
		30/08/2010	01:00	81.44	30.94	401	
		30/08/2010	06:00	81.40	21.33	185	

5. Broad scale spatial variation in zooplankton around the Svalbard archipelago

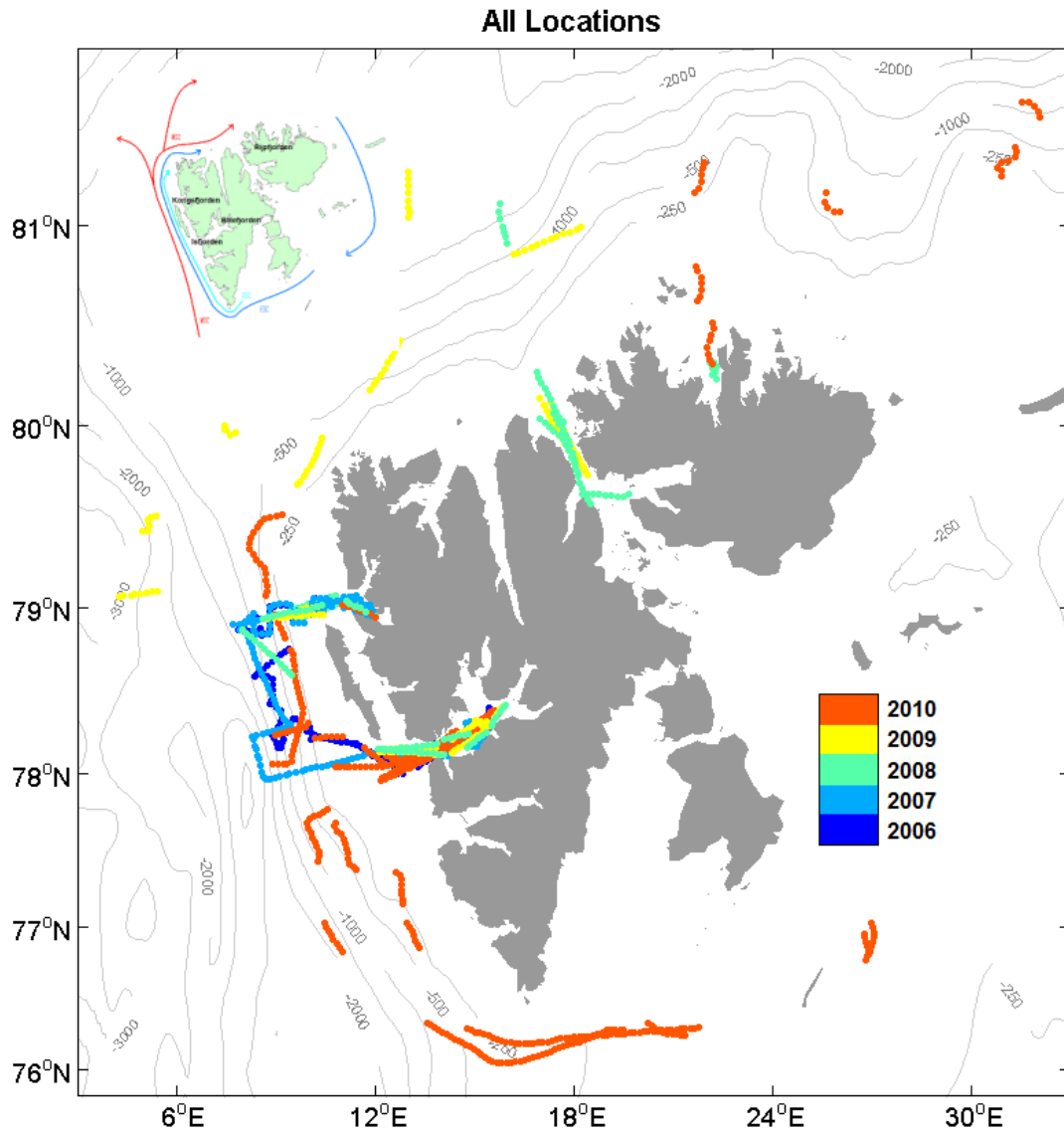


Fig 5.1) Map of the Svalbard archipelago displaying all acoustic data collection. Colours represent year of sampling. Inset (top left) displays dominant currents. [WSC carrying AtW (red), ESC carrying ArW (dark blue), SCC carrying Coastal Water (light blue)] and the key fjords investigated in this thesis [Isfjorden, Billefjorden, Kongsfjorden and Rijpfjorden].

Please see thesis section 1.3.1 for detailed hydrology of the Svalbard archipelago, as it is not repeated in this section. Although the main focus of this chapter is not linking zooplankton to hydrography (as this link has been well established by many previous studies and prior chapters in this thesis), monthly average sea surface temperature (SST) extractions were obtained from MODIS Aqua at 4.6 km resolution (in collaboration with Stanford University) in order to discuss the possible hydrographic drivers of

zooplankton variations highlighted by our spatial investigation. The Arctic sea-ice concentrations (observed by AMSR-E and projected using arctic grids from NSIDC at 6.25 km resolution by the University of Bremen) obtained as a daily average on July, August and September 15 in order to provide comparable broad-scale sea-ice conditions between years and described in section 1.3.1 will be referred to when discussing prevailing ice conditions.

5.2.2. Zooplankton sampling

Mesozooplankton sampling was conducted using a Multinet Plankton Sampler (see section 2.2 for details - sample times detailed in Table 5.1). Filtered water volume was derived from measurements made by flowmeters attached to the MPS, and all samples were fixed in 4% formalin/seawater solution and analysed for species composition post cruise as per Falk-Petersen et al. (1999) and Daase and Eiane (2007).

The depths of each sequential net were chosen at each station in order to allow comparable surface (i.e. 0-100 m) resolution while still sampling the entire water column. However, as depth strata varied between sampling events, mesozooplankton abundances were integrated over the entire sampled depth to allow comparison between all samples. Only net samples with at least 0 – 150 m of the water column sampled were used in the analysis in order to ensure the most abundant water layers were represented by all sampling events. However, maximum sampling depths do vary between stations (Table 5.1). Sample times also vary in terms of their position in the diel cycle, but the integration of abundances over the entire sampled depth should minimise differences between stations caused by vertical movements of zooplankton. Unfortunately, only information on *Calanus* was available from the net samples collected in 2008.

5.2.3. Acoustic observations

As in the previous chapter, downward facing, hull-mounted Simrad EK60 echosounders operating at frequencies of 18, 38 and 120 kHz and a ping rate of 0.5 pings s⁻¹ were used on all vessels to gather backscatter information from the water column (12 m to near seabed) (see 2.3. for calibration, noise removal and re-sampling details). Only data from the upper 175 m of the water column were used in the analysis due to range limitations at 120 kHz. The near field of 0-12 m (0-12 m at 38 kHz and 0-6.5 m at 120 kHz) was also excluded from analysis. Thus, data from 12-175 m were used in the acoustic analysis. Backscatter was partitioned using 120 kHz – 38 kHz into mesozooplankton, macrozooplankton and nekton echoes as per Madureira et al. (1993) (see 2.3. for details).

At each acoustic ‘station’ (i.e. stationary observations), 60 minutes of acoustic data were used to calculate a Mean Volume Backscattering Strength (MVBS = $10 \log_{10}$ [mean (S_v)], where S_v is the volume backscattering strength). All echo integration was carried out on a vertical grid of 12-20-30-40-50-60-80-100-125-150-175 m. This grid was chosen to emphasise the surface layers in our analysis, as these euphotic layers are known to contain the most zooplankton in Arctic waters (Kosobokova and Hopcroft 2009). For each acoustic transect of 10 nm length, echo integration was carried out using a 0.5 nm horizontal grid giving 20 samples per transect.

5.2.4. Multivariate clustering

Bray-Curtis similarity matrices created in PRIMER were used to cluster the MPS stations based on mesozooplankton community composition and the acoustic stations based on combined mesozooplankton, macrozooplankton and nekton depth stratified

5. Broad scale spatial variation in zooplankton around the Svalbard archipelago

backscatter. Net and acoustic stations sampled in each of the five years were clustered separately to avoid interannual variation affecting the clustering. Fourth-root transformation was chosen as the lowest level of transformation sufficient (see section 2.4 for details), and this was applied to both net and acoustic data. Clusters are presented at both 80 % and 70 % similarity for MPS stations, and 70 % and 60 % similarity for acoustic stations. These cluster similarities were chosen to create meaningful clusters and best display the broad scale clustering of locations around the archipelago. A weighted Spearman rank correlation was carried out between latitude, longitude and SST and acoustic stations to determine which variable was most responsible for the observed clustering between the acoustic stations.

5.2.5. Auto-correlation functions and characteristic scale

In order to compare spatial variation between locations during our study, the archipelago first had to be separated into sectors. This differentiation of sectors was based on a combination of latitude, longitude, and bathymetry, as bathymetry is well known to steer currents around the archipelago (Saloranta and Svendsen 2001), and latitude especially will affect the dominant water masses present and the extent of AtW influence. The chosen sectors are displayed in Fig 5.2.

5. Broad scale spatial variation in zooplankton around the Svalbard archipelago



Fig 5.2) Map of the Svalbard archipelago displaying sectors used to separate collected data. Light colours (purple, pink, light green and orange) indicate depths < 1000 m, while dark colours (dark green and red) indicate depths > 1000 m. Pink and purple sectors labelled A – H indicate sampled fjords and straits, while numbered sectors 1 – 11 indicate all other sampled sectors. Labelling starts at the bottom right of the map and moves around in a clockwise direction for each depth zone. Small brown dots indicate all acoustic stations.

5. Broad scale spatial variation in zooplankton around the Svalbard archipelago

The longitude of 22.50°E was chosen to separate sectors based on the likely furthest extent of AtW penetration to the northeast of Svalbard at Rijpfjorden (H). The central band of latitude (78.00°N – 80.00°N) was chosen to include Isfjorden (B), Kongsfjorden (D) and Smeerenburgfjorden (F), but exclude Rijpfjorden to the north and Hornsund (A) to the south. 81.00°N is further used to separate the sectors north of the archipelago, as latitudes above this are often dominated by sea-ice cover.

To calculate auto-correlation functions (ACF) of mesozooplankton, macrozooplankton and nekton backscatter, all transect data were first centred (i.e. vector x becomes $(x - \text{mean}(x))/\text{sd}(x)$) to create a fluctuation about the mean of all combined data. The auto-correlation function for each 10 nm transect from within each sector and year (with backscatter integrated at 0.5 nm intervals) was then calculated. A mean characteristic scale (L_s) was calculated for each sector by averaging all transect L_s . L_s was defined as the lag distance (k in nm) within which backscatter observations were more similar than expected from a random distribution, i.e. the shortest lag at which the ACF ceases to be significant. This was the lag within which $ACF(k) \leq \text{sig}.ACF_{(n,k)}$, where:

$$\text{sig}.ACF_{(n,k)} = \pm \frac{\sqrt{2}}{n - k} \quad (5.1)$$

which is the significance level of ACF at lag k , given a total of n lags (see Box and Jenkins 1976). r_{max} was also reported as the maximum ACF value within L_s , and a mean r_{max} was calculated for each sector by averaging all transect r_{max} . Our integration resolution of 0.5 nm along transect was chosen both to maximise the number of observations per transect, and also as zooplankton are known to aggregate in patches over short spatial scales (Folt and Burns 1999). When analysing each transect, mesozooplankton, macrozooplankton and nekton backscatter were integrated into three depth strata (12 – 50 m, 50 – 100 m and 100 – 175 m) and analysed separately in order to identify differences in characteristic scale between taxa and depth. The sectors

5. Broad scale spatial variation in zooplankton around the Svalbard archipelago

included in this analysis with their associated number of transects during each year are outlined in Table 5.2.

Table 5.2) Number of acoustic transects (10 nm) collected at each sector in each year of sampling.

Sector	Transect No (each = 10 nm)					Total (nm)
	2006	2007	2008	2009	2010	
1					2	20
2					11	110
3	5	6	6	6	11	340
4			2	3	1	60
7					1	10
8		2		1		30
9				1		10
10				1		10
B	3	3	4	4	9	230
D		1	2		1	40
G			3	2		50
H			1			10

5.3. Results

5.3.1. Broad scale station clustering

The MPS similarity clusters for each year and the dominant zooplankton species responsible are displayed below (Figs 5.3 – 5.5). For 2009 and 2010 when zooplankton abundances were available over a range of species, the clustering obtained using the *Calanus* copepods alone was very similar to that obtained using all the species available (Figs 5.4, 5.5).

In 2008, when only *Calanus* abundances were available, the locations of Billefjorden (blue – Fig 5.3), Kongsfjorden (light blue – Fig 5.3) and Rijpfjorden (red – Fig 5.3) clustered separately at 80 % similarity. This clustering was based primarily on the varying abundances of *Calanus finmarchicus* and *Calanus glacialis*, and as highlighted in chapters 3 and 4 of this thesis, Rijpfjorden contained a relatively high abundance of the AtW associated *C. finmarchicus*. Kongsfjorden was most dominated by *C. finmarchicus*, while Billefjorden contained the highest relative abundances of *C. glacialis*. *Calanus hyperboreus* was identified in its highest abundance deeper beyond the shelf break at latitude comparable to Rijpfjorden (Fig 5.3), and the deeper stations clustered separately to the fjords. At 70 % similarity (Fig 5.3 inset), Rijpfjorden and Kongsfjorden clustered together (yellow – Fig 5.3 inset), while Billefjorden remained separate, indicating it was the most distinct fjord in terms of its *Calanus* composition. All stations within the fjords clustered together at 80 % similarity.

In 2009, MPS data were only available from locations near Kongsfjorden (Fig 5.4), but this time the longer transect out to deeper waters beyond the shelf break indicated that a

gradient in zooplankton community occurred from the fjord (with locations within the fjord clustering together) through to the deep stations. This clustering was apparent at both 80 % and 70 % similarity. Deeper water associated species such as *C. hyperboreus* (Hirche 1997) and *Microcalanus* spp. (Brodsky 1950) were recorded in higher abundances at the deepest location, while the shelf associated *C. glacialis* (Conover and Huntley 1991) and larval animals were recorded in higher abundances within Kongsfjorden (Fig 5.4).

In 2010, MPS data were collected over a broad range of locations (Fig 5.5). At 80 % similarity, Rijpfjorden clustered together with stations on the shelf to the north of the fjord, with a *Calanus* community very similar to that recorded in 2008. As highlighted in chapter 4, *O. similis* was also recorded in comparatively high abundance at Rijpfjorden and the stations on the shelf nearby. However in 2010, Kongsfjorden clustered at 80 % similarity with both the deeper stations outside it, and with deeper water locations north of 81°N and eastwards of Rijpfjorden (red – Fig 5.5). The furthest northeast stations clustered together separately (yellow – Fig 5.5), and these stations contained very high relative abundances of *C. finmarchicus* well beyond 80°N and eastwards of 30°E. The most distinct cluster was located south of the archipelago between Sørkapp and Hopen, and this cluster contained relatively low abundance of *C. finmarchicus*, no *C. hyperboreus* and less *O. similis* (Fig 5.5). A high comparative abundance of copepod nauplii were also recorded here, and as this cluster was the only sampled in May, this may explain the presence of high numbers of nauplii during the spawning period.

5. Broad scale spatial variation in zooplankton around the Svalbard archipelago

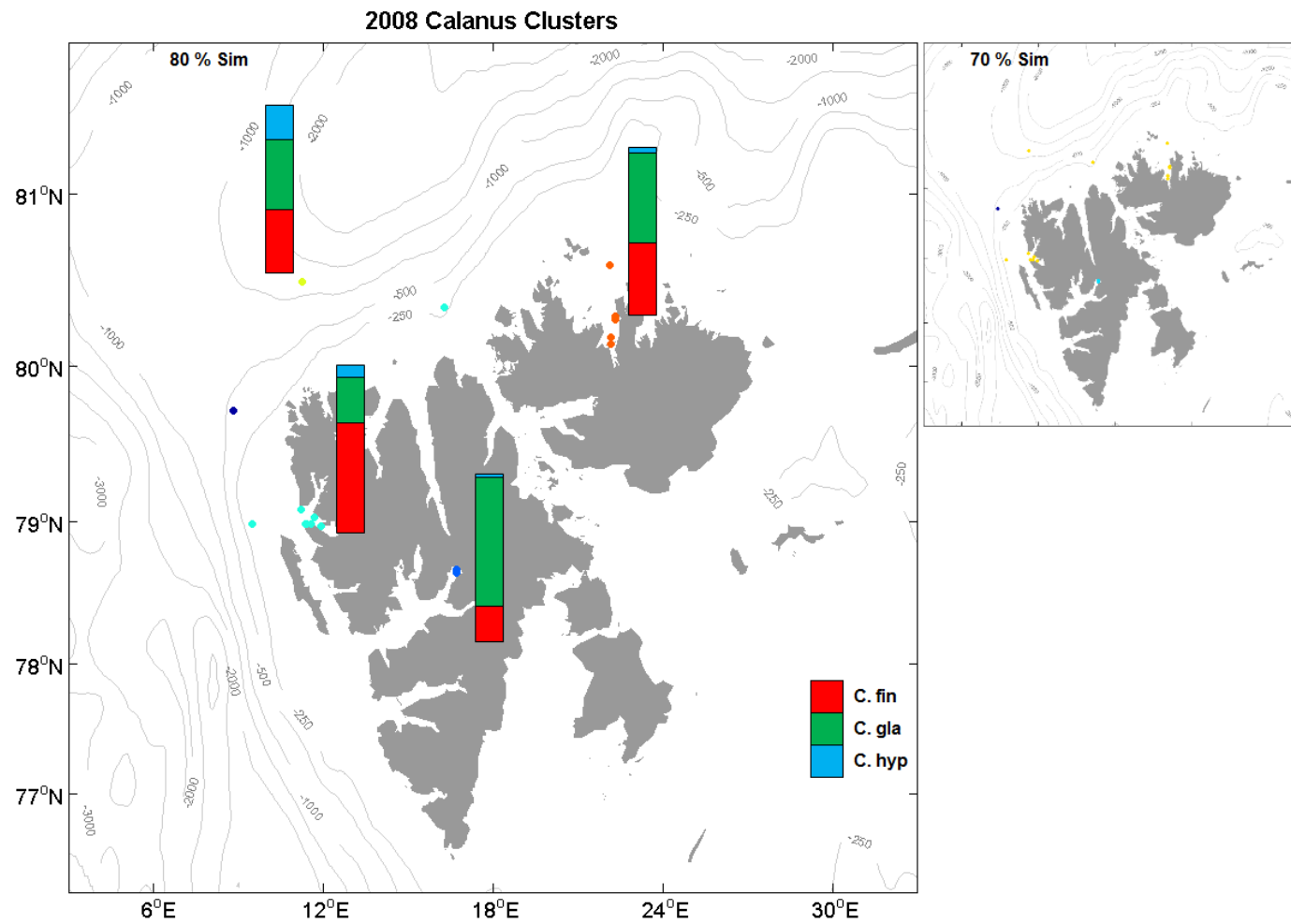


Fig 5.3) Main - map of the Svalbard archipelago displaying 2008 MPS *Calanus* 80 % similarity clusters. Each colour of spot represents members of a separate cluster. Percentage composition of *C. finmarchicus* (red), *C. glacialis* (green) and *C. hyperboreus* (blue) are displayed for chosen clusters. Inset (top-right) displays *Calanus* clusters at 70 % similarity.

5. Broad scale spatial variation in zooplankton around the Svalbard archipelago

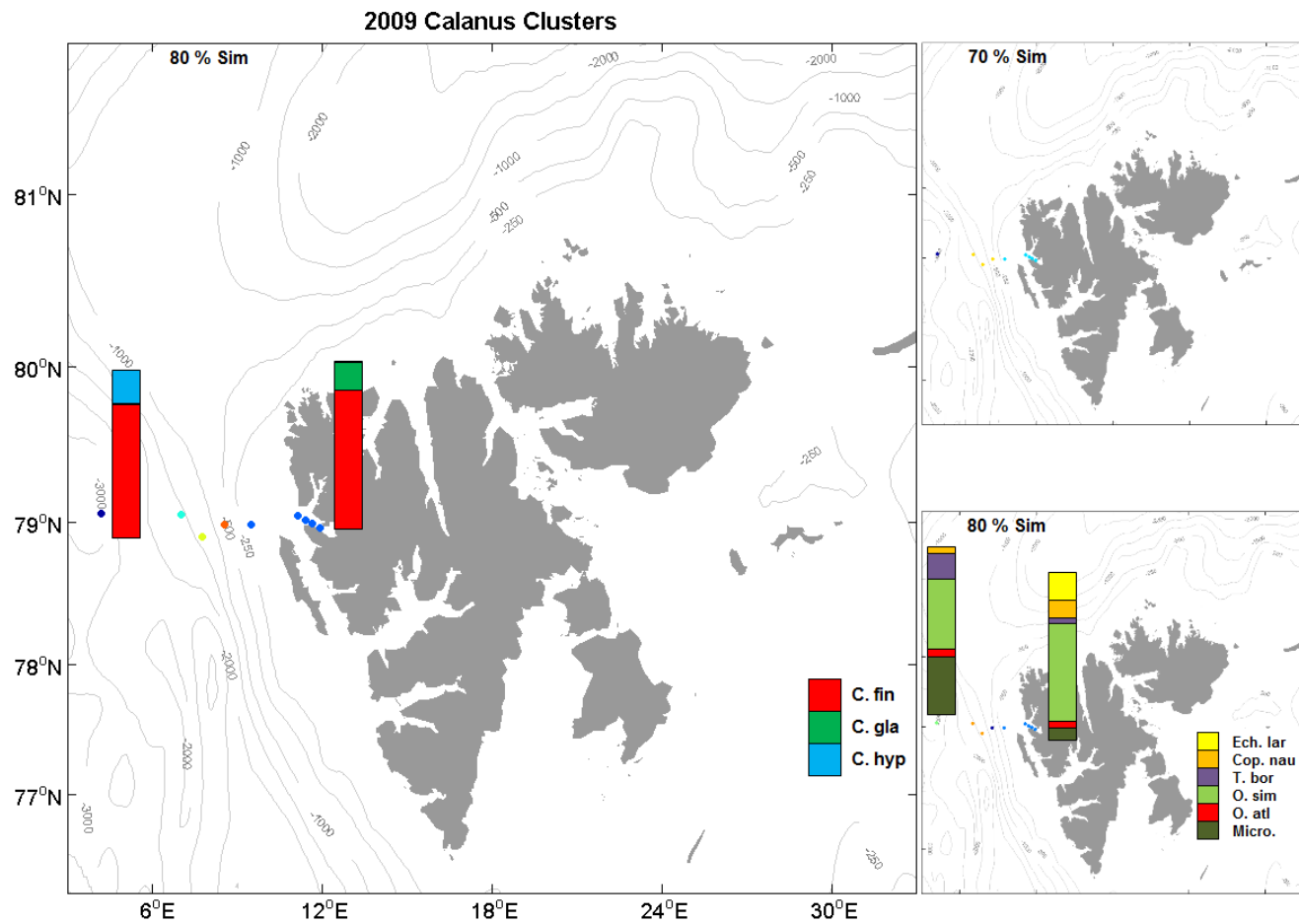


Fig 5.4) Main - map of the Svalbard archipelago displaying 2009 MPS *Calanus* 80 % similarity clusters. Each colour of spot represents members of a separate cluster. Percentage composition of *C. finmarchicus* (red), *C. glacialis* (green) and *C. hyperboreus* (blue) are displayed for chosen clusters. Inset (top-right) displays *Calanus* clusters at 70 % similarity. Inset (bottom-right) displays clusters at 80% similarity using all sampled zooplankton species. Percentage composition of echinoderm larvae (yellow), copepod nauplii (orange), *T. borealis* (purple), *O. similis* (light green), *O. atlantica* (red) and *Microcalanus* spp. (dark green) are displayed for chosen clusters.

5. Broad scale spatial variation in zooplankton around the Svalbard archipelago

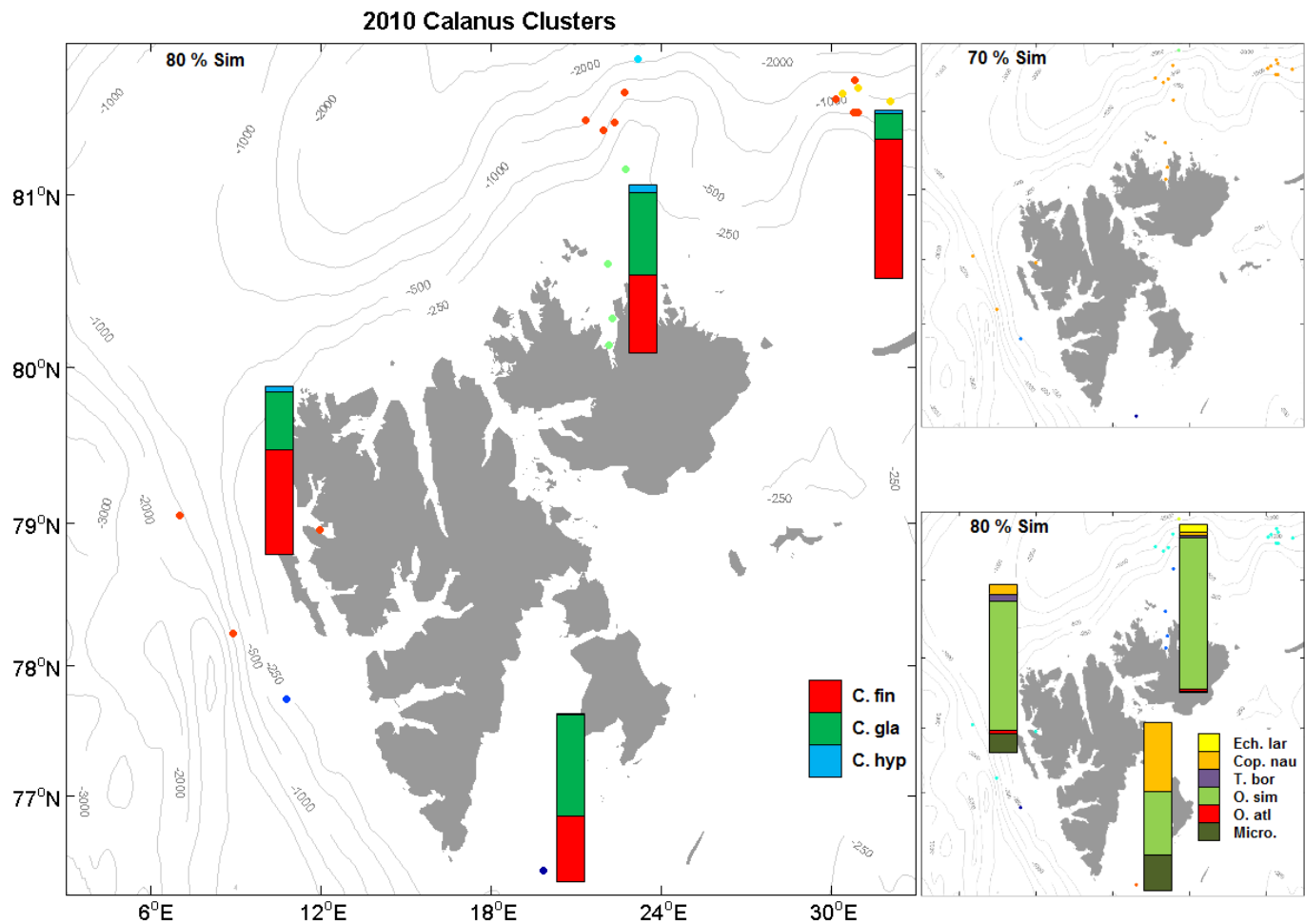


Fig 5.5) Main - map of the Svalbard archipelago displaying 2010 MPS *Calanus* 80 % similarity clusters. Each colour of spot represents members of a separate cluster. Percentage composition of *C. finmarchicus* (red), *C. glacialis* (green) and *C. hyperboreus* (blue) are displayed for chosen clusters. Inset (top-right) displays *Calanus* clusters at 70 % similarity. Inset (bottom-right) displays clusters at 80% similarity using all sampled zooplankton species. Percentage composition of echinoderm larvae (yellow), copepod nauplii (orange), *T. borealis* (purple), *O. similis* (light green), *O. atlantica* (red) and *Microcalanus* spp. (dark green) are displayed for chosen clusters.

The acoustic station data contained a better spatial resolution than the MPS data set, and data were available from 2006 and 2007 also. The similarity clusters for each year with mesozooplankton, macrozooplankton and nekton combined are displayed below (Figs 5.6 – 5.10). These clusters also included larger faster swimming taxa such as fish, euphausiids and amphipods which were not sampled proportionally by the MPS net. Clustering was also carried out with just mesozooplankton backscatter observations to highlight any differences between the taxa (Figs 5.6 – 5.10 bottom right).

Using combined backscatter in 2006, Kongsfjorden, Krossfjorden, Billefjorden, and much of outer Isfjorden and the adjacent shelf all clustered together at 70 % similarity (red – Fig 5.6). This clustering was very similar with just mesozooplankton backscatter, although greater variation was identified in outer Isfjorden (Fig 5.6 bottom right). In 2007, higher spatial resolution data were available from Kongsfjorden, and a gradient was observed at 70 % similarity between the inner fjord (blue – Fig 5.7), outer fjord (dark blue – Fig 5.7), shelf locations outside the fjord (light blue – Fig 5.7), and stations beyond the shelf break (red – Fig 5.7). When using just mesozooplankton backscatter, only two regions of similarity were identified – locations on the shelf (including the fjord) and locations off the shelf. In 2008, broader spatial coverage identified more clusters at 70% similarity using combined backscatter (Fig 5.8). The single Rijpfjorden station clustered with shelf locations to the west and south as far as outside Smeerenburgfjorden (light green – Fig 5.8). However, locations to the north both on and off the shelf clustered distinctly from Rijpfjorden. Locations within the Hinlopen strait were also clustered together (dark orange – Fig 5.8), and were similar to outer Isfjorden. A fjord gradient was still discernible at Kongsfjorden, and much of the outer fjord clustered together with Smeerenburgfjorden to the north at 70 % similarity. Billefjorden remained unique. Using just mesozooplankton backscatter, the outer stations at Kongsfjorden, Isfjorden and also Billefjorden clustered together with Rijpfjorden and the shelf (light green – Fig 5.8 bottom right). The locations within Hinlopen no longer clustered together based just on mesozooplankton backscatter.

5. Broad scale spatial variation in zooplankton around the Svalbard archipelago

In 2009, one large cluster dominated the map at 70 % similarity using combined backscatter (light green - Fig 5.9). This cluster included deep stations off the shelf outside Kongsfjorden, the shelf of northwest and northern Svalbard, much of central Hinlopen and also interestingly most of outer Rijpfjorden and the shelf to the north of the fjord. The innermost Rijpfjorden stations clustered separately from this large cluster, but together with scattered locations in outer Kongsfjorden and Isfjorden (green – Fig 5.9). Billefjorden remained distinct (orange – Fig 5.9), and a gradient was again observed at Kongsfjorden. The inner stations (dark blue – Fig 5.9) clustered separately to the central and outer stations, and these outer locations at Kongsfjorden clustered together with Smeerenburgfjorden again and also with outer Isfjorden. At 60 % similarity (Fig 5.9 top right), only inner Kongsfjorden and the northernmost deep stations remained distinctly clustered. Using just mesozooplankton backscatter, at 70 % similarity two clusters dominated the western shelf, outer Kongsfjorden and Isfjorden (blue-green and light green – Fig 5.9 bottom right), while a second large cluster included locations in inner Kongsfjorden, Hinlopen, the northern shelf and much of Rijpfjorden (light blue – Fig 5.9 bottom right).

As with the MPS data, spatial coverage was broadest within the acoustic data in 2010. At 70 % similarity, the map appears highly heterogeneous using combined backscatter, with many smaller different clusters. Rijpfjorden clustered together with much of the stations sampled at the shelf break to the far northeast of the archipelago (red – Fig 5.10), and Kongsfjorden clustered distinctly apart from one station on the shelf (light orange – Fig 5.10). Much of the western shelf was comprised of small individual clusters, and locations around Hopen to the southeast of the archipelago were distinct (light blue – Fig 5.10). A fjord gradient was also discernible at Isfjorden, with inner, central and outer stations clustered separately. However at 60 % similarity, much of the map is dominated by one large cluster which largely surrounded the archipelago and included Isfjorden, Kongsfjorden and Rijpfjorden. Locations in and around Magdalenefjorden however remained distinct (Fig 5.10 top right). Using just mesozooplankton backscatter, at 70 % similarity much of the southern and western shelf were dominated by two clusters (blue-green and light green – Fig 5.10 bottom right),

5. Broad scale spatial variation in zooplankton around the Svalbard archipelago

and Hopen was no longer distinct. These clusters also included outer Isfjorden, one station in outer Rijpfjorden and the stations sampled at the shelf break to the far northeast of the archipelago.

5. Broad scale spatial variation in zooplankton around the Svalbard archipelago

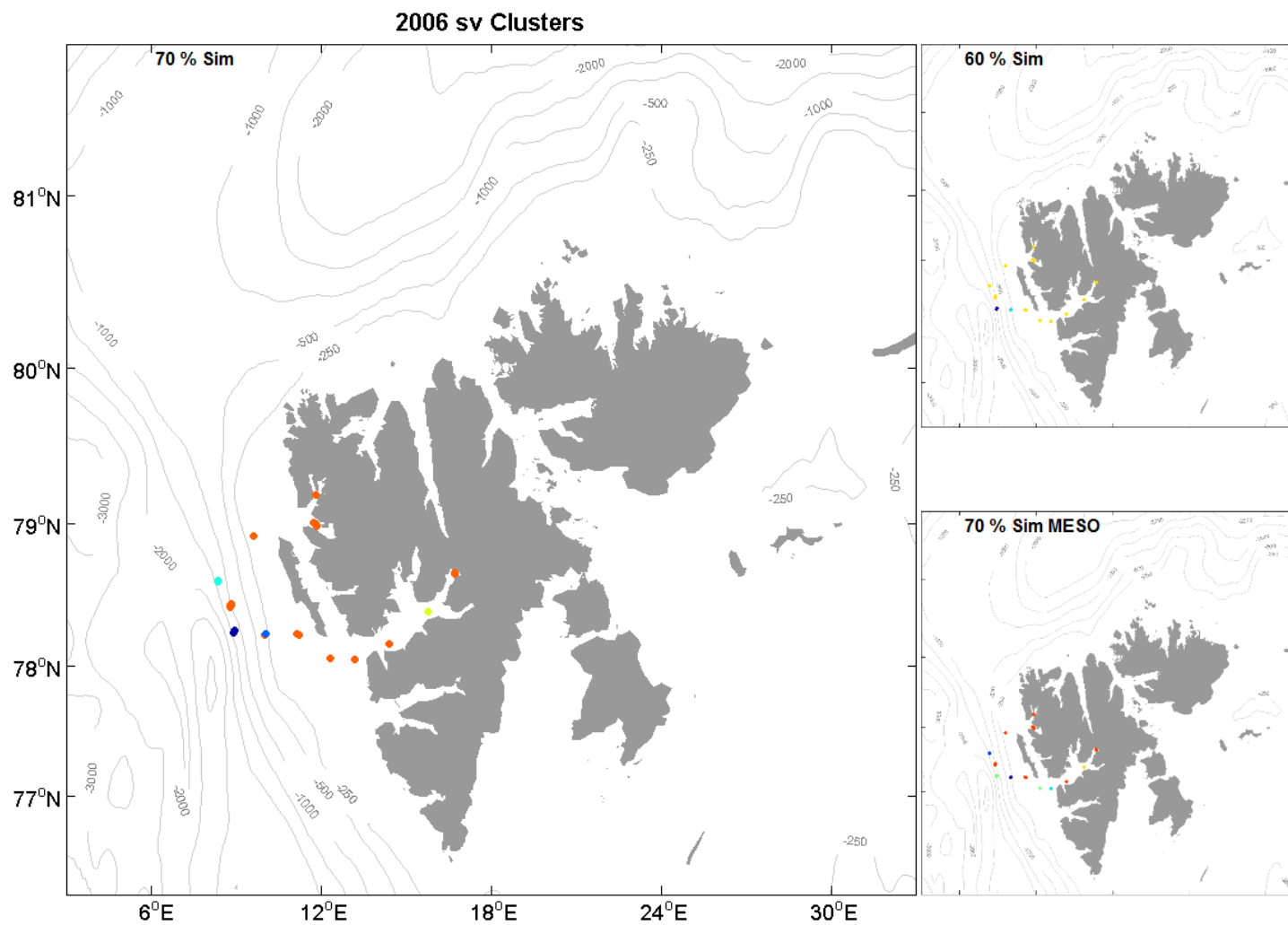


Fig 5.6) Main - map of the Svalbard archipelago displaying 2006 combined backscatter (sv - dB) 70 % similarity clusters. Each colour of spot represents members of a separate cluster. Inset (top-right) displays clusters at 60 % similarity. Inset (bottom-right) displays mesozooplankton (MESO) backscatter clusters at 70 % similarity.

5. Broad scale spatial variation in zooplankton around the Svalbard archipelago

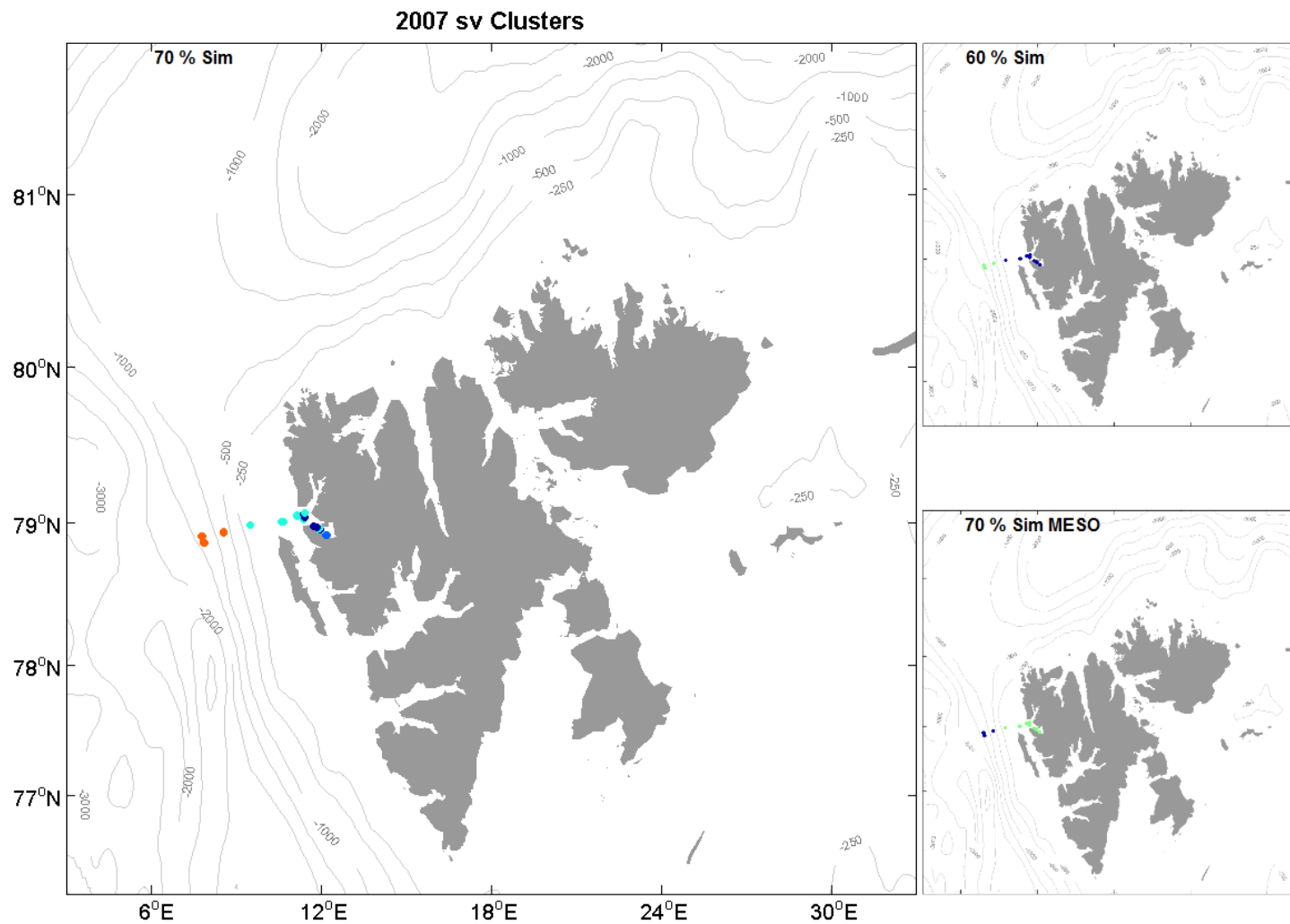


Fig 5.7) Main - map of the Svalbard archipelago displaying 2007 combined backscatter (sv - dB) 70 % similarity clusters. Each colour of spot represents members of a separate cluster. Inset (top-right) displays clusters at 60 % similarity. Inset (bottom-right) displays mesozooplankton (MESO) backscatter clusters at 70 % similarity.

5. Broad scale spatial variation in zooplankton around the Svalbard archipelago

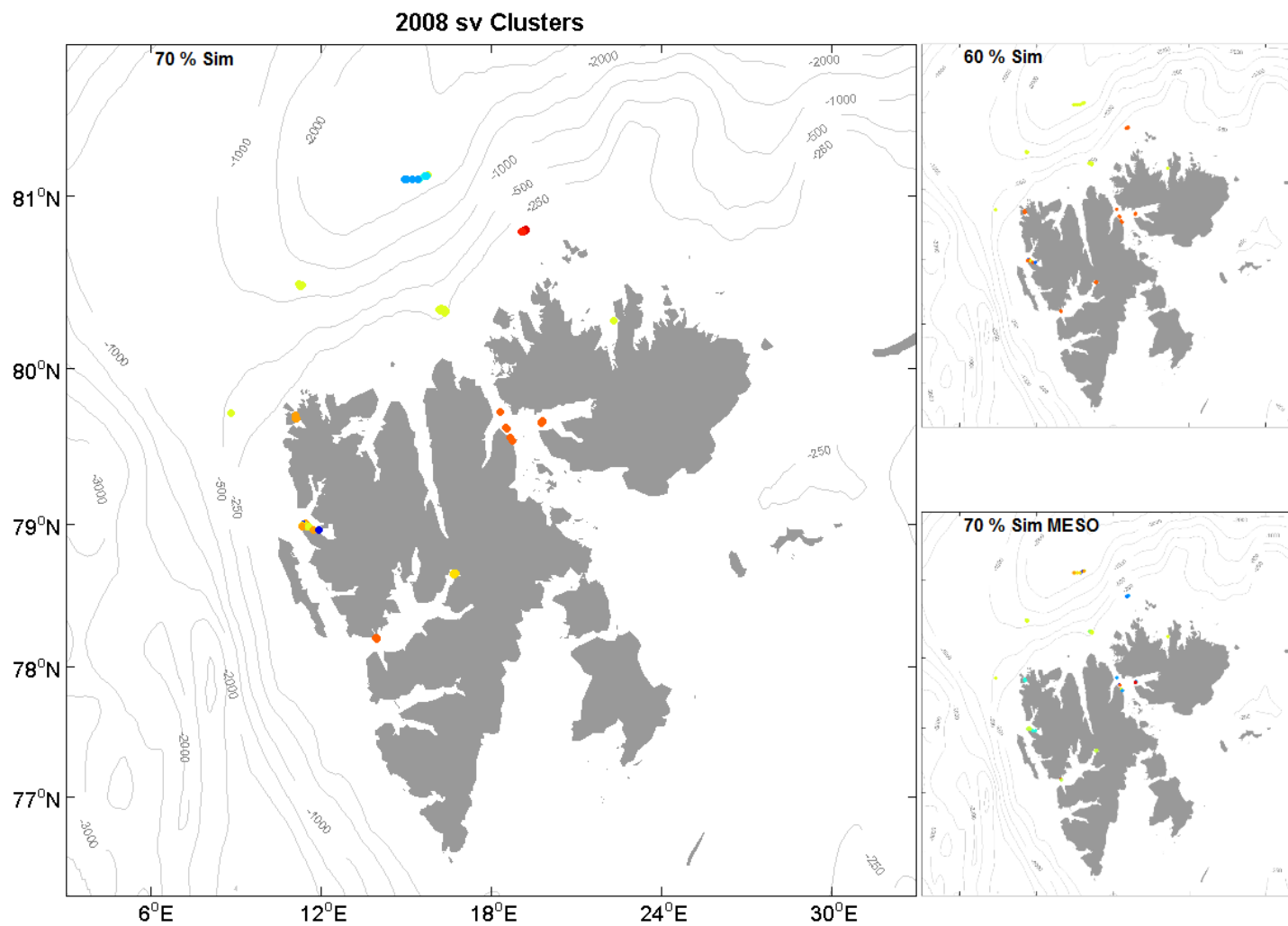


Fig 5.8) Main - map of the Svalbard archipelago displaying 2008 combined backscatter (sv - dB) 70 % similarity clusters. Each colour of spot represents members of a separate cluster. Inset (top-right) displays clusters at 60 % similarity. Inset (bottom-right) displays mesozooplankton (MESO) backscatter clusters at 70 % similarity.

5. Broad scale spatial variation in zooplankton around the Svalbard archipelago

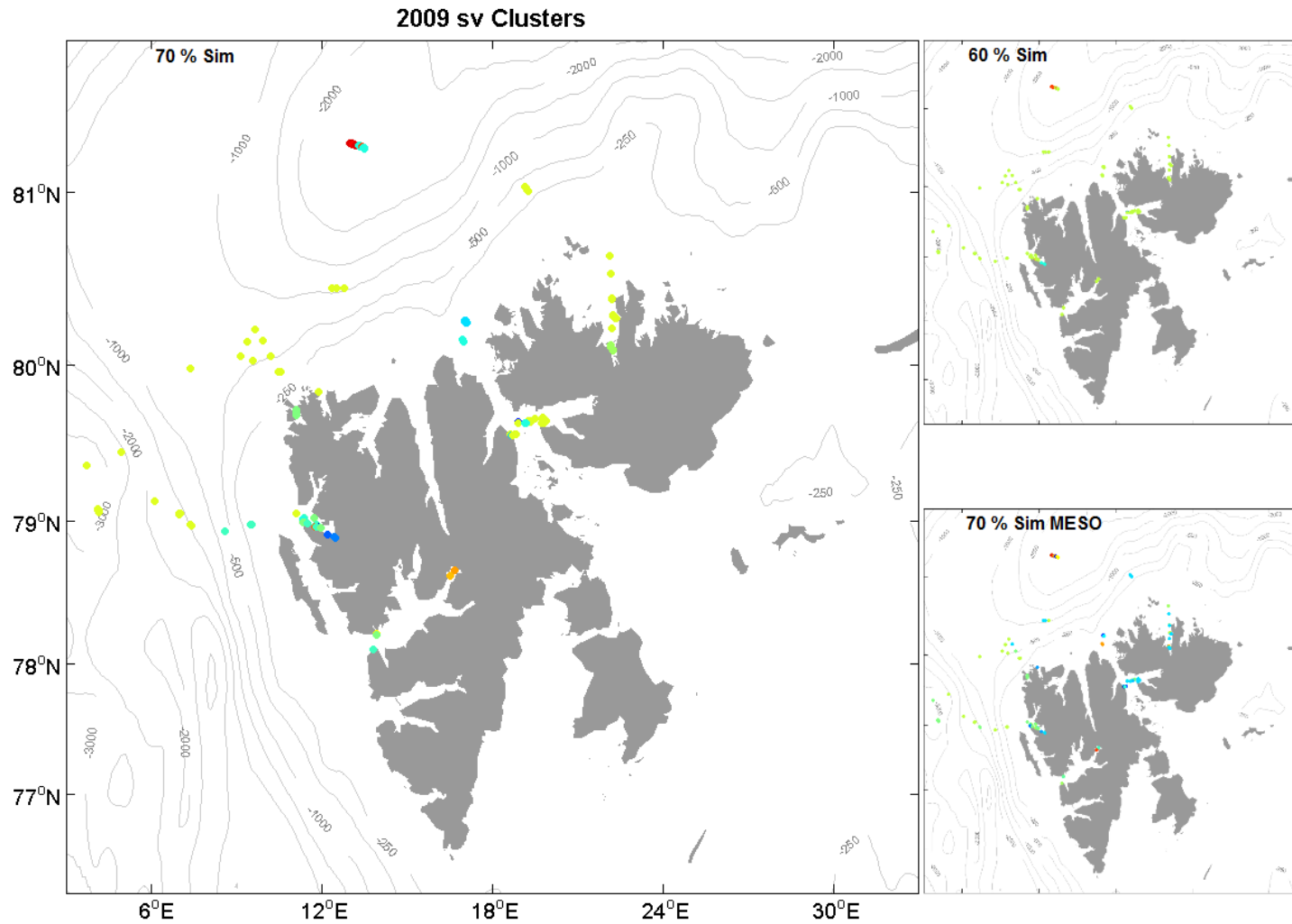


Fig 5.9) Main - map of the Svalbard archipelago displaying 2009 combined backscatter (sv - dB) 70 % similarity clusters. Each colour of spot represents members of a separate cluster. Inset (top-right) displays clusters at 60 % similarity. Inset (bottom-right) displays mesozooplankton (MESO) backscatter clusters at 70 % similarity.

5. Broad scale spatial variation in zooplankton around the Svalbard archipelago

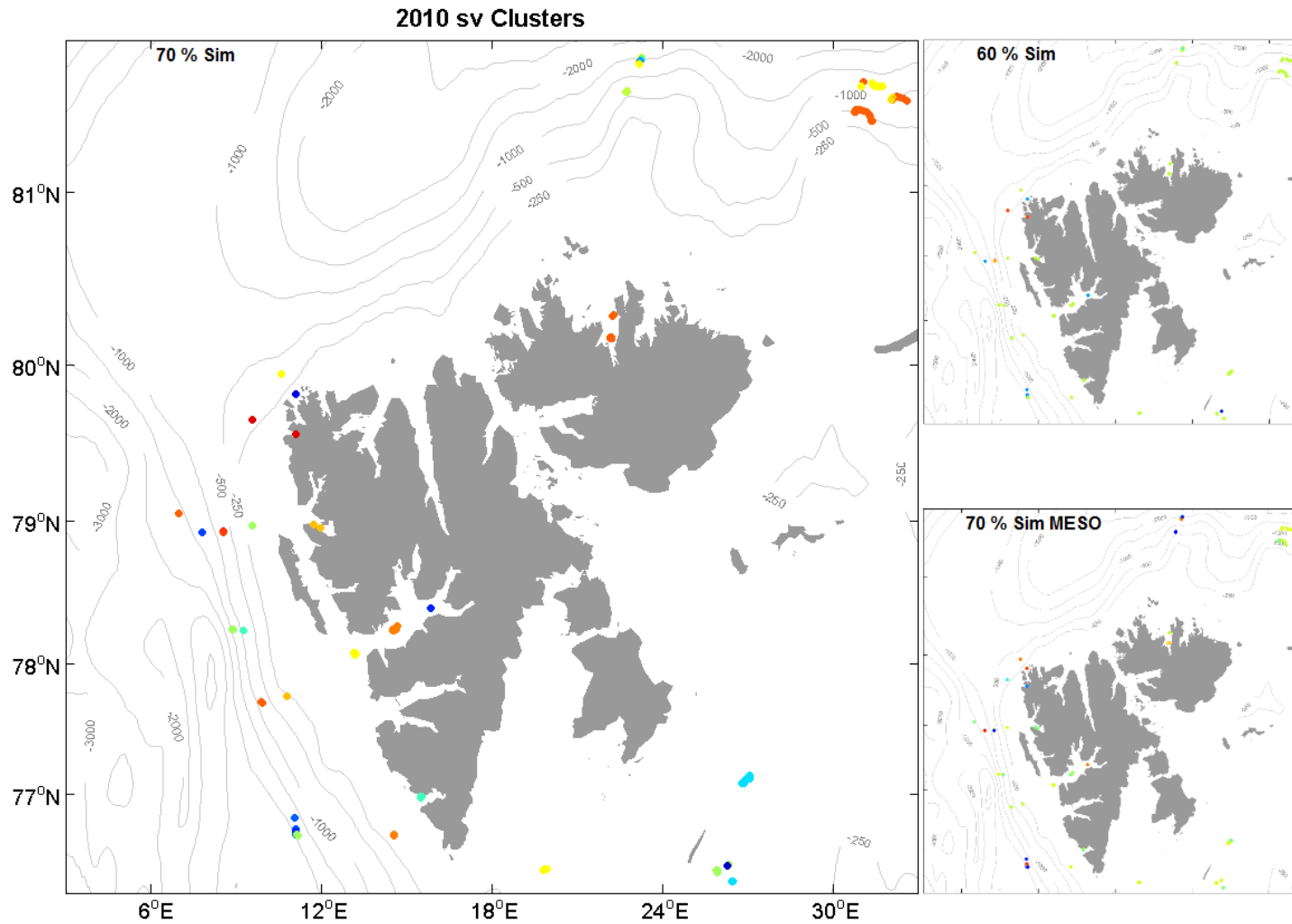


Fig 5.10) Main - map of the Svalbard archipelago displaying 2010 combined backscatter (sv - dB) 70 % similarity clusters. Each colour of spot represents members of a separate cluster. Inset (top-right) displays clusters at 60 % similarity. Inset (bottom-right) displays mesozooplankton (MESO) backscatter clusters at 70 % similarity.

Using SST extractions (see 5.2.1. for details), we correlated the spatial variability in our higher resolution backscatter observations to spatial variability in SST across a pan-Svalbard scale which has not been carried out before. The results of this correlation (weighted Spearman rank correlation of the Bray-Curtis similarity matrix between acoustic stations and Euclidean distance matrix between SST) are displayed in Table 5.3.

Table 5.3) Weighted Spearman rank correlation results (0 = no correlation, 1 = complete correlation) between SST, latitude and longitude and depth stratified (12 – 175 m) combined backscatter (All), mesozooplankton (ME), macrozooplankton (MA) and nekton (NE) backscatter for each year respectively. All acoustic stations collected in each year are used [n = 32 (2006), 31 (2007), 206 (2008), 156 (2009), 146 (2010)].

Year	SST				Lat				Lon			
	vs.				vs.				vs.			
	All	ME	MA	NE	All	ME	MA	NE	All	ME	MA	NE
2006	0.253	0.022	0.303	0.398	0.135	0.049	0.203	0.162	0.365	0.220	0.376	0.438
2007	0.007	0.022	0.013	0.000	0.272	0.463	0.147	0.160	0.705	0.731	0.617	0.512
2008	0.252	0.134	0.164	0.221	0.411	0.220	0.306	0.348	0.206	0.175	0.146	0.225
2009	0.293	0.023	0.139	0.453	0.440	0.316	0.358	0.288	0.021	0.009	0.000	0.057
2010	0.153	0.059	0.233	0.043	0.236	0.136	0.226	0.197	0.157	0.037	0.172	0.114

As we are most interested in smaller zooplankton communities in this thesis, maps of 12 – 50 m mesozooplankton backscatter and corresponding SST are displayed in Figs 5.11 and 5.12.

5. Broad scale spatial variation in zooplankton around the Svalbard archipelago

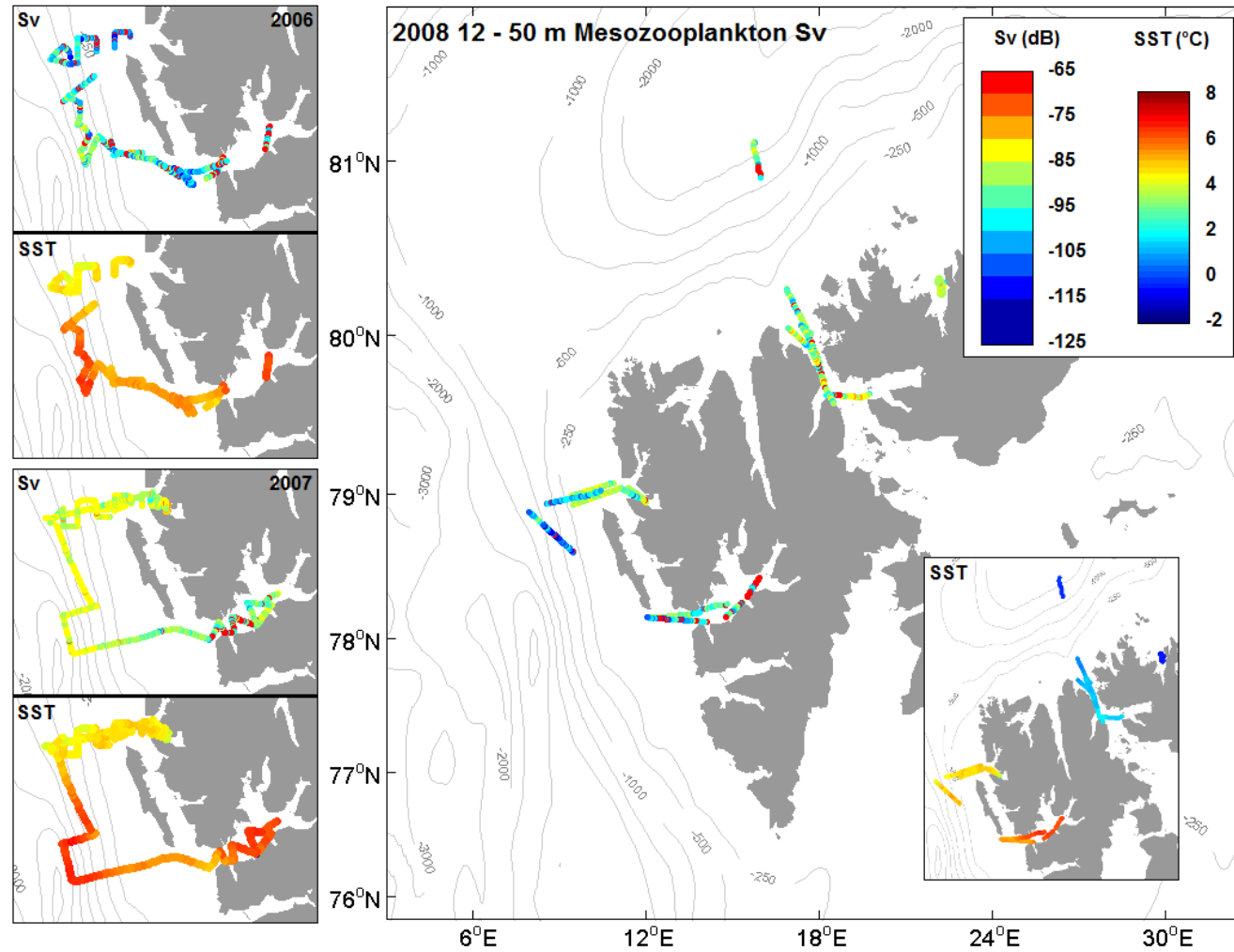


Fig 5.11) Map of the Svalbard archipelago displaying 12 – 50 m mesozooplankton Sv (120 kHz – dB at 0.5 nm horizontal resolution) and corresponding Sea Surface Temperature (SST monthly average corresponding to sample dates at 4.6 km resolution - °C) for all acoustic transects collected in 2006 (upper left), 2007 (lower left) and 2008 (main).

5. Broad scale spatial variation in zooplankton around the Svalbard archipelago

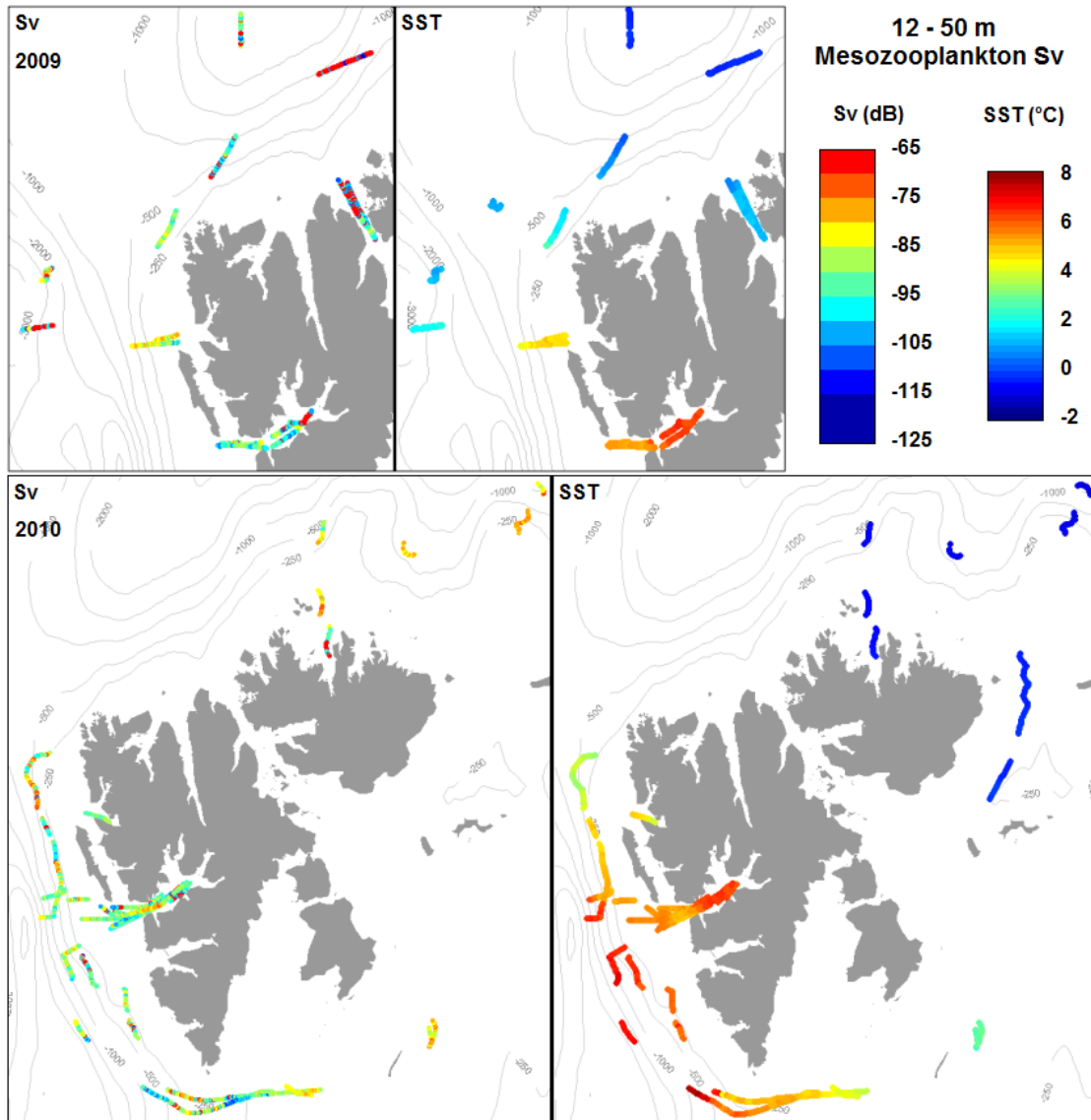


Fig 5.12) Map of the Svalbard archipelago displaying 12 – 50 m mesozooplankton Sv (120 kHz – dB at 0.5 nm horizontal resolution) and corresponding Sea Surface Temperature (SST monthly average corresponding to sample dates at 4.6 km resolution - °C) for all acoustic transects collected in 2009 (upper) and 2010 (lower).

5.3.2. Characteristic scale

Characteristic scale across all three taxa and depth strata was generally short and varied between 0.5 nm (i.e. no significant autocorrelation, as the data were analysed at 0.5 nm

intervals) and 2 nm. Mean characteristic scale within each sector however varied between 0.5 and 1.5 nm, an even shorter interval (Table 5.4). Across all taxa and depth strata, sector 1 (southeast of the archipelago around Hopen) had the longest mean characteristic scale of 0.86 nm, while of the three sectors with over 100 nm sampled, characteristic scale was longest within sector B (Isfjorden). Between the depth layers analysed, mean characteristic scale across all sectors was very similar, and shortest at 100 – 175 m. At 12 – 50 m (Fig 5.13), the euphotic layer commonly associated with the highest zooplankton biomass and ecological importance, Kongsfjorden contained the longest mesozooplankton mean characteristic scale (1 nm), while no significant autocorrelation was identified at Rijpfjorden across all three taxa. This result of high spatial variation at Rijpfjorden at this scale is consistent with findings in chapter 4 of this thesis.

The relatively high r_{\max} values across sectors and taxa (up to 0.82) indicate strong autocorrelation, but this drops significantly with increasing lag, resulting in our short characteristic scales. It is possible that our sample size per transect (20 samples) is insufficient to generate an accurate significance level (equation 5.1), resulting in our short characteristic scales. In an attempt to clarify this, the ACF within a few longer transects (> 30 nm) were calculated, but results were very similar with a short characteristic scale.

5. Broad scale spatial variation in zooplankton around the Svalbard archipelago

Table 5.4) mean characteristic scale (L_s - nm) of mesozooplankton (ME), macrozooplankton (MA) and nekton (NE) integrated into 12 – 50, 50 – 100 and 100 – 175 m depth layers and aggregated at 0.5 nm intervals along 10 nm transect(s) within each sector. r_{max} is the maximum autocorrelation function within L_s . For details, see section 5.2.5. Within sectors where more than one year of sampling were available (see Table 5.2), mean L_s , r_{max} and associated sd between years of sampling are presented. r_{max} NA indicates no significant autocorrelation within transect(s).

Taxon	Sector											
	1		2		3		4		7		8	
	L_s (sd)	r_{max} (sd)	L_s (sd)	r_{max} (sd)	L_s (sd)	r_{max} (sd)	L_s (sd)	r_{max} (sd)	L_s (sd)	r_{max} (sd)	L_s (sd)	r_{max} (sd)
ME 12-50 m	0.75	0.63	0.68	0.55	0.59 (0.09)	0.54 (0.03)	0.83 (0.58)	0.45 (0.00)	1.00	0.65	0.50 (0.00)	NA
ME 50-100 m	1.00	0.62	0.64	0.58	0.72 (0.21)	0.55 (0.05)	0.83 (0.29)	0.63 (0.01)	1.00	0.47	0.50 (0.00)	NA
ME 100-175 m	0.75	0.45	0.59	0.58	0.61 (0.05)	0.59 (0.08)	0.56 (0.10)	0.55 (0.00)	0.50	NA	0.50 (0.00)	NA
MA 12-50 m	1.25	0.72	0.82	0.59	0.63 (0.10)	0.50 (0.05)	0.75 (0.25)	0.68 (0.02)	0.50	NA	0.50 (0.00)	NA
MA 50-100 m	1.50	0.71	0.82	0.60	0.65 (0.15)	0.55 (0.09)	0.72 (0.25)	0.58 (0.11)	0.50	NA	0.63 (0.18)	0.51 (0.00)
MA 100-175 m	1.00	0.51	0.82	0.57	0.62 (0.09)	0.55 (0.03)	0.89 (0.54)	0.62 (0.19)	1.00	0.48	1.13 (0.53)	0.53 (0.13)
NE 12-50 m	0.50	NA	0.73	0.63	0.74 (0.10)	0.59 (0.05)	1.14 (0.38)	0.76 (0.06)	1.00	0.49	0.75 (0.35)	0.64 (0.00)
NE 50-100 m	0.50	NA	0.68	0.70	0.64 (0.13)	0.59 (0.10)	0.56 (0.10)	0.64 (0.00)	0.50	NA	0.50 (0.00)	NA
NE 100-175 m	0.50	NA	0.68	0.60	0.55 (0.05)	0.61 (0.08)	0.50 (0.00)	NA	0.50	NA	0.50 (0.00)	NA
	9		10		B		D		G		H	
	L_s (sd)	r_{max} (sd)	L_s (sd)	r_{max} (sd)	L_s (sd)	r_{max} (sd)	L_s (sd)	r_{max} (sd)	L_s (sd)	r_{max} (sd)	L_s (sd)	r_{max} (sd)
ME 12-50 m	0.50	NA	0.50	NA	0.69 (0.18)	0.63 (0.19)	1.00 (0.87)	0.81 (0.00)	0.79 (0.06)	0.50 (0.05)	0.50	NA
ME 50-100 m	0.50	NA	0.50	NA	0.83 (0.13)	0.61 (0.03)	0.92 (0.38)	0.74 (0.06)	0.50 (0.00)	NA	1.50	0.80
ME 100-175 m	0.50	NA	0.50	NA	0.78 (0.28)	0.62 (0.05)	0.83 (0.29)	0.64 (0.18)	0.58 (0.12)	0.62 (0.00)	0.50	NA
MA 12-50 m	1.00	0.60	0.50	NA	0.95 (0.19)	0.56 (0.05)	0.67 (0.29)	0.47 (0.00)	1.29 (0.65)	0.82 (0.03)	0.50	NA
MA 50-100 m	1.00	0.52	1.00	0.42	0.78 (0.17)	0.62 (0.06)	1.08 (0.80)	0.68 (0.21)	0.75 (0.35)	0.60 (0.00)	0.50	NA
MA 100-175 m	0.50	NA	0.50	NA	0.79 (0.25)	0.56 (0.14)	0.92 (0.52)	0.68 (0.03)	0.88 (0.18)	0.63 (0.04)	1.00	0.55
NE 12-50 m	0.50	NA	1.00	0.45	0.94 (0.23)	0.63 (0.03)	0.50 (0.00)	NA	0.63 (0.18)	0.45 (0.00)	0.50	NA
NE 50-100 m	1.00	0.45	1.00	0.51	0.93 (0.24)	0.62 (0.12)	0.50 (0.00)	NA	0.75 (0.35)	0.62 (0.00)	0.50	NA
NE 100-175 m	0.50	NA	0.50	NA	0.74 (0.09)	0.60 (0.09)	0.50 (0.00)	NA	0.58 (0.12)	0.54 (0.00)	0.50	NA

5. Broad scale spatial variation in zooplankton around the Svalbard archipelago

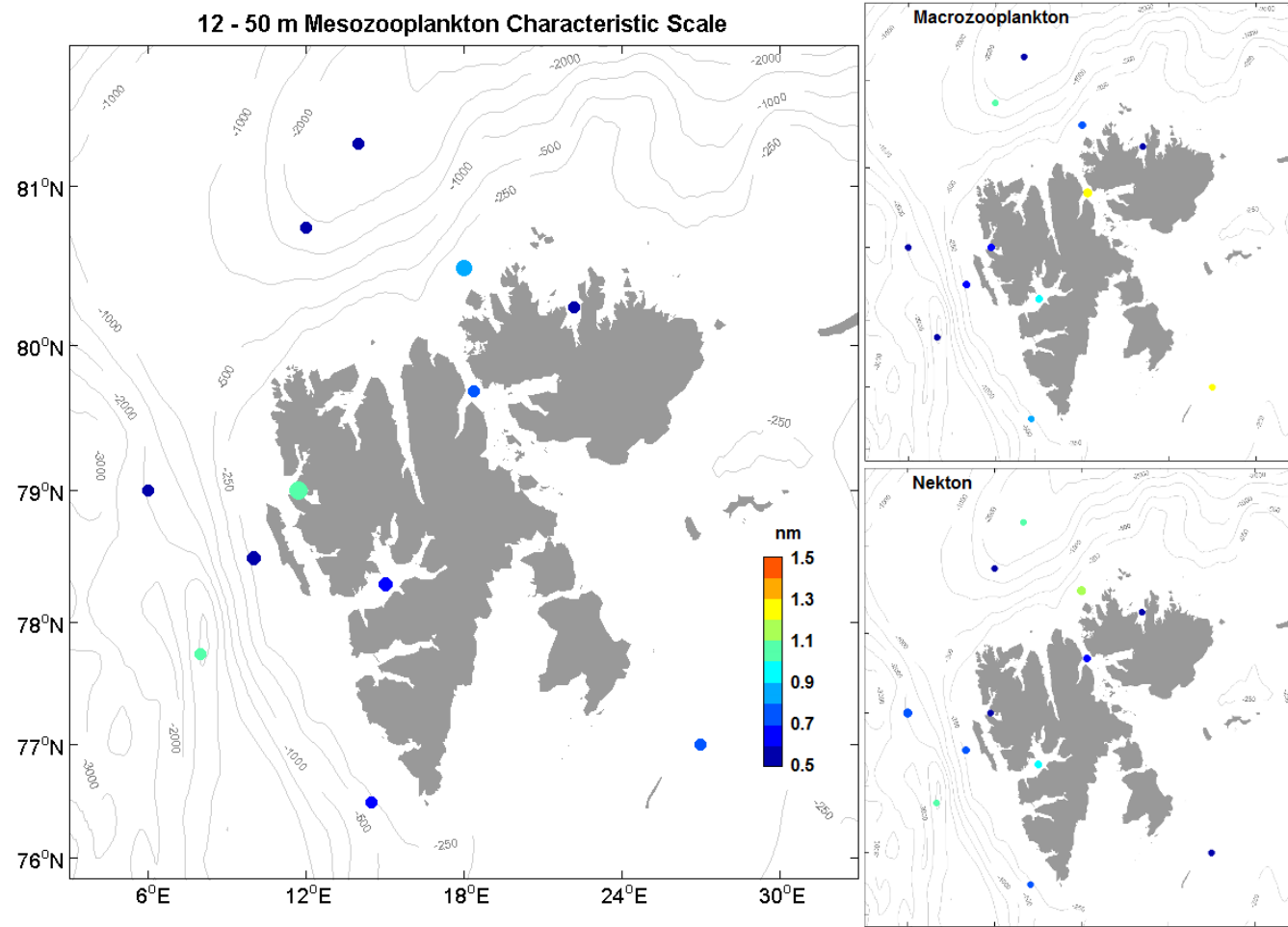


Fig 5.13) Map of the Svalbard archipelago displaying mean 12 – 50 m characteristic scale L_s (nm, 10 nm transects, 0.5 nm horizontal resolution) calculated at each sector for mesozooplankton (main), macrozooplankton (top right) and nekton (bottom right). Size of circle at each sector represents sd between years sampled i.e. the larger the circle, the greater the variation in L_s between years (detailed L_s in Table 5.4).

5.4. Discussion

5.4.1. Hydrodynamic control on zooplankton spatial distribution

It becomes apparent from our cluster analysis of both net and acoustically observed zooplankton that areas of similarity exist around the Svalbard archipelago, and this phenomenon has been well described (e.g. Daase and Eiane 2007; Blachowiak-Samolyk et al. 2008; Kwasniewski et al. 2010) although never with the coverage presented here. Chapter 4 of this thesis (on a smaller spatial scale) and numerous studies have linked plankton communities closely to hydrographic variability around the archipelago, and this pattern is to be expected throughout our broader scale investigation. We correlated the spatial variability in our higher resolution backscatter observations to spatial variability in SST (Table 5.3), and it was apparent from this analysis that the spatial range of observations in each year affected the relative correlations between backscatter and latitude or longitude, with 2007 displaying the highest correlation with longitude compared to latitude as hardly any latitudinal spread existed in the data set (Fig 5.7).

It was also apparent that with all taxa combined, correlations with latitude and longitude tended to be stronger than correlations with SST across all years, indicating further forcing factors were at work than simply SST (Table 5.3). Interestingly, the highest correlation with latitude occurred within the mesozooplankton in 2007, and it was apparent that latitude co-varied with sampling station depth (i.e. inner fjord, shelf and off-shelf locations at Kongsfjorden) during this year (Fig 5.7). The highest correlation with longitude was also recorded within the mesozooplankton during this year, and longitude co-varied to a greater extent along this depth gradient. The greater influence of this depth gradient on mesozooplankton vs. macrozooplankton or nekton is noteworthy, and indicates that smaller zooplankton were more closely associated with specific depths than larger animals. These gradients in community composition with depth were also observed at Kongsfjorden in 2008 (Fig 5.8), Rijpfjorden and

Kongsfjorden in 2009 (Fig 5.9) and Kongsfjorden and Isfjorden in 2010 (Fig 5.10). Deeper off shelf stations often clustered separately from shelf locations (e.g. light blue on Fig 5.8, red on Fig 5.9, numerous clusters on Fig 5.10). This phenomenon thus appeared to be fairly ubiquitous across years. Kwasniewski et al. (2010) reported that the separation of “fjord”, “shelf” and “open water” stations at Kongsfjorden was a manifestation of the ecological gradient between the inner fjord and open seas. This gradient is clearly highlighted in our study from a number of fjords, and was linked to specific species responsible via net sampling (Figs 5.3 – 5.5).

Within the correlations between backscatter and SST, the largest correlation across years was identified for nekton (mean of 0.223), while the lowest was identified for mesozooplankton. This result was surprising, as smaller plankton are known to be closely associated with water masses due to their inability to move against dominant currents (Pinel-Alloul 1995). Fish distributions are also well known to be linked to temperature (e.g. Brander et al. 2003). It is possible that our monthly average SST data at 4.6 km resolution did not contain the resolution required to properly explain changes in mesozooplankton, although the clustering of mesozooplankton backscatter (Figs 5.6 – 5.10 bottom right) generally displayed less spatial variation than the combined backscatter (i.e. fewer larger clusters). This indicates that macrozooplankton and nekton backscatter differed more between locations. Within the mesozooplankton backscatter, the highest correlation with SST was identified in 2008 (0.134), and this value increased marginally to 0.152 when only the 12 – 50 m depth layer was correlated to SST. This surface layer is most expected to vary with SST as temperatures and dominant water masses deeper in the water column may vary considerably from surface conditions.

Although surface temperature regimes were very similar between 2006 and 2007 in Isfjorden and just outside Kongsfjorden (Fig 5.11), higher intensities of mesozooplankton backscatter especially on the West Spitsbergen shelf were recorded in 2007 compared to 2006. This sector should also be most influenced by AtW advection. Thus it is likely that variations in advection between years at various depths (which will

not all be reflected by SST during the study period) caused the high interannual variation observed in this sector. It was also apparent during all years of sampling that SST inside Isfjorden and towards the inner fjord was considerably higher than on the shelf outside the fjord. AtW is known to penetrate and influence Isfjorden in a similar manner to Kongsfjorden (Nilsen et al. 2008), and alongside the warmer SST our study observed higher intensities of mesozooplankton backscatter within Isfjorden compared to the adjacent shelf (Figs 5.11 and 5.12), especially towards the innermost areas of the fjord. Macrozooplankton and nekton backscatter also followed this pattern especially in 2007 where highest intensities of nekton backscatter in particular were recorded within Isfjorden compared to all other sampled locations. In 2009, although SST was much lower compared to Isfjorden, mesozooplankton backscatter intensity was consistently high at the entrance to Hinlopen and further north at the shelf break beyond 81°N (Fig 5.12). This comparatively high backscatter at high latitude (with SST < 0°C) was also observed in 2010. The pattern of higher backscatter intensity at high latitude and low SST was only dominant in the mesozooplankton backscatter, and not noticeable in the nekton portion. These locations were sampled either within sea-ice or near the ice-edge (see Fig 1.9 for prevailing ice conditions), and were also close to or over the shelf break. These conditions are known to be highly productive due to intensive algal blooms (supported by the melting of sea-ice allowing light to penetrate the water column) and highly stratified surface waters keeping this bloom at the surface (Skjoldal and Rey 1989; Hegseth 1998; Falk-Petersen et al. 2000b; Søreide et al. 2003). Our study has recorded high mesozooplankton backscatter in particular at these locations.

High abundance of zooplankton (comparable to Kongsfjorden) within the Hinlopen strait has been documented before by Walkusz et al. (2003) in 2002. Their study hypothesised that this was due to some influence by AtW together with a highly dynamic system at Hinlopen with plenty of water mass mixing creating favourable conditions for zooplankton. Our study provides further evidence for this, with mesozooplankton backscatter intensity within Hinlopen reaching comparatively high levels in both 2008 and 2009 (Figs 5.11, 5.12). Our data from 2010 also showed that although SST was again comparatively low around Hopen to the southeast of the

archipelago, observed mesozooplankton backscatter intensity was relatively high (Fig 5.12). Net sampling at this location attributed this backscatter to ArW associated species such as *C. glacialis* (Fig 5.5), and this suggests that ArW dominated locations were not lower in zooplankton abundance.

5.4.2. Autocorrelation distances and implications for moored observations

Across all taxa and depths, the characteristic scale of autocorrelation (i.e. the distance within which observations were statistically autocorrelated to each other) determined using our 10 nm transects was shorter than 2 nm, and generally below 1 nm (Table 5.4). Within the important 12 – 50 m depth layer, this distance of similar observations within mesozooplankton backscatter was longest at Kongsfjorden and the off-shelf sector to the southwest of the archipelago (1 nm – Fig 5.13). Characteristic scale for macrozooplankton was longest at Hinlopen and around Hopen, two ArW dominated locations. However, the general conclusion is clear, and this is one of highly variable spatial distribution of zooplankton at 0.5 nm scale during summer. The transect plots of backscatter visually support this picture of high spatial variation around the archipelago at the 0.5 nm scale (Figs 5.11, 5.12). On this scale, our characteristic scales suggest observations by oceanic moorings can only be reliably extrapolated outwards by approximately 0.5 – 1 nm in any direction. This conclusion is supported by evidence from chapter 4 of this thesis. Our transect length of 10 nm however may be too short to properly assess spatial autocorrelation at varying scales, and we suggest further research cruises around the archipelago include dedicated multi-frequency acoustic sampling on lengthy transects designated to this purpose. Furthermore, an aggregation resolution of 0.5 nm may not be the most ecologically relevant scale of aggregation for zooplankton throughout the archipelago. However, as our transects were only 10 nm in length, using a larger scale resolution would have dramatically reduced the number of observations and made our estimates of L_s highly unreliable.

5. Broad scale spatial variation in zooplankton around the Svalbard archipelago

The mechanisms of sampling utilised by the moorings must also be considered when assessing their spatial relevance. As the moorings are fixed observation platforms within a dynamic environment influenced by advection (as described in chapters 3 and 4 of this thesis), the flow of water over the moored instruments will mean they sample more than just the volume of water directly above them over a period of time. The faster the horizontal currents, the greater the volume of water advected over the mooring and thus the larger the volume sampled by the sediment trap. In a patchy environment, currents may also bring zooplankton patches into contact with the mooring, increasing the chances that zooplankton are captured in the sediment trap. Monthly mean horizontal current velocities differed between mooring locations at Kongsfjorden and Rijpfjorden (Tables 1.2a – d). They varied between -69.5 and 52.2 mm/s at Kongsfjorden (with differences observed between the two positions in 2006/07 and 2008/09) and between -76.1 and 60.7 at Rijpfjorden. High standard deviations about these means also described a regime of variation amongst horizontal velocities. Thus although the range of monthly mean horizontal velocities appeared similar at the two locations, the currents at any particular point in time could be dramatically different between the mooring locations.

For example, hourly mean horizontal velocities described in chapter 4 of this thesis (Table 4.2) were highly variable over time and with changing depth. Northward velocities were far greater at Rijpfjorden in September 2009 (up to 10 times more for a particular depth) than Kongsfjorden in September 2009, while current velocities at Billefjorden in September 2008 were generally far lower than Kongsfjorden in September 2008. A steady current velocity of 100 mm/s through the water column will bring 18,000 m³ of water over a sediment trap (0.5 m² opening) located at 100 m depth every hour, meaning the fixed sediment trap is actually sampling a horizontal distance of 360 m. Due to the current, this is an extra 18 million litres of water passing over the sediment trap every hour. Although the sediment trap is not quantitatively sampling this volume, advection clearly influences the spatial relevance of moored observations. Although our characteristic scales suggest observations by oceanic moorings can only be reliably extrapolated outwards by approximately 0.5 – 1 nm, advection of water over

the mooring could increase this distance significantly through the duration of a sediment trap bottle. Our observed current velocities suggest that this effect will be greatest at Rijpfjorden (due to the greater observed range in horizontal current velocity at Rijpfjorden), and smallest at Billefjorden. Thus, the sediment trap at Rijpfjorden is likely to be representative of a wider area than at Billefjorden.

On a broader scale, important conclusions on how representative the moorings at Kongsfjorden and Rijpfjorden are can be drawn from this study. Based purely on net samples, the moored observations at Rijpfjorden appeared to be representative of the entire fjord and also the shelf northwards to the shelf break but not beyond it (Figs 5.3, 5.5). This area was also distinct from all other locations sampled. However, using combined backscatter observations, the outer and inner fjord appeared to be different during some years (Fig 5.9), while Rijpfjorden was now similar to large areas of the shelf to the north and west all the way to Smeerenburgfjorden (Figs 5.8, 5.9). Relatively high abundances of the AtW associated *C. finmarchicus* were also recorded both within Rijpfjorden and at the stations far to the north east (Fig 5.5), indicating the influence of AtW at latitudes well beyond 81°N.

Although the similar observed backscatter intensities could be due to different species of zooplankton associated with different dominant water masses, we suggest that evidence from this clustering as well as from net and sediment trap samples collected within Rijpfjorden in this thesis strongly support the influence of AtW at Rijpfjorden during summer in certain years although physical conditions remain largely indicative of Arctic dominance. Thus, if the aim of the mooring at Rijpfjorden is to act as an indicator for the northward reach of AtW, we argue it is already occurring at this location during summer. If however the aim of the mooring is to observe true year round Arctic conditions for comparison with Atlantic influenced locations, we suggest a better shelf area would be to the east of the archipelago free of the influence of AtW (e.g. somewhere on the east coast or around Hopen). Using combined backscatter we have shown the area around Hopen to cluster distinctly from all other locations and also

5. Broad scale spatial variation in zooplankton around the Svalbard archipelago

to contain higher proportional abundances of the ArW associated species *C. glacialis* with fewer of the small copepod *O. similis*. Clearly ice conditions at these latitudes will remain largely ice-free and be very different to Rijpfjorden and the Arctic basin to the north, but as a deeper water mooring to the north east of the archipelago is impractical due to ice cover and logistical difficulties, the shelf to the east and even south east of Rijpfjorden would be a better option for observing consistently Arctic conditions. The prevailing hydrographic regime around the Svalbard archipelago (Fig 1.4) indicates ArW dominance most strongly to the east of the archipelago compared to the north. However, our conclusions regarding Hopen are based on comparatively few observations during one year of sampling, and the location appears less distinct when only considering mesozooplankton backscatter. We suggest further sampling effort to the east of the archipelago to substantiate our claims.

Also, Billefjorden consistently clustered distinctly from Isfjorden, Kongsfjorden and also from Rijpfjorden using combined backscatter. Net sampling at Billefjorden displayed the highest proportional abundances of *C. glacialis* (as identified before in 2001/02 by Arnkvaern et al. 2005), so although this fjord is largely dominated by locally produced waters, the zooplankton community here is more likely to be consistently representative of year round Arctic conditions. We propose that this seasonally ice-covered fjord maintains the oceanic mooring most representative of Arctic conditions during the summer period sampled in this investigation. The previous chapters of this thesis have already documented that although the zooplankton community at Rijpfjorden remains strongly indicative of ArW conditions through much of the year, the summer influence of AtW is noteworthy and more marked than at Billefjorden. SAMS and NPI have maintained a mooring at Billefjorden in 2008/09 and 2010/11, and results from these deployments are expected soon. However, our net samples from Billefjorden and Rijpfjorden did not include the larger macrozooplankton species that were identified in sediment trap samples (chapter 3) and high intensity macrozooplankton backscatter (chapter 4) at Rijpfjorden. Thus although Billefjorden may be more 'Arctic' in terms of its *Calanus* and other copepods, it may not be so in terms of its macrozooplankton.

The location of the mooring at Kongsfjorden changed considerably between deployments and varied from the centre of the fjord to the very entrance and just outside (see <http://martech.sams.ac.uk/arctictimeseries/> for details). We suggest that this change in position of the mooring can have a significant influence on which zooplankton community it observes. Although net samples throughout the length of Kongsfjorden and the close adjacent shelf largely clustered together at a broad scale, higher resolution acoustic observations that include more taxa did not. Observations from 2007, 2009 and 2010 (Figs 5.7, 5.9, 5.10) illustrate this particularly well with an inner-fjord – outer-fjord – shelf – off-shelf gradient present in the clustering. A strong ecological gradient at Kongsfjorden has also been documented before by Hop et al. (2002) and Kwasniewski et al (2003). Thus a movement of the mooring between years within the fjord may place it within a different zooplankton community and make comparisons between years more difficult. Furthermore, the relationship between backscatter within Kongsfjorden and backscatter on the adjacent shelf varies between years. Backscatter within Kongsfjorden however largely clusters separately to the adjacent shelf. Thus, the zooplankton community within Kongsfjorden has been observed to be distinct to the community on the adjacent shelf (within a regime of variation), and so the mooring is observing a unique zooplankton community that cannot be assumed to be the same as the community outside.

5.4.3. Conclusion

At a scale of 0.5 nautical miles during summer, zooplankton distribution was highly variable around the Svalbard archipelago and moored observations could only be reliably extrapolated outwards to a maximum of 1 nautical mile. On a broader scale, Billefjorden was most distinct from all other locations and could be considered most representative of Arctic mesozooplankton during summer. Backscatter in Kongsfjorden was largely unique from observations on the adjacent shelf and was subject to a gradient along the fjords length. This relationship between fjord and adjacent shelf was highly

5. Broad scale spatial variation in zooplankton around the Svalbard archipelago

variable between years. During certain years, combined backscatter at Kongsfjorden in summer was similar to that recorded at Rijpfjorden. Generally, mesozooplankton backscatter observations contained less broad scale variation than combined backscatter observations, indicating mesozooplankton distribution was more similar across the archipelago than macrozooplankton and nekton.

6. Seasonal and diel vertical migration of zooplankton at Svalbard¹

¹The work described in this chapter has been published as: Rabindranath, A., Daase, M., Falk-Petersen S., Wold, A., Wallace, M.I., Berge J., Brierley, A.S., 2011. Seasonal and diel vertical migration of zooplankton in the High Arctic during the autumn midnight sun of 2008. *Marine Biodiversity*. 41, 365-382.

I estimate I contributed 70 % of the total effort toward this paper. Net abundances (raw) were supplied to me by the Norwegian Polar Institute, and acoustic data (raw) by M.I. Wallace. CTD data (processed) were supplied to me by SAMS. Net and acoustic data processing (from raw data) and all analysis were conducted by myself, although assistance was received with net sample processing from NPI. 90 % of the effort towards figure creation was mine, and all writing was done by myself with inputs from all authors.

6.1. Introduction

The depth distribution of *Calanus* in colder regions is characterised by strong seasonality and linked closely to the annual cycle of primary production (Vinogradov, 1997). Copepods are found in shallow waters during the productive summer months and in deeper waters during winter (Varpe et al., 2007). The widely accepted paradigm of polar marine biology is that the seasonal changes in sea-ice cover have a dramatic influence on ecosystem processes (Cisewski et al., 2009; Søreide et al., 2010; Leu et al., 2011). For much of the year in seasonally ice covered areas such as the high Arctic, most of the primary production occurs in the overlying sea-ice and not in the water column (Arrigo & Thomas, 2004), and ice cover is known to have a significant negative effect on phytoplankton primary production in the Arctic (Gosselin et al., 1997). However, as the sea-ice melts, phytoplankton production peaks in summer and autumn and is accompanied by peak abundances of *Calanus* close to the surface (Smith & Sakshaug, 1990; Falk-Petersen et al., 2008, 2009). The phytoplankton bloom follows the receding ice edge as it melts during spring/summer (Zenkevitch, 1963; Sakshaug &

Slagstad, 1991), and the onset of the Arctic phytoplankton bloom varies widely in the Svalbard region due to large differences in prevailing sea-ice conditions (Søreide et al., 2008).

Along the western coast of Svalbard, where the influence of ice is diminished by the dominance of warmer Atlantic Water ($> 3^{\circ}\text{C}$), the phytoplankton bloom starts in April/May (Leu et al., 2006). In contrast, the phytoplankton bloom in northern and eastern Svalbard is strongly influenced by the reduction in light levels beneath sea-ice cover, and the bloom onset may be delayed until the sea-ice thins sufficiently to permit illumination, which may occur as late as August (Falk-Petersen et al., 2000; Hegseth & Sundfjord, 2008). When primary production decreases following the phytoplankton bloom, copepods descend to depth and overwinter in a state of dormancy (Heath et al., 2004), during which time they survive on large lipid reserves accumulated during the summer (Conover & Huntley, 1991; Hagen & Auel, 2001). Whether *Calanus* ascend later in areas with heavier sea-ice cover due to a delay in the Arctic bloom is largely unknown, although Falk-Petersen et al. (2009) and Søreide et al (2010) suggest that the seasonal ascent of *Calanus glacialis* is timed with the Arctic bloom, and that ice algae may be as important as phytoplankton in terms of a food source for copepods in ice covered seas (Søreide et al., 2006). Hunt et al (2002) suggest that in ice covered waters, an early ice retreat in late winter (when there is insufficient light to support a bloom) will delay the phytoplankton bloom until late spring when the water column is stratified sufficiently to prevent the algae sinking. In contrast, a later ice retreat in spring (when there is sufficient light to support a bloom), allows an earlier ice associated bloom to develop in 'ice-melt-stabilised' water (Hunt et al., 2002).

Whilst populations migrate on a large scale seasonally, individuals also migrate on a daily basis. The vertical migration of copepods is considered to be an effective strategy for coping with variations in food availability and predation risk throughout the water column (Longhurst, 1976). DVM is considered less important at high latitudes than seasonal migration patterns (Kosobokova, 1978; Longhurst et al., 1984; Falkenhaug et

al., 1997). Previous studies of zooplankton in Arctic regions have largely failed to demonstrate any coordinated vertical migration during the period of midnight sun, when there is little variability in insolation throughout the diel cycle, or during the winter period in the high Arctic due to low food availability in the water column (see 1.3.3. for details). In recent years however, a variety of acoustic instruments and techniques have been used to identify vertical migrations in high Arctic zooplankton both during summer and winter (see 1.3.3 for details). A better understanding of zooplankton vertical migration throughout the annual cycle is of critical importance in the context of carbon flux in the oceans. Diel migrants ingest organic material in near-surface waters and produce faecal pellets at depth (Cisewski et al., 2009). This process has the potential to contribute considerably to the vertical transport of carbon and nutrients (Longhurst et al., 1990; Longhurst & Williams, 1992; Wexels Riser et al., 2002; Sampei et al., 2004). Disruption of zooplankton vertical migration in the Arctic by ice melt for example will thus have important consequences.

The aim of this study was to integrate net sampling and acoustic measurements at a number of locations reflecting a variety of Arctic environments from early to post bloom, and observe copepod seasonal and diel migration patterns. Depth stratified net sampling was used to identify the migrants, while simultaneous multi-frequency acoustic sampling permitted identification of migration patterns at a high temporal and vertical resolution. Six stations across a large spatial area north and west of the Svalbard archipelago were sampled, enabling the observation of various intensities of the high Arctic bloom. This permitted the assessment of zooplankton vertical migration behaviour in the context of the influences of difference water masses (i.e. Atlantic and Arctic dominated locations) and variability in the intensity of primary productivity. 200 kHz acoustic observations were also available during this study compared to 120 kHz throughout the rest of this thesis, and this higher frequency will generate higher proportional backscatter from small zooplankton but only be effective at shorted ranges.

6.2. Materials and methods

6.2.1. Sampling location

The study was undertaken during the period of midnight sun, 2 – 20 Aug 2008, aboard the ice strengthened British Antarctic Survey (National Environment Research Council) research vessel “*RRS James Clark Ross*” [Cruise JR210]. Samples were collected at six stations around Svalbard (Table 6.1, Fig 6.1). See 1.3.1 for detailed Svalbard hydrology.

Table 6.1) Sampling station details including start date and time, station location and maximum water depth

Station	Start Date	Start Time (UTC)	Latitude (N)	Longitude (E)	Depth (m)	MPS depth strata	MPS sampling time (day; night)
Rijpfjorden (RF)	14/08/2008	20:58	80.285	22.304	225	210-175, 175-100, 100-50, 50-20, 20-0	09:30;20:45
Ice (ICE)	06/08/2008	09:14	80.812	19.218	138	100-50, 50-20, 20-0	14:00;23:00
Marginal Ice Zone (MIZ)	08/08/2008	21:43	80.347	16.269	386	375-200, 200-100, 100-50, 50-20, 20-0	12:00;22:00
Shelf break (SHB)	12/08/2008	08:45	80.487	11.307	753	740-600, 600-200, 200-100, 100-50, 50-0	16:30;22:30
Shelf (SH)	02/08/2008	14:19	79.725	8.833	449	370-200, 200-100, 100-50, 50-20, 20-0	15:00;23:00
Kongsfjorden (KF)	18/08/2008	17:58	78.960	11.890	345	320-200, 200-100, 100-50, 50-20, 20-0	06:00;21:00

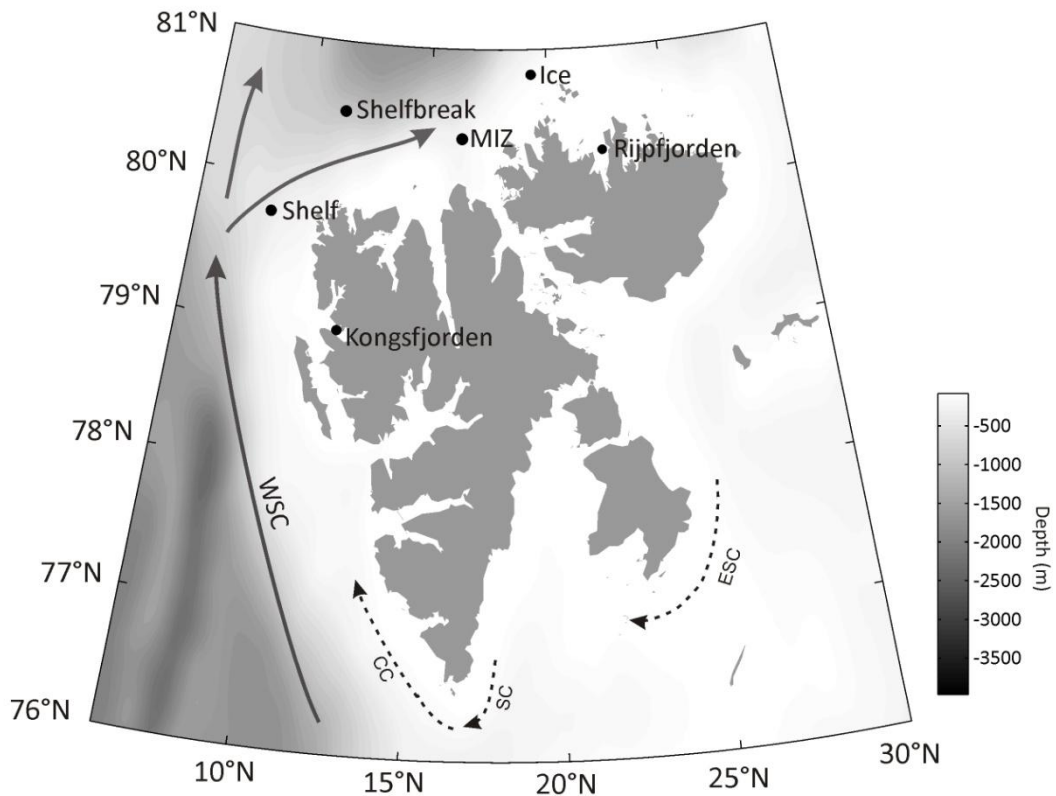


Fig 6.1) Sampling station locations and current systems North and West of Svalbard. Solid arrows indicate warm water currents, dotted arrows cold water currents. ESC = East Spitsbergen Current, SC = South Cape Current, CC = Coastal Current, WSC = West Spitsbergen Current (see 1.3.1. for details).

6.2.2. Environmental parameters

The positions of the sea-ice edge were extracted from sea-ice maps produced by NPI (Fig 6.2). Photosynthetically Active Radiation (PAR, 400 to 700 nm) was measured at the surface at all stations (Fig 6.3) using a cosine-corrected flat-head sensor (Quantum Li-190 SA, LiCor, USA). Salinity, temperature, depth and fluorescence were measured by Seabird CTD and processed following standard Sea Bird Electronics (SBE) data processing procedures by SAMS. CTD profiles measuring temperature, salinity and fluorescence were undertaken immediately prior to all zooplankton sampling events.

6.2.3. Zooplankton sampling

Mesozooplankton samples were collected at each station as close to local midday and midnight as possible using a Multi Plankton Sampler (MPS, Hydrobios, Kiel) (detailed in Table 6.1). The depths of each sequential net were chosen at each station in order to allow comparable surface (i.e. 0-100 m) resolution while still sampling the entire water column. This procedure was undertaken twice for each sampling event. Filtered water volume was calculated using deployed wire length and the net mouth dimensions, assuming 100% filtration efficiency.

All samples were fixed in 4% formaldehyde and analysed for species composition post cruise as per Falk-Petersen et al. (1999). *Calanus* species were distinguished on the basis of prosome length (Unstad & Tande, 1991; Kwasniewski et al., 2003) and staged from C1-adult. *Calanus* biomass was determined from the collected net abundance data by calculating an average dry weight (DW) value using a collection of published methods (Mumm, 1991; Hirche, 1991; Richter, 1994; Hirche, 1997) and published species-specific mass-length relationships (Karnovsky et al., 2003).

6.2.4. Acoustic observations

A hull mounted Simrad EK60 downward facing echosounder operating at frequencies of 38, 120 and 200 kHz and a ping rate of 0.5 pings s⁻¹ was used to gather backscatter information from the water column (12 m depth to near sea bed). At all stations, the ship remained stationary for approximately 24 hours while EK60 data were collected, thereby spanning the midday and midnight net sampling regimes. Only data from the upper 125 m of the water column were used due to range limitations at 200 kHz, and the near field at 38 kHz (12 m) was also excluded from analysis (see 2.3. for calibration and noise removal details).

We sought to compare data from net samples collected at midday and midnight with acoustic sample data. In order to do this, acoustic data were chosen from each 24 hour station to match the zooplankton net sampling times as closely as possible. Whenever possible, two hours of acoustic data were used to calculate a mean volume backscattering strength ($MVBS = 10 \log_{10} [\text{mean}(S_v)]$), and in no cases was less than one hour of data used. 120 kHz – 38 kHz MVBS partitions into mesozooplankton, macrozooplankton and nekton echoes were carried out using a 1 m x 60 ping grid (Benoit et al., 2008) over the entire acoustic sampling period as per Madureira et al. (1993) (see 2.3. for details).

$\Delta MVBS$ values were used to partition 200 kHz data from equivalent cells into these three classes. 200 kHz was chosen as it returns proportionally stronger backscatter from the small *Calanus* zooplankton targeted in this study. Echo integration was then carried out for each taxon using a 25 m x 20 min grid. Nautical Area Scattering Coefficient (NASC = scaled area scattering [$4\pi(1852)^2 s_a$]) values were extracted from the echo integration grids (25 m x 20 min), as these provide linear representations of zooplankton backscatter.

Although $\Delta MVBS$ differentiations were carried out using a 60 ping x 1 m depth grid to generate accurate backscatter partitions, the echo integration resolutions were made coarser (25 m x 20 min). This coarser resolution was chosen after inspection of the acoustic data revealed that any DVM signal would be of low amplitude and easily ‘masked’ amongst a large number of echo integrations over a very fine scale.

6.2.5. Multivariate analysis

Similarity matrices created in PRIMER were used to test for differences between the stations based on (1) hydrography, (2) *Calanus* community composition, and (3) zooplankton vertical distributions.

(1) 10 m averages of temperature, salinity and fluorescence were calculated over the upper 150 m at each station and then normalised (ranges converted to numerical values with a mean average of zero and standard deviation of one) in order to summarise the hydrographic conditions. These data were then compared using a Euclidean distance similarity matrix and presented using a hierarchical cluster dendrogram (Fig 6.4).

(2) Fourth root transformed MPS determined zooplankton abundances were compared between stations using a Bray-Curtis similarity matrix. The differences between day and night depth stratified communities, and also between different depth strata at each station were quantified using Analysis of Similarity (ANOSIM). Similarity Percentage (SIMPER) analysis was carried out to determine which species were most responsible for the observed differences in community structure between day and night samples and different depths in terms of percentage contribution (see 2.4 for equations and details of these methods).

(3) The partitioned 200 kHz backscatter (mesozooplankton/macrozooplankton/nekton) data were standardised using a fourth root transformation and compared between stations using a Bray-Curtis similarity matrix. The differences between day and night samples and between stations were quantified using ANOSIM and displayed using a Multi-Dimensional Scaling plot (MDS – Fig 6.8). The mesozooplankton, macrozooplankton and nekton were also analysed individually between stations to highlight any differences between the different taxa (Fig 6.9).

In order to distinguish between advection and vertical migration effects within the *Calanus* community, the net-determined depth stratified abundances were modified and compared. Firstly, the abundances of all three *Calanus* copepods and *Metridia longa* were summed together at each depth stratum, yielding one value for each depth that represented all the copepods combined. This maintained the depth stratification of the data, but lost all community diversity. The transformed abundance data by this first method shall be referred to subsequently as Depth Stratified Total Abundance.

Differences between the day and night samples using this method can be attributed primarily to changing numbers of copepods at each depth stratum. These changes are likely to be good indicators of vertical migration amongst the copepod populations.

Secondly, in order to compare vertical migration effects with possible advection effects, the abundances of each stage of *Calanus* and *Metridia longa* were integrated over the entire water column at each station, resulting in one value for each copepod stage that represented the entire water column depth. This maintained the community diversity within the data, but lost the depth stratification. The transformed abundance data by this second method shall be referred to as Water Column Community Diversity. Differences between the day and night samples using this method will not be a result of changes in vertical position, but rather changing numbers of individuals at the station. This method can be used to assess the advection of copepods in or out of the population.

6.2.6. ANOVA analysis

The partitioned 200 kHz backscatter (mesozooplankton/macrozooplankton/nekton) data were also compared using ANOVA statistical analyses. Firstly, the partitioned backscatter was separated into five depth strata (0 – 25 m, 25 – 50 m, 50 – 75 m, 75 – 100 m, and 100 – 125 m). Each depth stratum was then analysed using a three way ANOVA test, with station, taxa and time being the three factors tested for significance. Secondly, all depth strata were combined and the backscatter was analysed using a four way ANOVA test – with station, taxa, time, and depth now the four factors tested for

significance. This allowed the influence of the four primary variables to be ranked and tested for significance.

6.3. Results

6.3.1. Ice cover

In June 2008 (prior to our study), most of the Svalbard coast had landfast ice. This ice cover continued around the southern tip of Svalbard and only parts of the west coast were ice free. However, by the time of our study (August 2008), most of this ice cover had broken up and Kongsfjorden (KF) and the Shelf station (SH) were ice-free. In contrast, the Marginal Ice Zone (MIZ) and Shelf break (SHB) stations were sampled in areas of large leads and broken ice cover, whilst in Rijpfjorden (RF) the fast ice broke up the day before sampling. Ice concentration at the northernmost station, Ice Station (ICE, Fig 6.2), was 0.95 at the time of sampling. Continued sea-ice melting and breakup led to large areas north of Svalbard being ice free by October 2008.

6. Seasonal and diel vertical migration of zooplankton at Svalbard

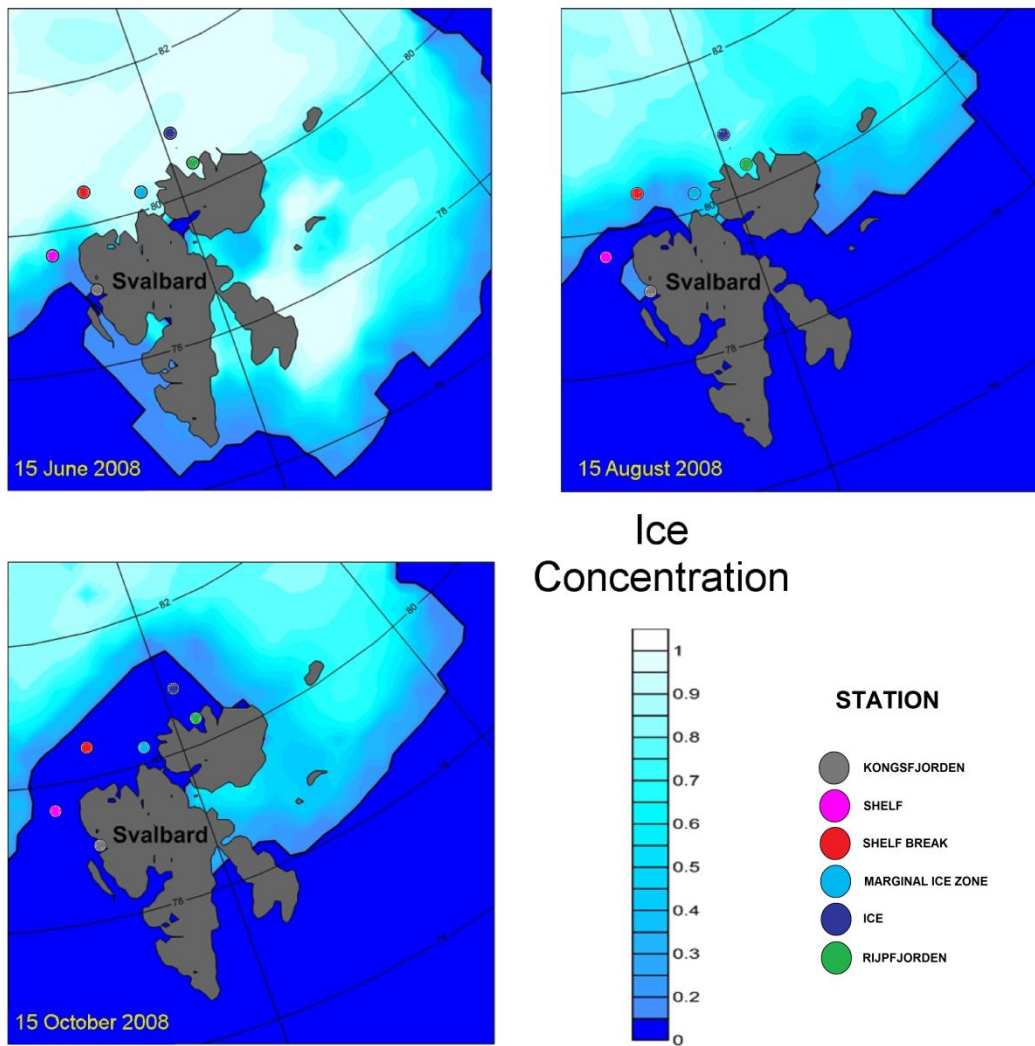


Fig 6.2) Ice maps from the Svalbard region (courtesy of NPI) between 15 June and 15 October 2008.

6.3.2. Environmental conditions

Although this study occurred during the period of midnight sun in the High Arctic, a diurnal PAR cycle was observed at all stations (Fig 6.3), with daily insolation ranges of 1.2 to 1243 $\mu\text{Em}^{-2}\text{s}^{-1}$. Variability between successive days at the same sampling location was also observed: for example, ICE day one (06 Aug) experienced a range of 92.9 to 543.5 $\mu\text{Em}^{-2}\text{s}^{-1}$, while ICE day two (07 Aug) experienced a range of 70.4 to 1159.8 $\mu\text{Em}^{-2}\text{s}^{-1}$.

6. Seasonal and diel vertical migration of zooplankton at Svalbard

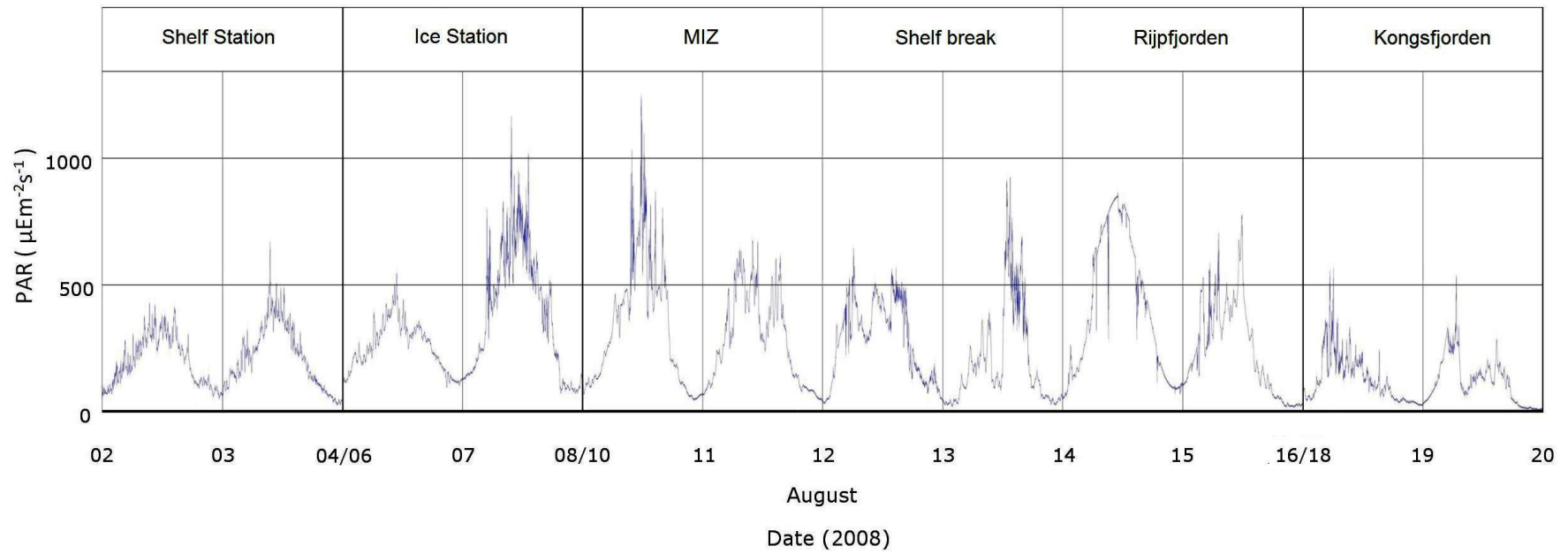


Fig 6.3) Surface Photosynthetically Active Radiation (PAR, 400 to 700 nm) sampled from the vessel deck at all stations. Stations run in chronological order starting on 02 August 2008 (SH) and ending at 20 August 2008 (KF).

Relatively fresh (salinity of 32 to 33) and cold (-2 to 0 °C) water was found over approximately the upper 10 m at ICE, MIZ, SHB, and RF (Fig 6.5). However, at MIZ and SHB, water temperatures of 4 to 4.5 °C and higher salinities of around 34 to 35 were observed between 25 and 30 m depth. Temperatures at RF never exceeded 0 °C, while ICE reached approximately 1 °C at approximately 100 m depth. A pronounced fluorescence maximum was observed at all four of these ice-influenced stations, corresponding to the boundary between surface MW and deeper AtW/ArW. The precise depth of this fluorescence maximum differed between the ice-influenced stations, but all were found between 20 and 40 m depth. The maximum was most pronounced at ICE and RF, which experienced the most recent sea-ice cover.

SH was dominated by AtW, with temperatures in excess of 6 °C and salinities as high as approximately 35 at the surface. A pronounced fluorescence maximum was observed here too. KF was ice-free all year. Although glacial MW influenced the fjord, temperatures and salinities indicated AtW dominance. The fluorescence maximum at this station was less pronounced than at the other stations, and this location also experienced only minor changes in light intensity during the diel light cycle compared with the rest of the study area (Fig 6.3, 6.5).

Cluster analysis comparing the stations in terms of temperature, salinity and fluorescence resulted in RF and KF being most extreme in terms of their physical characteristics and the other stations falling between them (Fig 6.4).

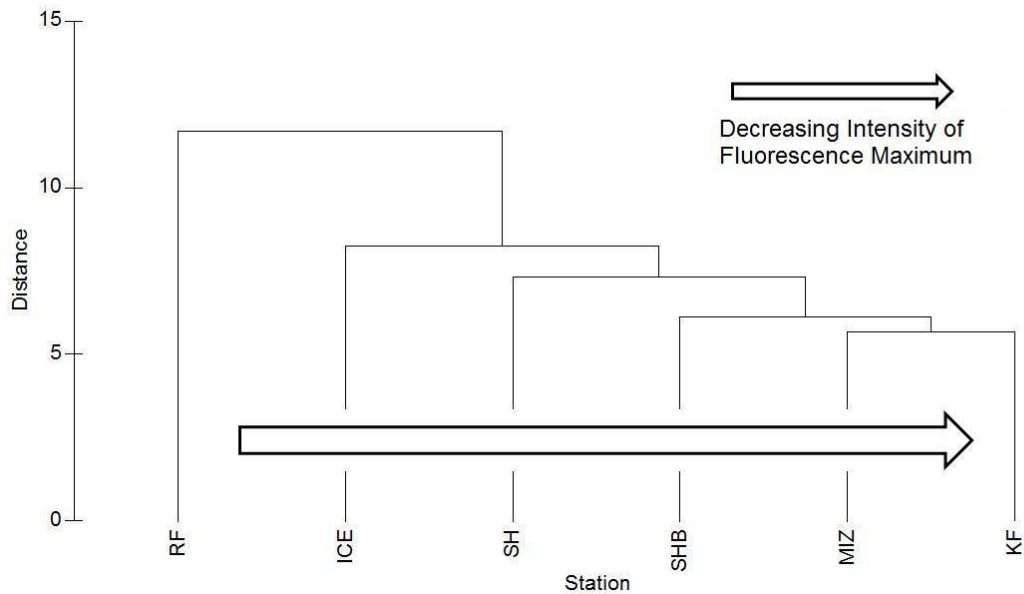


Fig 6.4) Dendrogram displaying the Euclidean distance grouping between normalised (ranges converted to numerical values with a mean average of zero and standard deviation of one) CTD data (10 m averages of temperature, salinity and fluorescence calculated over the top 150 m at each station) at each of the six stations.

6.3.3. Copepod populations and vertical distribution

At RF and ICE, young stages (CI-CIII) of *C. finmarchicus* and *C. glacialis* dominated the upper 50 m (> 70% of total 0 to 50 m abundance). *C. hyperboreus* was primarily found as CIV copepodites between 20 to 50 m depth (2.7 to 7.1 ind m⁻³). *M. longa* was found in comparatively low abundances (≤ 2.6 ind m⁻³) and only at depths below 50 m at RF and below 20 m at the ICE. The population at both stations was dominated by CV copepodites and adults. RF and ICE displayed the lowest abundances of *C. finmarchicus* (≤ 187.3 ind m⁻³, Fig 6.5). Higher abundances of *C. finmarchicus* CI-CIII (117 ind m⁻³), *C. glacialis* CV (40 ind m⁻³) and CIV (20 ind m⁻³) were found between 0-20 m during the day than at night at RF, while *M. longa* adults were found in higher abundance (1.9 ind m⁻³) towards the surface (20-50 m) at night at ICE.

At SH, *C. finmarchicus* dominated ($> 5000 \text{ ind m}^{-3}$), and its population was composed almost entirely of CI-CIII copepodites. Higher abundances were found towards the surface (0 to 20 m) at night (4920 ind m^{-3} at night compared to 2076 ind m^{-3} during the day). Here, *C. hyperboreus* was rare, and a *C. glacialis* population dominated by CV copepodites was found between 0 to 50 m in comparatively low abundance ($\leq 24 \text{ ind m}^{-3}$). *M. longa* was found in comparatively high numbers ($> 15 \text{ ind m}^{-3}$) and across all stages (CI – adult), and this *M. longa* population was found almost entirely below 100 m.

At the deeper SHB, a bimodal depth distribution was observed for all the copepod populations. *C. finmarchicus* dominated in higher abundances than at RF, ICE and MIZ (in excess of 500 ind m^{-3}) (Fig 6.5). A younger population composed primarily of CI-CIII copepodites was found between 50 to 200 m ($> 90\%$ of total 50 to 200 m abundance). In addition, an older population composed almost entirely of CV and adults was found at depths below 600 m. The *C. glacialis* and *C. hyperboreus* populations were found in low abundances at SHB (under 20 ind m^{-3}), but again displayed a bimodal depth distribution with the older stages at depth. *M. longa* was found in its highest abundances (in excess of 75 ind m^{-3}), and almost entirely below 600 m. This *M. longa* population was of mostly early stage animals, being composed $> 50\%$ of CI-CIII copepodites.

At MIZ, *C. finmarchicus* and *C. hyperboreus* were more abundant than *C. glacialis* and *M. longa*, although abundances were similar to those at RF and ICE. The *C. finmarchicus* population at MIZ was dominated by the older copepodites (CV) and adults ($> 65\%$ *C. finmarchicus* abundance), and was located primarily below 100 m. The *C. glacialis* population at MIZ was also dominated by CV ($> 90\%$ *C. glacialis* abundance) and located below 100 m. More *C. finmarchicus* and *C. glacialis* individuals were found between 100 to 200 m during the night, and between 200 to 300 m during the day. The *C. hyperboreus* population here was composed more of CV

copepodites and adults, and was located below 200 m. *M. longa* was found in high abundances (in excess of 70 ind m⁻³) and predominantly below 200 m.

In KF, bimodal depth distributions (as at SHB) were observed among the copepods (Fig 6.5). Again, *C. finmarchicus* dominated in terms of abundance (up to 1966 ind m⁻³). The *C. finmarchicus* population above 50 m represented > 90% of the total *C. finmarchicus* abundance, and was composed mainly of CI-CIII copepodites. The population at depth was older, and composed almost entirely of CV copepodites. In KF, *C. glacialis* was found in its highest abundance, (up to 473 ind m⁻³). *C. glacialis* also displayed a bimodal depth distribution, but the two populations were similar in terms of abundance. The surface population (0 to 50 m depth) was composed almost entirely of CV copepodites, while the deeper population below 100 m was younger and composed of approximately 50% CIV copepodites alongside the CV stages. *C. hyperboreus* was also found here in comparatively high numbers, and almost entirely below 100 m. The *C. hyperboreus* stage composition was similar to *C. glacialis*, with CIV and CV dominating. *M. longa* had fairly high abundances in KF (in excess of 40 ind m⁻³), and > 70% of the population was located between 100 to 200 m; with considerably lower abundance (5.9 ind m⁻³) at 200 to 300 m depth. The differences between day and night abundances were highest at KF, with considerably more copepods present in the day samples.

6. Seasonal and diel vertical migration of zooplankton at Svalbard

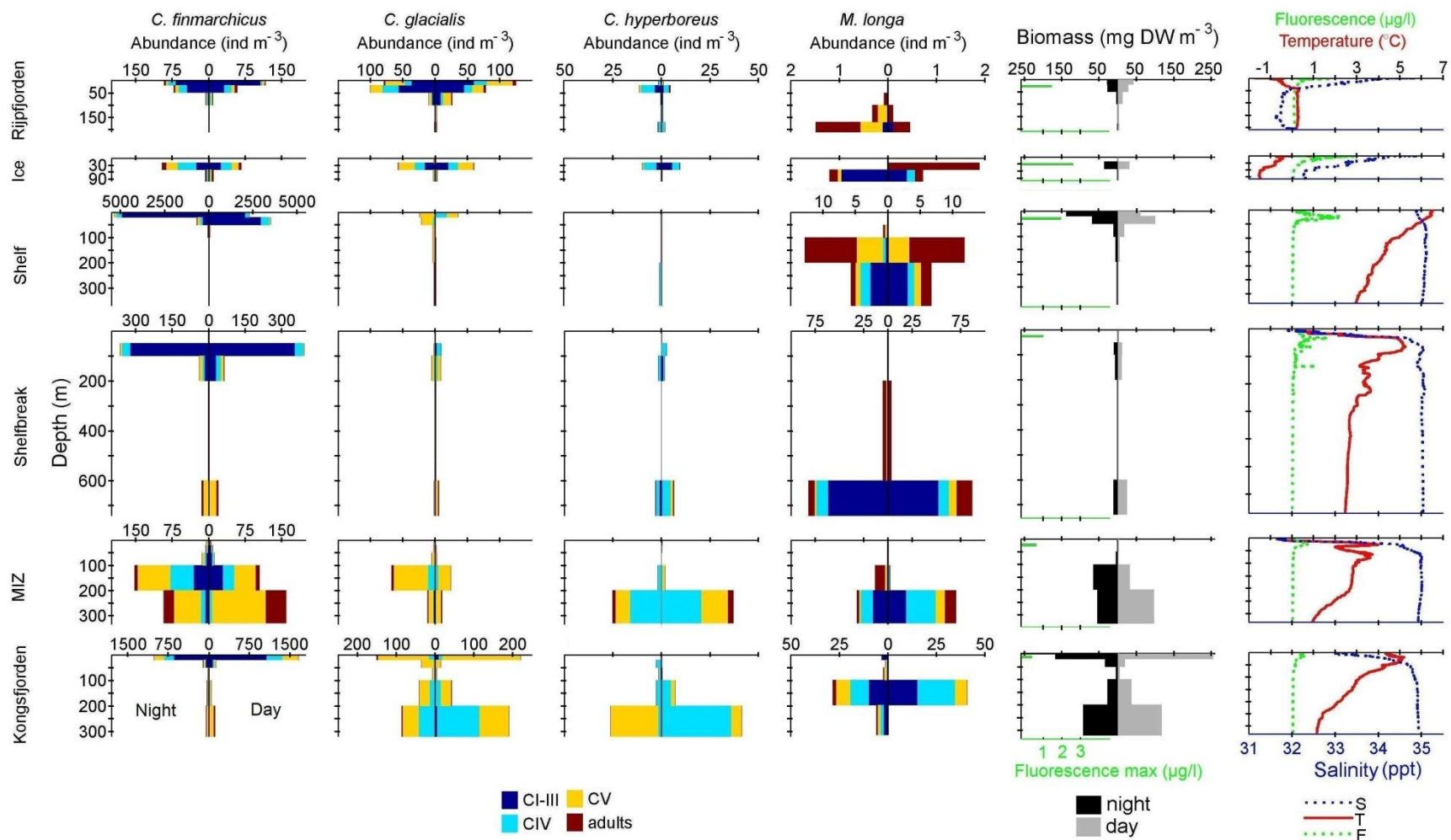


Fig 6.5) Vertical profiles of *C. finmarchicus*, *C. glacialis*, *C. hyperboreus* and *M. longa* (individuals m^{-3}), *Calanus* biomass ($mg DW m^{-3}$), salinity, temperature ($^{\circ}C$), and fluorescence ($\mu g l^{-1}$). Day samples are on the right axis of each plot, while night samples are on the left axis. The depth and intensity of the fluorescence maximum at each station is displayed on the biomass plots.

6.3.4. Vertical distribution of *Calanus* biomass

Converting the *Calanus* abundances to biomass revealed considerably more biomass at shallow depths during the night than during the day at MIZ and SH (Fig 6.5). In RF, more biomass was observed close to the surface during the day than at night. At MIZ, SHB and KF, most of the biomass was located below 200 m, while at RF, SH and ICE, most biomass was found in the upper 50 m.

6.3.5. Multivariate analysis of net samples

When the MPS determined abundances were compared between stations using a Bray-Curtis similarity matrix and one way ANOSIM, significant differences were found between the depth stratified communities at each station ($R = 0.129$, $p = 0.001$), and between the depth strata at each station ($R = 0.224$, $p = 0.001$). SIMPER identified *C. finmarchicus* CI-CIII and *C. glacialis* CV as being most responsible for the differences in community between stations, while *C. finmarchicus* CI-CIII was most responsible for the differences between surface waters and deeper depths and *M. longa* CIII and CV were most responsible for the differences between 50 to 200 m and ≥ 200 m. Using these data, no significant difference was found between day and night samples ($R = -0.022$, $p = 0.829$). Although the day and night samples were not significantly different to each other, SIMPER identified *C. finmarchicus* CI-CIII as being responsible for 25.31% of the differences between the day and night samples. Two way ANOSIM analysis using station and time as the chosen factors resulted in no significant differences between stations ($R = 0.042$, $p = 0.192$) or day and night samples ($R = -0.146$, $p = 0.995$).

Cluster analysis and ANOSIM of Depth Stratified Total Abundance showed significant differences between the stations ($R = 1$, $p = 0.002$), but high levels of similarity at all stations between the day and night samples taken at the same station ($R = -0.164$, $p =$

0.952) (Fig 6.6a). The highest similarities between day and night samples were found at ICE and SHB (> 95% similar), and the lowest similarity at SH (< 90% similar). When Depth Stratified Total Abundance was compared between stations, the ICE and RF were 75% similar, SHB and MIZ were > 80% similar, and KF and SH were also > 80% similar. SIMPER identified the 0 to 20 m depth strata as being most responsible (30%) for the differences between the day and night samples.

Cluster analysis and ANOSIM of the Water Column Community Diversity at each station again showed significant differences between the stations ($R = 1$, $p = 0.002$), but less similarity between the day and night samples compared with the Depth Stratified Total Abundance (Fig 6.6b). The difference however was very small ($R = -0.154$, $p = 0.922$). The highest similarity between day and night samples was found at SH and SHB (> 90% similar), and the lowest similarity at ICE (< 90% similar).

6. Seasonal and diel vertical migration of zooplankton at Svalbard

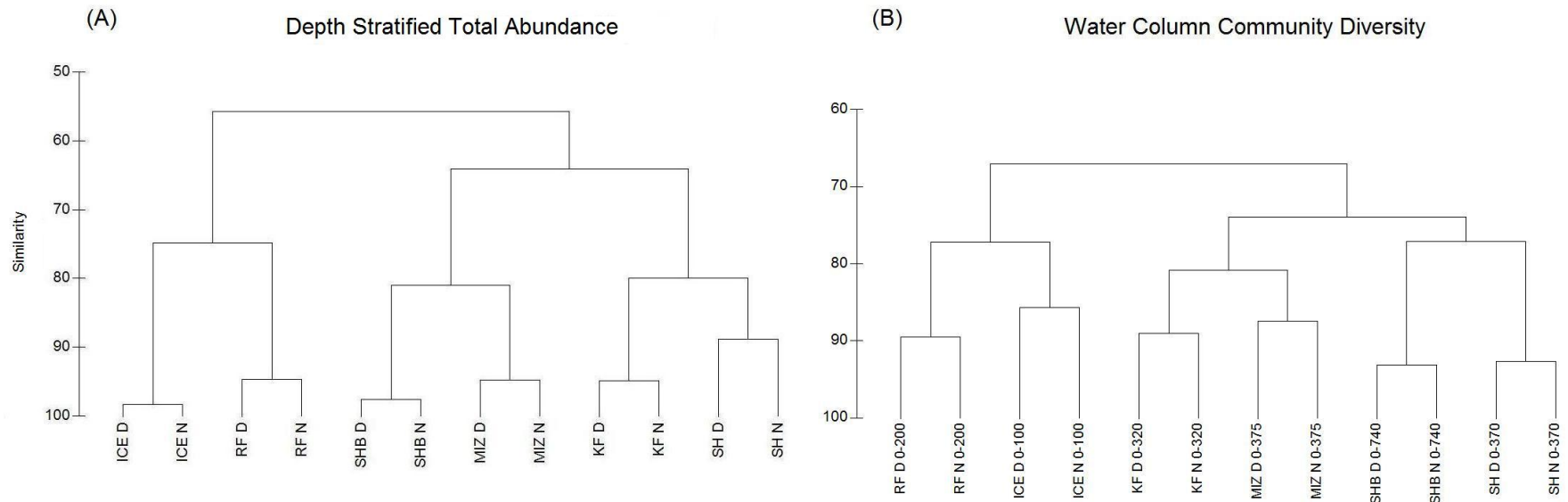


Fig 6.6 a & b) Hierarchical cluster dendrograms based on Bray Curtis similarity analysis on 4th root transformed net abundance data. Similarity scale on cluster dendrograms represents percentage similarity between samples. D = Day sample, N = Night sample. (A) [**Depth Stratified Total Abundance**] displays similarities between day and night samples at each station in terms of *Calanus* and *M. longa* abundance at each depth stratum. (B) [**Water Column Community Diversity**] displays similarities between day and night samples at each station in terms of the abundance of every *Calanus* and *M. longa* stage integrated over the entire water column. The water column depths over which abundances are integrated are displayed on the dendrogram.

6.3.6. Acoustic observations

Across all six stations, MVBS (S_v) was generally low (Fig 6.7).

At RF, the 200 kHz data displayed low S_v values (-133 to -51 dB) throughout the upper 125 m during the day, with a scattering layer at approximately 0 – 85 m and a mean S_v of -80.68 dB. A scattering layer of higher mean S_v (-71.2 dB) was identified between 0 to 30 m during the night. This surface scattering layer at night appeared to be primarily composed of mesozooplankton and macrozooplankton, but also contained some nekton echoes (Fig 6.7). At ICE, a similar pattern was observed but with higher S_v (-130 to -39 dB) and two backscattering layers: one between 0 to 80 m (-75 dB) during the day and 0 to 30 m (-68 dB) at night, the other near the bottom below 120 m (-88 dB) during the day and below 100 m (-81 dB) at night. Backscatter attributable to nekton was observed between 50 – 110 m during both the day and night, and appeared to be present mainly below the surface scattering layer. Mesozooplankton backscatter was found primarily in the two scattering layers during the day, and was more evenly spread throughout 0 – 125 m at night. Smaller mesozooplankton (Δ MVBS > 20 dB) echoes were more prevalent within the surface scattering layer at night compared to the day. Echoes attributable to macrozooplankton (Δ MVBS of 2 to 12 dB) were found in both layers during the day and night, but at higher S_v (-79 to -77 dB) in the upper layer (Fig 6.7).

At SH, the echograms were characterised by the lowest S_v of any station. However, a generally diffuse distribution of backscatter during the day became more concentrated between 0 to 30 m at night. Though much of the backscatter deeper than 50 m during the day and night was attributed to mesozooplankton, the surface scattering layer appeared to be due to nekton during the day (Fig 6.7), with more macrozooplankton and mesozooplankton backscatter towards the surface at night. At SHB, increased S_v below 100 m was observed at night (-87 to -76 dB at night compared with -99 to -81 dB during the day), and this was largely attributed to mesozooplankton. A patchy scattering layer was observed between 0 to 100 m during the day, and this scattering layer appears to be

mostly due to macrozooplankton aggregations. Backscatter attributable to nekton was found between 0 – 125 m during both the day and night, but was most prevalent in a surface scattering layer between 0 – 50 m.

At MIZ, the day echogram was characterised by lower S_v (-89 to -78 dB) compared with the night echogram, with patches during the day being attributed more to macrozooplankton and mesozooplankton rather than nekton, and no clear scattering layer in the upper 125 m. However, S_v increased considerably at night in a similar manner to SHB, especially below 100 m (-81 to -72 dB) and in a surface scattering layer. This increase in backscatter below 100 m at night was largely attributed to mesozooplankton (Fig 6.7). Echoes attributable to nekton were far more prevalent during the night than the day, especially between 0 -75 m in a mixed scattering layer with macrozooplankton. At KF, a dense scattering layer of high S_v (-50 to -55 dB) was located below 100 m during the day. This backscatter was not attributed to nekton alone (as the $\Delta MVBS$ is primarily > 2 dB), and seemed to indicate a mixed layer of macrozooplankton and nekton. Amphipod backscatter should fall within this range, and the dense aggregation may have been composed of amphipods. A mesozooplankton scattering layer was also found at the same depth. However, at night, the dense high S_v scattering layer disappeared almost completely, and a scattering layer dominated by mesozooplankton remained. This layer was found below 50 m depth, with a higher $\Delta MVBS$ (> 20 dB) indicating smaller mesozooplankton between 25 – 60 m and echoes mainly attributable to macrozooplankton between 0 -20 m (Fig 6.7).

6. Seasonal and diel vertical migration of zooplankton at Svalbard

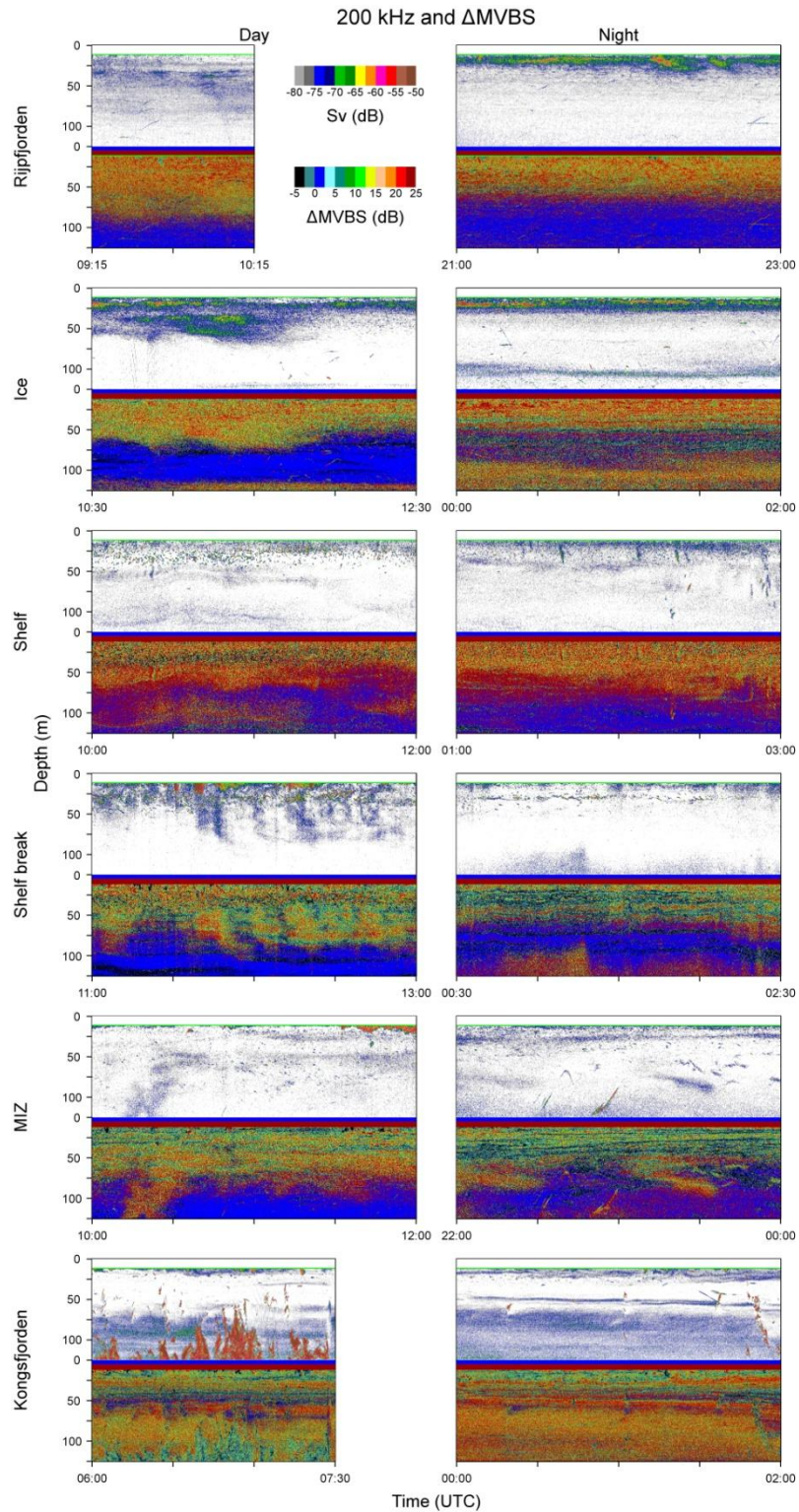


Fig 6.7) 200 kHz backscatter (above) and Δ MVBS (below) from each of the six stations [0 – 125 m depth]. Volume backscatter (S_v) is expressed using a colour scale between -80 and -50 decibels (dB). Δ MVBS is expressed using a colour scale between -5 and 25 dB. The top 11 m of each echogram are discarded due to near-field and noise (i.e. white in the 200 kHz echogram and dark blue/red solid stripe on the Δ MVBS display). Δ MVBS echoes with yellow-red shades represent stronger scattering at 120 kHz, while Δ MVBS echoes with grey-black shades represent stronger scattering at 38 kHz. Day echograms are displayed on the left and night echograms on the right.

6.3.7. Multivariate analysis of acoustic observations

When the partitioned fourth root transformed 200 kHz acoustic backscatter (25 m x 20 min grid, $n = 1020$) were compared between all sampled stations using a Bray-Curtis similarity matrix and one way ANOSIM, significant differences were found between stations ($R = 0.15$, $p = 0.001$) but not between day and night samples ($R = 0.019$, $p = 0.151$). This difference between depth stratified stations is similar to the difference found using the net determined abundance data. However, when using a two way ANOSIM with Station and Time as the chosen factors, significant differences were found between the depth stratified backscatter at each station ($R = 0.277$, $p = 0.001$), and also between the day and night samples ($R = 0.136$, $p = 0.044$). Significant differences were also found between the three classes of backscatter (mesozooplankton, macrozooplankton, nekton) at all stations using a one way ANOSIM ($R = 0.055$, $p = 0.018$). The partitioned 200 kHz acoustic data are displayed as a MDS plot (Fig 6.8A). Night mesozooplankton backscatter from RF, SH and KF along with night macrozooplankton backscatter from KF were the four outlying samples, with all other data being closely clustered. All six stations appeared to cluster with similar distances between samples, although RF (Fig 6.8B) and KF (Fig 6.8G) appeared to display the clearest and widest day/night separation.

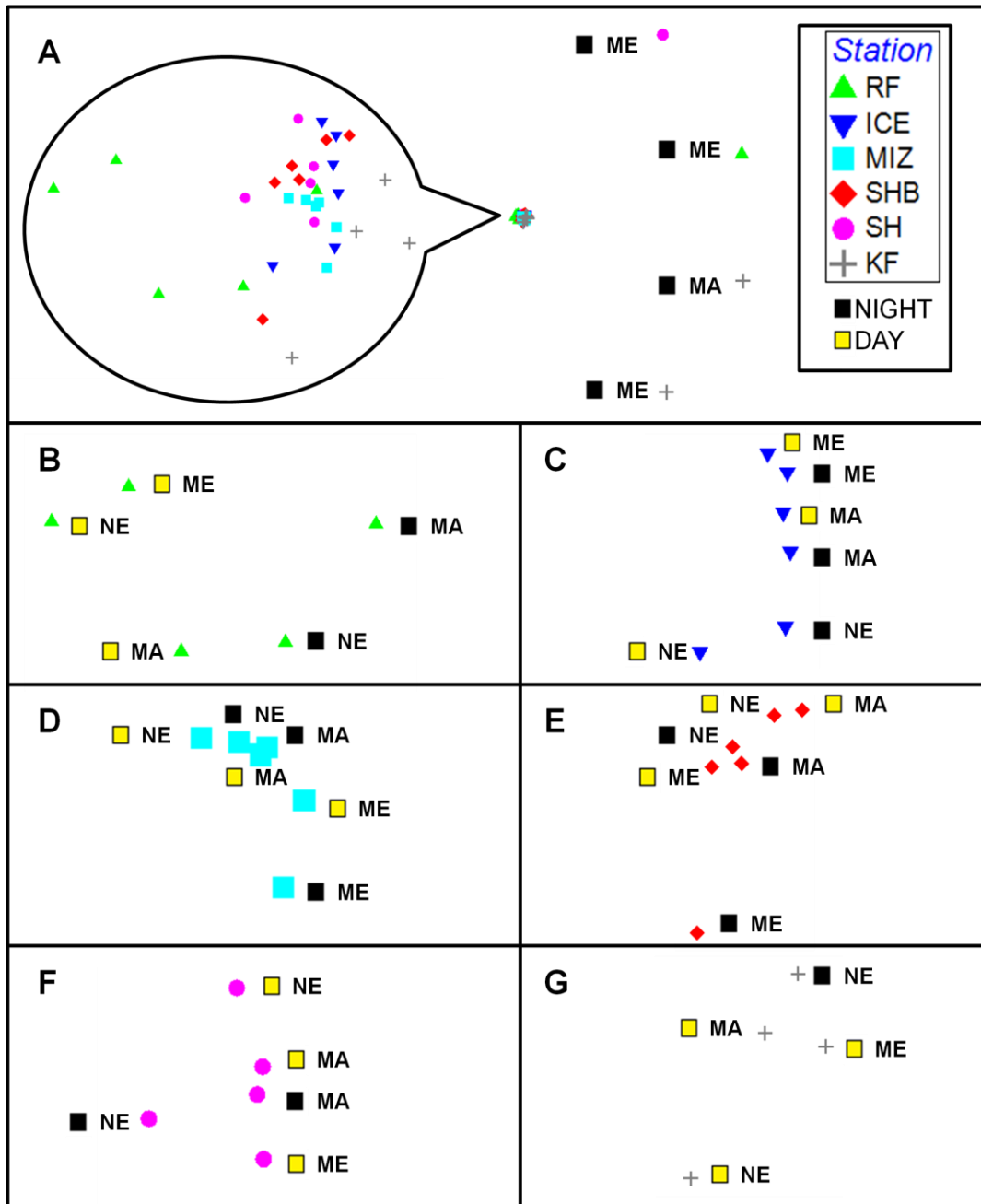


Fig 6.8) A = Multi Dimensional Scaling (MDS) Plot based on Bray Curtis Similarity analysis on fourth root transformed depth stratified acoustic data collected at 200 kHz at all stations (60 ping x 1 m grid – 0 – 125 m, n = 1020). Each station displays 6 points on the MDS plot – one each for mesozooplankton (ME), macrozooplankton (MA), and nekton (NE) during both the day (x3) and night (x3). Distances between points on the MDS represent similarity, with closer points being more similar. Stations and Day/Night symbols are indicated on the legend. Inset represents x 9 zoom on the close cluster in A. B (RF), C (ICE), D (MIZ), E (SHB), F (SH), and G (KF) are all expanded versions of A inset and display individual stations for clarity.

When the three different size groups were separated and analysed individually between stations, the resulting MDS plots (Fig 6.9) confirmed RF and KF as most different in terms of their day and night acoustic data across all three classes of partitioned backscatter. RF and KF also displayed much greater distances between day and night backscatter at the macrozooplankton partition compared with the other stations (Fig 6.9B), indicating that changes in macrozooplankton between day and night were of highest magnitude at these two stations. MIZ day and night data appeared to be most closely clustered and showed the least day/night differences of all stations. SH macrozooplankton (Fig 6.9B) and nekton (Fig 6.9C) day and night backscatter were relatively closely clustered, but the mesozooplankton (Fig 6.9A) backscatter were not, indicating that mesozooplankton day/night differences were greater compared with the other stations and were therefore most important at SH. All p values were not significant during this analysis, although they indicated that day/night backscatter differences were largest for mesozooplankton and smallest for nekton.

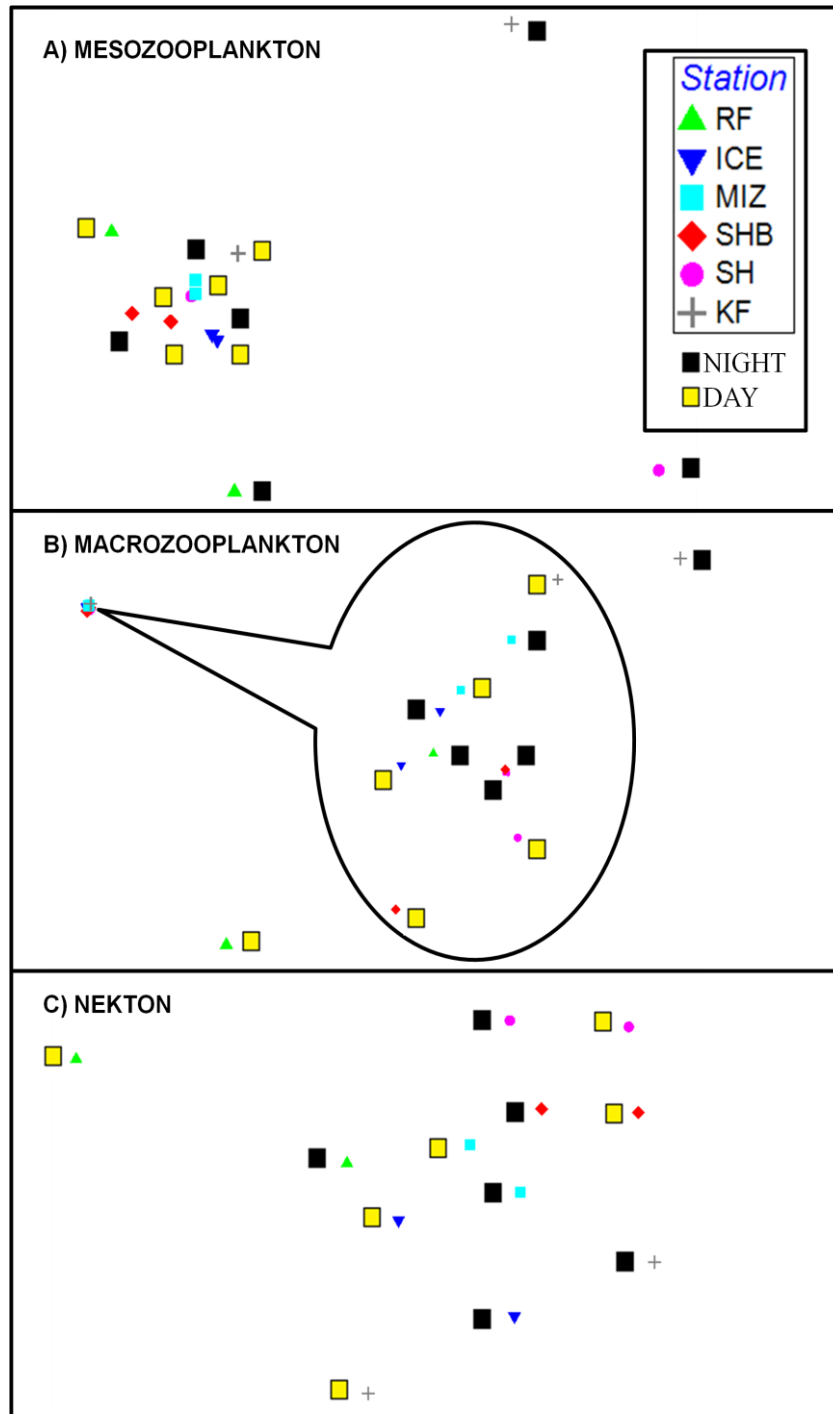


Fig 6.9) Multi Dimensional Scaling (MDS) Plots based on Bray Curtis Similarity analysis on fourth root transformed depth stratified acoustic data collected at 200 kHz at all stations (60 ping x 1 m grid – 0 – 125 m, n = 1020). Acoustic data is split at each station based on Δ MVBS into A) Mesozooplankton (top), B) Macrozooplankton (centre), and C) Nekton (bottom) backscatter. Each station displays 2 points on each MDS plot – one for day and one for night backscatter. Distances between points on the MDS represent similarity, with closer points being more similar. Inset represents x 10 zoom on the close cluster in B). Stations and Day/Night symbols are indicated on the legend.

6.3.8. ANOVA of acoustic observations

When the partitioned fourth root transformed 200 kHz acoustic backscatter ($n = 1020$) data were examined using a four way ANOVA with station, taxa, time, and depth being the four tested factors, the only factor that exhibited significant influence was depth ($F = 2.7996$, $p = 0.02496$). However, when the other factors were ranked, time was the next most influential factor ($F = 2.5674$, $p = 0.10940$), followed by size ($F = 1.2213$, $p = 0.29529$) and station ($F = 1.0580$, $p = 0.38223$). In order to better resolve the differences between day and night measurements, depth was removed as an influencing factor by carrying out three way ANOVA tests on individual depth strata (with station, taxa, and time now the only tested factors). These tests highlighted station as a significant influencing factor at 25 – 50 m, 50 – 75 m, and 75 – 100 m ($4.2506 < F < 11.0649$, $2.149e-9 < p < 0.001085$). The different taxa were never found to be a significant influencing factor on the differences in backscatter. However, time was a significant influencing factor at 25 – 50 m depth ($F = 6.1926$, $p = 0.013666$) and at 75 – 100 m depth ($F = 3.3836$, $p = 0.06737$). At 25 – 50 m, time was the strongest influencing factor on backscatter. Time was also the strongest influencing factor at 100 – 125 m, but the result was not significant ($F = 2.5918$, $p = 0.1090$).

6.4. Discussion

6.4.1. Seasonal ‘snapshot’

The occurrence and timing of the High Arctic phytoplankton bloom is an important phenomenon (Zenkevitch, 1963; Falk-Petersen et al., 2007; Søreide et al., 2008), and the bloom is shortest at higher latitudes. *Calanus* leave their over-wintering hibernations at depth and resume feeding at the surface in order to take advantage of the brief bloom in high latitude primary production (Hagen, 1999; Hagen & Auel, 2001; Lee et al.,

2006; Søreide et al., 2010), although the specific environmental signal that triggers the ascent from dormancy is unknown (Miller et al., 1991; Hirche, 1996). This bloom period, which is habitually accompanied by higher intensities of light penetration in the water column, is associated with copepod DVM behaviour due to the trade-off between the need to feed at the surface and the need to escape visual predation by moving to depth. Although the six stations in our study were sampled at approximately the same time, they can be placed on a seasonal scale regarding their respective fluorescence maxima, and a clear seasonal pattern in the depth distribution and stage composition of the *Calanus* species can be observed.

ICE and RF can be considered ‘spring’ stations in terms of their physical characteristics. At both of these stations, a noticeable fluorescence maximum was present at 25 to 30 m depth corresponding to the boundary between surface MW and deeper AtW/ArW. Of all our sites, these stations were most recently dominated by ice cover (Fig 6.2), and at RF in particular the ice cover had disappeared a day prior to sampling, which is consistent with the pronounced stratification and characterised an early bloom. Fluorescence data recorded by the mooring in Rjippfjorden indicated that the peak of the Arctic bloom had occurred very recently at this location (Wallace et al., 2010). Consequently, the *C. finmarchicus* and *C. glacialis* populations consisted predominantly of young stages concentrated in the upper 50 m, indicating that these stages were still actively feeding. Leu et al. (2011) described how the pelagic Arctic bloom in Rjippfjorden took place under the ice, just days/weeks before the ice break up, and that the first feeding stages of *C. glacialis* nauplii and copepodites were feeding actively on this phytoplankton bloom.

SH was influenced primarily by AtW and a pronounced fluorescence maximum existed there also (Fig 6.5), indicating that bloom conditions prevailed at this location. As at RF and ICE, the mean depth of *C. finmarchicus* at SH was shallower than 50 m. However, *C. glacialis* and *C. hyperboreus* were concentrated below 100 m and up to 300 m depth at this location. The abundances of these species were very low at SH and SHB, as these

areas were outside their dominant areas of distribution (Daase & Eiane, 2007; Blachowiak-Samolyk et al., 2008).

MIZ displayed a less pronounced fluorescence maximum, and a similarly low intensity fluorescence maximum was observed at SHB. The conditions at the two stations sampled in areas of broken sea-ice cover and large leads indicated either that the Arctic bloom had not yet occurred due to insufficient ice break up and light penetration into the water column, or that the annual season had progressed further at this location despite the relative closeness to the ice edge. The latter seems more likely due to the large leads present at the two stations. *C. finmarchicus* was concentrated considerably deeper here than at RF, ICE and SH (CI-CIII at 150 m and CIV-Adults at 225 m) suggesting that the season had progressed far enough to prompt a descent to over-wintering depth. The *C. glacialis* and *C. hyperboreus* populations at MIZ and SHB followed a similar distribution that was deeper than their respective distributions at RF, ICE and SH. The pattern of seasonal vertical migration we observed, with copepods being found closer to the surface during the bloom and at depth (over-wintering) once the bloom had retreated with the ice edge (Wassmann et al., 2006) was in agreement with the widely documented seasonal regime in the High Arctic (Falk-Petersen et al., 2007, 2009; Varpe et al., 2007).

KF had a low fluorescence maximum at the time of sampling and, in terms of physical characteristics, can be considered the 'furthest' from High Arctic spring conditions. Fluorescence data recorded by the mooring in Kongsfjorden confirmed that the peak of the spring bloom had occurred 2 to 3 months prior to sampling (Wallace et al., 2010).

At SHB and KF, a bimodal *Calanus* depth distribution was observed. *C. finmarchicus* CI-CIV were found primarily at the surface (0 to 75 m), while CV and adults dominated at depth (below 600 m at SHB and below 200 m at KF). This distribution indicated continued feeding at the surface from the younger copepodites, and a need to build lipid

reserves even 2 to 3 months after the spring bloom. It is possible to infer that primary production and the food supply available to copepods was more plentiful at MIZ than at SHB and KF, as even the younger stages of *C. finmarchicus* at MIZ had retreated to depth, having presumably built up sufficient lipid reserves during the bloom. Furthermore, the respective depth distributions of copepods implied that the phytoplankton bloom was earlier at MIZ than at SHB, as more copepods are found over-wintering at depth. This inference is supported by the 'seasonal' cluster dendrogram (Fig 6.4), which places MIZ closer to KF and thus further from spring bloom conditions.

The 'seasonal' separation of the sampling locations was reflected in the cluster dendrogram based on temperature, salinity and fluorescence data at each station (Fig 6.4). However, dominant water mass characteristics at each station may have also played a key role in this clustering, with RF and ICE being heavily influenced by ArW (water temperature never exceeding 1 °C), while all other stations appeared to be influenced by AtW (water temperatures of 4 °C recorded). Heavy influence by AtW at KF is the primary factor keeping this fjord ice-free all year, thereby modifying the timing of the annual seasonal progression in the High Arctic.

6.4.2. Copepod DVM behaviour

Much of the debate surrounding the presence or absence of DVM amongst copepods revolves around both the seasonal variability and the mode of the behaviour. No conclusive evidence of synchronised DVM has been found using traditional depth stratified net sampling alone during the period of midnight sun (May) in the High Arctic (Blachowiak-Samolyk et al., 2006) and in early autumn (September) (Daase et al., 2008). However, substantial evidence of synchronised DVM during the autumn period (September) with a pronounced diel light cycle has been obtained using acoustic observation techniques alongside net sampling (Falk-Petersen et al. 2008). During the transitional period from summer to autumn, Cottier et al. (2006) determined that the

period from July to September is the transitional period for a shift from unsynchronised vertical migration behaviour during midnight sun to a more classical synchronised DVM during autumn. However, that study used ADCP data primarily and was thus unable to identify the migrants involved. Our study falls within this transitional period, and a diel cycle was apparent at all stations in the PAR data. As our study was earlier in autumn than Falk-Petersen et al. (2008) (August 2 – 20 compared with September 2 – 9), we had the opportunity to study the transitional period at an earlier phase, and the broad spatial coverage of our six sampling locations allowed the comparison of sites with different phytoplankton bloom conditions during this period.

The MPS data indicated a classic DVM pattern at MIZ and SH, and reverse DVM signals in the abundances at RF (*C. finmarchicus* and *C. glacialis*) (Fig 6.5) and ICE (*M. longa*). This apparent reverse DVM appeared to be strongest at RF, as suggested by the biomass distribution (Fig 6.5). It is important to note that a combination of classic and reverse DVM will be difficult to detect amongst the acoustic backscatter, as the signals will effectively cancel one another out. Importantly, these observed differences in MPS abundance between the day and night samples were not statistically significant at any station, and the day and night samples were found to be very similar in terms of their total abundance at each depth stratum (Fig 6.6a). SH day and night samples were most different from one another, and SIMPER analysis identified 0 to 20 m as being the depth stratum most responsible (30%) for the difference. The greatest change in abundance between the day and night samples at this depth was by *C. finmarchicus*. These observations indicate that *C. finmarchicus* may be the dominant vertical migrator in and out of the surface 20 m.

The day and night samples from each station were less similar in terms of their community diversity at each station regardless of depth distribution (Fig 6.6b), suggesting advective influences between day and night samples were stronger than vertical migration effects. However, the differences were very slight and not statistically significant. ICE day and night samples were most different from one another,

suggesting that advection was more important at this location. Conversely, SH displayed the highest similarity between day and night community composition, but the lowest similarity in terms of copepod depth distribution, suggesting vertical migration was a stronger influence here.

Regardless of the day and night differences, copepod community depth distributions seemed to be grouped primarily by the dominant water masses influencing the stations (Fig 6.6a). ICE and RF were 75% similar (ArW dominance); SHB and MIZ were > 80% similar (transformed AtW dominance); and KF and SH were also > 80% similar (AtW dominance). This result suggests that the different depth preferences between species that dominate in AtW (*C. finmarchicus*) and the species that dominate in ArW (*C. hyperboreus*) (Blachowiak-Samolyk et al., 2008) played a key role in copepod depth distribution.

Although ‘indications’ of zooplankton DVM behaviour were gathered from the net-determined depth stratified abundances, no significant differences were found between the day and night samples ($-0.165 < R < -0.022$). However, the 200 kHz acoustic measurements were made at higher vertical and temporal resolutions than the net samples, with 25 m depth resolution and six repeats every 20 minutes analysed. The 25 m depth resolution chosen ultimately provides better vertical resolution than the MPS system, and so is more effective at identifying smaller scale vertical signals.

Multivariate analysis of these acoustic measurements resulted in significant differences between day and night backscatter across all stations, and using ANOVA allowed us to describe at which depths these day and night differences were significant. Although ANOVA described depth as being the strongest influencing factor on backscatter, time (day and night) was a significant influencing factor at 25 – 50 m and at 75 – 100 m.

KF and RF displayed the greatest differences between their day and night backscatter (Fig 6.8). When these differences were compared with the advection vs. vertical

migration technique applied to the MPS samples (Fig 6.6), it appeared that the differences could be in part due to advection. However, given that the largest contrasts between day and night MPS abundances were observed at KF (Fig 6.5). It appears that this station is more likely than RF to be influenced by strong advection. This apparent advection signal is further complicated by the phenomenon of zooplankton distribution being very patchy in the marine ecosystem (Gallager et al., 1996). The previous chapters of this thesis have highlighted the patchiness around Svalbard. As the research vessel was drifting while on station, day and night MPS samples may have been taken in different ‘patches’ of zooplankton. This sampling problem is partially addressed by using acoustic data collected continuously over a two hour period.

As the acoustic measurements were made at higher spatial and temporal resolutions than the MPS abundance data, the MPS data cannot be used effectively to inform the acoustic results. Unfortunately, only two MPS hauls (one day and one night) were available from each station. The day and night net hauls were also taken at different times of the day and night between stations (Table 6.1). This lack of directly comparable repeat data casts doubts over the results gathered from the MPS alone. However, these doubts can be addressed effectively by utilising the corroborating acoustic data, and this study illustrates how the two sampling methods can be used effectively in future studies, especially with repeated net sampling regimes.

Furthermore, acoustic targets outside the copepods studied here may be responsible for much of the acoustic DVM signal. These targets may be pteropods such as *Limacina helicina*, or pelagic amphipods such as *Themisto libellula* (Falk-Petersen et al., 2008) that are known to occur in high densities. At lower latitudes, pteropods are known to cause strong backscattering layers and to migrate vertically in diel cycles (Tarling et al., 2001), and these should be considered for future study. Notably, the MPS zooplankton net is not designed to catch fast swimming species like *T. libellula*. Our 200 kHz acoustic data contained backscatter contributions from both macrozooplankton and nekton (Fig 6.7). The differences between day and night measurements of

macrozooplankton in particular is strongest at RF and KF compared to the other stations, and this apparent macrozooplankton vertical migration could be largely responsible for the observed acoustic DVM signals at these two stations. However, multivariate analysis results showed that mesozooplankton backscatter had the greatest day/night differences overall across all the stations, making this taxa the most widespread vertical migrators across the study area.

Calanus populations feeding in near-surface waters appeared to undertake classic DVM to a greater extent than *Calanus* populations that were no longer influenced by a pronounced fluorescence maximum. Both the acoustic and net data displayed a shallow water DVM signal at RF, ICE and SH where a large portion of the population were still utilising the phytoplankton production at the surface. Thus the copepods were located closer to the surface, and behaviour such as classic DVM that protects them from visual predation is a useful adaptation. *C. finmarchicus*, especially the younger stages (CI-CIII), appears to be most responsible for the differences between the sampled depths at all stations and also for the observed difference between the day and night samples (and *C. glacialis* CV to a lesser extent). This observation is in contrast to other studies that found the young developmental stages to be more stationary and confined to surface waters, while older stages displayed DVM behaviour (Tande, 1988; Dale & Kaartvedt, 2000; Daase et al., 2008). However, these observed differences among the younger stages of *C. finmarchicus* may not be good indications of a DVM signal, as advective effects and a lack of repeat MPS data influence any conclusion based solely on the net data. The observations may indicate instead that *C. finmarchicus* CI-CIII were subjected to the highest levels of advection, which is why their abundance was most different between day and night samples.

6.4.3. Conclusion

Evidence suggests zooplankton DVM occurs in the High Arctic during late summer/early autumn when changes in the diel light cycle are apparent, especially at 25 – 50 m depth. This low amplitude DVM is linked to the existence of a pronounced fluorescence maximum (approximately 30 m deep), and previous studies have shown that this tends to be most common during the Arctic bloom. Thus, the occurrence of DVM should not be discussed in the context of annual timing and seasonal progression alone, but rather in the context of the High Arctic phytoplankton bloom that is potentially highly variable spatially, temporally, and in intensity. The analyses here indicate that advection is an important influence on zooplankton distributions, and has the potential to mask the signature of vertical migration. Evidence from the previous chapters of this thesis indicates high levels of advection around the Svalbard archipelago. In addition to mesozooplankton DVM signals, macrozooplankton and nekton DVM can be important. Pronounced day/night differences in macrozooplankton vertical distribution were found at the fjord stations in particular, and as these predators may influence mesozooplankton behaviour, a thorough understanding of the interactions between the different species is of optimal importance. Such knowledge could be gained in future studies via a thorough and intensive net sampling regime.

7. Summer diel vertical migration of zooplankton in ice-covered waters²

²The work described in this chapter is under review for publication as: Rabindranath, A., Daase, M., Hop, H., Falk-Petersen S., Brierley, A.S., 2012. Zooplankton diel vertical migration during summer-autumn in the High Arctic. *Journal of Marine Systems*.

I estimate I contributed 75 % of the total effort toward this paper. Net abundances (raw) and CTD data (processed) were supplied to me by NPI. LADCP velocities (processed) were supplied to me by NPI. Net and acoustic data processing (from raw data) and all analysis were conducted by myself, although assistance was received with net sample processing from NPI. 90 % of the effort towards figure creation was mine, and all writing was done by myself with inputs from all authors.

7.1. Introduction

Following on from the previous broad scale study of DVM around the Svalbard archipelago, the aim of this study was to thoroughly investigate zooplankton DVM during continual daylight in ice-covered waters using an integrated multi-disciplinary approach. Locations dominated by sea ice cover were chosen in order to investigate zooplankton vertical migration not just during continual daylight, but also where sea ice cover attenuates irradiance that arrives at the ocean surface. DVM in these areas of drifting sea ice has rarely been investigated using net samples in the past. However, Wallace et al. (2010) have provided evidence for zooplankton vertical migration within a sea-ice covered fjord using an ADCP, making this an interesting area for study. A multi-disciplinary approach is important in DVM studies (as highlighted in the previous chapter), as investigations of vertical migration using day/night net samples alone facilitate the identification of migrants, but generally lack spatial and temporal resolution (Blachowiak-Samolyk et al. 2006; Cisewski et al. 2009). The use of multi-

frequency acoustic scattering however can add higher vertical resolution when studying DVM along with net sampling.

7.2. Materials and methods

7.2.1. Sampling location

The study was carried out towards the end of the ‘midnight sun’, 27–30 August 2010, on board RV *Lance* (Cruise ICE 10-16). Samples were collected at two stations northeast of Svalbard (ICE19 & ICE22; Table 7.1, Fig 7.1). The two stations sampled in this study were in the north-eastern extension of the AtW from the WSC (Hegseth and Sundfjord 2008).

7. Summer diel vertical migration of zooplankton in ice-covered waters

Table 7.1) Sampling details including start date and time, station location and maximum water depth

Station	Start date (2010)	Start time (UTC)	Latitude (N)	Longitude (E)	Depth (m)	MPS depth strata (m)	MPS sampling Time (UTC)
ICE19 D1	27/08	09:40	81.568	30.963	1303	200-160, 160-120, 120-80, 80-40, 40-0; 100-80, 80-60, 60-40, 40-20, 20-0	11:00;11:30
ICE19 N1	27/08	21:00	81.542	30.408	832	200-160, 160-120, 120-80, 80-40, 40-0; 100-80, 80-60, 60-40, 40-20, 20-0	23:00;23:30
ICE19 D2	28/08	11:00	81.503	32.091	581	200-160, 160-120, 120-80, 80-40, 40-0; 100-80, 80-60, 60-40, 40-20, 20-0	11:00;11:30
ICE22 D3	29/08	10:30	81.508	30.193	858		
ICE22 D4	29/08	13:20	81.509	30.422	858		
ICE22 N2	29/08	23:00	81.438	30.793	401	250-200, 200-150, 150-100, 100-50, 50-0	23:00
ICE22 N3	30/08	00:00	81.441	30.853	401	250-200, 200-150, 150-100, 100-50, 50-0	00:00
ICE22 N4	30/08	01:00	81.441	30.937	401	250-200, 200-150, 150-100, 100-50, 50-0	01:00
ICE22 D5	30/08	06:00	81.401	21.334	185	180-150, 150-100, 100-50, 50-0	06:00

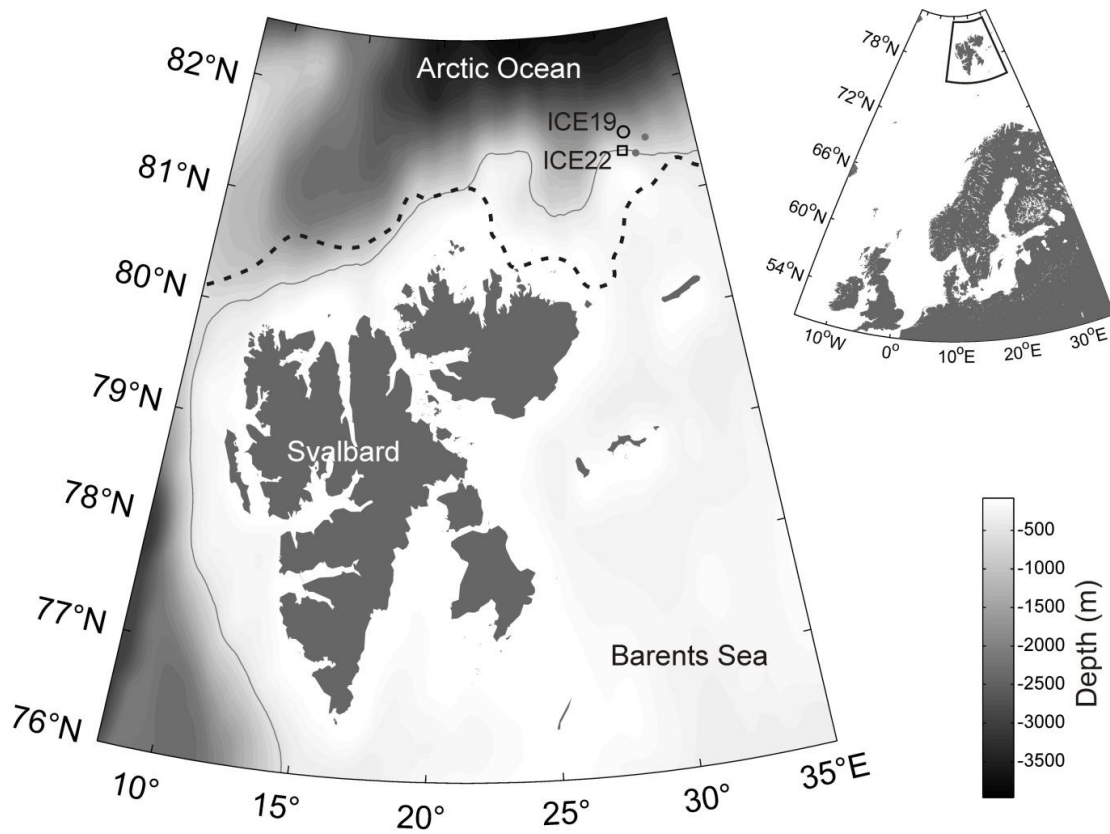


Fig 7.1) Sampling locations (ICE19 & ICE22) north-east of Svalbard. Grey dots alongside station markers indicate vessel position at the end of each station (due to drift). Dashed line indicates position of ice edge at time of sampling (courtesy of NPI), while grey line indicates 500 m bathymetry line (shelf break). Inset (top right) displays the location of Svalbard on a wider scale.

7.2.2. Environmental parameters

Photosynthetically Active Radiation (PAR, 400-700 nm) was measured at the surface at both stations (Fig 7.2) using a cosine-corrected flat-head sensor (Quantum Li-190 SA, LiCor, USA). Salinity, temperature, depth and PAR were measured using a conductivity-temperature-depth profiler (CTD) and processed following standard Sea Bird Electronics (SBE) procedures by the Norwegian Polar Institute. CTD profiles were taken immediately prior to mesozooplankton sampling when possible, depending on ice conditions. Horizontal currents were observed between 0-250 m simultaneously with CTD observations using a downward looking Lowered ADCP (LADCP) mounted to the

bottom of the CTD rosette. Due to strong tidal currents in the study area (up to 15 – 20 cm/s), all current observations were corrected using the results of the Arctic Ocean Tidal Inverse Model AOTIM-5. The drift of the ship during sampling was also plotted using GPS fixes. At both stations (ICE19 and ICE22), water samples were collected from 0-5-10-25-50-100 m for chlorophyll-*a* and phaeopigment determinations. Three replicates of 500-1000 ml from each depth were filtered through 25 mm GF/F filters. Filters were frozen at -20°C and analysed immediately after the cruise. Chlorophyll-*a* was analysed fluorometrically with methanol as the extracting solvent (Holm-Hansen and Rieman 1978) using a Turner Design 10-AU fluorometer (Sunnyvale, California).

7.2.3. Zooplankton sampling

Previous DVM studies may have used depth resolutions during net sampling that were too coarse to detect migrations (Masson et al. 2001). To maximise our chances of detecting fine-scale vertical migrations, we used a finer scale depth resolution for our net sampling regime. Mesozooplankton sampling was conducted with a Multinet Plankton Sampler (MPS, Hydro-Bios, Kiel). At ICE19, mesozooplankton samples were collected on 27 August as close to local midday and midnight as possible (11:00 and 23:00 UTC), and again at 11:00 UTC on 28 August. At each sampling time, two MPS hauls were performed – the first at 40 m depth intervals (200-160-120-80-40 m) and the second at 20 m depth intervals (100-80-60-40-20 m) (Table 7.1). To simplify further analysis, data from these two hauls were combined. Results and figures are thus based on abundances from 0-20, 20-40, 40-60, 60-80 (from the haul taken at 20 m depth intervals), and 80-120, 120-160 and 160-200 m (from the haul taken at 40 m depth intervals). While the net sampling regime at ICE19 was designed primarily to assess DVM behaviour, the sampling regime at ICE22 was designed to assess midnight sinking behaviour alongside DVM and 50 m depth intervals were chosen here. MPS hauls were collected every hour between 23:00 and 01:00 UTC at ICE22 on 29-30 August (250-200-150-100-50 m), and at 06:00 UTC on 30 August (180-150-100-50 m).

This difference in depth intervals for the MPS hauls between night and morning at ICE22 was due to the research vessel drifting overnight to shallower waters. Filtered water volume was derived from measurements made by flowmeters attached to the MPS. All samples were fixed in 4% formalin/seawater solution and analysed for species composition post cruise following procedures described by Daase and Eiane (2007). The mean depth (Z_m) of mesozooplankton species and corresponding standard deviations (Z_s) were calculated following the procedure described by Daase et al. (2008) (see 2.2 for equations).

Macrozooplankton sampling was conducted using a single vertical Method-Isaac-Kidd (MIK; 1.5 mm mesh size, 3.14 m² opening) net haul at both ICE19 (1000-0 m, 27 August 17:00 UTC) and ICE22 (750-0 m, 29 August 13:00 UTC). Samples were split, with 50% frozen and 50% fixed in 4% formalin/seawater solution. Amphipods and euphausiids were identified and counted from the sample fixed in formalin following procedures described by Dalpadado (2002).

7.2.4. Acoustic observations

A downward facing, hull-mounted Simrad EK60 echosounder operating at frequencies of 18, 38 and 120 kHz and a ping rate of 0.5 pings s⁻¹ was used to gather backscatter information from the water column (12 m to near seabed). Only data from the upper 175 m of the water column were used in the analysis due to range limitations and the shallow-water station at ICE22 D5. The near field of 0-12 m at 38 kHz was also excluded from analysis. Thus, data from 12-175 m were used in the acoustic statistical analysis. However, when displaying and discussing the acoustic record, 0-300 m is used to allow the entire water column to be visualised and thereby fully investigate and better explain all apparent DVM signals.

In order to combine and compare acoustic data and mesozooplankton net hauls, acoustic data were chosen from each station to match the mesozooplankton net sampling times as closely as possible. At ICE19, one hour of acoustic data was used to calculate a Mean Volume Backscattering Strength ($MVBS = 10 \log_{10} [\text{mean}(S_v)]$, where S_v is the volume backscattering strength), at each net sampling event (3 h total at ICE19). At ICE22, 20 min of acoustic data was used at each net sampling event due to the tighter sampling schedule, as well as 40 min at noon (10:30 – 13:55 UTC) on 29 August (2 h total at ICE22). This allowed the acoustic data to include further daytime samples at ICE22 (ICE22 D3 and ICE22 D4) compared to the net samples. The backscatter was classified using 120 kHz – 38 kHz dB differences as per Madureira et al. (1993) (see 2.3 for details).

Echo integration was then carried out for each taxon using a 25 m x 20 min grid. Nautical Area Scattering Coefficients ($NASC = \text{scaled area scattering} [4\pi(1852)^2 s_a]$, where s_a is the area backscattering coefficient) were extracted from the echo integration grids, as these provide linear representations of zooplankton backscatter. The mean depth (Z_m) of mesozooplankton, macrozooplankton and nekton NASC and corresponding standard deviations (Z_s) were calculated following the procedure described by Daase et al. (2008) and using our 25 m depth resolution and 12-175 m sampling depth. The integration cells (25 m X 20 min) were first averaged to create one cell at each sampling event (i.e. one hour at each ICE19 station, 20 min at each ICE22 station), and these were used in the Z_m and Z_s calculations (see equations in 2.2, with f_j being NASC ($\text{m}^2 \text{nm}^{-2}$) in this case).

7.2.5. Multivariate analysis

Similarity matrices created in PRIMER were used to test for differences between the stations based on 1) hydrography, 2) mesozooplankton community composition, and 3) mesozooplankton vertical distribution.

1) 10-m averages of temperature, salinity and fluorescence were calculated over the upper 180 m at each station and normalised (ranges converted to numerical values with a grand mean of zero and standard deviation of one) in order to summarise the hydrographic conditions. These data were then compared using a Euclidean distance similarity matrix and presented using a hierarchical cluster dendrogram.

2) Fourth-root transformed MPS-determined abundances of mesozooplankton were compared using a Bray-Curtis similarity matrix. Samples collected at ICE22 on 30 August at 06:00 UTC (ICE22 D5) were classified as both ‘morning’ and ‘day’ samples in two replicates of the analysis, while all other samples were classified as either day or night. The differences between stations (ICE19 and ICE22), sampling time (day/night/morning) and different depth strata were quantified using Analysis of Similarity (ANOSIM). Similarity Percentage (SIMPER) analysis was also carried out to determine which species were most responsible for the observed differences in community structure between day and night samples and different depths in terms of percentage contribution. Mesozooplankton abundances were also combined over 0-200 m at each sampling event and analysed using ANOSIM to assess the differences between samples irrespective of depth stratification, and the comparison of these two results will allow us to determine the importance of vertical movements of mesozooplankton.

3) Fourth-root transformed partitioned 120 kHz NASC data ($\text{m}^2 \text{nm}^{-2}$) were compared between stations (ICE19 and ICE22), sampling time (day/night/morning) and taxa (mesozooplankton/macrozooplankton/nekton) using a Bray-Curtis similarity matrix and Analysis of similarity (as above). Similarity percentage analysis was carried out to determine which depth strata were most responsible for the observed differences in NASC from the three taxonomic groups between day, night and morning samples and also between stations. Mean depth information (Z_m) for each species (calculated from net abundances) was also standardised using a fourth-root transformation and compared between stations (ICE19 and ICE22) and sampling time (day/night/morning) using a Bray-Curtis similarity matrix. The resulting dendrogram allows us to visualise the differences between stations and day/night.

7.2.6. Kruskal-Wallis and ANOVA analysis of mean depth (Z_m)

In addition to multivariate analysis, Kruskal-Wallis and ANOVA tests were used to isolate specific taxa responsible for differences in vertical structure between day and night. For these tests, the 120-kHz NASC mean depth (Z_m) data (ICE19 and ICE22 combined, and partitioned into mesozooplankton, macrozooplankton and nekton) and the mean depth (Z_m) of Multinet mesozooplankton species (ICE19 and ICE22 combined, and separated into individual species and stages) were used. Only Z_m information from *Calanus finmarchicus*, *Calanus glacialis*, *Calanus hyperboreus* (when sufficient numbers of animals were present), *Metridia longa* (when sufficient numbers of animals were present), *Oithona similis*, *Oithona atlantica*, *Triconia borealis*, *Microcalanus* spp. and *Pseudocalanus* spp. were included in the analysis of Multinet mesozooplankton. All data were tested for normality and homogeneity of variance using the Lilliefors normality test (Abdi and Molin 2007) and Bartlett's homogeneity of variance test (Bartlett 1936). If the data (NASC or abundance mean depth) were considered normally distributed with homogenous variances across groups by these tests, then ANOVA was used to determine the effect of the independent variables (taxa,

station, and time) on observed differences in the mean depths. However, if the data were non-normally distributed, then the Kruskal-Wallis test was used.

To determine whether the morning station at ICE22 (06:00 UTC, ICE22 D5) could be included as a day station, two replicates of the analysis were carried out, one including NASC Z_m calculated from this station as a day station, and another with this data excluded from analysis. All test statistics and p-values remained similar, and so this station was included as a day station at ICE22 to ensure the largest possible sample size. This similarity in the NASC Z_m analysis allowed the Multinet sample collected at 06:00 UTC at ICE22 to be considered a day sample also and thus allowed a day/night comparison using net determined mesozooplankton Z_m at ICE22. These tests allowed the influence of the three primary variables to be ranked and tested for significance, including differences between day and night samples which are relevant when assessing DVM behaviour.

In order to quantify differences in day/night mean depth variations within particular species between ICE19 and ICE22, analysis by Wilcoxon signed-rank test was carried out on Multinet determined mesozooplankton Z_m (when data were available at both day and night for each particular stage) and NASC Z_m for each station (ICE19 and ICE22) separately. In order to make this a fair test with the same n at each station, average Z_m was calculated at ICE19 from the two day net samples and corresponding NASC data to compare with the one night sample, and at ICE22 from the three night net samples to compare with the one day net sample. When average Z_m is calculated in this manner at ICE19 and ICE22, n becomes too small to test for day/night differences within each individual stage at the separate stations.

7.3. Results

7.3.1. Environmental conditions

A diurnal PAR cycle was observed at both stations (Fig 7.2), with irradiance varying from $1.1 \mu\text{Em}^{-2}\text{s}^{-1}$ at midnight to $651 \mu\text{Em}^{-2}\text{s}^{-1}$ at mid-day. Throughout the study, irradiance began to increase from minimal levels at approximately 23:00 UTC, peaking between 09:00 – 13:30 UTC. Irradiance reached minimal levels between approximately 20:30 – 21:00 UTC. At both stations, a layer of melt water was observed in the upper 20 m characterised by low temperature and salinity (-1.5°C , salinity 32).

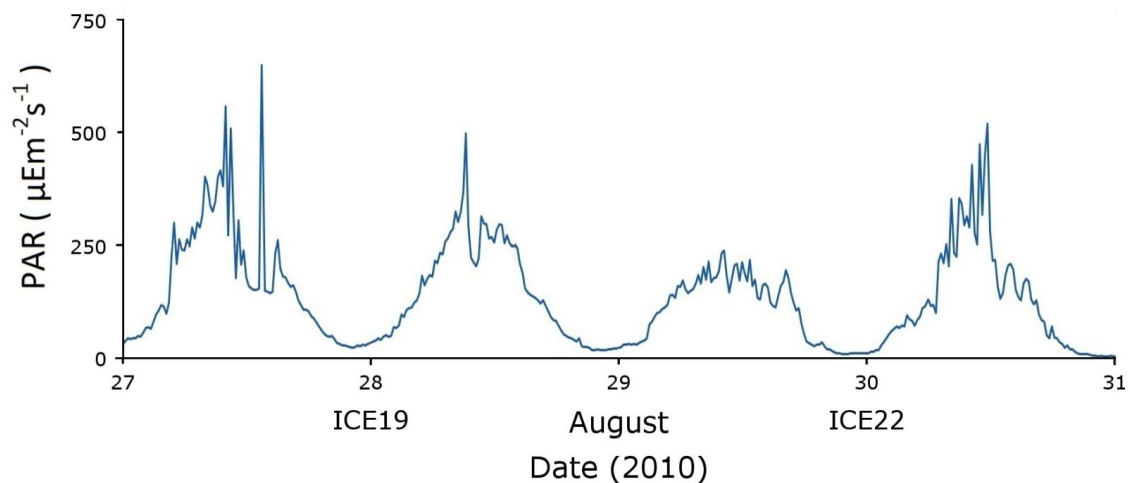


Fig 7.2) Surface PAR sampled from the vessel deck at both stations. Station ICE19 begins on 27 August, while station ICE22 begins on 29 August, 2010

Temperature and salinity increased rapidly between 20 and 30 m, and AtW was observed below 40 m depth (2°C , salinity 35; Fig 7.3). PAR in the water column differed significantly between day and night casts. At ICE19, PAR approached zero at approximately 20 m at midnight and 40 m at noon (Fig 7.3). At ICE22, there were CTD casts at 22:30 and 05:30 UTC. PAR was low at night (almost zero below 10 m) but higher in the morning (only approaching zero below 35 m). The Chl-*a* concentration in

7. Summer diel vertical migration of zooplankton in ice-covered waters

the upper 100 m varied between 0.02-0.45 mg m⁻³, with highest concentrations at 25 m at both stations (Fig 7.3).

7. Summer diel vertical migration of zooplankton in ice-covered waters

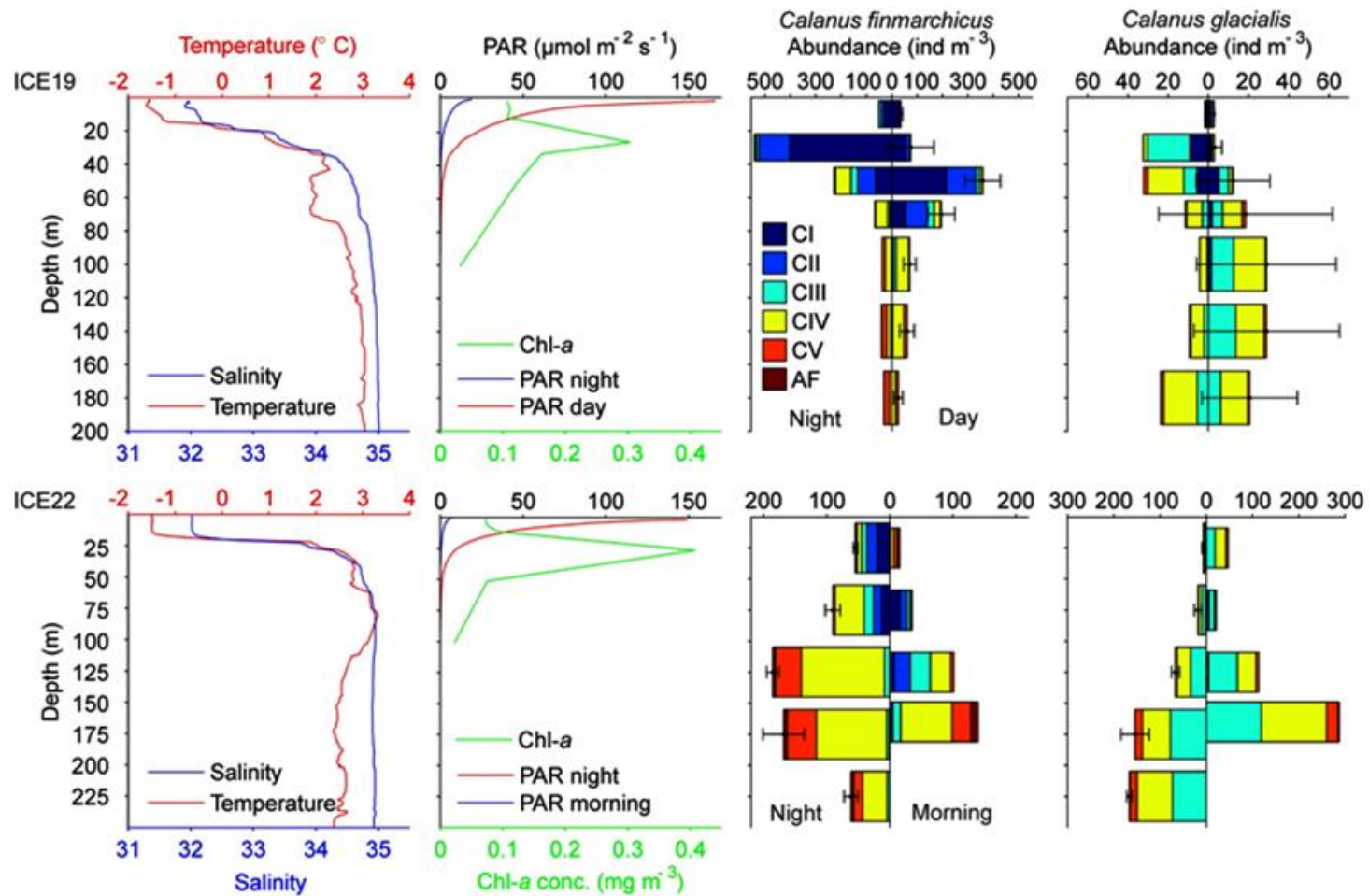


Fig 7.3) Vertical profiles of salinity, temperature ($^{\circ}\text{C}$), chlorophyll-*a* concentration (mg m^{-3}), PAR ($\mu\text{mol m}^{-2}\text{s}^{-1}$), *Calanus finmarchicus* and *C. glacialis* (individual's m^{-3}). Day (1100 UTC) and morning (0600 UTC) samples are on the right axis of each plot, while night (2300 UTC) samples are on the left axis. To aid display, the two day sampling events at ICE19 and the three night sampling events at ICE22 are combined using averages. Error bars display standard deviation.

Analysis of similarity on 10-m averages of temperature, salinity and fluorescence over the upper 180 m resulted in no significant differences identified between ICE19 and ICE22 ($R = 0.333$, $p = 0.200$) or between day/night casts ($R = 0.179$, $p = 0.267$). However, the corresponding dendrogram (Fig 7.4) highlights sampling date as the primary differentiating factor between the sampled physical environments. These differences in environmental conditions were mostly due to fluorescence values (45% contribution determined by similarity percentage analysis).

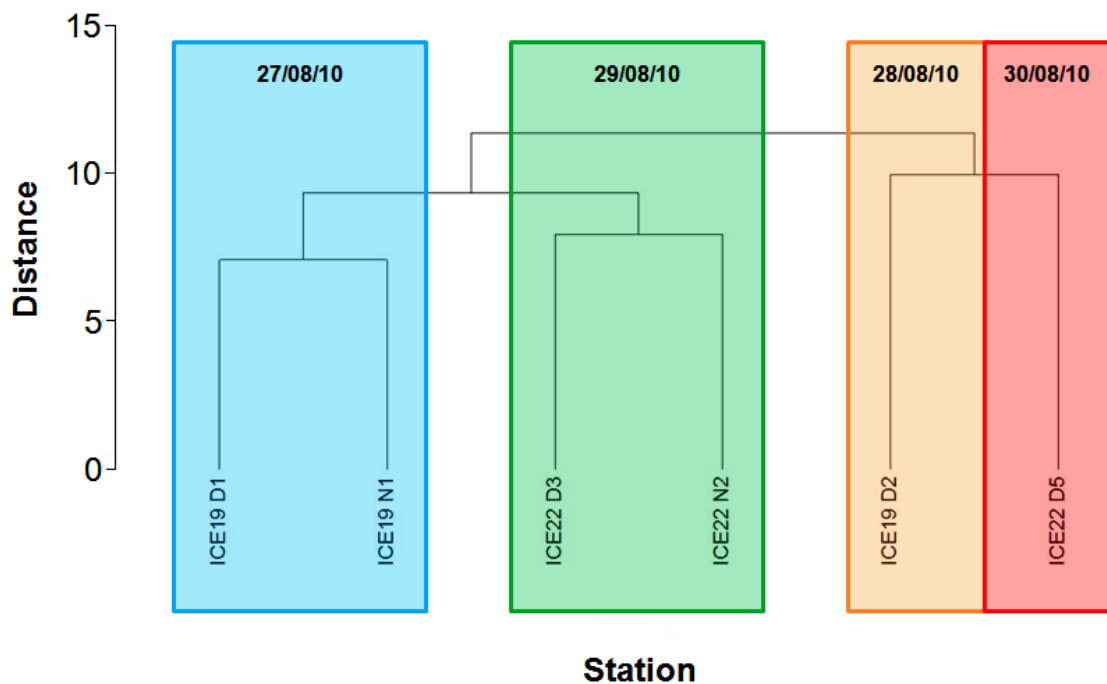


Fig 7.4) Dendrogram displaying the Euclidean distance grouping between normalised (ranges converted to numerical values with a grand mean of zero and standard deviation of one) CTD data (10 m averages of temperature, salinity and fluorescence calculated from the surface to 180 m depth at each station) at ICE19 & ICE22. Colours outline different days of sampling

Currents in the study area were generally observed as having an eastward direction (Fig 7.5). At ICE19, almost all currents between 0 – 250 m flowed in a north-easterly direction. At ICE19 D1 and ICE19 N1, the velocity of currents in the surface layers ranged between 200 – 370 mm/s. However, at ICE19 D2, currents between 0 – 100 m were slower at 100 – 120 mm/s, while current velocities were slower still between 100 – 300 m (20 – 50 mm/s). At ICE22 D3 and ICE22 N2, currents flowed in an

easterly/south-easterly direction and had surface velocities of 200 – 250 mm/s (Fig 7.5). Maximal velocities (400 – 450 mm/s) were observed at ICE22 N2 between 200 – 250 m. At ICE22 D5, the currents flowed in a south-easterly direction at 150 – 190 mm/s between 0 – 50 m but were much weaker (40 – 70 mm/s) with variable direction below 50 m depth.

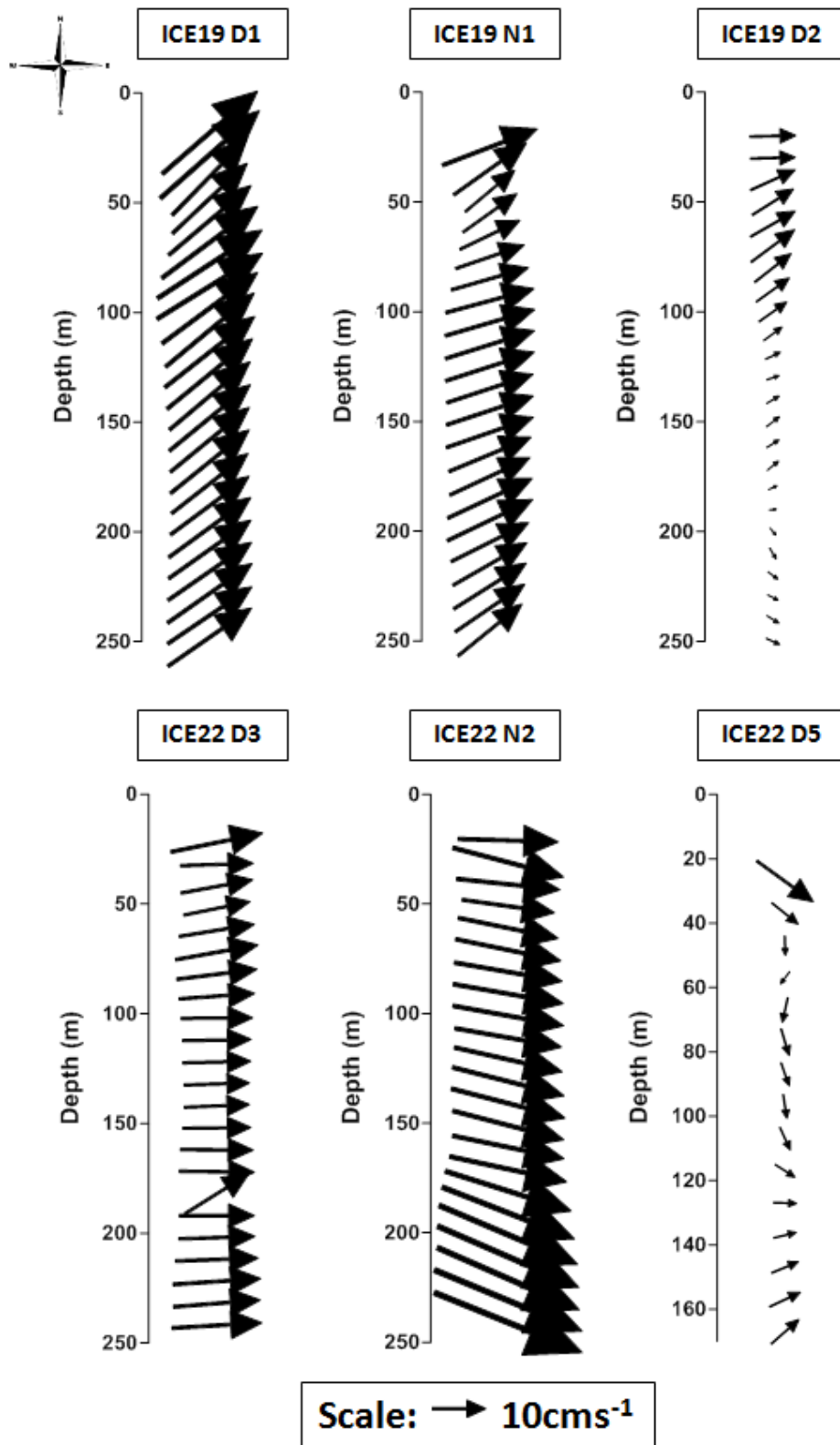


Fig 7.5) Vertical profiles of current vectors (0 – 250 m) at stations ICE19 and ICE22 observed using an LADCP mounted to the CTD rosette during the day (D) and night (N). Observations were collected immediately prior to mesozooplankton sampling (see Table 7.1 for details). Direction of arrows indicate horizontal direction of flow – N = \uparrow

As the ship was forced to drift with the ice, the winds and currents created significant drift (Fig 7.6).

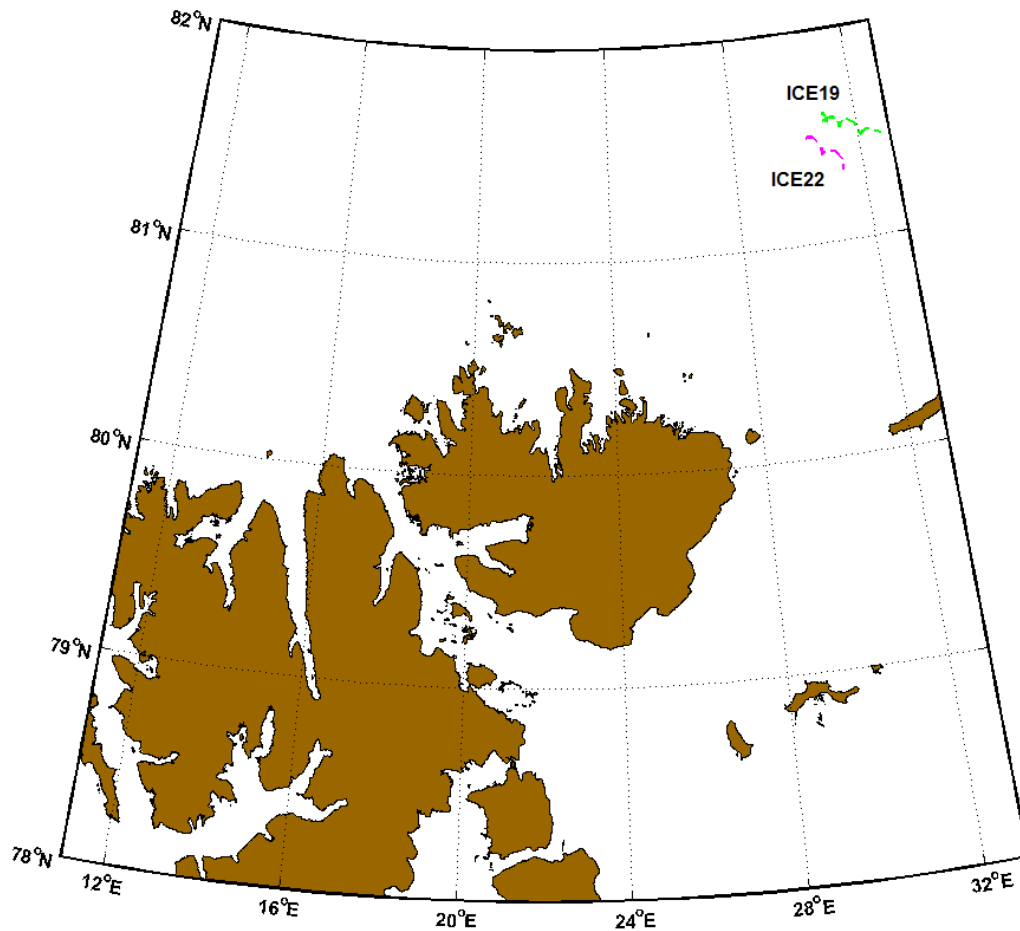


Fig 7.6) Ship drift plotted using GPS fixes during sampling at ICE19 (green) and ICE22 (pink). The land mass in brown is the Svalbard archipelago.

7.3.2. Copepod populations and vertical distribution

Copepods dominated numerically in all MPS samples. The copepod *Oithona similis* was the most abundant species and accounted for > 55% of the total number of individuals recorded in all samples (Table 7.2). Apart from *O. similis*, the most abundant species were *Calanus finmarchicus*, *Pseudocalanus* spp. and *Microcalanus* spp., accounting

together for approximately 30% of the zooplankton community at both stations. *Calanus glacialis*, *Triconia borealis*, *Oithona atlantica* and copepod nauplii were recorded in almost all samples. *Metridia longa* was rare at ICE19, but more abundant at ICE22. Other copepod species were rare and only found in a few samples at low abundance. MIK samples of larger zooplankton indicated highest relative abundances of *Themisto abyssorum* (> 60%), followed by *Themisto libellula* and *Thysanoessa longicaudata* (33%) in the water column for both ICE19 and ICE22 (Table 7.2). Lesser abundant macrozooplankton (< 5%) included *Thysanoessa inermis* and *Meganyctiphanes norvegica* (< 5%).

Table 7.2) Relative abundance (%) of the 10 most abundant species sampled at ICE19 and ICE22 using the combined MPS hauls at each station (top), and of the 5 most abundant euphausiids and amphipods sampled using the MIK haul at each station (bottom)

Sampling net	ICE19 (%)		ICE22 (%)
MPS			
<i>Oithona similis</i>	60.10	<i>Oithona similis</i>	55.39
<i>Microcalanus</i> spp.	9.63	<i>Pseudocalanus</i> spp.	12.97
<i>Calanus finmarchicus</i>	9.25	<i>Calanus finmarchicus</i>	8.93
<i>Pseudocalanus</i> spp.	5.78	<i>Calanus glacialis</i>	7.68
<i>Fritillaria borealis</i>	5.34	<i>Microcalanus</i> spp.	7.33
copepod nauplii	4.47	<i>Triconia borealis</i>	1.78
<i>Triconia borealis</i>	2.27	<i>Oithona atlantica</i>	1.77
<i>Calanus glacialis</i>	1.66	<i>Metridia longa</i>	1.10
<i>Oithona atlantica</i>	0.78	<i>Fritillaria borealis</i>	1.07
<i>Limacina helicina</i>	0.32	Copepod nauplii	0.99
Others	0.40		0.99
MIK			
<i>Themisto abyssorum</i>	61.66	<i>Themisto abyssorum</i>	61.02
<i>Themisto libellula</i>	17.38	<i>Thysanoessa longicaudata</i>	21.42
<i>Thysanoessa longicaudata</i>	16.34	<i>Themisto libellula</i>	11.71
<i>Thysanoessa inermis</i>	3.12	<i>Thysanoessa inermis</i>	3.08
<i>Meganyctiphanes norvegica</i>	1.04	<i>Meganyctiphanes norvegica</i>	1.85
Others	0.45		0.92

Amongst the three *Calanus* species, *C. finmarchicus* was most abundant at ICE19 representing > 80% of the *Calanus* population. *Calanus glacialis* was more common at

ICE22, making up approximately 45% of the *Calanus* population there. The abundance of *C. hyperboreus* was very low at both stations (< 2%), thus its vertical distribution is not further reported in this section.

Although abundances varied for some species between noon sampling events at ICE19, the depth distributions of most species were similar in samples taken at noon on 27 and 28 August. In order to report and display the results more concisely, the samples were treated as replicates and means were calculated for all abundances (creating one ICE19 'day' sample; Fig 7.3). At ICE22, the mesozooplankton vertical distributions at 23:00, 01:00 and 02:00 UTC remained largely the same for most species, and means were again calculated for all abundances (creating one ICE22 'night' sample). As some populations collected in the Multinet were normally distributed and others were not, both ANOVA and the Kruskal-Wallis test had to be used to test for differences in mean depths (Z_m) when ICE19 and ICE22 were combined. A Chi-sq test statistic in this section signifies a Kruskal-Wallis test, while an F value signifies ANOVA. To test for day/night differences within each station, Wilcoxon signed-rank tests are denoted by a V test statistic.

Over 70% of the *C. finmarchicus* population at ICE19 consisted of copepodid stages CI and CII, which were concentrated in the upper 80 m (144 ind. m^{-3} mean abundance between 0-80 m during the day) and largely absent below 80 m (Fig 7.3). During the day, these stages were concentrated between 40-80 m with highest abundance between 40-60 m depth (331 ind. m^{-3}). At night, stages CI-II were concentrated in the upper 20-60 m with highest abundance between 20-40 m depth (525 ind. m^{-3}). At ICE19, the mean depth of stage CI was calculated as 32 m during the night and 47 m during the day. The mean depths of stage CII were deeper in comparison to CI (37 m at night and 57 m during the day) (Fig 7.7). The abundance of older stages of *C. finmarchicus* CIII-CV (< 49 ind. m^{-3}) was lower than that of CI-CII and most were observed below 40 m depth (Fig 7.3). Differences in mean depth were observed for stages CIII and CIV between day (77 m and 118 m, respectively) and night (48 m and 89 m, respectively)

(Fig 7.7). The mean depth (140-150 m) of stage CV and adults differed little between the day and night samples. At ICE19, *C. finmarchicus* Z_m (CI to adult female) differed significantly between day and night ($V = 21$, $p = 0.031$). The upper 20 m were avoided by all stages during both day and night.

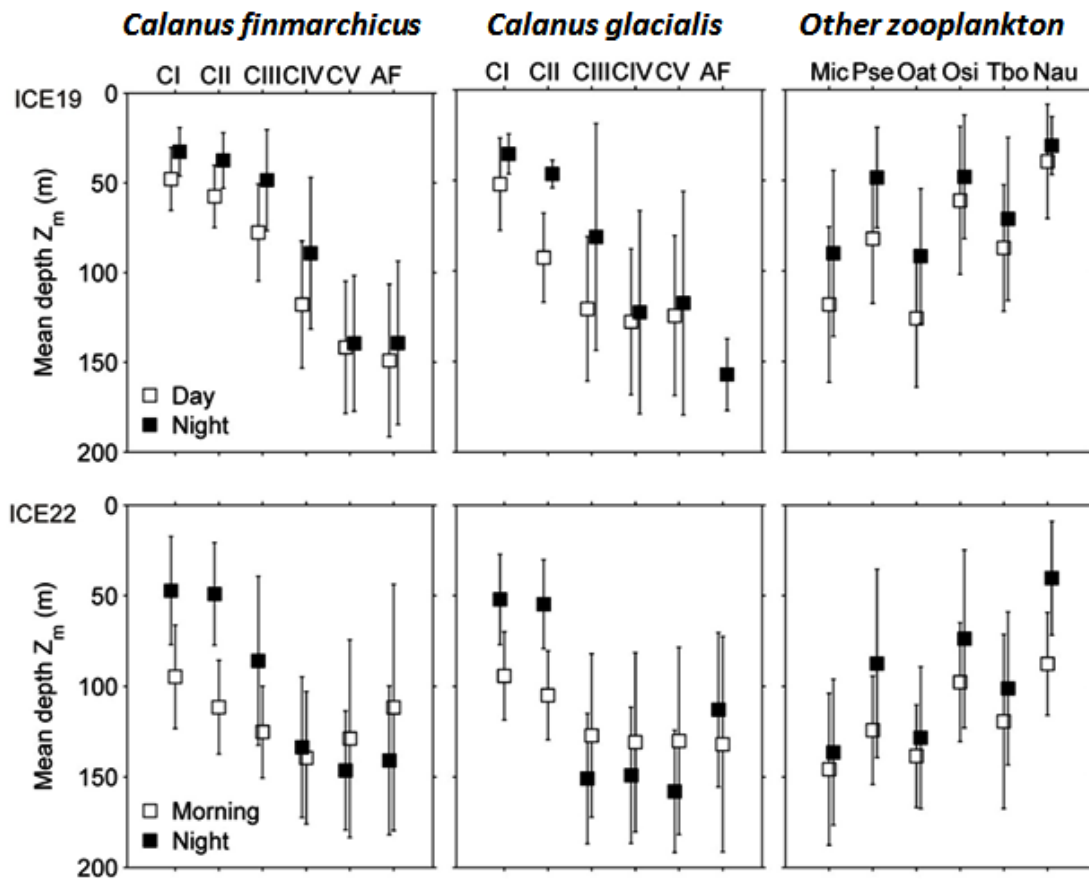


Fig 7.7) Mean depths (Z_m) of copepodid stages CI-CV and adult females (AF) of *C. finmarchicus*, *C. glacialis* and selected copepod species at ICE19 (upper panel) and ICE22 (lower panel). Day/morning depths are displayed as white boxes, while night depths are black boxes. Error bars display standard deviation (Z_s). Mic = *Microcalanus* spp.; Pse = *Pseudocalanus* spp.; Oat = *Oithona atlantica*; Osi = *Oithona similis*; Tbo = *Triconia borealis*; Nau = *Calanus* nauplii. To aid in display, the two day-sampling events at ICE19 and the three night-sampling events at ICE22 are combined prior to calculation of Z_m and Z_s .

At ICE22, the *C. finmarchicus* population consisted mainly of copepodid stage CIV (up to 149 ind. m⁻³) and was primarily found deeper than 100 m (Fig 7.3). Younger, less abundant stages were concentrated in the upper 50 m. At dawn (06:00 UTC), the mean depths of stages CI and CII were deeper (100 m and 110 m, respectively) than at night (50 m for both stages), indicating DVM behaviour for these stages and corroborating with the observations at ICE19 (Fig 7.7). The mean depths of the older *C. finmarchicus* stages (140-150 m) did not differ greatly between the dawn and night samples. In contrast to ICE19, at ICE22 *C. finmarchicus* Z_m (CI to adult female) did not differ significantly between day and night ($V = 16$, $p = 0.312$).

The *C. glacialis* population consisted mainly of stages CIII and CIV at both locations. At ICE19, the population in the upper 200 m consisted primarily of stages CIII (< 13 ind. m⁻³) and CIV (< 17 ind. m⁻³), while adult females were almost completely absent (Fig 7.3). As with *C. finmarchicus*, very few individuals were observed in the upper 20 m during either day or night. The abundance of *C. glacialis* was highest between 20-60 m at night (mean abundance 32 ind. m⁻³) and deeper than 60 m during the day (Fig 7.3). Stages CI, CII and CIII were concentrated shallower in the water column at night (mean depths of 35, 46 and 81 m, respectively) compared to the day (52, 92 and 120 m, respectively) (Fig 7.7). At ICE19, *C. glacialis* Z_m (CI to adult female) did not differ significantly between day and night ($V = 15$, $p = 0.063$), although the p value here was just outside the 95% confidence interval.

At ICE22, the *C. glacialis* population was largely concentrated deeper than 150 m (< 287 ind. m⁻³). Abundance was lowest in the upper 50 m (8 ind. m⁻³). As with *C. finmarchicus*, its depth distribution did not vary between 23:00-01:00 UTC. Stages CI and CII were distributed deeper at dawn than at night, although the abundances of these stages were very low (< 5 ind. m⁻³). In contrast to *C. finmarchicus* CI and CII, the *C. glacialis* CIII, CIV and CV were deeper during the night (average of 153 m) than during the day (average of 129 m). As at ICE19, at ICE22 *C. glacialis* Z_m (CI to adult female) did not differ significantly between day and night ($V = 10$, $p = 1.000$). The lower V

statistic and considerably higher p indicate less day/night difference in *C. glacialis* mean depth at ICE22 compared to ICE19.

Higher abundances of the copepods *Microcalanus* spp., *Pseudocalanus* spp., *O. atlantica* and *T. borealis* and copepod nauplii were observed in the upper water column (< 80 m depth) at night compared to during the day at ICE19. This pattern was also observed for *Pseudocalanus* spp., *O. similis* and *T. borealis* at ICE22 (Fig 7.7). Vertical migration appeared to be restricted to the upper 20-80 m, with species being more abundant at 20-40 m during the night and at 40-80 m during the day. Again, as with the *Calanus* copepods, the upper 20 m were largely avoided by all species. Although the mean depths of these copepod taxa and of copepod nauplii were generally shallower at night than during the day at both stations, the depth distributions themselves were spread over a large portion of the sampled water column (Fig 7.7). The largest differences between mean depths during the day and night were observed for *Pseudocalanus* spp. at both stations and for nauplii at ICE22 (Fig 7.7).

When the mean depths of *Calanus finmarchicus*, *Calanus glacialis*, *Calanus hyperboreus*, *Metridia longa*, *Oithona similis*, *Oithona atlantica*, *Triconia borealis*, *Microcalanus* spp. and *Pseudocalanus* spp. from ICE19 and ICE22 were tested together ($n = 203$), species (Chi-sq = 47.26, $P = 1.4e-7$) and stage (Chi-sq = 35.02, $P = 4.3e-6$) had significant influences on Z_m while station and time did not (Table 7.3a). As the species displayed such differing Z_m , each species and stage was then tested individually to determine any day/night differences in Z_m . However, for these tests, sample size was smaller ($n = 7$ for each individual stage). *Calanus finmarchicus* CIII ($F = 20.88$, $P = 0.010$), CII (Chi-sq = 4.50, $P = 0.034$), *Metridia longa* CV ($F = 9.55$, $P = 0.037$), CIV (Chi-sq = 4.50, $P = 0.034$), *Pseudocalanus* spp. ($F = 293.14$, $P = 6.8e-5$), *Oithona similis* ($F = 8.76$, $P = 0.042$), and *Triconia borealis* ($F = 8.01$, $P = 0.047$) displayed significant differences between day and night mean depths. Of these species and stages, *C. finmarchicus* CII, and *M. longa* CV, CIV also displayed no significant difference between stations (Table 7.3a), indicating that day/night was the only influencing factor

7. Summer diel vertical migration of zooplankton in ice-covered waters

on mean depth. Species and stages that showed day/night differences in Z_m at 10% significance are also displayed in Table 7.3a,b.

7. Summer diel vertical migration of zooplankton in ice-covered waters

Table 7.3a) Sample statistic and p values from ANOVA and Kruskal-Wallis tests on NASC and Multinet abundance mean depth (Z_m) data (m). NASC Z_m is calculated from all 120 kHz data (25 m x 20 min grid – see Fig. 7.10 for data collection periods, n = 27 combined, n = 9 for each taxa), mesozooplankton Z_m is calculated from all MultiNet abundances (see Table 7.1 for MultiNet details, n = 203 combined, n = 7 for each individual stage). Only Z_m information from *Calanus finmarchicus* (C fin), *Calanus glacialis* (C gla), *Calanus hyperboreus* (C hyp), *Metridia longa* (M lon), *Oithona similis* (O sim), *Oithona atlantica* (O atl), *Triconia borealis* (T bor), *Microcalanus* spp (Micro), and *Pseudocalanus* spp. (Pseudo) are tested. The independent variables are taxa (mesozooplankton [meso], macrozooplankton [macro] and nekton [nekto]), species, stage, station (ICE19 and ICE22), and time (day, night). This table only contains individual taxa or species/stages that have significant differences between day and night Z_m at 5% or 10%. [Table continues in 7.3b]. When testing the difference between day and night (time), the p values significant at 5% are highlighted with bold and italics, while the p values significant at 10% are highlighted in italics

Dependent Variable [Z_m (m)]	Independent Variable	ANOVA Test					Kruskal-Wallis Test		
		Sum Sq	Mean Sq	df	F	p	df	Chi-squared	p
Meso, Macro, Nekto NASC	Taxa	1562.0	1562.0	1	1.955	0.175			
	Station	649.2	649.2	1	0.813	0.377			
	Time	5283.4	5283.4	1	6.613	0.017			
	Residual	18376.4	799.0	23					
Meso NASC	Station	288.3	288.3	1	0.281	0.615			
	Time	4884.7	4884.7	1	4.763	<i>0.072</i>			
	Residual	6153.4	1025.6	6					
C fin, C gla, C hyp, M lon, Micro, Pseudo, O sim, O atl, T bor	Species						8	47.26	0.000
	Stage						6	35.02	0.000
	Station						1	2.39	0.122
	Time						1	1.43	0.233
C fin CIII	Station	1383.5	1383.5	1	17.459	0.014			
	Time	1654.1	1654.1	1	20.875	0.010			
	Residual	317.0	79.2	4					
C fin CII	Station						1	0.00	1.000
	Time						1	4.50	0.034
C gla CII	Station	34.9	34.9	1	0.072	0.802			
	Time	2804.2	2804.2	1	5.789	<i>0.074</i>			
	Residual	1937.5	484.4	4					
C gla CI	Station	230.6	230.6	1	0.896	0.397			
	Time	1571.1	1571.1	1	6.107	<i>0.069</i>			
	Residual	1029.1	257.3	4					
M lon AF	Station						1	2.00	0.157
	Time						1	3.13	<i>0.077</i>
M lon CV	Station	4524.0	4524.0	1	2.210	0.211			
	Time	19538.3	19538.3	1	9.545	0.037			
	Residual	8187.7	2046.9	4					
M lon CIV	Station						1	0.13	0.724
	Time						1	4.50	0.034
M lon CIII	Station	1935.8	1935.8	1	2.001	0.230			
	Time	4486.7	4486.7	1	4.639	<i>0.098</i>			
	Residual	3869.0	967.3	4					

7. Summer diel vertical migration of zooplankton in ice-covered waters

Table 7.3b) Continuation from Table 7.3a. Sample statistic and p values from ANOVA tests on Multinet abundance mean depth (Z_m) data (m). Z_m is calculated from all MultiNet abundances (see Table 7.1 for MultiNet details, $n = 203$ combined, $n = 7$ for each individual stage). The independent variables are station (ICE19 and ICE22), and time (day, night). This table only contains individual taxa or species/stages that have significant differences between day and night Z_m at 5% or 10%. When testing the difference between day and night (time), the p values significant at 5% are highlighted with bold and italics, while the p values significant at 10% are highlighted in italics

Dependent Variable [Z_m (m)]	Independent Variable	ANOVA Test					Kruskal-Wallis Test		
		Sum Sq	Mean Sq	df	F	p	df	Chi-squared	p
Micro	Station	1480.5	1480.5	1	20.551	0.011			
	Time	478.5	478.5	1	6.642	<i>0.062</i>			
	Residual	288.2	72.0	4					
Pseudo	Station	1156.9	1156.9	1	193.980	0.000			
	Time	1748.3	1748.3	1	293.140	<i>0.000</i>			
	Residual	23.9	6.0	4					
O sim	Station	882.7	882.7	1	15.164	0.018			
	Time	509.7	509.7	1	8.757	<i>0.042</i>			
	Residual	232.8	58.2	4					
O atl	Station	482.0	482.0	1	4.640	0.098			
	Time	632.1	632.1	1	6.085	<i>0.069</i>			
	Residual	415.5	103.9	4					
T bor	Station	922.9	922.9	1	16.896	0.015			
	Time	437.4	437.4	1	8.008	<i>0.047</i>			
	Residual	218.5	54.6	4					

Amongst the non-copepods from the MPS samples, the chaetognath *Eukrohnia hamata*, the larvacean *Fritillaria borealis* and the pteropod *Limacina helicina* were the most abundant species. The amphipod *Themisto libellula*, the euphausiid *Thysanoessa longicaudata*, the chaetognath *Sagitta elegans* and various larval stages of echinoderms and bivalves were found in some of the samples. *Eukrohnia hamata* was located shallower in the water column at ICE19 at night compared to the day, but this was not observed at ICE22 (Fig 7.8). However, at ICE22 *Fritillaria* spp. and *L. helicina* were found at higher concentrations in the upper water column at night compared to the day. This was not observed at ICE19 (*L. helicina* was not present there in the night samples).

7. Summer diel vertical migration of zooplankton in ice-covered waters

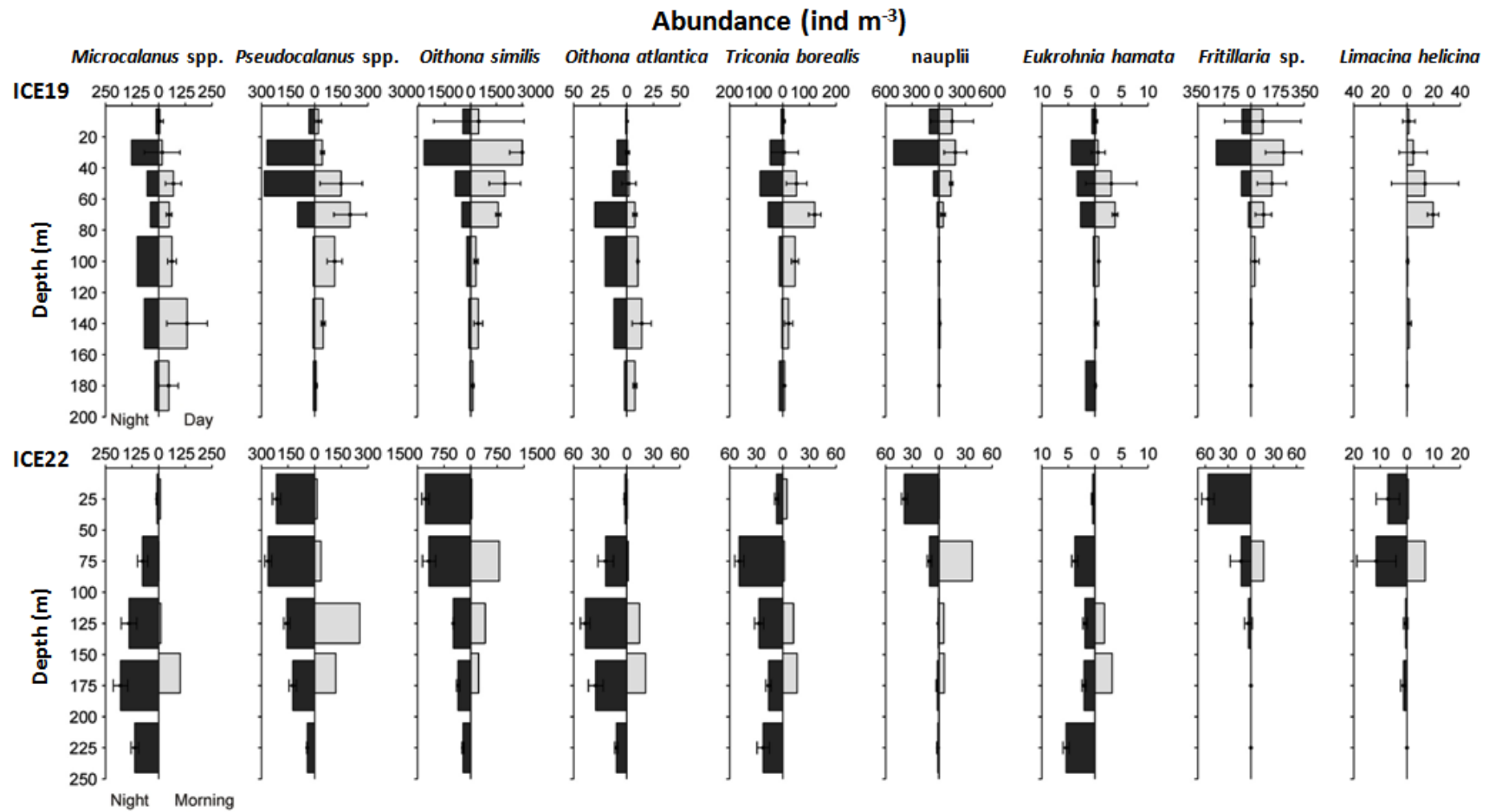


Fig 7.8) Vertical profiles of the most numerically dominant zooplankton taxa (apart from *Calanus*) recorded in the MPS hauls (ind. m⁻³). Day/morning samples are on the right axis of each plot and night samples on the left. To aid in display, the two day-sampling events at ICE19 and the three night-sampling events at ICE22 are combined means. Error bars display standard deviation.

7.3.3. Multivariate analysis of net samples

Significant differences in MPS-determined abundances were found between the depth-stratified communities at each station (analysis of similarity $R = 0.206$, $P = 0.003$), among the depth strata at each station ($R = 0.662$, $P = 0.001$) and also between sampling times ($R = 0.144$, $P = 0.016$). When the abundances were combined over 0-200 m at each sampling event, analysis of similarity revealed significant differences between stations ($R = 0.963$, $P = 0.029$) and sampling times ($R = 0.592$, $P = 0.038$). The higher R values here signify the effect of removing the depth stratification from the samples. When the morning samples taken at ICE22 were classified as 'day' samples and combined with all other day samples, a significant difference was still found between sampling time, although of lesser magnitude ($R = 0.077$, $P = 0.045$). The magnitude of the difference found between day and night samples increased ($R = 0.242$, $P = 0.002$) when the 40 m depth resolution samples (0-200 m) at ICE19 were discarded from the analysis (leaving only the 20 m resolution samples taken between 0-100 m). Similarity percentage analysis identified *F. borealis*, *C. finmarchicus* CI-CII, *O. similis* and copepod nauplii as being most responsible for the differences in community structure between stations. These same species were most responsible (accounting for 37% dissimilarity) for the differences between surface waters (0-40 m) and deeper depths (> 160 m). *Metridia longa* CV was most responsible for the difference between the 160-200 m and the ≥ 200 m depth layers.

When the mean depths (Z_m) for all species (see 7.2.6 for species list) were compared between stations using Bray Curtis similarity and then plotted as a dendrogram, the day/night differences at both stations can be visualised (Fig 7.9). Day 2 at ICE19 is the most different to all other stations, and the next most prominent difference is between the remaining ICE19 stations and ICE22 (Fig 7.9). Within ICE19, day 1 and night 1 are very similar, while there is a clear difference at ICE22 between the day station and the three night stations.

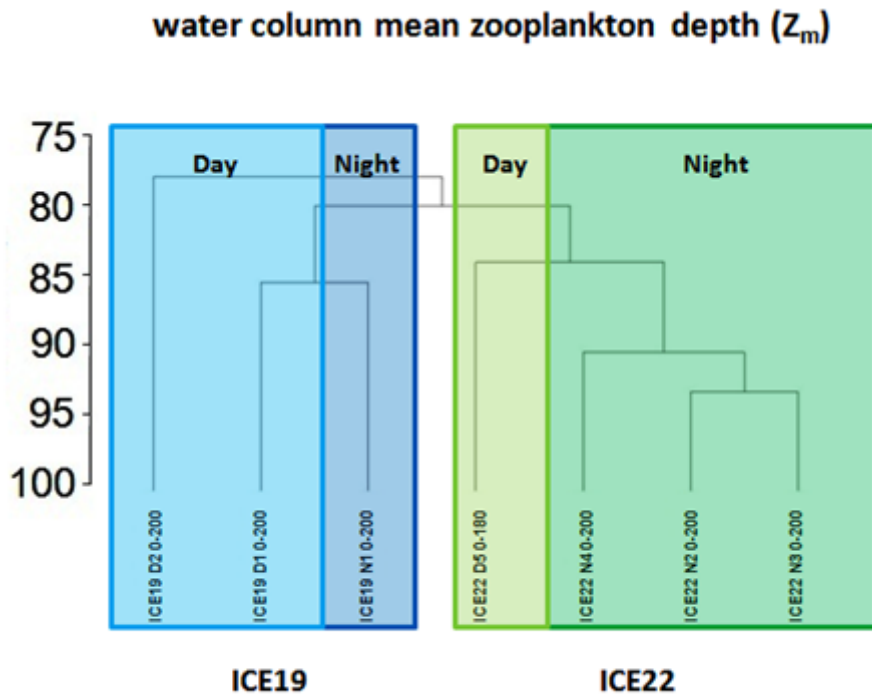


Fig 7.9) Hierarchical cluster dendrogram based on Bray Curtis similarity analysis of fourth-root transformed Multinet mesozooplankton mean depth (Z_m). Similarity scale on cluster dendrogram represents percentage similarity between samples. In all cases (apart from ICE22 D5), net abundances are integrated between 0-200 m. At ICE22 D5, the integration layer is 0-180 m. Shaded areas represent station and day/night groupings.

7.3.4. Acoustic observations

MVBS (S_v) was generally low at both stations (Fig7.10). Below, ‘*’ denotes S_v values based on echo integration carried out on a 25 m x 20 min grid. At ICE19, the two day-stations (ICE19 D1 and ICE19 D2) displayed similar patterns of backscatter, apart from the patches of high S_v (up to -48 dB) at ICE19 D2 recorded between 100-300 m. The ‘day’ 120 kHz data displayed two distinct scattering layers, one between approximately 0-100 m (-89 to -73 dB*), and the other largely at > 250 m depth (-100 to -71 dB*). The layer between 0-100 m consisted mostly of macrozooplankton and mesozooplankton, with echoes attributed to nekton being more prevalent deeper than 100 m. The backscatter pattern appeared different during the night (ICE19 N1), with a narrower

scattering layer at the surface between 0-50 m (-84 to -75 dB*), and a more defined scattering layer between approximately 200-270 m (-83 to -74 dB*). Again, the scattering layers appeared to be composed mainly of macrozooplankton and mesozooplankton, although echoes attributable to smaller mesozooplankton ($\Delta MVBS > 20$) were more dominant during the night, especially between 50-200 m. Echoes attributable to nekton were found just below this layer, largely at > 300 m depth.

At ICE22, the two day-stations on 29 August (ICE22 D3 and ICE 22 D4), which were only 1.5 h apart, appeared different in terms of their backscatter pattern (Fig 7.10). At ICE22 D3, two distinct scattering layers existed, one between 0-30 m (-74 dB*) and the other between 200-300 m (-82 to -78 dB*). Both layers appeared to consist primarily of macrozooplankton and mesozooplankton, with smaller mesozooplankton ($\Delta MVBS > 20$) being more dominant between 200-300 m. At ICE22 D4, the scattering layer between 200-300 m was completely absent, and the surface scattering layer was broader (0-50 m). However, this deeper scattering layer is not included in our 12-175 m acoustic analysis depth. As at ICE19, the backscatter pattern appeared different during the night compared to the day (ICE22 N2, ICE22 N3 and ICE22 N4; Fig 7.10). A surface scattering layer was found between approximately 0-70 m (-81 to -78 dB*), and a more patchy scattering layer was found between 100-300 m (-90 to -70 dB*), with patch S_v as high as -51 dB. This scattering layer was shallower at 23:15 (100-250 m) than at 01:45 (150-300 m). At night, the echoes at < 250 m depth were largely attributable to macrozooplankton and larger mesozooplankton, while echoes attributable to nekton dominated > 300 m depth. The final dawn station (ICE22 D5) was sampled in much shallower water (180 m depth), and the entire water column above this depth contained backscatter (-82 to -69 dB*), with higher S_v towards the surface than at any other station.

7. Summer diel vertical migration of zooplankton in ice-covered waters

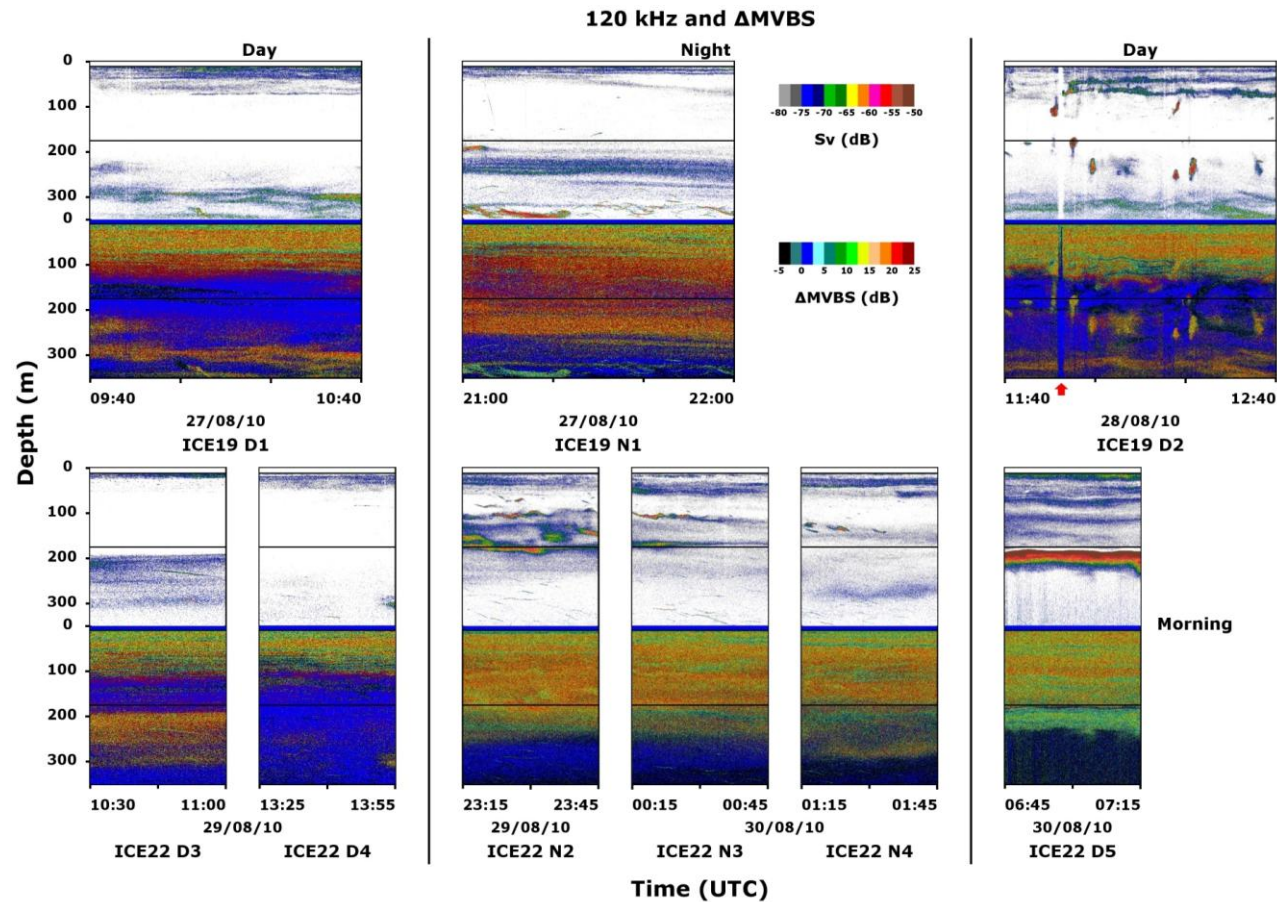


Fig 7.10) 120 kHz backscatter (above) and Δ MVBS (below) from the two stations [0 – 350 m depth]. ICE19 is displayed on the top row, with ICE22 on the bottom row. Volume backscatter (S_v) is expressed using a colour scale between -80 and -50 decibels (dB). Δ MVBS is expressed using a colour scale between -5 and 25 dB. The top 12 m of each echogram are discarded due to near-field and noise (i.e. white in the 120 kHz echogram and dark blue solid stripe on the Δ MVBS display). Black horizontal lines (12 & 175 m) represent cut-off depths for data used in acoustic analysis. Δ MVBS echoes with yellow-red shades represent stronger scattering at 120 kHz, while Δ MVBS echoes with grey-black shades represent stronger scattering at 38 kHz. Day echograms are displayed on the far left and far right (morning for ICE22 D5), and night echograms in the centre. Red arrow below the ICE19 D2 plot highlights lost pings due to sea ice impact

At ICE19, a Wilcoxon signed-rank test on combined mesozooplankton, macrozooplankton and nekton NASC Z_m showed no significant difference between day/night NASC ($n = 6$). This is likely because in contrast to the similarity found in the net samples, NASC mean depth (Z_m) values varied significantly between noon sampling events at ICE19 (27 and 28 August), and this was due to the patches of high S_v at ICE19 D2 (Fig 7.10). NASC mean depth also varied between the two day sampling events at ICE22 (29 and 30 August). In order to report and display the results as concisely as possible, NASC mean depth (Z_m) was averaged between ICE22 D3 and ICE22 D4 to create one ICE22 day sample on the 29 August, and between ICE22 N2, ICE22 N3 and ICE22 N4 to create one ICE22 night sample for the plot (Fig 7.11). Due to the deeper patches of high S_v at ICE19 D2, NASC mean depth is deepest at ICE19 during the second day station (mesozooplankton = 97 m, macrozooplankton = 95 m, nekton = 79 m) and shallowest during the first day station (mesozooplankton = 35 m, macrozooplankton = 25 m, nekton = 30 m). At ICE19, the amplitude between the shallowest and deepest NASC mean depths is smallest within the nekton.

At ICE22, mesozooplankton and macrozooplankton NASC mean depth (Z_m) were shallower during both daytime sampling events (i.e. noon on the 29 August and morning on the 30 August) compared to the night (Fig 7.11). NASC mean depth was deeper in the morning samples (mesozooplankton = 49 m, macrozooplankton = 63 m) compared to the noon samples (mesozooplankton = 27 m, macrozooplankton = 23 m). However, both taxa had mean depths deepest at night (mesozooplankton = 114 m, macrozooplankton = 97 m). When combined mesozooplankton, macrozooplankton and nekton NASC Z_m at ICE22 were tested by Wilcoxon signed-rank, NASC Z_m differed significantly between the day and night ($V = 3$, $p = 0.019$, $n = 18$). Based on the echograms (Fig 7.10) and comparing ICE22 D3 with ICE22 N2, this high NASC at depth during the night appears to be from scattering layers which have moved into the analysed 12-175 m layer from below. Nekton NASC mean depth at ICE22 displayed a different pattern, with mean depth deeper during the morning (79 m) than at night (57 m). The amplitude between the shallowest and deepest NASC mean depths is again smallest within the nekton as at ICE19, indicating least vertical movement within this

group. As with the net determined mesozooplankton mean depths (Fig 7.9), NASC mean depths (which include a further noon sampling event at ICE22) indicate more consistent day/night differences at ICE22 compared to ICE19, especially within mesozooplankton and macrozooplankton NASC.

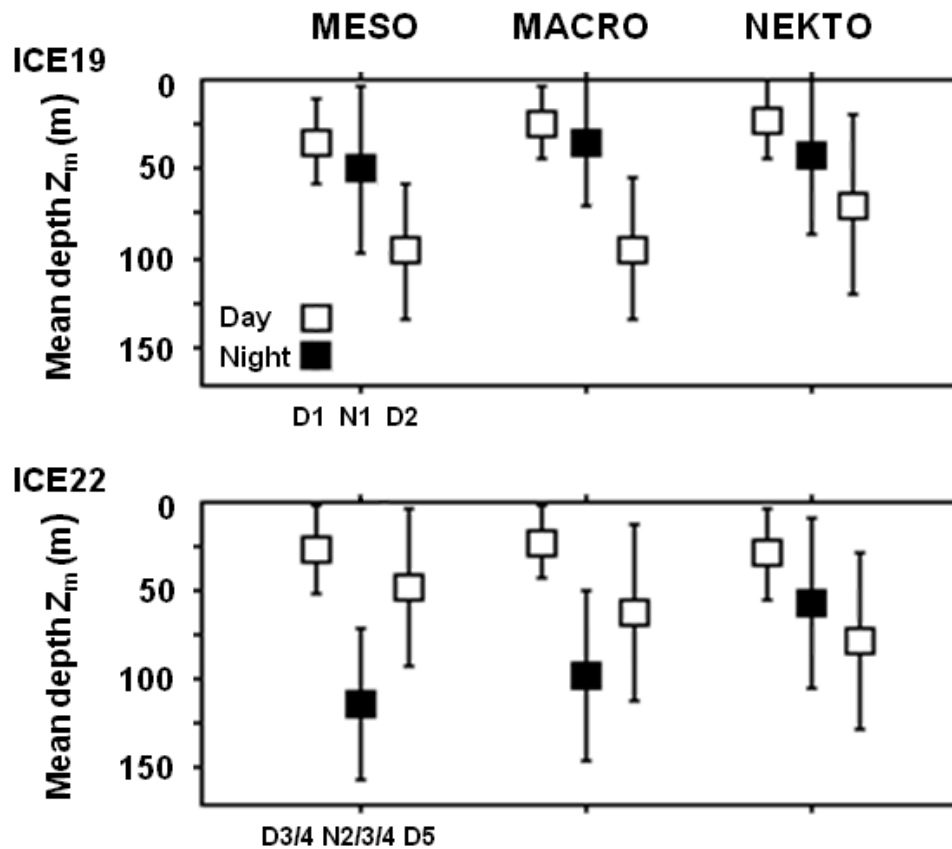


Fig 7.11) Mean depths (Z_m) of mesozooplankton (meso), macrozooplankton (macro) and nekton (nekto) NASC at ICE19 (upper panel) and ICE22 (lower panel). Day depths are displayed as white boxes, while night depths are black boxes. At ICE22, NASC is combined between D3 and D4 and between N2, N3 and N4 prior to calculation of Z_m and Z_s to aid in display. ICE22 D5 (06:45 – 07:15) is considered a day sample. Error bars display standard deviation (Z_s).

As the NASC mean depths were normally distributed with homogenous variance between groups, ANOVA was also used to test whether taxa (mesozooplankton/macrozooplankton/nekton), station (ICE19/ICE22) or time

(day/night) had any significant effects on the combined (ICE19 and ICE22 together, $n = 27$) NASC mean depths (Z_m). Taxa ($F = 1.96$, $P = 0.175$) and station ($F = 0.81$, $P = 0.377$) had no significant influence on NASC Z_m , but time ($F = 6.61$, $P = 0.017$) did (Table 7.3a). When mesozooplankton, macrozooplankton and nekton NASC Z_m at ICE19 and ICE22 combined were separated and tested individually ($n = 9$) to determine which taxa showed the largest differences between day and night, mesozooplankton ($F = 4.76$, $P = 0.072$) displayed the largest day/night difference and was the only taxa with a day/night difference that would pass a significance test at 10%. This change in p-value from the day/night test on combined NASC Z_m is likely due to the smaller sample size. The day/night difference was also larger than the difference between stations ($F = 0.28$, $P = 0.615$).

As significant vessel drift (Fig 7.6) and strong currents (Fig 7.5) were identified during sampling, observing and reporting day/night differences in depth distribution based purely on the day/night sections of echogram may not be considered sufficient evidence for vertical migration within a dynamic and patchy environment. Thus, a 32 hour continual echogram of the surface 100 m (where much of the day/night changes were identified) is plotted for ICE19 (Fig 7.12). On this echogram, a typical DVM signal can be observed, with backscatter spread between the surface and approximately 75 m depth at noon, before the scattering layer moves closer to the surface (reaching < 40 m depth at midnight) then back down at dawn to reach 75 m by noon the following day. Unfortunately the 0 – 12 m depth layer is not available due to near-field effects and large levels of noise.

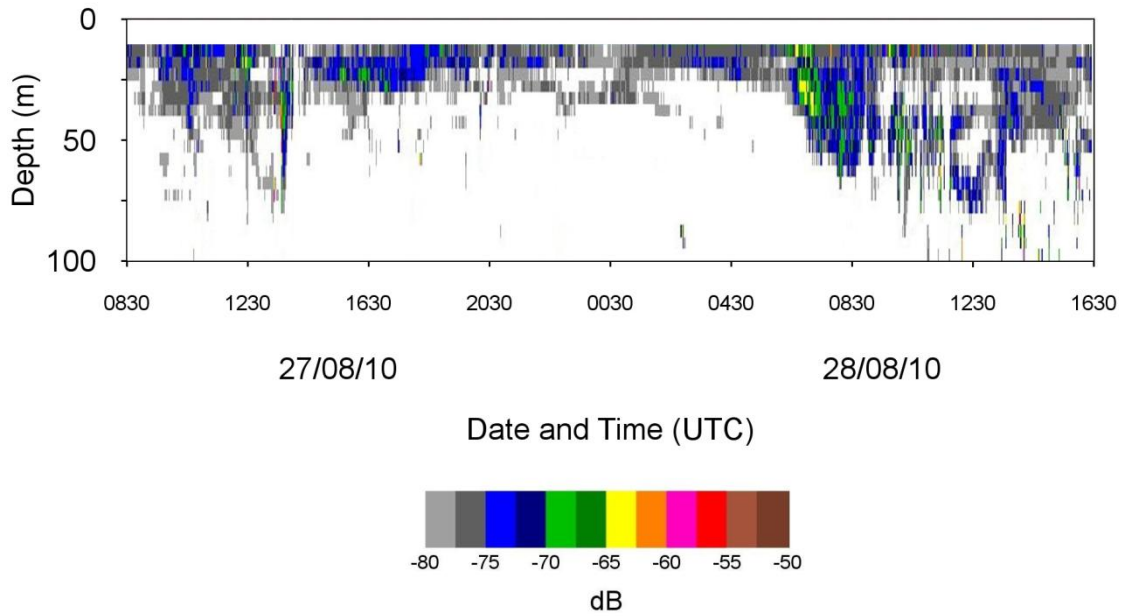


Fig 7.12) Volume backscatter [S_v (dB)] at 120 kHz (mean backscatter re-sampled every 100 seconds to condense echogram) from ICE19 (0 – 100 m depth). S_v is expressed using a colour scale between -80 and -50 decibels (dB). The top 12 m of the echogram are discarded due to near-field and noise (i.e. white section). NB – due to other instruments being run at periods during this 32 hour section, some interference will be included in this echogram.

7.3.5. Multivariate analysis of acoustic observations

No significant difference in the partitioned fourth-root transformed 120 kHz NASC data (25 m \times 20 min grid, $n = 315$) was found between ICE19 and ICE22 (analysis of similarity $R = 0.056$, $P = 0.086$), but a significant difference was found among day/night/morning samples ($R = 0.109$, $P = 0.026$). This difference between sampling times was similar to that found using the net-determined abundance data. When the morning sample (ICE22 D5) was excluded from the analysis, a significant difference still persisted between just the day and night NASC ($R = 0.103$, $P = 0.030$). Using similarity percentage analysis, depth layers 100-125 m and 150-175 m were highlighted as most responsible for the differences between day and night NASC (38% responsible). Significant differences were also found between the three classes of NASC

(mesozooplankton, macrozooplankton, nekton; $R = 0.411$, $P = 0.001$). Depth-stratified mesozooplankton and macrozooplankton NASC are comparatively similar (similarity percentage dissimilarity = 22.40) compared to the nekton depth-stratified NASC, with dissimilarity of 34.66 to mesozooplankton and 29.08 to macrozooplankton.

7.4. Discussion

7.4.1. Zooplankton DVM behaviour at ice-covered locations

Our data show differences in the depth distribution of some of the mesozooplankton species between day and night at both stations. Clearest signs of DVM were observed for *Calanus finmarchicus* (CI to adults) at ICE19 and for *Calanus finmarchicus* CII, CIII, *Metridia longa* CIV, CV, *Pseudocalanus* spp., *Oithona similis* and *Triconia borealis* at ICE19 and ICE22 combined. These differences were supported by ANOVA analysis on mean depth (Z_m) at ICE19 and ICE22. Abundance of *C. finmarchicus* CI and CII was however much higher at ICE19 compared to ICE22. *Calanus finmarchicus* is known as an indicator species for AtW masses (Søreide et al. 2008), and advection of AtW into the study area is the most likely origin of the young *C. finmarchicus* population.

The observed migrations in young stages of *C. finmarchicus* and in *Pseudocalanus* spp. appeared to be small-scale (approx. 20 m). The copepods avoided the well lit upper 40 m during the day and migrated into the 20-40 m layer at night. Highest Chl-*a* concentration in the 20-40 m layer indicates that food was available in this layer. As the light intensity (PAR) was very low below 20 m at night, the copepods may utilise the food source at 20-40 m with some protection from visual predators. During the day, light intensities reached minimal levels below 40 m, and migrating below this depth

may thus provide copepods with refuge from visual predators (Lampert 1989). The metabolic-demographic advantage hypothesis (*sensu* McLaren 1963) states that migrating copepods may gain a metabolic advantage by leaving the food-rich surface waters for deeper layers. However, in our study at high latitude, water temperature actually increases with depth within the observed migratory layers. This temperature increase makes it unlikely therefore that any metabolic advantage exists for migrants (Fortier et al. 2001). The avoidance of visual predators is thus likely to be the main driver of DVM in our study.

The surface layer (0-20 m) provided less favourable conditions for copepods. This was probably due to a combination of poor food supply (approximately $0.1 \text{ mg Chl-}a \text{ m}^{-3}$ compared to peak concentrations of $0.3\text{-}0.4 \text{ mg Chl-}a \text{ m}^{-3}$) and high visibility to predators due to higher light intensity. The surface layer (0-20 m) at both stations was largely melt water, with lower temperatures (approximately -1.5°C compared to $2\text{-}3^\circ\text{C}$ below the thermocline at 20-30 m) and salinities (approximately 32.3 compared to 34-35 below 20-30 m). Although other studies have shown high concentrations of *Calanus* in brackish meltwater below landfast sea ice when phytoplankton biomass was available for grazing (Hop et al. 2011), there is little phytoplankton biomass available at this depth in our study location. It is unlikely that ultraviolet radiation avoidance (Alonso et al. 2004) is creating this effect, as any negative effects to organisms from ultraviolet radiation are expected to be limited to the upper 5-10 m only (Tartarotti et al. 2000; Hanelt et al. 2001). Thus, the main reason for avoidance is likely a combination of little food and increased vulnerability to predation.

Throughout this thesis, the influence of advection on our observations of zooplankton has been important, and currents have often been observed to be strongest within the surface layers. In this chapter unlike chapter 6, LADCP measurements gave us current observations that were very closely matched temporally with net sampling events. Currents at ICE19 and ICE22 were generally stronger than observed elsewhere in this thesis, and horizontal velocities ranged between 20 – 450 mm/s. Indications of vertical migration in young stages of *C. finmarchicus* for example were most prominent in the upper 50 m, so if this layer in particular were subject to stronger currents, we may

expect greater day/night differences to be observed due to advection rather than vertical migration. However, current velocities at ICE19 D1, ICE19 N1, ICE22 D3 and ICE22 N2 remained relatively constant in both magnitude and direction between 0 – 250 m (Fig 7.5). These observations suggest that advective effects would occur equally throughout the 0 – 250 m layer, and observed day/night differences were more likely due to vertical migrations. However, high current velocities of > 100 mm/s would suggest that advection has some effect on our observations. As described in Fig 7.6, the ship drifted significantly during sampling at ICE19 and ICE22 with the strong currents. Thus although different (albeit close) locations were sampled during the day and night, if the patches of zooplankton drifted with the currents in a similar manner to the ship, we observed largely the same patch of zooplankton each time. If the ship was kept stationary however, advection would have brought different patches of zooplankton into contact with it. Regardless of drift and advection, a clear indication of typical DVM can be observed in the 32 hour echogram at ICE19 (Fig 7.12). It is less likely that this pattern was created by advective influences, and this lends weight to our conclusions of vertical migration creating the observed day/night differences

Older *Calanus* stages remained deeper in the water column and showed less signs of DVM. Abundances of stage CV and adult individuals in the upper 200 m were also very low for both *C. finmarchicus* and *C. glacialis*. MPS hauls taken from below 200 m at ICE 19 showed that these stages were concentrated deeper than 200 m (unpubl. data). This low abundance in surface waters and higher concentration well below 200 m indicates that a larger part of the population has already descended to overwintering depth at the end of August (Marshall and Orr 1958; Hirche 1983, Falk-Petersen et al. 2009). *Calanus finmarchicus* stage CIII still remaining in the upper 100 m displayed signs of DVM, and this was statistically supported by analysis of the day/night differences in combined mean depth (Z_m) at ICE19 and ICE22. These individuals still needed to feed in order to accumulate sufficient lipid stores and develop to overwintering stage (CV), and thus needed the food provided closer to the surface (Falk-Petersen et al. 2008). Although numbers of individuals were very low (especially at ICE19), mean depths indicated that the older stages of *Metridia longa* (CIV and CV) did carry out DVM at ICE22. These stages were located largely deeper than 150 m at

night, and were found in the upper 50 m during the day. *Metridia longa*, especially the larger stages, is known to be a diel vertical migrator (Hays 1995), but the very small number of individuals must be taken into account when assessing our evidence for this. *Fritillaria borealis* also appeared to contribute to the DVM signal, especially at ICE22.

The exhibition of DVM in *Pseudocalanus* spp. was consistent with previous studies from ice covered waters (Conover et al. 1988; Runge and Ingram 1991; Hattori and Saito 1997; Saito and Hattori 1997). Fortier et al. (2001) recorded a DVM magnitude of 20-40 m exhibited by *Pseudocalanus acuspes* in the Barrow Strait of the Canadian Arctic, which was similar to the DVM observed in *Pseudocalanus* spp. here. As a comparison with lower latitudes, Frost and Bollens (1992) observed highly variable migration behaviour in *Pseudocalanus newmani* at Dabob Bay (Washington) over a period of 3 years. The magnitudes of migration ranged between no-migration to DVM of approximately 40 m, which was similar to these observations in the Arctic. DVM has also been observed previously in *Calanus* species at high latitudes during midnight sun, but mainly for older stages (CIII-AF) of *C. glacialis* (Runge and Ingram 1991; Fortier et al. 2001). Fortier et al. (2001) recorded vertical migration magnitudes of circa 40 m within the 40-100 m depth layer by late copepodids and females of both *C. hyperboreus* and *C. glacialis* in early June, but no apparent DVM by these same stages and species earlier in May when they were observed mainly in deeper water. As this study was conducted later in the annual season, the older stages had likely built up sufficient lipid stores to overwinter at depth.

DVM in CI and CII has not been widely reported for the Arctic/Atlantic *Calanus* species specifically to date. Dale and Kaartvedt (2000) found that *C. finmarchicus* CI-III in the Norwegian Sea occurred higher in the water column at night. At lower latitudes, Osgood and Frost (1994) found indications of DVM in *Calanus pacificus* from Dabob Bay (Washington) for CII and CIII in the upper 25 m. These migrations were small-scale movements from the 0-25 m depth layer into the 0-10 m depth layer, and the magnitude of this vertical movement was similar to observations in this study for *C. finmarchicus* CI and CII. Durbin et al. (1995) studied *C. finmarchicus* at a temperate latitude (Gulf of Maine) during late spring, and found the magnitude of vertical

migration in all stages of *C. finmarchicus* (including CI and CII) to be as large as 50 m. These studies at lower latitude indicate that *C. finmarchicus* CI is capable of the observed vertical migrations in the Arctic. These prior studies also indicate that the vertical migrations of *Pseudocalanus* spp. and *Calanus* copepods in ice-covered waters (when present) are of a similar magnitude to their counterparts at lower latitudes.

Pseudocalanus and CI/CII of *Calanus* are similar in size (0.4-1.2 mm), indicating that they may avoid the same type of predator specialising on prey of this size-class. Predators that tend to hunt prey of this size include *T. libellula*, *E. hamata* and euphausiids (Øresland 1990; Auel and Werner 2003), and all these species were present in the net samples. These larger macrozooplankton species were likely to be responsible for much of the macrozooplankton backscatter identified in this study. *Eukrohnia hamata* was the only larger zooplankton species that showed signs of DVM based on abundance data derived from the Multinet samples. This species was absent in the upper 40 m at ICE19 during the day and in the upper 100 m at ICE22 at dawn. Other prey species of similar size, such as *O. similis*, *O. atlantica*, *Microcalanus* spp. and *T. borealis*, also indicated vertical migration behaviour. *Oithona similis* was abundant in the shallower layers, as has been observed in other studies (Auel and Hagen 2002; Walkusz et al. 2003; Blachowiak-Samolyk et al. 2006). *Microcalanus* spp., *O. atlantica* and *T. borealis* were concentrated deeper in the water column, largely avoiding the upper 40 m during both the day and night. These species are more omnivorous and may be less dependent on feeding in the algal-rich surface layer. These species are often found deeper in the water column (e.g. Blachowiak-Samolyk et al. 2006) and appear to be associated with Atlantic water. There are signs of deeper-water DVM in *O. atlantica* and *T. borealis*, since these species were found shallower at night (60-80 m and 40-60 m, respectively) than during the day (120-160 m and 60-80 m, respectively). Nekton NASC values were higher during the day at 50-75 m ($0.41 \text{ m}^2 \text{ nm}^{-2}$) and 100-125 m ($0.66 \text{ m}^2 \text{ nm}^{-2}$) than at night (0.17 and $0.30 \text{ m}^2 \text{ nm}^{-2}$, respectively), indicating the increased presence of predators at the depths which are avoided by these species during the day.

Although the DVM signal was not fully consistent in the acoustic record, combined mesozooplankton, macrozooplankton and nekton depth-stratified NASC at ICE19 and ICE22 displayed a small but significant difference between day and night samples during multivariate analysis, supporting the existence of a vertical migration signal. At ICE22, a significant difference was identified between the day and night NASC mean depth, possibly assisted by the higher number of acoustic sampling stations at ICE22 compared to ICE19. The mean depths of mesozooplankton and macrozooplankton NASC here were deeper in the morning compared to the noon samples, but deepest at night. This result is in contrast to ICE19, where no significant difference in NASC mean depth was identified. This difference between ICE19 and ICE22 is likely to be due to the variations in daytime NASC mean depth between the two sampling days and the smaller number of acoustic sampling stations at ICE19, and highlights the patchiness found in marine environments.

It is clear from the echograms that significant backscatter was present at both stations below 175 m, and an upward movement of this layer into the surface 175 m at night (i.e. classic DVM) would have created higher NASC in the deepest layers within our analysis framework. This made it difficult to conclude whether vertical migrations were classic or reverse DVM based on day/night differences in the upper 175 m. The methods used in this study, both acoustic and net based, were also potentially integrating both upward and downward movements within the water column (Tarling et al. 2002), masking signals and making them more difficult to detect.

The acoustic observations also provided insight into the vertical migration behaviour of the different groups (mesozooplankton, macrozooplankton and nekton) which could not be derived from the Multinet samples. The depth-stratified NASC of mesozooplankton and macrozooplankton were relatively similar to each other compared to the nekton depth-stratified NASC (Bray Curtis similarity matrix), and when day and night values were compared, the backscatter of nekton had insignificant R and p values and also the smallest magnitude between deepest and shallowest mean depth, indicating that this group was least responsible for DVM. In contrast to this apparent lack of coupling between nekton and mesozooplankton NASC, the close linkage of mesozooplankton

and macrozooplankton NASC showed that macrozooplankton predator species identified in net hauls (i.e. *Themisto libellula*, *Eukrohnia hamata* and *Thysanoessa longicaudata*) were situated in similar water depths to their prey throughout the diel cycle. This relationship indicated that any vertical movements by mesozooplankton prey species were tracked by macrozooplankton predators.

While net-samples identified the surface 20-40 m as a primary zone for small-scale DVM behaviour of younger copepodids, the 120 kHz backscatter identified the 100-125 m depth layer as most responsible for differences between day/night combined NASC values. The 120 kHz backscatter also included large zooplankton species which only appeared in small numbers in the Multinet. Larger and faster swimming species, such as amphipods (*Themisto*) and euphausiids were abundant in MIK net hauls and we suggest that these species account for the deeper vertical migration signal identified in the acoustic record.

When NASC was averaged across all stations, both mesozooplankton and macrozooplankton had higher NASC during the day (22.54 and 9.70 m² nm⁻² respectively) than at night (17.51 and 6.57 m² nm⁻² respectively) between 100-125 m. Mesozooplankton, macrozooplankton and nekton had higher NASC at night (8.55, 2.43 and 0.10 m² nm⁻² respectively) compared to the day (0.55, 0.38 and 0.07 m² nm⁻² respectively) in the 125-150 m layer just below. This higher mesozooplankton NASC at depth during the night compared to the day was likely due to the more mature, larger copepod stages (CIV – adults), which would create proportionally greater backscatter at 120 kHz even though they were less abundant. This signal may indicate reverse DVM, and this observation was supported by the net samples which displayed a statistically significant difference in mean depth for *M. longa* CIV and CV which were deeper during the night than during the day. Such patterns of reverse DVM by more mature stages of *M. longa* have been observed at higher latitudes in the previous chapter of this thesis.

For our study, the combined use of acoustic and net sampling effectively covered a broad range of taxa, and allowed us to accurately identify the smaller zooplankton

migrants while collecting DVM signals from larger taxa as well. Although specific predator species were not identified in this study, the primary depth layers at which nekton predators occur were identified, and future targeted pelagic sampling can aid in better identification of these species.

None of the species that dominated the Multinet samples showed any sign of midnight sinking. One possible reason may be that the depth resolution at ICE22 (50 m) was too coarse to observe small-scale sinking. As our results from ICE19 show, vertical migration can occur over a narrow range of 20-40 m. At ICE22, the acoustic record appeared to show sinking occurring between 00:45 and 01:15 UTC, with the scattering layer shifting from approximately 100-250 m to 150-300 m. The deeper section of this scattering layer (below 200 m) was below our sampling depth-range with the Multinet, and was largely composed of macrozooplankton and nekton backscatter. Thus, another reason for the lack of a midnight sinking signal in the net-collected abundances may be that the species responsible were not caught quantitatively by the Multinet. However, the acoustic record was not continuous enough at ICE22 to clearly determine any midnight sinking signal.

All our vertical migration conclusions must be interpreted within a dynamic system of advection much highlighted in this thesis. When mesozooplankton abundances were combined over 0-200 m at each location and compared, the R and p values quantifying the differences between day and night samples increased. This suggested that the overall abundances of mesozooplankton were changing between day and night sampling events and not just their depth distributions, signifying possible advection of animals through the study area. However, it should also be noted that the echograms at ICE22 in particular displayed zooplankton layers migrating up into the 0-200 m layer from below, and this vertical migration movement would create higher abundances in the net samples. Furthermore, our DVM inferences appear valid as the scattering layers within the acoustic record do not change greatly within the 1-h timescale chosen for data collection despite the prevailing currents.

7.4.3. Conclusion

This study provides further evidence supporting the existence of zooplankton DVM under ice in the high Arctic during late summer/autumn, when changes in the diel light cycle are apparent. The clearest classic DVM signals were displayed by younger *Calanus* copepodids within the surface 20-80 m (small-scale vertical migrations of approx. 20-40 m) and by *Pseudocalanus* spp. over a similar scale of magnitude but across a broader depth range of 20-150 m. This study also provides some evidence for reverse DVM by more mature stages below 125 m. These results were consistent with those from chapter 6 of this thesis. The low amplitude near-surface DVM was linked to the existence of a pronounced chlorophyll-*a* maximum at 25 m. Acoustic measurements and macrozooplankton net hauls have also identified the presence of nekton and macrozooplankton predators, and have shown that differences between day and night macrozooplankton backscatter were of a lesser magnitude compared to mesozooplankton. However, vertical migration was indicated far more strongly in mesozooplankton and macrozooplankton backscatter compared to nekton backscatter. In order to better describe the predator-prey relationships and vertical structure, targeted depth-stratified pelagic sampling designed to catch larger macrozooplankton and nekton is suggested during future investigations.

8. General discussion

This thesis has primarily focussed on the fjords of Svalbard that contain long term oceanic moorings, and has investigated both temporal and spatial aspects of zooplankton distribution at these locations. In this chapter I will focus primarily on the novel aspects of this research, the new conclusions drawn from them and the direction suggested for future studies.

8.1. Hydrodynamic control of zooplankton

As mentioned throughout this thesis, numerous studies at the Svalbard archipelago prior to this research have linked zooplankton community composition and abundances to prevailing hydrographic conditions (e.g. Kwasniewski et al. 2003; Willis et al. 2006; Daase and Eiane 2007; Blachowiak-Samolyk et al. 2008). This established link has been further described in this thesis for specific species of zooplankton and developmental stages of copepods, and as the spatial scale of this thesis was broader than any previously published work, it was able to compare many contrasting locations. The main results are:

- 1) Influxes of AtW strongly influence Kongsfjorden especially during spring/early summer, and these influxes vary both with depth (i.e. surface conditions alone cannot accurately indicate AtW influence) and between years. Species most associated with this advection include all three *Calanus* copepods, *Sagitta elegans*, and *Oikopleura* spp. Importantly, sediment trap evidence indicates almost all zooplankton appear unable to maintain continual residency within Kongsfjorden without advection into the fjord from the adjacent shelf during 'cold' years.

- 2) Arctic species (e.g. *Calanus glacialis*) currently persist at Kongsfjorden at comparatively high abundance despite the AtW influence
- 3) AtW associated *Calanus finmarchicus* in particular has been identified in high abundances at Rijpfjorden during summer, even when hydrography did not indicate the influence of AtW (temperature < 3°C and salinity < 33.5). Thus, high modification of AtW at Rijpfjorden is likely. AtW influence at Rijpfjorden is further indicated by the presence of *Themisto abyssorum*. Furthermore, *Calanus finmarchicus* has been identified in high abundances well beyond 81°N, indicating AtW reaches further north and east along the shelf break.
- 4) The appendicularians *Oikopleura* spp. and *Fritellaria borealis* are the quickest members of the zooplankton community to respond to rising temperatures at Rijpfjorden after the cold winter and can peak at very high abundances before other animals. This is likely promoted by advection into the fjord.
- 5) Advection at Rijpfjorden plays an important influencing role on zooplankton community composition as it does at Kongsfjorden. Numerous species are associated with this advection including all three *Calanus* copepods, *Pseudocalanus* spp, *Oikopleura* spp, and *Fritellaria borealis*. Larval stages of many organisms and younger copepodids are also advected into Rijpfjorden from the adjacent shelf.
- 6) Billefjorden during summer can be considered more ‘Arctic’ in terms of its *Calanus* complex than Rijpfjorden, with higher abundance of *Calanus glacialis* and lower abundance of *Calanus finmarchicus*. Rijpfjorden however continues to maintain high abundances of Arctic macrozooplankton (e.g. *Gammarus wilkitzkii*, *Themisto libellula*) and nekton which can vary considerably in abundance between years.
- 7) *Metridia longa* is consistently associated with colder Arctic conditions, dominating the zooplankton more during colder periods in the annual season and at colder locations.

Much of this hydrodynamic influence can be illustrated by a scheme of seasonal progression at Kongsfjorden and Rijpfjorden determined during this thesis (Fig 8.1).

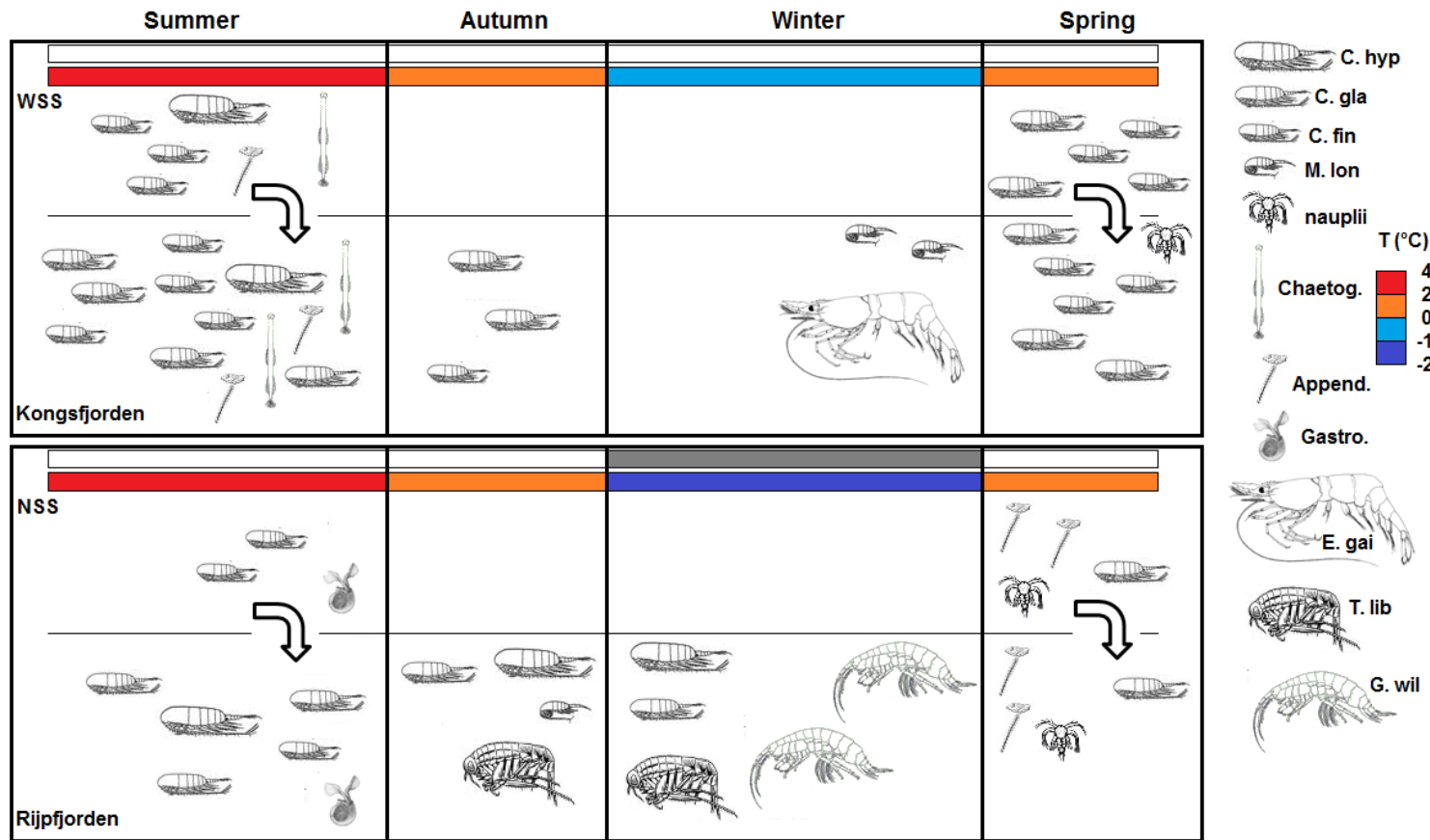


Fig 8.1) Generalised seasonal progression at Kongsfjorden (upper) and Rijpfjorden (lower). WSS = West Spitsbergen Shelf adjacent to Kongsfjorden, NSS = North Svalbard Shelf adjacent to Rijpfjorden. Arrows indicate dominant advection events into fjords. Grey represents sea ice cover. All temperature(s) are generalised approximations, and the timing of each 'season' varies considerably between years and location. [Chaetog. = Chaetognaths, Append. = Appendicularians, Gastro = Gastropods, all others are shortened species names]. Image density approximates animal abundance within a regime of variation. Only dominant animals recorded in sediment trap samples during each season are included. [All animal images gathered from the Arctic Ocean Diversity website and taxonomic keys supplied by NPI].

The new evidence from Rijpfjorden in particular has implications for climate change in the Arctic. As Rijpfjorden is now periodically influenced by AtW in summer, I suggest it should no longer be considered a consistent indicator of year round high Arctic zooplankton conditions. However, the lower latitude Kongsfjorden which has long been associated with strong AtW influence still maintains high abundances of ArW associated zooplankton species. Recently, Kwasniewski et al. (2010) described similar abundances of *Calanus glacialis* at two locations of contrasting hydrology (AtW vs. ArW) along the West coast of Svalbard, but vastly different abundances of *Calanus finmarchicus*. *Calanus glacialis* thus appears flexible enough to persist in locations influenced by AtW. I consider these observations evidence that the two fjords in particular and the western/northern shelf of the archipelago as a whole are becoming more homogenous in terms of their *Calanus* complex, which is now a mix of both Arctic and Atlantic associated species. Since this research began, a submitted study in 2009 (Tverberg et al. 2009) emphasised prevailing warm conditions on the West Spitsbergen Shelf between 2006 and 2008. Although prevailing ice and hydrographic conditions indicate colder and variable conditions since then, the evidence from this thesis suggests AtW influence continues within a regime of variation.

It should be noted that a certain amount of caution is required when linking species to water masses in this manner. Daase and Eiane (2007) reported an unexpected relationship between *Oithona similis* and temperature although indicators suggested this species should be largely indifferent to environmental forcing. Their study also highlighted how *Calanus glacialis* and *Pseudocalanus* spp. scaled better with latitude and bottom depth than with temperature and salinity, suggesting these factors may be stronger drivers of zooplankton spatial structure. This thesis has provided further evidence that factors such as bathymetry in particular play an important role in distributing zooplankton. The advection of AtW around Svalbard is well correlated with bathymetry (Saloranta and Svendsen 2001), making it difficult to separate the two.

Furthermore, using the *Calanus* complex as climate indicators may not be as straightforward as traditionally assumed. A very recent study (Gabrielsen et al. 2012) used molecular tools to compare the morphological and genetic identification of *Calanus* copepods from a number of regions around Svalbard. They found that morphological identification systematically overestimates the abundance of *Calanus finmarchicus* at the expense of *Calanus glacialis*, and thus the relative abundances of these species so heavily relied upon in this thesis and many other studies may be inaccurate. However, further indicator species from various taxa have been identified during this research to support the main conclusions.

I suggest the following further research is required to assess the results from this thesis:

- 1) High resolution bathymetry and physical observations (CTD casts to capture the water column profile) modelled against backscatter, especially along transects of similar depth to effectively remove bathymetry as an influencing factor and determine the effect of temperature alone on zooplankton.
- 2) The macrozooplankton community at Kongsfjorden, Billefjorden and Rijpfjorden should be compared using net samples to assess the relative abundances of ArW and AtW associated species at these sites and compare this relationship to the *Calanus* complex. This will indicate whether macrozooplankton are becoming more homogeneous around the archipelago alongside the *Calanus* complex, and assess the use of macrozooplankton as indicator species for climate changes. Macrozooplankton backscatter in this thesis was responsible both for DVM signals and for high levels of spatial heterogeneity, indicating an interesting avenue for study.

8.2. Spatial relevance of moored observations

At 0.5 nautical mile scale, zooplankton distribution has been identified as highly heterogeneous around the entire Svalbard archipelago. Backscatter observations highlighted the longest characteristic scales (i.e. distance of similar observations) within macrozooplankton, indicating larger zooplankton were aggregated in larger patches at this scale of observation. However, we are most interested in mesozooplankton in this thesis and in particular the fjords that contain moorings.

Within surface waters, the longest mesozooplankton characteristic scale of 1 nm was identified at Kongsfjorden. This was twice the distance identified at Rijpfjorden, which displayed no autocorrelation at 0.5 nm scale. Although this result must be treated with caution as sampling effort was vastly different at these locations (with only one transect available from Rijpfjorden), net samples collected in the two fjords at a similar spatial scale support the conclusion that Rijpfjorden is more heterogeneous at this scale than Kongsfjorden. The animals primarily responsible for the patchiness at both locations included larval forms, appendicularians, small gastropods and small copepods – all weak swimmers highly susceptible to advection. Since the work in this thesis began, Wallace et al. (2010) have reported that dominant current regimes vary between the two fjords, with currents at Rijpfjorden varying far more in direction throughout the year. This thesis has also put forward strong evidence of a highly dynamic system of advection around Svalbard. These changeable currents may be promoting higher levels of patchiness in Rijpfjorden compared to Kongsfjorden. This thesis has put forward evidence that advection is a dominant factor affecting small scale spatial variation in zooplankton. The highly patchy environment at both fjords indicates that at any one point in time, the moorings will only be sampling an area of approximately 1 nm^2 or less. This new information is important when considering moored observations. However, over a lengthy period of time within a dynamic environment highly influenced by advection, it is likely that moored observations will ultimately integrate observations from various patches.

This effect can be demonstrated using two 10 nautical mile transects from chapter 5 of this thesis, one from Kongsfjorden in 2008, and the other from Rijpfjorden in 2008 (Fig 8.2). We can imagine that these transects begin at two mooring locations at distance 0, and then extend out for 10 nautical miles. Assuming zooplankton are advected within water masses at the same rate as the water itself and with a constant current of 100 mm/s running from right to left along the echograms (i.e. bringing the water mass observed in the echogram directly towards the mooring at distance 0), the time scale describes how long it would take before the mooring observes each section of the transect (Fig 8.2). In this scenario, it would take the mooring at Kongsfjorden approximately 30 hours to observe the large patch of zooplankton (blue on Fig 8.2) which started approximately 6 nautical miles away from the mooring. Under these conditions, the moorings would observe zooplankton over a 10 nautical mile range in approximately 48 hours although they themselves are fixed in place. As observations in this thesis suggest that Rijpfjorden maintains a more variable current regime with greater horizontal velocities, we might expect the mooring at Rijpfjorden to integrate a greater spatial range into its observations than the moorings at Kongsfjorden and Billefjorden. However, although this simplistic model allows us to visualise how moorings increase their spatial range of observation under increasing levels of advection, currents are continually changing their direction and magnitude (as described in this thesis) and thus the spatial relevance of each mooring will be continually changing.

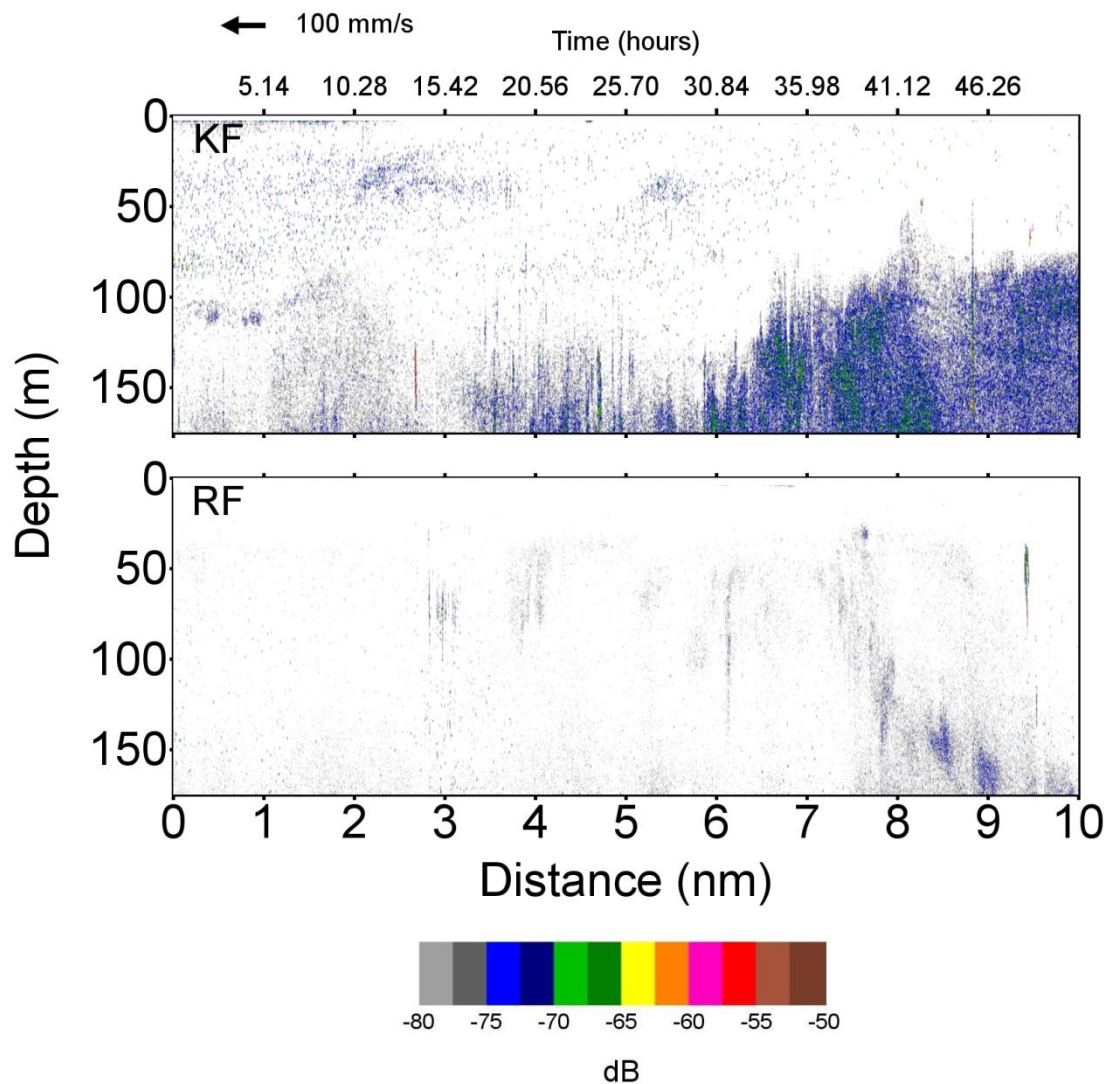


Fig 8.2) Volume backscatter [S_v (dB)] at 120 kHz along a 10 nm transect at Kongsfjorden 2008 (KF – above) and Rijpfjorden 2008 (RF – below) [0 – 175 m depth]. S_v is expressed using a colour scale between -80 and -50 decibels (dB). The top 6 m of the echogram are discarded due to near-field and noise (i.e. white section). Arrow represents theoretical horizontal current velocity of 100 mm/s running from right to left along the echogram throughout the entire water column, and time scale (in hours) represents the length of time required before the horizontal current brings a particular portion of the echogram to the zero distance mark (i.e. x axis origin).

On a broader scale, this research suggests that the dominating regime around the Svalbard archipelago is one of variation. Recently, Trudnowska et al. (2012) used an Optical Plankton Counter alongside acoustic observations to describe zooplankton

assemblages up to a few km in size along the northern WSS, highlighting this regime of variation. The variation identified in this thesis affects interannual zooplankton distributions within a certain location, and also the relationship between locations in different years. A similar regime of variation in zooplankton between regions was identified recently among northeast Atlantic regions subject to climate change (McGinty et al. 2011).

However, one common theme from this research is that deeper off-shelf locations cluster together separately from shelf locations, indicating depth is a significant factor affecting the distribution of animals around the archipelago. Within the regime of variation, this thesis has compared both Kongsfjorden and Rijpfjorden to the pan-Svalbard system as a whole.

Firstly, it becomes apparent that the similarity between Kongsfjorden, Rijpfjorden, the adjacent shelf or Svalbard as a whole depends largely on the animals in question. When net abundances of mesozooplankton were clustered, Kongsfjorden was largely similar to the adjacent WSS and was different to Rijpfjorden. Similarly, Rijpfjorden clustered together with the adjacent shelf to the north. No fjord gradients were discernible with this broad scale clustering. Thus, with these clusters, the moorings within each fjord appear to be sampling different regions and are representative of the entire fjord length and the adjacent shelf. However, these net abundances were integrated over the water column in order to avoid the effects of vertical migration between samples collected at different times, and so this clustering does not include changes in vertical distribution. It is based purely on the relative abundances of mesozooplankton species. A recent study has highlighted how the input of glacial meltwater can affect the vertical distribution of zooplankton (Hylander et al. 2011), and so we would expect a spatial gradient in vertical distributions along our glacial fjords.

Two main biological observations are routinely carried out by the oceanic moorings. ADCP's collect information on zooplankton movements (which can be used in studies of vertical migration but cannot identify which species are responsible for the observations), and sediment traps collect zooplankton species present in the water column. Thus, spatial changes in the relative depth distributions of animals are important when assessing the relevance of ADCP observations, and more taxa should be included when assessing the spatial relevance of sediment trap samples that include macrozooplankton species. When depth stratified backscatter observations were clustered (including macrozooplankton and nekton backscatter alongside mesozooplankton), a more variable picture of the archipelago was created. Kongsfjorden became different to the adjacent shelf in some years (e.g. 2007, 2010) but not in others (e.g. 2006), and the variation from inner – outer fjord also differed between years. The relationship between Rijpfjorden and the adjacent shelf was also variable. In 2008 and 2009 Rijpfjorden clustered together with locations on the shelf eastward beyond 12°E. When stations beyond the shelf break to the northeast were sampled in 2010, Rijpfjorden clustered with many of them. In 2008 and 2009, locations from Rijpfjorden and Kongsfjorden also clustered together. Thus when depth stratification and further taxa were included, the area represented by each mooring changed dramatically and was more variable between years. In general however the picture was now one of greater similarity between Kongsfjorden and Rijpfjorden but greater variation within each fjord along the fjord gradients.

These results further support our conclusion of spatial heterogeneity within the fjords, and this variation appears to be greater within macrozooplankton and nekton compared to mesozooplankton. On a broad scale however, Kongsfjorden and Rijpfjorden appear more similar based on their respective backscatter profiles than their mesozooplankton community compositions.

Ultimately, if the aim of the mooring at Kongsfjorden is to consistently observe conditions characteristic of AtW influence (note the use of 'conditions' rather than

‘mesozooplankton community composition’ as backscatter observations include numerous taxa), then I suggest the mooring should be placed on the shelf adjacent to Kongsfjorden. The adjacent shelf can be different to conditions within the fjord but is more representative of broader conditions along the WSS and further north influenced by AtW. Similarly at Rijpfjorden, if the aim of the mooring is to consistently observe Arctic conditions, I suggest the east Svalbard coast or Barents Sea east/southeast of the archipelago is a better location. However, the value of the long term ecosystem monitoring data sets at Kongsfjorden and Rijpfjorden within the wider regime of a warming Arctic and the wealth of information from these locations will ensure the current moorings stay in place. Thus, locating moored platforms at the areas suggested in this thesis is suggested if future opportunities arise.

In order to build on these results, especially if informing the positioning of a future mooring, I suggest the following research is required:

- 1) Longer transects along designed sampling grids are required to accurately assess the characteristic scale of backscatter observations at a number of integration scales around the archipelago, and especially within the fjords that contain the moorings (i.e. Kongsfjorden, Rijpfjorden and Billefjorden). Considering multiple scales for the aggregation of pelagic organisms is considered highly important (Lavoie et al. 2000). Furthermore, in order to classify regions for comparison, a recent study (McGinty et al. 2011) used satellite derived chl-*a* measurements to define areas over which to combine Continuous Plankton Recorder data. I suggest a similar approach is used to define sectors around Svalbard for comparison.
- 2) Observations should be made at more points in the annual cycle in order to assess differences in spatial aggregation throughout the highly seasonal Arctic regime.
- 3) More observations should be made along the east coast and south east of the archipelago around Hopen (mesozooplankton and macrozooplankton net hauls

and acoustic sampling) to determine if these locations are better year round indicators of Arctic conditions than Rjippfjorden, and assess any differences.

8.3. The prevalence of summer diel vertical migration

The evidence generated in this thesis for DVM behaviour during summer at high latitude is largely for low amplitude DVM in surface waters when a food source is available to copepods. The importance of a food source as a factor in driving vertical migrations has recently been suggested to be greater than the requirement of a strong diel light cycle (Wallace et al. 2010), and our evidence supports this. Younger copepodids were identified as performing these migrations, and this information is new to DVM studies at this latitude. Our investigations utilised both higher vertical resolution net samples than prior studies and acoustic observations to observe these low amplitude migrations. During this research, it became clear that vertical migration signals were more prevalent within the acoustic observations, and this was due to two main factors:

- 1) The higher temporal and vertical resolution of the observations (i.e. integrated over a longer period of time and at higher vertical resolution)
- 2) The inclusion of taxa and targets not sampled representatively by the MPS

Both chapters 6 and 7 of this thesis stress the need for depth stratified pelagic sampling designed to sample larger macrozooplankton and nekton and relate the vertical movements of these predators to their mesozooplankton prey. Any future DVM studies should include this sampling regime alongside MPS sampling and multi-frequency acoustic observations.

This thesis has put forward evidence for high levels of advection within the fjords of Svalbard. During the investigation of DVM at these locations, it became difficult to determine whether diel changes were due to the advection of zooplankton or their vertical movements. Advection was identified as being most significant within surface layers, with the greatest effects on weak swimmers. This coincides with both the depth layer and mesozooplankton type deemed most responsible for DVM. To clarify this, I suggest future studies on DVM should use a sampling regime which is a combination of chapters 4 and 7 of this thesis. At each extreme of the diel cycle, depth stratified net hauls of mesozooplankton and macrozooplankton alongside multi-frequency acoustic observations should be gathered from three locations 0.5 – 1 nm apart. Although this triples the sampling effort, the comparison of variation within each set of three samples vs. the extremes of the diel cycle should create a framework for answering the ‘advection or DVM’ problem. In addition, replicate samples should be gathered at each extreme of the diel cycle. If the same signals are observed through a number of replicates, advection is unlikely to be the dominant driver of day/night differences.

Transect data may also be used to assess how much advection will affect our DVM conclusions (for example the transects from Kongsfjorden and Rijpfjorden displayed in Fig 8.2). Although the Kongsfjorden transect contains higher density patches and greater volume backscatter, the Rijpfjorden transect may be considered patchier in terms of its heterogeneity. Evidence from this thesis suggests that Rijpfjorden is the patchier of the two fjords overall, and it also maintains a more variable current regime with greater horizontal velocities. In this patchier fjord, advection will have a greater influence on any point sampling method (such as vertical zooplankton net hauls), as two repeat samples may observe significantly different patches of zooplankton. Thus, conclusions of DVM based on day/night differences may be less reliable at Rijpfjorden compared to Kongsfjorden. However, longer term sampling methods (such as the sediment trap deployed on a mooring and acoustic observation of DVM) will integrate such patches over time leading to more robust results. Under the influence of advection, samples collected at one point in space over a long period of time essentially increase their spatial range (see Fig 8.2). In order to best incorporate these factors, this thesis

uses a combination of sampling techniques to create a robust set of conclusions that combine spatial and temporal aspects of zooplankton observation

Finally I should note that a frequency of 120 kHz may not be sufficient to generate significant proportions of backscatter from the smaller mesozooplankton found at Svalbard. However, 200 kHz is limited to 125 m effective depth. Thus, the use of a high frequency profiler which can be lowered into the water column and located closer to the required targets would be beneficiary. The latest studies of zooplankton are following this trend and integrate a number of high frequency observations (e.g. Warren and Patrician 2011), and this technology should be used as far as possible in the future.

References

- Aagaard, K., Greisman, P., 1975. Towards new mass and heat budgets in the Arctic Ocean. *Journal of Geophysical Research*. 80, 3821-3827.
- Abdi, H., Molin, P., 2007. Lilliefors/Van Soest's test of normality. In: Salkind, N.J., Rasmussen, K. (eds.), *Encyclopedia of measurement and statistics*. Sage Publications, Thousand Oaks, California.
- ACIA, 2004. *Impacts of a Warming Arctic. Summary report of the Arctic Climate Impact Assessment*. Cambridge University Press, Cambridge, UK.
- Aksnes, D.L., Aure, J., Kaartvedt, S., Magnesen, T., Richard, J., 1989. Significance of advection for the carrying capacities of fjord populations. *Marine Ecology Progress Series*. 50, 263-274.
- Alexandrov, Ye.I., Maistrova, V.V., 1998. The comparison of the air temperature measurements for the polar regions. *The Antarctica*. 34, 60-72.
- Allredge, A.L., Hamner, W.M., 1980. Recurring aggregation of Zooplankton by a tidal current. *Estuarine and Coastal Marine Science*. 10(1), 31-37.
- Alonso, C., Rocco, V., Barriga, J.P., Battini, M.A., Zagarese, H., 2004. Surface avoidance by freshwater zooplankton: Field evidence on the role of ultraviolet radiation. *Limnology and Oceanography*. 49, 225-232.
- Ambrose, W.G., Renaud, P.E., 1995. Benthic response to water column productivity patterns: evidence for benthic–pelagic coupling in the Northeast Water Polynya. *Journal of Geophysical Research*. 100, 4411–4421.
- Anisimov, O.A., Fitzharris, B., 2001. 'Polar regions (Arctic and Antarctic)', in McCarthy, O.F.C. J., Leary, N.A., Dokken, D.J., White, F.S. (eds.), *Climate Change 2001: Impacts, Adaptation, and Vulnerability. Contribution of Working group II to the Third Assessment Report of the Intergovernmental Panel on Climate Change*, Cambridge University Press, Cambridge, 801-841.
- Arashkevich, E., Wassmann, P., Pasternak, A., Riser, C.W., 2002. Seasonal and spatial changes in biomass, structure, and development progress of the zooplankton community in the Barents Sea. *Journal of Marine Systems*. 38, 125-145.
- Arrigo, K.R., Thomas, D.N., 2004. Large scale importance of sea-ice biology in the Southern Ocean. *Antarctic Science*. 16, 471-486.

- Arnkvaern, G., Daase, M., Eiane, K., 2005. Dynamics of coexisting *Calanus finmarchicus*, *Calanus glacialis* and *Calanus hyperboreus* populations in a high-Arctic fjord. *Polar Biology*. 28, 528-538.
- Ashjian, C.J., Campbell, R.G., Welch, H.E., Butler, M., Van Keuren, D., 2003. Annual cycle in abundance, distribution, and size in relation to hydrography of important copepod species in the western Arctic Ocean. *Deep Sea Research II*. 50(10-11), 1235-1261.
- Auel, H., Hagen, W., 2002. Mesozooplankton community structure, abundance and biomass in the central Arctic Ocean. *Marine Biology*. 140, 1013-1021.
- Auel, H., Werner, I., 2003. Feeding, respiration and life history of the hyperiid amphipod *Themisto libellula* in the Arctic marginal ice zone of the Greenland Sea. *Journal of Experimental Marine Biology and Ecology*. 296, 183-197.
- Bainbridge, R., 1957. The size, shape and density of marine phytoplankton concentrations. *Biological Reviews*. 32, 91-115.
- Båmstedt, U., Tande, K.S., Nicolajsen, H. 1985. Local variations in size and activity among *Calanus finmarchicus* and *Metridia longa* overwintering on the west coast of Norway. *Journal of Plankton Research*. 6, 843-857.
- Barthel, C-G., 1995. Zooplankton dynamics in Balsfjorden, northern Norway. In: Skjoldal, H.R., Hopkins, C., Erikstad, K.E., Leinaas, H.P., (eds). *Ecology of fjords and coastal waters*. Elsevier, Amsterdam, 113-126.
- Bartlett, M., S., 1936. The information available in small samples. *Proceedings of the Cambridge Philosophical Society*. 32, 560-566.
- Basedow, S.L., Eiane, K., Tverberg, V., Spindler, M., 2004. Advection of zooplankton in an Arctic fjord (Kongsfjorden, Svalbard). *Estuarine, Coastal and Shelf Science*. 60, 113-124.
- Beaugrand, G., Reid, P.C., Ibanez, F., Lindley, J.A., 2002. Diversity of calanoid copepods in the North Atlantic and adjacent seas: species associations and biogeography. *Marine Ecology Progress Series*. 232, 179-195.
- Beever, E.A., Swihart, R.K., Bestelmeyer, B.T., 2006. Linking the concept of scale to studies of biological diversity: evolving approaches and tools. *Diversity and Distributions*. 12, 229-235.
- Benoit, D., Simard, Y., Fortier, L., 2008. Hydro-acoustic detection of large winter aggregations of Arctic cod (*Boreogadus saida*) at depth in ice-covered Franklin Bay (Beaufort Sea). *Journal of Geophysical Research - Oceans*. 113. C06S90. doi:10.1029/2007JC004276

- Berge, J., Cottier, F., Last, K.S., Varpe, Ø., Leu, E., Søreide, J., Eiane, K., Falk-Petersen, S., Willis, K., Nygård, H., Vogedes, D., Griffiths, C., Johnsen, G., Lorentzen, D., Brierley, A.S., 2009. Diel vertical migration of Arctic zooplankton during the polar night. *Biology Letters*. 5, 69-72.
- Berge, J., Johnsen, G., Nilsen, F., Gulliksen, B., Slagstad, D., 2005. Ocean temperature oscillations enable reappearance of blue mussel *Mytilus edulis* in Svalbard after 1000 yr absence. *Marine Ecology Progress Series*. 303, 167-175.
- Bigelow, H.B., 1926. Plankton of the offshore waters of the Gulf of Maine. *Bulletin of the Bureau of Fisheries*. 40, 1-509.
- Blachowiak-Samolyk, K., Kwasniewski, S., Richardson, K., Dmoch, K., Hop, H., Falk-Petersen, S., Mouritsen, L.T., 2006. Arctic zooplankton do not perform diel vertical migration (DVM) during periods of midnight sun. *Marine Ecology Progress Series*. 308, 101-116.
- Blachowiak-Samolyk, K., Søreide, J.E., Kwasniewski, S., Sundfjord, A., Hop, H., Falk-Petersen, S., Hegseth, E.N., 2008. Hydrodynamic control of mesozooplankton abundance and biomass in northern Svalbard waters (79-81°N). *Deep Sea Research II*. doi:10.1016/j.dsr2.2008.05.018.
- Bollens, S.M., Frost, B.W., 1989. Zooplanktivorous fish and variable diel vertical migration in the marine planktonic copepod *Calanus pacificus*. *Limnology and Oceanography*. 34, 1072-1083.
- Bond, G.C., Showers, W., Elliot, M., Evans, M., Lotti, R., Hajdas, I., Bonani, G., Johnson, S., 1999. The North Atlantic's 1–2 kyr climate rhythm: Relation to Heinrich events, Dansgaard/Oeschger cycles and the Little Ice Age. In *Mechanisms of millennial-scale global climate change*, eds. Clark, P.U., Webb, R.S., Keigwin, L.D., AGU Monograph, 385-394.
- Borzenkova, I.I., 1999. Environmental indicators of recent global warming. In: *Environmental Indices* [Pykh, Y.A., Yuri, A., Hyatt, D.E., Lenz, R.J.M., (eds.)]. EOLSS Publishing Company, Baldwin House, London, United Kingdom, 455-465.
- Bouchard, C., Fortier, L., 2008. Effects of polynyas on the hatching season, early growth and survival of polar cod *Boreogadus saida* in the Laptev Sea. *Marine Ecology Progress Series*. 355, 247-256.
- Box, G., Jenkins, G., 1976. *Time series analysis: forecasting and control*. Holden-Day, San Francisco.
- Bracco, A., Provenzale, A., Scheuring, I., 2000. Mesoscale vortices and the paradox of the plankton. *Proceedings of the Royal Society of London B*. 267, 1795-1800.

- Brander, K.M., Blom G., Borges, M.F., Erzini, K., Henderson, G., MacKenzie, B.R., Mendes, H., Santos, A.M.P., Toresen, P., 2003. Changes in fish distribution in the eastern North Atlantic: are we seeing a coherent response to changing temperature? ICES Marine Science Symposia. 219, 260-273.
- Brentnall, S.J., Richards, K.J., Brindley, J., Murphy, E., 2003. Plankton patchiness and its effect on larger-scale productivity. *Journal of Plankton Research*. 25, 121-140.
- Breur, A., 2003. Influences of advection on local dynamics of overwintering zooplankton in an arctic sill fjord. Thesis, Wageningen University, 1-38.
- Brierley, A.S., Axelsen, B.E., Buecher, E., Sparks, C.A.J., Boyer, H., Gibbons, M.J., 2001. Acoustic observations of jellyfish in the Namibian Benguela. *Marine Ecology Progress Series*. 210, 55-66.
- Brierley, A.S., Boyer, D.C., Axelsen, B.E., Lynam, C.P., Sparks, C.A.J., Boyer, H.J., Gibbons, M.J., 2005. Towards the acoustic estimation of jellyfish abundance. *Marine Ecology Progress Series*. 295, 105-111.
- Brierley, A.S., Ward, P., Watkins, J.L., Goss, C., 1998. Acoustic discrimination of Southern Ocean zooplankton. *Deep Sea Research II*. 45, 1155-1173.
- Brierley, A.S., Watkins, J.L., Murray, A.W.A., 1997. Interannual variability in krill abundance at South Georgia. *Marine Ecology Progress Series*. 150, 87-98.
- Brodeur, R.D., Mills, C.E., Overland, J.E., Walters, G.E., Schumacher, J.D., 1999. Evidence for a substantial increase in gelatinous zooplankton in the Bering Sea, with possible links to climate change. *Fisheries Oceanography*. 8, 296-306.
- Brodsky, K.A., 1950. Calanoida of the Far Eastern Seas and Polar Basin of the USSR. *Opred. Fauna SSSR vol 35*. Publishing House of the USSR Academy of Sciences, Leningrad.
- Brodsky, K.A., 1967. Calanoida of the Far Eastern Seas and Polar Basin of the USSR. *Keys to the Fauna of the USSR*. 35, 440 (Translated from Russian).
- Cassie, R.M., 1959. Some correlation in replicate plankton samples. *New Zealand Journal of Science*. 2, 473-484.
- Cassie, R.M., 1963. Microdistribution of plankton. *Oceanography and Marine Biology: Annual Review*. 1, 223-252.
- Cavaleri, D.J., Gloersen, P., Parkinson, C.L., Comiso, J.C., Zwally, H.J., 1997. Observed hemispheric asymmetry in global sea ice changes. *Science*. 278, 1104-1106.
- Chapman, W.L., Walsh, J.E., 1993. Recent variations of sea ice and air temperatures in high latitudes, *Bulletin of the American Meteorological Society*. 74, 33-47.

- Cisewski, B., Strass, V.H., Rhein, M., Krägefsky, S., 2009. Seasonal variation of diel vertical migration of zooplankton from ADCP backscatter time series data in the Lazarev Sea, Antarctica. *Deep Sea Research I*. doi:10.1016/j.dsr.2009.10.005.
- Clark, D.R., Aazem, K.V., Hays, G.C., 2001. Zooplankton abundance and community structure over a 4000 km transect in the North-east Atlantic. *Journal of Plankton Research*. 23, 365-372.
- Clarke, K.R., Gorley, R.N., 2006. Primer v6: user manual/tutorial. Primer-E Ltd, Plymouth.
- Clay, C.S., Medwin, H., 1977. In McCormick, M., (ed.). *Acoustical Oceanography: Principles and Applications*. John Wiley and Sons, New York, pp 544.
- Conover, R.J., 1988. Comparative life histories in the genera *Calanus* and *Neocalanus* in high latitudes of the Northern Hemisphere. In Boxhall, G.A., Schminke, H.K., (eds), *Biology of Copepods*. *Hydrobiologia*. 167/168, 127-142.
- Conover, R.J., Bedo, A.W., Herman, A.W., Head, E.J.H., Harris, L.R., Horne, E.P.W., 1988. Never trust a copepod - Some observations on their behavior in the Canadian Arctic. *Bulletin of Marine Science*. 43, 650-662.
- Conover, R., Huntley, M., 1991. Copepods in ice covered seas – Distribution, adaptations to seasonally limited food, metabolism, growth patterns and life cycle strategies in polar seas. *Journal of Marine Systems*. 2, 1-41.
- Cottier, F.R., Nilsen, F., Inall, M.E., Gerland, S., Tverberg, V., Svendsen, H., 2007. Wintertime warming of an Arctic shelf in response to large-scale atmospheric circulation. *Geophysical Research Letters*. 34(L10607), 5. doi:10.1029/2007GL029948.
- Cottier, F.R., Tarling, G.A., Wold, A., Falk-Petersen, S., 2006. Unsynchronised and synchronised vertical migration of zooplankton in a high arctic fjord. *Limnology and Oceanography*. 51(6), 2586-2599.
- Cottier, F., Tverberg, V., Inall, M., Svendsen, H., Nilsen, F., Griffiths, C., 2005. Water mass modifications in an Arctic fjord trough cross-shelf exchange: the seasonal Hydrography of Kongsfjorden. Svalbard. *Journal of Geophysical Research*. 110, C12005. doi:10.1029/2004JC002757.
- Cushing, D.H., 1951. The vertical migration of planktonic Crustacea. *Biological Reviews*. 26, 158-192.
- Cushing, D., 1982. *Climate and Fisheries*. Academic Press, London. 373.
- Daase, M., Eiane, K., 2007. Mesozooplankton distribution in northern Svalbard waters in relation to hydrography. *Polar Biology*. 30, 969-981.

- Daase, M., Eiane, K., Aksnes, D.L., Vogedes, D., 2008. Vertical distribution of *Calanus* spp. and *Metridia longa* at four Arctic locations. *Marine Biology Research*. 4, 193-207.
- Daase, M., Vik, J.O., Bagøien, E., Stenseth, N.C., Eiane, E., 2007. The influence of advection on *Calanus* near Svalbard: statistical relations between salinity, temperature and copepod abundance. *Journal of Plankton Research*. 29(10), 903-911.
- Dagg, M.J., Frost, B.W., Newton, J., 1998. Diel vertical migration and feeding in adult female *Calanus pacificus*, *Metridia lucens* and *Pseudocalanus newmani* during a spring bloom in Dabob Bay, a fjord in Washington USA. *Journal of Marine Systems*. 15, 503-509.
- Dale, T., Kaartvedt, S., 2000. Diel patterns in stage-specific vertical migration of *Calanus finmarchicus* in habitats with midnight sun. *ICES Journal of Marine Science*. 57, 1800-1818.
- Dalpadado, P., 2002. Inter-specific variations in distribution, abundance and possible life-cycle patterns of *Themisto* spp. (Amphipoda) in the Barents Sea. *Polar Biology*. 25(9), 656-666.
- Dalpadado, P., Borkner, N., Bogstad, B., Mehl, S., 2001. Distribution of *Themisto* (Amphipoda) spp. in the Barents Sea and predator-prey interactions. *ICES Journal of Marine Science*. 58, 876-895.
- De Robertis, A., Higginbottom, I., 2007. A post-processing technique to estimate the signal-to-noise ratio and remove echosounder background noise. *ICES Journal of Marine Science*. 64, 1282-1291.
- De Robertis, A., Jaffe, J.S., Ohman, M.D., 2000. Size-dependent predation risk and the timing of vertical migration in zooplankton. *Limnology and Oceanography*. 45, 1838-1844.
- Deser, C., 2000. On the teleconnectivity of the “Arctic Oscillation”. *Geophysical Research Letters*. 27, 779-82.
- Dickson, R.R., Osborn, T.J., Hurrell, J.W., Meincke, J., Blindheim, J., Adlandsvik, B., et al., 2000. The Arctic Ocean response to the North Atlantic oscillation. *Journal of Climate*. 13, 2671-96.
- Diel, S., Tande, K., 1992. Does the spawning of *Calanus finmarchicus* in high-latitudes follow a reproducible pattern. *Marine Biology*. 113(1), 21-31.
- Dippner, J., Ottersen, G., 2001. Cod and climate variability in the Barents Sea. *Climate Research*. 17, 73-82.
- Douglas, M.S.V., Smol, J.P., Blake Jr., W., 1994. Marked post-18th century environmental change in high arctic ecosystems. *Science*. 226, 416-419.

- Durbin, E.G., Gilman, S.L., Campbell, R.G., Durbin, A.G., 1995. Abundance, biomass, vertical migration and estimated development rate of the copepod *Calanus finmarchicus* in the southern Gulf of Maine during late spring. *Continental Shelf Research*. 15, 571-591.
- Edvardsen, A., Slagstad, D., Tande, K.S., Jaccard, P., 2003. Assessing zooplankton advection in the Barents Sea using underway measurements and modelling. *Fisheries Oceanography*. 12, 61-74.
- Engelsen, O., Hegseth, E.N., Hop, H., Hansen, E., Falk-Petersen, S., 2002. Spatial variability of chlorophyll a in the marginal ice zone of the Barents Sea, with relations to sea ice and oceanographic conditions. *Journal of Marine Systems*. 35(1-2), 79-97.
- Falkenhaus, T., Tande, K.S., Semenova, T., 1997. Diel, seasonal and ontogenetic variations in the vertical distributions of four marine copepods. *Marine Ecology Progress Series*. 149, 105-119.
- Falk-Petersen, S., Hagen, W., Kattner, G., Clarke, A., Sargent, J.R., 2000. Lipids, trophic relationships and biodiversity in Arctic and Antarctic Krill. *Canadian Journal of Fisheries and Aquatic Sciences*. 57, 178-191.
- Falk-Petersen, S., Hop, H., Budgell, W.P., Hegseth, E.N., Korsnes, R., Løyning, T.B., Ørbæk, J.B., Kawamura, T., Shirasawa, K., 2000b. Physical and ecological processes in the marginal ice zone of the northern Barents Sea during the summer melt periods. *Journal of Marine Systems*. 27(1-3), 131-159.
- Falk-Petersen, S., Hopkins, C.C.E., Sargent, J.R., 1990. Trophic relationships in the pelagic food web. In: Barnes, M., Gibson, R.N., (eds.) *Trophic Relationships in the Marine Environment*. Aberdeen University Press, Aberdeen, 315-333.
- Falk-Petersen, S., Leu, E., Berge, J., Kwasniewski, S., Nygard, H., Rostad, A., Keskinen, E., Thormar, J., von Quillfeldt, C., Wold, A., Gulliksen, B., 2008. Vertical migration in high Arctic waters during autumn 2004. *Deep Sea Research II*. 55, 2275-2284.
- Falk-Petersen, S., Mayzaud, P., Kattner, G., 2009. Lipids, life strategy and trophic relationships of *Calanus hyperboreus*, *C. glacialis* and *C. finmarchicus* in the Arctic. *Marine Biology Research*. 5(1), 18-39.
- Falk-Petersen, S., Pedersen, G., Kwasniewski, S., Hegseth, E.N., Hop, H., 1999. Spatial distribution and life cycle timing of zooplankton in the marginal ice zone of the Barents Sea during the summer melt season in 1995. *Journal of Plankton Research*. 21, 1249-1264.

- Falk-Petersen, S., Timofeev, S., Pavlov, V., Sargent, J.R., 2007. Climate variability and possible effects on arctic food chains: The role of *Calanus*. In: Ørbæk, J.B., Tombre, T., Kallenborn, R., Hegseth, E.N., Falk-Petersen, S., Hoel, A.H. (Eds.), *Arctic-Alpine Ecosystems and People in a Changing Environment*. Springer, Berlin. 147–166.
- Fasham, M.J., Angel, M.V., Roe, H.S.J., 1974. An investigation of the spatial pattern of zooplankton using the Longhurst-Hardy Plankton Recorder. *Journal of Experimental Marine Biology and Ecology*. 16, 93-112.
- Feder, H.M., Norton, D.W., Geller, J.B., 2003. A review of apparent 20th Century changes in the presence of mussels (*Mytilus trossulus*) and macroalgae in Arctic Alaska, and of historical and paleontological evidence used to relate mollusc distributions to climate change. *Arctic*. 56, 391-407.
- Fields, D.M., Yen J., 1997. The escape behaviour of marine copepods in response to a quantifiable fluid mechanical disturbance. *Journal of Plankton Research*. 19, 1289-1304.
- Fiksen, Ø., Carlotti, F., 1998. A model of optimal life history and diel vertical migration in *Calanus finmarchicus*. *Sarsia*. 83, 129-147.
- Fischer, J., Visbeck, M., 1993. Seasonal variation of the daily zooplankton migration in the Greenland Sea. *Deep Sea Research I - Oceanographic Research Papers*. 40, 1547-1557.
- Fitzharris, B.B., 1996. The cryosphere: Changes and their impacts. In: *Climate Change 1995. Impacts, Adaptions, and Mitigation of Climate Change: Scientific- Technical Analyses. Contribution of Working Group II to the Second Assessment Report for the Intergovernmental Panel on Climate Change* [Watson, R.T., Zinyowera, M.C., Moss, R.H. (eds.)]. Cambridge University Press, Cambridge, United Kingdom and New York, NY, USA, 880.
- Flato G.M., Boer, G.J., 2001. Warming asymmetry in climate change simulations. *Geophysical Research Letters*. 28, 195-198.
- Folt, C.L., Burns, C.W., 1999. Biological drivers of zooplankton patchiness. *Trends in Ecology and Evolution*. 14(8), 300-305.
- Folt, C., Schulze, P.C., Baumgartner, K., 1993. Characterizing a zooplankton neighbourhood: small scale patterns of association and abundance. *Freshwater Biology*. 30, 289-300.
- Forbes, J.R., Macdonald, R.W., Carmack, E.C., Iseki, K., O'Brien, M.C., 1992. Zooplankton retained in sequential sediment traps along the Beaufort Sea shelf break during winter. *Canadian Journal of Fisheries and Aquatic Sciences*. 49, 663-670.

- Fortier, M., Fortier, L., Hattori, H., Saito, H., Legendre, L., 2001. Visual predators and the diel vertical migration of copepods under arctic sea ice during the midnight sun. *Journal of Plankton Research*. 23, 1263-1278.
- Forward, R.B., 1988. Diel vertical migration - zooplankton photobiology and behaviour. *Oceanography and Marine Biology*. 26, 361-393.
- Frank, T.M., Widder, E.A., 1997. The correlation of downwelling irradiance and staggered vertical migration patterns of zooplankton in Wilkinson Basin, Gulf of Maine. *Journal of Plankton Research*. 19, 1975-1991.
- Frost, B.W., Bollens, S.M., 1992. Variability of diel vertical migration in the marine planktonic copepod *Pseudocalanus newmani* in relation to its predators. *Canadian Journal of Fisheries and Aquatic Sciences*. 49, 1137-1141.
- Gabrielsen, T.M., Merkel, B., Søreide, J.E., Johansson-Karlsen, E., Bailey, A., Vogedes, D., Nygard, H., Varpe, Ø., Berge, J., 2012. Potential misidentifications of two climate indicator species of the marine arctic ecosystem: *Calanus glacialis* and *C. finmarchicus*. *Polar Biology*. 35, 1621-1628.
- Gallager, S.M., Davis, C.S., Epstein, A.W., Solow, A., Beardsley, R.C., 1996. High-resolution observations of plankton spatial distributions correlated with hydrography in the Great South Channel, Georges Bank. *Deep Sea Research II*. 43(7-8), 1627-1663.
- Gosselin, M., Levasseur, M., Wheeler, P.A., Horner, R.A., Booth, B.C., 1997. New measurements of phytoplankton and ice algal production in the Arctic Ocean. *Deep Sea Research II*. 44(8), 1623-1644.
- Grebmeier, J.M., Dunton, K., 2000. Benthic processes in the northern Bering/Chukchi seas: status and global change. In: Huntington, H.P., ed. *Impacts of changes in sea ice and other environmental parameters in the Arctic*. Alaska. Girdwood. 80-93.
- Greene, C.H., Pershing, A.J., 2000. The response of *Calanus finmarchicus* populations to climate variability in the Northwest Atlantic: basin-scale forcing associated with the North Atlantic Oscillation. *ICES Journal of Marine Science*. 57, 1536-1544.
- Greene, C.H., Wiebe, P.H., Pelkie, C., Benfield, M.C., Popp, J.M., 1998. Three-dimensional acoustic visualization of zooplankton patchiness. *Deep Sea Research II*. 45, 1201-1217.
- Greenlaw, C.F., 1979. Acoustical estimation of zooplankton populations. *Limnology and Oceanography*. 24, 226-242.
- Gulliksen, B., Lønne, O.J., 1989. Distribution, abundance, and ecological importance of marine sympagic fauna in the Arctic. *Rapports et proces-verbaux des reunions / conseil permanent international pour l'exploration de la mer*. 188, 133-138.

- Hagen, W., 1999. Reproductive strategies and energetic adaptations of polar zooplankton. *Invertebrate Reproduction and Development*. 36(1-3), 25-34.
- Hagen, W., Auel, H., 2001. Seasonal adaptations and the role of lipids in oceanic zooplankton. *Zoology - Analysis of Complex Systems*. 104(3-4), 313-326.
- Hanelt, D., Tug, H., Bischof, K., Groß, C., Lippert, H., Sawall, T., Wiencke, C., 2001. Light regime in an Arctic fjord: a study related to stratospheric ozone depletion as a basis for determination of UV effects on algal growth. *Marine Biology*. 138, 649-658.
- Hansen, A.S., Nielsen, T.G., Levinsen, H., Madsen, S.D., Thingstad, F., Hansen, B.W., 2003. Impact of changing ice cover on pelagic productivity and food web structure in Disko Bay, West Greenland: a dynamic model approach. *Deep Sea Research I*. 50, 171-187.
- Hardy, A.C., 1953. Some problems of pelagic life. In: *Essays in Marine Biology (Richard Elmhirst memorial lectures)* (Marshall, S.M., Orr, A.P., eds.) Oliver and Boyd, Edinburgh. 101-121.
- Hardy, A.C., 1936. Observations on the uneven distribution of oceanic plankton. *Discovery Reports*. 11, 511-538.
- Hardy, A.C., Gunther, E.R., 1935. The plankton of the south Georgia whaling grounds and adjacent waters. *Discovery Reports*. 11, 1-456.
- Hargrave, B.T., von Bodungen, B., Conover, R.J., Fraser, A.J., Vass, W.P., 1989. Seasonal changes in sedimentation of particulate material and lipid content of zooplankton collected by sediment trap in the Arctic Ocean off Heiberg Island. *Polar Biology*. 9, 467-475.
- Harris, C., Plueddemann, A., Gawarkiewicz, G., 1998. Water mass distribution and polar front structure in the western Barents Sea. *Journal of Geophysical Research - Oceans*. 103(C2), 2905-2917.
- Harvey, M., Therriault, J.C., Simard, N., 2001. Hydrodynamic control of late summer species composition and abundance of zooplankton in Hudson Bay and Hudson Strait (Canada). *Journal of Plankton Research*. 23, 481-496.
- Hattori, H., Saito, H., 1997. Diel changes in vertical distribution and feeding activity of copepods in ice-covered Resolute Passage, Canadian Arctic, in spring 1992. *Journal of Marine Systems*. 11, 205-219.
- Haury, L.R., 1976. A comparison of zooplankton patterns in the California Current and North Pacific central gyre. *Marine Biology*. 37, 159-167.

- Haury, L.R., McGowan, J.A., Wiebe, P.H., 1978. Patterns and processes in the time-space scales of plankton distribution. In: Spatial pattern in plankton communities. Steele, J.H., ed. Plenum Press, New York. 277-328.
- Hays, G.C., 1995. Ontogenetic and seasonal variation in the diel vertical migration of the copepods *Metridia lucens* and *Metridia longa*. *Limnology and Oceanography*. 40(8), 1461-1465.
- Hays, G.C., 2001 Individual variability in diel vertical migration of a marine copepod: Why some individuals remain at depth when others migrate. *Limnology and Oceanography*. 46(8), 2050-2054.
- Hays, G.C., 2003. A review of the adaptive significance and ecosystem consequences of zooplankton diel vertical migrations. *Hydrobiologia*. 503, 163-170.
- Hays, G.C., Richardson, A.J., Robinson, C., 2005. Climate change and marine plankton. *Trends in Ecology and Evolution*. 20(6), 337-344.
- Head, E.J.H., Harris, L.R., Yashayaev, I., 2003. Distributions of *Calanus* spp. and other mesozooplankton in the Labrador Sea in relation to hydrography in spring and summer (1995–2000). *Progress in Oceanography*. 59, 1-30.
- Heath, M.R., Boyle, P.R., Gislason, A., Gurney, W.S.C., Hay, S.J., Head, E.J.H., Holmes, S., et al., 2004. Comparative ecology of over-wintering *Calanus finmarchicus* in the northern North Atlantic, and implications for life-cycle patterns. *ICES Journal of Marine Science*. 61, 698-708.
- Hegseth, E.N., 1998. Primary production of the northern Barents Sea. *Polar Research*. 17(2), 113-123.
- Hegseth, E.N., Sundfjord, A., 2008. Intrusion and blooming of Atlantic phytoplankton species in the high Arctic. *Journal of Marine Systems*. 74(1-2), 108-119.
- Heim, A., 1900. Der Schlammabsatz am Grund des Vierwaldstättersees. *Vjschr. Naturf. Ges. Zurich*. 45, 164-182.
- Hinzman, L.D., Bettez, N.D., Bolton, W.R., et al., 2005. Evidence and implications of recent climate change in Northern Alaska and other Arctic regions. *Climate Change*. 72, 251-298. DOI: 10.1007/s10584-005-5352-2.
- Hirche, H-J., 1983. Overwintering of *Calanus finmarchicus* and *Calanus helgolandicus*. *Marine Ecology Progress Series*. 11, 281-290.
- Hirche, H-J., 1991. Distribution of dominant calanoid copepod species in the Greenland sea during late fall. *Polar Biology*. 11(6), 351-362.
- Hirche, H-J., 1996. Diapause in the marine copepod *Calanus finmarchicus* – a review. *Ophelia*. 44, 129-143.

- Hirche, H-J., 1997. Life cycle of the copepod *Calanus hyperboreus* in the Greenland Sea. *Marine Biology*. 128, 607-618.
- Hirche, H-J., Mumm, N., 1992. Distribution of dominant copepods in the Nansen Basin, Arctic Ocean, in summer. *Deep Sea Research*. 39(S2), S485-S505.
- Hobson, L.A., 1989. Paradox of the plankton-an overview. *Biological Oceanography*. 6, 493-504.
- Hodges, G., 2000. The new cold war; stalking arctic climate change by submarine. *National Geographic*. March, 30-41.
- Holland, M.M., Bitz, C.M., 2003. Polar amplification of climate change in coupled models. *Climate Dynamics*. 21, 221-232.
- Holliday, D.V., Pieper, R.E., 1995. Bioacoustical oceanography at high frequencies. *ICES Journal of Marine Science*. 52, 279-296.
- Holm-Hansen, O., Rieman, B., 1978. Chlorophyll *a* determination: Improvement of the methodology. *Oikos*. 30, 438-447.
- Holtcamp, W., 2010. The tiniest catch. *Nature*. 468, 26-27.
- Hop, H., Falk-Petersen, S., Svendsen, H., Kwasniewski, S., Pavlov, V., Pavlova, O., Søreide, J.E., 2006. Physical and biological characteristics of the pelagic system across Fram Strait to Kongsfjorden. *Progress in Oceanography*. 71, 182-231.
- Hop, H., Mundy, C.J., Gosselin, M., Rossnagel, A.L., Barber, D.G., 2011. Zooplankton boom and ice amphipod bust below melting sea ice in the Amundsen Gulf, Arctic Canada. *Polar Biology*. 34, 1947-1958.
- Hop, H., Pearson, T., Hegseth, E.N., Kovacs, K.M., Wiencke, C., Kwasniewski, S., Eiane, K., Mehlum, F., Gulliksen, B., Wlodarska-Kowalezuk, M., Lydersen, C., Weslawski, J.M., Cochrane, S., Gabrielsen, G.W., Leakey, R.J.G., Lønne, O.J., Zajaczkowski, M., Falk-Petersen, S., Kendall, M., Wangberg, S.A., Bischof, K., Voronkov, A.Y., Kovaltchouk, N.A., Wiktor, J., Poltermann, M., Di Prisco, G., Papucci, C., Gerland, S., 2002. The marine ecosystem of Kongsfjorden, Svalbard. *Polar Research*. 21(1), 167-208.
- Hop, H., Poltermann, M., Lønne, O.J., Falk-Petersen, S., Korsnes, R., Budgell, W.P., 2000. Ice amphipod distribution relative to ice density and under-ice topography in the northern Barents Sea. *Polar Biology*. 23, 367.
- Hopkins, C.C.E., Nilssen, E.M., 1991. The rise and fall of the Barents Sea capelin (*Mallotus villosus*): a multivariate scenario. *Polar Research*. 10, 535-596.
- Horne, J.K., 2000. Acoustic approaches to remote species identification: a review. *Fisheries Oceanography*. 9(4), 356-371.

- Horne, J.K., Clay, C.S., 1998. Sonar systems and aquatic organisms: matching equipment and model parameters. *Canadian Journal of Fisheries and Aquatic Sciences*. 55, 1296-1306.
- Horwood, J.W., 1981. Variation of fluorescence, particle-size groups and environmental parameters in the southern North Sea. *Journal du conseil / Conseil international pour l'exploration de la mer*. 39, 261-270.
- Houghton, J. T., Filho, L.G.M., Callandar, B.A., Harris, N., Kattenberg, A., Maskell, K., eds. 1996. *Climate change 1995. Contribution of Working Group I to the Second Assessment Report of the Intergovernmental Panel on Climate Change*. New York: Cambridge University Press.
- Houghton, J. T., Ding, Y., Griggs, D.J., Noguer, M., van der Linden, P.J., Xiaosu, D., eds. 2001. *Climate change 2001: The scientific basis. Third Assessment Report. IPCC Working Group I*. Cambridge, United Kingdom: Cambridge University Press.
- Howe, J.A., Harland, R., Cottier, F.R., Brand, T., Willis, K.J., Berge, J.R., Grosfjeld, K., Eriksson, A., 2010. Dinoflagellate cysts as proxies for palaeoceanographic conditions in Arctic fjords. In Howe, J.A., Austin, W.E.N., Forwick, M., Paetzel, M., (eds) *Fjord Systems and Archives*. Geological Society, London, Special Publications. 344, 61-74.
- Hunt, G.L.Jr., Stabeno, P., Walters, G., Sinclair, E., Brodeur, R.D., Napp, J.M., Bond, N.A., 2002. Climate change and control of the southeastern Bering Sea pelagic ecosystem. *Deep Sea Research II*. 49, 5821-5853.
- Huntley, M., Strong, K.W., Dengler, A.T., 1983, Dynamics and community structure of zooplankton in the Davis Strait and northern Labrador Sea. *Arctic*. 36, 143-161.
- Hunt, G.L., Baduini, C.L., Brodeur, R.D., Coyle, K.O., Kachel, N.B., Napp, J.M., et al., 1999. The Bering Sea in 1998: the second consecutive year of extreme weather-forced anomalies. *Eos Transactions, American Geophysical Union*. 80(561), 565-6.
- Hylander, S., Jephson, T., Lebet, K., Von Einem, J., Fagberg, T., Balseiro, E., Modenutti, B., Sol Souza, M., Laspoumaderes, C., Jonsson, M., Ljungberg, P., Nicolle, A., Nilsson, P.A., Ranaker, L., Hansson, L-A., 2011. Climate-induced input of turbid glacial meltwater affects vertical distribution and community composition of phyto- and zooplankton. *Journal of Plankton Research*. 33(8), 1239-1248.
- ICES, 1949. Climatic changes in the Arctic in relation to plants and animals. *Rapports et Proces-Verbaux des Reunions du Conseil International pour l'Exploration de la Mer*. 125, 5-52.
- Ingvaldsen, R., Loeng, H., 2009. Physical oceanography. In *Ecosystem Barents Sea*, eds. Sakshaug, E., Johnsen, G., Kovacs, K. Tapir Academic Press, Trondheim, Norway. 33-64.

- IPCC, 2001. Climate Change 2001: The Scientific Basis. Contribution of Working Group I to the Third Assessment Report of the Intergovernmental Panel on Climate Change [Houghton J. T., Ding Y., Griggs D. J., Noguer M., van der Linden P. J., Dai X., Maskell K., & Johnson C. A. (eds.)] Cambridge University Press, Cambridge, United Kingdom & New York, NY, 881.
- Ito, H., Kudoh, S., 1997. Characteristics of water in Kongsfjorden, Svalbard. Proceedings of the NIPR Symposium on Polar Meteorology and Glaciology. 11, 211-232.
- Ivanov, I.V., Polyakov, V.V., et al. 2008. Seasonal variability in AW off Spitsbergen. Deep Sea Research I. 56, 1-14.
- Jaschnov, V.A., 1970. Distribution of *Calanus* species in the seas of the Northern Hemisphere. International Review of Ges. Hydrobiology. 55, 197-212.
- Jensen, T., Ugland, K. I., Anstensrud, M., 1991. Aspects of growth in Arctic cod, *Boreogadus saida* (Lepechin 1773). Polar Research. 10, 547-552.
- Johannessen, O.M., Miles, M.W., 2000. Arctic sea ice and climate change-will the ice disappear in this century? Science Progress. 83, 209-22.
- Johannessen, O.M., Shalina, E.V., Miles, M.W., 1999. Satellite evidence for an arctic sea ice cover in transformation. Science. 286, 1937-1939.
- Jones, P.D., New, M., Parker, D.E., Martin, S., Rigor, I.G., 1999. Surface air temperature and its changes over the past 150 years. Reviews of Geophysics. 37, 173-199.
- Karnovsky, N.J., Kwasniewski, S., Weslawski, J.M., Walkusz, W., Beszczyska-Möller, A., 2003. Foraging behavior of Little Auks in a heterogeneous environment. Marine Ecology Progress Series. 253, 289-303.
- Kasatkina, S.M., Goss, C., Emery, J.H., Takao, Y., Litvinov, F.F., Malyshko, A.P., Shnar, V.N., Berezhinsky, O.A., 2004. A comparison of net and acoustic estimates of krill density in the Scotia Sea during the CCAMLR 2000 survey. Deep Sea Research II. 51, 1289-1300.
- Kattsov, V.M., Kallen, E., 2005. Future climate change: modeling and scenarios for the Arctic In: Arctic Climate Impact Assessment-Scientific Report. Cambridge University Press, Cambridge, 99-150.
- Kielhorn, W.V., 1952. The biology of the surface zone zooplankton of a boreo-arctic Atlantic Ocean area. Journal of the Fisheries Research Board of Canada. 9, 223-264.
- Kloser, R.J., Ryan, T., Sakov, P., Williams, A., Koslow, J.A., 2002. Species identification in deep water using multiple acoustic frequencies. Canadian Journal of Fisheries and Aquatic Sciences. 59, 1065-1077.

- Koerner, R.M., Lundgaard, L., 1996. Glaciers and global warming. *Geographie Physique et Quaternaire*. 49, 429–434.
- Kosobokova, K.N., 1978. Diurnal vertical distribution of *Calanus hyperboreus* Kroyer and *Calanus glacialis* Jaschnov in central polar Basin. *Okeanologiya*. 18, 722-728.
- Kosobokova, K.N., Hopcroft, R.R., 2009. Diversity and vertical distribution of mesozooplankton in the Arctic's Canada Basin. *Deep Sea Research II*. doi:10.1016/j.dsr2.2009.08.009
- Kotlyakov, B.M., 1997. Quickly warming Arctic basin. *The Earth and the World*. 4, 107.
- Krabill, W., Frederick, E., Manizade, S., Martin, C., Sonntag, J., Swift, R., Thomas, R., Wright, W., Jungel, J., 1999. Rapid thinning of parts of the southern Greenland ice sheet. *Science*. 283, 1522-1524.
- Krabill, W., Abdalati, W., Frederick, E., Manizade, S., Martin, C., Sonntag, J., Swift, R., Thomas, R., Wright, W., Jungel, J., 2000. Greenland ice sheet: high elevation-balance and peripheral thinning. *Science*. 289, 428-430.
- Kwasniewski, S., Gluchowska, M., Jakubus, D., Wojczulanis-Jakubas K., Walkusz, W., Karnovsky, N., Blachowiak-Samolyk, K., Cisek, M., Stempniewicz, L., 2010. The impact of different hydrographic conditions and zooplankton communities on provisioning Little Auks along the West coast of Spitsbergen. *Progress in Oceanography*. 87, 72-82.
- Kwasniewski, S., Hop, H., Falk-Petersen, S., Pedersen, G., 2003. Distribution of *Calanus* species in Kongsfjorden, a glacial fjord in Svalbard. *Journal of plankton research*. 25(1), 1-20.
- Kwasniewski, S., Walkusz, W., Cottier, F., Leu, E., 2012. Mesozooplankton dynamics in relation to food availability during spring and early summer in a high latitude glaciated fjord (Kongsfjorden), with focus on *Calanus*. *Journal of Marine Systems*. <http://dx.doi.org/10.1016/j.jmarsys.2012.09.012>.
- Lampert, W., 1989. The adaptive significance of diel vertical migration of zooplankton. *Functional Ecology*. 3, 21-27.
- Lavoie, D., Simard, Y., Saucier, F.J., 2000. Aggregation and dispersion of krill at channel heads and shelf edges: the dynamics in the Saguenay – St. Lawrence Marine Park. *Canadian Journal of Fisheries and Aquatic Sciences*. 57, 1853-1869.
- Lawson, G.L., Wiebe, P.H., Ashjian, C.J., Gallagher, S.M., Davis, C.S., Warren, J.D., 2004. Acoustically-inferred zooplankton distribution in relation to hydrography west of the Antarctic Peninsula. *Deep Sea Research II*. 51(17-19), 2041-2071.

- Lee, R.F., Hagen, W., Kattner, G., 2006. Lipid storage in marine zooplankton. *Marine Ecology Progress Series*. 307, 273-306.
- Legendre, L., Ackley, S.F., Dieckmann, G.S., Gulliksen, B., Horner, R., Hoshiai, T., Melnikov, I.A., Reeburgh, W.S., Spindler, M., Sullivan, C.W., 1992. Ecology of sea ice biota. 2. Global significance. *Polar Biology*. 12(3-4), 429-444.
- Legendre, P., Legendre, L., 1998. *Numerical Ecology*. Number 20 in *Developments in Environmental Modelling*. Elsevier, Oxford, 2nd ed.
- Lenton, T.M., Held, H., Kriegler, E., Hall, J.W., Lucht, W., Rahmstorf, S., Schellnhuber, H.J., 2008. Tipping elements in the Earth's climate system. *Proceedings of the National Academy of Sciences*. 105(6), 1786-1793.
- Leu, E., Falk-Petersen, S., Kwasniewski, S., Wulff, A., Edwardsen, K., Hessen, D.O., 2006. Fatty acid dynamics during the spring bloom in a high Arctic fjord: importance of abiotic factors vs. community changes. *Canadian Journal of Fisheries and Aquatic Sciences*. 63(12), 2760-2779.
- Leu, E., Søreide J.E., Hessen, D.O., Falk-Petersen, S., Berge, J., 2011. Consequences of changing sea-ice cover for primary and secondary producers in the European Arctic shelf seas: Timing, quantity, and quality. *Progress in Oceanography*. 90(1-4), 18-32.
- Levin, S.A., Morin, A., Powell, T.M., 1988. Patterns and processes in the distribution and dynamics of Antarctic krill. In: *Selected scientific papers, 1988 (SC-CAMLR-SSP/5) CCAMLR*, Hobart, Australia. 281-286.
- Lindsay, R.W., Zhang, J., 2005. The thinning of Arctic sea ice, 1988-2003: Have we passed a tipping point? *Journal of Climate*. 18, 4879-4894.
- Loeng, H., 1991. Features of the physical oceanographic conditions of the Barents Sea. *Polar Research*. 25, 5-18.
- Longhurst, A.R., 1976. Interactions between zooplankton and phytoplankton profiles in the eastern tropical Pacific Ocean. *Deep Sea Research*. 23, 729-754.
- Longhurst, A.R., Bedo, A.W., Harrison, W.G., Head, E.J.H., Sameoto, D.D., 1990. Vertical flux of respiratory carbon by oceanic diel migrant biota. *Deep Sea Research*. 37, 685-694.
- Longhurst, A.R., Sameoto, D., Herman, A., 1984. Vertical distribution of Arctic zooplankton in summer: eastern Canadian archipelago. *Journal of Plankton Research*. 6(1), 137-168.
- Longhurst, A.R., Williams, R., 1992. Carbon flux by seasonal vertical migrant copepods is a small number. *Journal of Plankton Research*. 14, 1495-1509.

- Lønne, O. J., Gulliksen, B., 1989. Size, age, and diet of polar cod, *Boreogadus saida* (Lepechin 1773), in ice-covered waters. *Polar Biology*. 9, 187-191.
- Lønne, O.J., Gulliksen, B., 1991. On the distribution of sympagic macro-fauna in the seasonally ice covered Barents Sea. *Polar Biology*. 11, 457-469.
- Macdonald, R.W., Harner, T., Fyfe, J., 2005. Recent climate change in the Arctic and its impact on contaminant pathways and interpretation of temporal trend data. *Science of the Total Environment*. 342, 5-86.
- MacLennan, D.N., Fernandes, P.G., Dalen, J., 2002. A consistent approach to definitions and symbols in fisheries acoustics. *ICES Journal of Marine Science*. 59, 365-369.
- Madureira, L.S.P., Everson, I., Murphy, E.J., 1993. Interpretation of acoustic data at two frequencies to discriminate between Antarctic krill (*Euphausia superba* Dana) and other scatterers. *Journal of Plankton Research*. 15(7), 787-802.
- Manabe, S., Stouffer, R.J., Spelman, M.J., Bryan, K., 1991. Transient responses of a coupled ocean-atmosphere model to gradual changes of atmospheric CO₂. Part I: Annual mean response. *Journal of Climate*. 4(8), 785-818.
- Manabe, S., Spelman, M.M., Stouffer, R.J., 1992. Transient responses of a coupled ocean-atmosphere model to gradual changes in atmospheric CO₂. *Journal of Climate*. 5, 105-26.
- Manabe, S., Stouffer, R.J., 1995. Simulation of abrupt climate change induced by freshwater input to the North Atlantic Ocean. *Nature*. 378, 165-167.
- Marshall, J., Kushnir, Y., Battisti, D., Chang, P., Czaja, A., Dickson, R., Hurrell, J., McCarney, M., Saravanan, R., Visbeck, M., 2001. North Atlantic climate variability: Phenomena, impacts and mechanisms. *International Journal of Climatology*. 21, 1863-1898.
- Marshall, S.M., Orr A.P., 1958. On the biology of *Calanus finmarchicus* X. Seasonal changes in oxygen consumption. *Journal of the Marine Biological Association of the U.K.* 37, 459-472.
- Martin, A.P., Richards, K.J., Bracco, A., Provenzale, A., 2002. Patchy productivity in the open ocean. *Global Biogeochemical Cycles*. 29, 2213. 10.1029/2001GB001449.
- Maslanik, J.A., Serreze, M.C., Barry, R.G., 1996. Recent decreases in Arctic summer ice cover and linkages to atmospheric circulation anomalies. *Geophysical Research Letters*. 23, 1677-1680.
- Maslowski, W., Newton, B., Schlosser, P., Semtner, A., Martinson, D., 2000. Modeling recent climate variability in the Arctic Ocean. *Geophysical Research Letters*. 27, 3743-3746.

- Masson, S., Angeli, N., Guillard, J., Pinel-Alloul, B., 2001. Diel vertical and horizontal distribution of crustacean zooplankton and young of the year fish in a sub-alpine lake: an approach based on high frequency sampling. *Journal of Plankton Research*. 23(10), 1041-1060.
- Matthews, J.B., Heimdal, B.R., 1980. Pelagic productivity and food chains in fjord systems. In: Freeland, H.J., Farmer, D.M., Levings, C.D. (eds.). *Fjord Oceanography*. Plenum Publication Corp, New York, 377–398.
- McGhee, R., 1996. *Ancient People of the Arctic*. UBC Press in association with Canadian Museum of Civilization, Vancouver. 244.
- McGinty, N., Power, A.M., Johnson, A.M., 2011. Variation among northeast Atlantic regions in the responses of zooplankton to climate change: Not all areas follow the same path. *Journal of Experimental Marine Biology and Ecology*. 400(1-2), 120-131.
- McLaren, I.A., 1963. Effect of temperature on growth of zooplankton and the adaptive value of vertical migration. *Journal of the Fisheries Research Board of Canada*. 20, 685-727.
- McLaughlin, F.A., Carmack, E.C., Macdonald, R.W., Bishop, J.K.B., 1996. Physical and geochemical properties across the Atlantic/Pacific water mass boundary in the southern Canadian Basin. *Journal of Geophysical Research*. 101(C1), 1183-1197.
- McNaught, D.C., 1968. Acoustical determination of zooplankton distribution. in *Proceedings of the 11th Conference on Great Lakes Research*. 76-84.
- McNaught, D.C., Buzzard, M., Levine, S., 1975. Zooplankton production in Lake Ontario as influenced by environmental perturbations. U.S. EPA Report. E/M-660/3-75-021, 40-63.
- Megard, R.O. et al., 1997. Spatial distributions of zooplankton during coastal upwelling in western Lake Superior. *Limnology and Oceanography*. 42, 827-840.
- Michel, C., Legendre, L., Ingram, R.G., Gosselin, M., Levasseur, M., 1996. Carbon budget of sea-ice algae in spring: evidence of a significant transfer to zooplankton grazers. *Journal of Geophysical Research - Oceans*. 101(C8), 18345-18360.
- Miller, C.B., Cowles, T.J., Wiebe, P.H., Copley, N.J., Grigg, H., 1991. Phenology in *Calanus finmarchicus*; hypotheses about control mechanisms. *Marine Ecology Progress Series*. 72, 97-91.
- Mitchell, J.F.B., Johns, T.C., Gergory, J.M., Tett, S.F.B., 1995. Climate response to increasing levels of greenhouse gases and sulphate aerosols. *Nature*. 376, 501-4.

- Moline, M.A., Karnovsky, N.J., Brown, Z., Divoky, G.J., Frazer, T.K., Jacoby, C.A., Torres, J.J., Fraser, W.R., 2008. High latitude changes in ice dynamics and their impact on polar marine ecosystems. *Annals of the New York Academy of Sciences*. 1134, 267-319.
- Molineró, J.C., Ibanez, F., Souissi, F., Bosc, E., Nival, P., 2008. Surface patterns of zooplankton spatial variability detected by high frequency sampling in the NW Mediterranean. Role of density fronts. *Journal of Marine Systems*. 69, 271-282.
- Monsen, N.E., Cloern, E.J., Lucas, L., 2002. A comment on the use of flushing time, residence time, and age as transport time. *Limnology and Oceanography*. 47, 1545-1553.
- Morison, J., Aagaard, K., Steele, M., 2000. Recent environmental changes in the Arctic: a review. *Arctic*. 53, 359-371.
- Morison, J.H., Steele, M., Andersen, R., 1998. Hydrography of the upper Arctic Ocean measured from the nuclear submarine USS Pargo. *Deep Sea Research I*. 45, 15-38.
- Mumm, N., 1991. On the summerly distribution of mesozooplankton in the Nansen Basin, Arctic Ocean (in German). *Rep. Polar Research*. 92, 1-173.
- Mumm, N., 1993. Composition and distribution of mesozooplankton in the Nansen Basin, Arctic Ocean, during summer. *Polar Biology*. 13, 451-461.
- Mysak, L.A., Venegas, S.S., 1998. Decadal climate oscillations in the Arctic: a new feedback loop for atmosphere-ice-ocean interactions. *Geophysical Research Letters*. 25, 3609-3610.
- Neill, W.E., 1990. Induced vertical migration in copepods as a defence against invertebrate predation. *Nature*. 345, 524-526.
- Niebauer, N.J., Alexander, V., 1985. Oceanographic frontal structure and biological production at an ice edge. *Continental Shelf Research*. 4, 367-88.
- Nilsen, F., Cottier, F., Skogseth, R., Mattsson, S., 2008. Fjord-shelf exchanges controlled by ice and brine production: The interannual variation of Atlantic Water in Isfjorden, Svalbard. *Continental Shelf Research*. 28, 1838-1853.
- NSIDC, 2012. Arctic sea ice extent settles at record seasonal minimum. Online announcement. <http://nsidc.org/arcticseaicenews/2012/09/arctic-sea-ice-extent-settles-at-record-seasonal-minimum/> accessed 25/12/12.
- Orcutt, J.D. Jr., Porter, K.G., 1983. Diel vertical migration by zooplankton: constant and fluctuating temperature effects on life history parameters of *Daphnia*. *Limnology and Oceanography*. 28, 720-730.

- Øresland, V., 1990. Feeding and predation impact of the chaetognath *Eukrohnia hamata* in Gerlache Strait, Antarctic Peninsula. *Marine Ecology Progress Series*. 63, 201-209.
- Osgood, K.E., Frost, B.W., 1994. Ontogenic diel vertical migration behaviors of the marine planktonic copepods *Calanus pacificus* and *Metridia lucens*. *Marine Ecology Progress Series*. 104, 13-25.
- Østvedt, O. J., 1955. Zooplankton investigations from weather ship M in the Norwegian Sea, 1948-49. *Hvalrådets Skr.* 40, 93.
- Overland, J.E., Roach, A.T., 1987. Northward flow in the Bering and Chukchi Seas. *Journal of Geophysical Research*. 92, 7097-7105.
- Overpeck, J.T., 1996. Warm climate surprises. *Science*. 271, 1,820-1,821.
- Overpeck, J., Hughen, K., Hardy, D., Bradley, R., Case, R., Douglas, M., Finney, B., Gajewski, K., Jacoby, G., Jennings, A., Lamoureux, S., Lasca, A., MacDonald, G., Moore, J., Retelle, M., Smith, S., Wolfe, A., Zielinski, G., 1997. Arctic environmental change of the last four centuries. *Science*. 278, 1,251-1,256.
- Parkinson, C., Cavalieri, D., Gloersen, P., Zwally, H., Comiso, J., 1999. Arctic sea ice extents, areas, and trends, 1978–1996. *Journal of Geophysical Research (Oceans)*. C9, 20837-20856.
- Pearre, S., 2003. Eat and run? The hunger/satiation hypothesis in vertical migration: History, evidence and consequences. *Biology Reviews*. 78, 1-79.
- Pedersen, G., 1995. Factors influencing the size and distribution of the copepod community in the Barents Sea with special emphasis on *Calanus finmarchicus* (Gunnerus). Dr. Thesis, Norwegian College of Fishery Science, University of Tromsø.
- Pedersen, G., Tande, K.S., Nilssen, E.M., 1995. Temporal and regional variation in the copepod community in the central Barents Sea during spring and early summer 1988 and 1989. *Journal of Plankton Research*. 17, 263-282.
- Petersen, G.H., Curtis, M.A., 1980. Differences in energy flow through major components of subarctic, temperate and tropical marine shelf communities. *Dana*. 1, 53-64.
- Pfirman, S., Bauch, D., Gammelrød, T., 1994. The Northern Barents Sea: water mass distribution and modification. In: Johannesen, O., Muench, R., Overland, J., The polar oceans and their Role in Shaping the global Environment, American Geophysical Union, Washington. *Geophysical Monograph Series*. 85, 77-94.

- Pieper, R.E., McGehee, D.E., Greenlaw, C.F., Holliday, D.V., 2001. Acoustically measured seasonal patterns of zooplankton in the Arabian Sea. *Deep Sea Research II*. 48, 1325-1343.
- Piepenburg, D., 2005. Recent research on Arctic benthos: common notions need to be revised. *Polar Biology*. 28, 733-755.
- Pierson, J.J., 2008. Forays and foraging in marine zooplankton. (Online at: <http://www.hpl.umces.edu/~jpierson/forays.html>)
- Pinel-Alloul, B., 1995. Spatial heterogeneity as a multiscale characteristic of zooplankton community. *Hydrobiologia*. 300/301, 17-42.
- Piontkovski, S.A., Williams, R., Melnik, T.A., 1995. Spatial heterogeneity, biomass and size structure of plankton of the Indian Ocean: some general trends. *Marine Ecology Progress Series*. 117, 219-227.
- Poltermann, M., 1997. Biology and ecology of cryopelagic amphipods from Arctic sea ice. *Berichte der Polarforschung*. 225, 1-170.
- Powell, T.M., 1989. Perspectives in Ecological Theory, chapter: Physical and biological scales of variability in lakes, estuaries, and the coastal ocean, Princeton, NJ. 157-176.
- Reigstad, M., Wassmann, P., Wexels Riser, C., Øygarden, S., Rey, F., 2002. Variations in hydrography, nutrients and chlorophyll a in the marginal ice-zone and the central Barents Sea. *Journal of Marine Systems*. 38(1-2), 9-29.
- Renaud, P.E., Morata, N., Carroll, M.L., Denisenko, S.G., Reigstad, M., 2008. Pelagic-benthic coupling in the western Barents Sea: Processes and time scales. *Deep Sea Research II*. 55(20-21), 2372-2380.
- Renaud, P.E., Reidel, A., Michel, C., Morata, N., Gosselin, M., Juul-Pedersen, T., Chiuchiolo, A., 2007. Seasonal variation in benthic community oxygen demand: a response to an ice algal bloom in the Beaufort Sea, Canadian Arctic? *Journal of Marine Systems*. 67(1-2), 1-12.
- Resgalla Jr., C., De la Rocha, C., Montu, M., 2001. The influence of Ekman transport on zooplankton biomass variability off southern Brazil. *Journal of Plankton Research*. 23, 641-650.
- Richter, C., 1994. Regional and seasonal variability in the vertical distribution of mesozooplankton in the Greenland Sea. *Reports on Polar Research*. 154, 87.
- Ringelberg, J., 1995. Changes in light intensity and diel vertical migration – a comparison of marine and fresh-water environments. *Journal of the Marine Biological Association of the UK*. 75, 15-25.

- Rios-Jara, E., 1998. Spatial and temporal variations in the zooplankton community of Phosphorescent Bay, Puerto Rico. *Estuarine, Coastal and Shelf Science*. 46, 797-809.
- Riser, C.W., Wassmann, P., Reigstad, M., Seuthe, L., 2008. Vertical flux regulation by zooplankton in the northern Barents Sea during Arctic spring. *Deep Sea Research II*. 55(20-21), 2320-2329.
- Rothrock, D.A., Yu, Y., Maykut, G.A., 1999. Thinning of the Arctic sea-ice cover. *Geophysical Research Letters*. 26, 3469-3472.
- Rudels, B., Jones, E.P., Anderson, L.G., Katner, G., 1994. On the intermediate depth waters of the Arctic Ocean. [In: Johannessen, O.M., Muench, R.D., Overland, J.E., ed]. *The polar oceans and their role in shaping the global environment*. 85. Washington (DC) American Geophysical Union. 33-46.
- Runge, J.A., Ingram, R.G., 1991. Under-ice feeding and diel migration by the planktonic copepods *Calanus glacialis* and *Pseudocalanus minutus* in relation to the ice algal production cycle in southeastern Hudson Bay, Canada. *Marine Biology*. 108, 217-225.
- Saar, R.A., 2000. The unbearable capriciousness of Bering. *Science*. 287, 1388-9.
- Sabine, C.L., Feely, R.A., Gruber, N., Key, R.M., Lee, K., Bullister, J.L., Wanninkhof, R., Wong, C.S., Wallace, D.W.R., Tilbrook, B., Millero, F.J., Peng, T.H., Kozyr, A., Ono, T., Rios, A.F., 2004. The oceanic sink for anthropogenic CO₂. *Science*. 305, 367-370.
- Saito, H., Hattori, H., 1997. Diel vertical migration and feeding rhythm of copepods under sea ice at Saroma-ko Lagoon. *Journal of Marine Systems*. 11, 191-203.
- Sakshaug, E., Hopkins, C.C.E., Øritsland, N.A., 1991. Proceedings of the pro mare symposium on polar marine ecology, Trondheim, 12-16 May, 1990. *Polar Research*. 1-610.
- Sakshaug, E., Slagstad, D., 1991. Light and productivity of phytoplankton in marine ecosystems: a physiological view. *Polar Research*. 10, 69-85.
- Saloranta, T., Svendsen, H., 2001. Across the Arctic front west of Spitsbergen: high resolution CTD sections from 1998-200. *Polar Research*. 20, 177-184.
- Sampei, M., Sasaki, H., Hattori, H., Fukuchi, M., Hargrave, B.T., 2004. Fate of sinking particles, especially faecal pellets, within the epipelagic zone in the North Water (NOW) polynya of northern Baffin Bay. *Marine Ecology Progress Series*. 278, 17-25.
- Saunders, J.E., 2008. Measuring and understanding biogenic influences upon cohesive sediment stability in intertidal systems. PhD thesis submitted at the University of St Andrews.

- Schauer, U., Fahrbach, E., Østerhus, S., Rohardt, G., 2004. Arctic warming through the Fram Strait: Oceanic heat transport from 3 years of measurements. *Journal of Geophysical Research*. 109, C06026.
- Schlosser, P., Swift, J.H., Lewis, D., Pfirman, S.L., 1995. The role of the large-scale Arctic Ocean circulation in the transport of contaminants. *Deep Sea Research II*. 42(6), 1341-1367.
- Schlüter, M., Rachor, E., 2001. Meroplankton distribution in the central Barents Sea in relation to local oceanographic patterns. *Polar Biology*. 24, 582-592.
- Schneider, D., 2001. The Rise of the Concept of Scale in Ecology. *BioScience*. 51(7), 545-553.
- Scott, C.L., Kwasniewski, S., Falk-Petersen, S., Sargent, J.R., 2000. Lipids and life strategies of *Calanus finmarchicus*, *Calanus glacialis* and *Calanus hyperboreus* in late autumn, Kongsfjorden, Svalbard. *Polar Biology*. 23, 510-516.
- Sekino, T., Yamamura, N., 1999. Diel vertical migration of zooplankton: optimum migrating schedule based on energy accumulation. *Evolutionary Ecology*. 13, 267-282.
- Sekino, T., Yoshioka, T., 1995. The relationship between nutritional condition and diel vertical migration of *Daphnia galeata*. *Japanese Journal of Limnology*. 56, 145-150.
- Semiletov, I.P., Pipko, I.I., Repina, I., Shakhova, N.E., 2007. Carbonate chemistry dynamics and carbon dioxide fluxes across the atmosphere–ice–water interfaces in the Arctic Ocean: Pacific sector of the Arctic. *Journal of Marine Systems*. 66, 204-226.
- Serreze, M.C., Walsh, J.E., Chapin III, F.S., Osterkamp, T., Dyurgerov, M., Romanovsky, V., Oechel, W.C., Morison, J., Zhang, T., Barry, R.G., 2000. Observational evidence of recent change in the northern high latitude environment. *Climatic Change*. 46, 159-207.
- Skjoldal, H.R., Hassel, A., Rey, F., 1987. Spring phytoplankton development and zooplankton reproduction in the central Barents Sea in the period 1979-1984. In: Loeng, H. (ed.) *The effect of oceanographic conditions on distribution and population dynamics of commercial fish stocks in the Barents Sea*, Proceedings of the 3rd Soviet–Norwegian Symposium. IMR/PINRO, Bergen, 59-89.
- Skjoldal, H.R., Rey, F., 1989 Pelagic production and variability of the Barents Sea ecosystem. In: Sherman, K., Alexander, L.M., (eds) *Biomass yields and geography of large marine ecosystems*. AAAS selected symposium 111. Westview Press, Washington. 241-286.

- Slagstad, D., McClimans, T., 2005. Modelling the ecosystem dynamics of the marginal ice zone and central Barents Sea. I. Physical and chemical oceanography. *Journal of Marine Systems*. 58, 1-18.
- Slubowska-Woldengen, M., Rasmussen, T.L., Koc, N., Klitgaard-Kristensen, D., Nilsen, F., Solheim, A., 2007. Advection of Atlantic Water to the western and northern Svalbard shelf since 17,500 cal yr BP. *Quaternary Science Reviews*. 26, 463-478.
- Smetacek, V., Nicol, S., 2005. Review Polar ocean ecosystems in a changing world. *Nature*. 437, 362-368.
- Smith, D.M., 1998. Recent increase in the length of the melt season of perennial Arctic sea ice. *Geophysical Research Letters*. 25, 655-658.
- Smith, P.E., Ohman, M.D., Eber, L.E., 1989. Analysis of the patterns of distribution of zooplankton aggregations from an ADCP. *CalCOFI Report*. 30, 88-103.
- Smith, S.L., 1990. Egg production and feeding by copepods prior to the spring bloom of phytoplankton in Fram Strait, Greenland Sea. *Marine Biology*. 106, 59-69.
- Smith, W.O., Sakshaug, E., 1990. Autotrophic processes in polar regions. In: Smith, W.O., (ed.), *Polar Oceanography, Part B*. Academic Press, San Diego, 477-525.
- Søreide, J.E., Falk-Petersen, S., Hegseth, E.N., Hop, H., Carroll, M.L., Hobson, K.A., Blachowiak-Samolyk, K., 2008. Seasonal feeding strategies of *Calanus* in the high-Arctic Svalbard region. *Deep Sea Research II*. 55, 2225-2244.
- Søreide, J.E., Hop, H., Carroll, M.L., Falk-Petersen, S., Hegseth, E.N., 2006. Seasonal food web structures and sympagic–pelagic coupling in the European Arctic revealed by stable isotopes and a two-source food web model. *Progress in Oceanography*. 71(1), 59-87.
- Søreide, J.E., Hop, H., Falk-Petersen, S., Gulliksen, B., Hansen, E., 2003. Macrozooplankton communities and environmental variables in the Barents Sea marginal ice zone in late winter and spring. *Marine Ecology Progress Series*. 263, 43-64.
- Søreide, J.E., Leu, E., Berge, J., Graeve, M., Falk-Petersen, S., 2010. Effects of omega-3 fatty acid production on *Calanus glacialis* reproduction and growth in a changing marine Arctic. *Global Change Biology*. doi: 10.1111/j.1365-2486.2010.02175.x
- Stanton, T.K., Chu, D., 2000. Review and recommendations for the modelling of acoustic scattering by fluid-like elongated zooplankton: euphausiids and copepods. *ICES Journal of Marine Science*. 57, 793-807.

- Stanton, T.K., Wiebe, P.H., Chu, D., Benfield, M.C., Scanlon, L., Martin, L., Eastwood, R.L., 1994. On acoustic estimates of zooplankton biomass. *ICES Journal of Marine Science*. 51, 505-512.
- Steele, M., Boyd, T., 1998. Retreat of the cold halocline layer in the Arctic Ocean. *Journal of Geophysical Research*. 103, 10419-10435.
- Stein, R., Schubert, C., Vogt, C., Futterer, D., 1994 Stable isotope stratigraphy, sedimentation rates, and salinity changes in the Latest Pleistocene to Holocene eastern central Arctic Ocean. *Marine Geology*. 119, 333-355.
- Stein, R., Boucsein, B., Fahl, K., Garcia de Oteyza, T., Knies, J., Niessen, F., 2001. Accumulation of particulate organic carbon at the Eurasian continental margin during late Quaternary times: controlling mechanisms and paleoenvironmental significance. *Global and Planetary Change*. 31, 87-102.
- Stempniewicz, L., 2001. Alle alle Little Auk, BWP Update. *The Journal of the Birds of the Western Palearctic*. 3, Oxford University Press, Oxford, 175-201.
- Stempniewicz, L., Blachowiak-Samolyk, K., Weslawski, J.M. 2007. Impact of climate change on zooplankton communities, seabird populations and arctic terrestrial ecosystem – A scenario. *Deep Sea Research 2*. 54, 2934-2945.
- Stich, H.B., Lampert, W., 1981. Predator evasion as an explanation of diurnal vertical migration by zooplankton. *Nature*. 293, 396-398.
- Strickler, J.R., 1998. Observing free-swimming copepods mating. *Philosophical Transactions of the Royal Society of London B*. 353, 671-680.
- Strutton, P.G. et al., 1997. Phytoplankton patchiness: quantifying the biological contribution using fast repetition rate fluorometry. *Journal of Plankton Research*. 19, 1265-1274.
- Svendsen, H., Beszczynska-Moeller, A., Hagen, J., Lefauconnier, B., Tveberg, V., Gerland, S., Oebaeck, J., Bischhof, K., Papucci, C., Zajaczkowski, M., Attoni, R., Bruland, O., Wiencke, C., Winther, J., Dallmann, W., 2002. The physical environment of Kongsfjorden-Krossfjorden, an Arctic fjord system in Svalbard. *Polar Research*. 21(1), 133-166.
- Szczucinski, W., Kajaczkowski, M., 2012. Factors controlling downward fluxes of particulate matter in glacier-contact and non-glacier contact settings in a subpolar fjord (Billefjorden, Svalbard). In Li, M.Z., Sherwood, C.R., Hill, P.R (eds) *Sediments, Morphology and Sedimentary Processes on Continental Shelves: Advances in technologies, research and applications*. Special publication 44 of the International Association of Sedimentologists. Wiley-Blackwell, UK, 369-389.

- Takahashi, T., Feely, R.A., Weiss, R.F., Wanninkhof, R.H., Chipman, D.W., Sutherland, S.C., Takahashi, T.T., 1997. Global air-sea flux of CO₂: an estimate based on measurements of sea-air pCO₂ difference. Proceedings of the National Academy of Sciences of the United States of America. 94, 8292-8299.
- Tande, K.S., 1982. Ecological investigation on the zooplankton community of Balsfjorden, northern Norway: generation cycles, and variations in body weight and body content of carbon and nitrogen related to overwintering and reproduction in the copepod *Calanus finmarchicus* (Gunnerus). Journal of Experimental Marine Biology and Ecology. 62, 129-142.
- Tande, K.S., 1988. An evaluation of factors affecting vertical distribution among recruits of *Calanus finmarchicus* in three adjacent high latitude localities. Hydrobiologia. 167, 115-126.
- Tande, K.S., 1991. *Calanus* in North Norwegian fjords and in the Barents Sea. Polar Research. 10, 389-407.
- Tande, K.S., Henderson, R.J., 1988. Lipid composition of copepodite stages and adult females of *Calanus glacialis* in Arctic waters of the Barents Sea. Polar Biology. 8, 333-339.
- Tarling, G.A., Jarvis, T., Emsley, S.M., Matthews, J.B.L., 2002. Midnight sinking behaviour in *Calanus finmarchicus*: a response to satiation or krill predation? Marine Ecology Progress Series. 240, 183-194.
- Tarling, G.A., Matthews, J.B.L., David, P., Guerin, O., Buchholz, F., 2001. The swarm dynamics of northern krill (*Meganyctiphanes norvegica*) and pteropods (*Cavolinia inflexa*) during vertical migration in the Ligurian Sea observed by an acoustic Doppler current profiler. Deep Sea Research I. 48(7), 1671-1686.
- Tartarotti, B., Cravero, W., Zagarese, H.E., 2000. Biological weighting function for the mortality of *Boeckella gracilipes* (Copepoda, Crustacea) derived from experiments with natural solar radiation. Photochemistry and Photobiology. 72, 314-319.
- Taylor, A.H., Allen, J.I., Clark, P.A., 2002. Extraction of a weak climatic signal by an ecosystem. Nature. 416, 629-632.
- Thibault, D., Head, E.J., Wheeler, P.A., 1999. Mesozooplankton in the Arctic Ocean in summer. Deep Sea Research I. 46, 1391-1415.
- Tiselius, P., 1998. An in situ camera for plankton studies: design and preliminary observations. Marine Ecology Progress Series. 164, 293-299.
- Trevorrow, M.V., Tanaka, Y., 1997. Acoustic and in situ measurements of freshwater amphipods (*Jesogammarus annandalei*) in Lake Biwa, Japan. Limnology and Oceanography. 42, 121-132.

- Trudnowska, E., Szczucka, J., Hoppe, L., Boehnke, R., Hop, H., Blachowiak-Samolyk, K., 2012. Multidimensional zooplankton observations on the northern West Spitsbergen Shelf. *Journal of Marine Systems*. 98-99, 18-25.
- Tverberg, V., Cottier, F.R., Nilsen, F., Nøst, O.A., Svendsen, H., 2009. Warming of an arctic shelf - the recent Atlantic Water dominance of west Spitsbergen. *Geophysical Research Letters* (submitted).
- Tynan, C.T., DeMaster, D.P., 1997. Observations and predictions of Arctic climatic change: potential effects on marine mammals. *Arctic*. 50, 308-322.
- Unstad, K.H., Tande, K., 1991. Depth distribution of *Calanus finmarchicus* and *C. glacialis* in relation to environmental conditions in the Barents Sea. *Polar Research*. 10, 409-420.
- Varpe, Ø., Jørgensen, C., Tarling, G.A., Fiksen, Ø., 2007. Early is better: seasonal egg fitness and timing of reproduction in a zooplankton life-history perspective. *Oikos*, 116, 1331-1342. doi:10.1111/j.2007.0030-1299.15893.x
- Vinje, T., 1999. Barents Sea ice edge variation over the past 400 years. In: Report of the Workshop on Sea Ice Charts of the Arctic. WCRP no.108.
- Vinnikov, K.Y., Robock, A., Stouffer, R.J., Walsh, J.E., Parkinson, C.L., Cavalieri, D.J., Mitchell, J.F.B., Garrett, D., Zakharov, V.F., 1999. Global warming and Northern Hemisphere sea ice extent. *Science*. 286, 1934-1937.
- Vinogradov, G.M., 1997. Some problems of vertical distribution of meso- and macrozooplankton in the ocean. *Advances in Marine Biology*. 32, 1-9.
- Walczowski, W., Piechura, J., 2007. Pathways of the Greenland Sea warming. *Geophysical Research Letters*. 34, L10608. doi:10.1029/2007GL029974.
- Walkusz, W., Storemark, K., et al., 2003. Zooplankton community structure; a comparison of fjords, open water and ice stations in the Svalbard area. *Polish Polar Research*. 24(2), 149-165.
- Wallace, M.I., Cottier, F.R., Berge, J., Tarling, G.A., Griffiths, C., Brierley, A.S., 2010. Comparison of zooplankton vertical migration in an ice-free and a seasonally ice-covered Arctic fjord: An insight into the influence of sea ice cover on zooplankton behaviour. *Limnology and Oceanography*. 55(2), 831-845.
- Wang, J., Ikeda, M., 2001. Arctic sea-ice oscillation: regional and seasonal perspectives. *Annals of Glaciology*. 33, 481-492.
- Warren, J.D., Patrician, M., 2011. Multiple frequency acoustic backscatter discrimination of zooplankton and fish scatterers in Cape Cod Bay in Spring 2010. *Journal of the Acoustical Society of America*. 129(4), 2691-2691 [submitted abstract]

- Wassmann, P., 2001. Vernal export and retention of biogenic matter in the north-eastern North Atlantic and adjacent Arctic Ocean: the role of the Norwegian Atlantic Current and topography. National Institute of Polar Research, Special Issue. 54, 377-392.
- Wassmann, P., Olli, K., Wexels Riser, C., Svensen, C., 2003. Ecosystem function, biodiversity, and vertical flux regulation in the twilight zone. In: Wefer, G., Lamy, F., Mantoura, F., (eds.) Marine Science Frontiers for Europe. Springer, Berlin. 279-287.
- Wassmann, P., Reigstad, M., Haug, T., Rudels, B., Carroll, M.L., Hop, H., Gabrielsen, G.W., Falk-Petersen, S., Denisenko, S.G., Arashkevich, E., Slagstad, D., Pavlova, O., 2006. Food webs and carbon flux in the Barents Sea. Progress in Oceanography. 71, 232-287.
- Watkins, J.L., Brierley, A.S., 1996. A post-processing technique to remove background noise from echo integration data. ICES Journal of Marine Science. 53, 339-344.
- Watkins, J.L., Brierley, A.S., 2002. Verification of the acoustic techniques used to identify Antarctic krill. ICES Journal of Marine Science. 59, 1326-1336.
- Watson, R. T., Zinyowera, M., Moss, R.H., eds. 1998. The regional impacts of climate change: An assessment of vulnerability. Cambridge, United Kingdom: Cambridge University Press.
- Weaver, A.J., Bitz, C.M., Fanning, A.F., Holland, M.M., 1999. THERMOHALINE CIRCULATION: High-Latitude Phenomena and the Difference Between the Pacific and Atlantic. Annual Review of Earth and Planetary Sciences. 27, 231-285.
- Wenneck, T.de L., Falkenhaus, T., Bergstad, O.A., 2008. Strategies, methods, and technologies adopted on the R.V. *G.O Sars* MAR-ECO expedition to the Mid-Atlantic Ridge in 2004. Deep Sea Research II. 55(1-2), 6-28.
- Weslawski, J.M., Jankowski, A., Kwasniewski, S., Swerpel, S., Ryg, M., 1991. Summer hydrology and zooplankton in two Svalbard fjords. Polish Polar Research. 12, 445-460.
- Weslawski, J.M., Ryg, M., Smith, T., Oritsland, N., 1994. Diet of ringed seals (*Phoca hispida*) in a fjord of West Svalbard. Arctic. 47(2), 109-114.
- Weslawski, J.M., Stempniewicz, L., Mehlum, F., Kwasniewski, S., 1999. Summer feeding strategy of the Little Auk (*Alle alle*) from Bjørnøya, Barents Sea. Polar Biology. 21, 129-134.
- Wexels Riser, C., Wassmann, P., Olli, K., Pasternak, A., Arashkevich, E., 2002. Seasonal variation in production, retention and export of zooplankton faecal pellets in the marginal ice zone and the central Barents Sea. Journal of Marine Systems. 38, 175-188.

- Wiafe, G., Frid, C.L.J., 1996. Short-term temporal variation in coastal zooplankton communities: the relative importance of physical and biological mechanisms. *Journal of Plankton Research*. 18, 1485-1501.
- Wiborg, K.F., 1955. Zooplankton in relation to hydrography in the Norwegian Sea. *Fisk Dir Skr. Ser. Havunders.* 11, 1-66.
- Wiebe, P.H., 1970. Small-scale spatial distribution in oceanic zooplankton. *Limnology and Oceanography*. 15, 205-217.
- Wiebe, P.H., Copley, N.J., Boyd, S.H., 1992. Coarse-scale horizontal patchiness and vertical migration of zooplankton in Gulf Stream warm-core ring 82-H. *Deep Sea Research*. 39, 247-278.
- Williamson, C.E., Sanders, R.W., Moeller, R.E., Stutzman, P.L., 1996. Utilization of subsurface food resources for zooplankton reproduction: Implications for diel vertical migration theory. *Limnology and Oceanography*. 41(2), 224-233.
- Willis, K.J., Cottier, F.R., Kwasniewski, S., 2008. Impact of warm water advection on the winter zooplankton community in an Arctic fjord. *Polar Biology*. 31, 475-481.
- Willis, K., Cottier, F., Kwasniewski, S., Wold, A., Falk-Petersen, S., 2006. The influence of advection on zooplankton community composition in an Arctic fjord (Kongsfjorden, Svalbard). *Journal of Marine Systems*. 61, 39-54.
- Woodgate, R.A., Aagaard, K., Muench, R.D., Gunn, J., Bjork, G., Rudels, B., Roach, A.T., Schauer, U., 2001. The Arctic Ocean boundary current along the Eurasian slope and adjacent Lomonosov Ridge: water mass properties, transports and transformations from moored instruments. *Deep Sea Research*. 48, 1757-92.
- Zaret, T.M., Suffern, J.S., 1976. Vertical migration in zooplankton as a predator avoidance mechanism. *Limnology and Oceanography*. 21, 804-813.
- Zenkevitch, L., 1963. *Biology of the Seas of the USSR*. Georg Allen and Unwin, London. 955.
- Zhou, M., Nordhausen, W., Huntley, M.E., 1994 ADCP measurements of the distribution and abundance of euphausiids near the Antarctic Peninsula in winter. *Deep Sea Research*. 41, 1425-1445.
- Zwiers, F.W., 2002. The 20-year forecast. *Nature*. 416, 690-691.